frontiers | Research Topics

Chordoma: Advances in biology and clinical management

Edited by
Jiwei Bai, Sebastien Froelich, Paul Gardner, Xiaohong Rose Yang and Cheng Yang

Published in
Frontiers in Oncology
Frontiers in Neurology

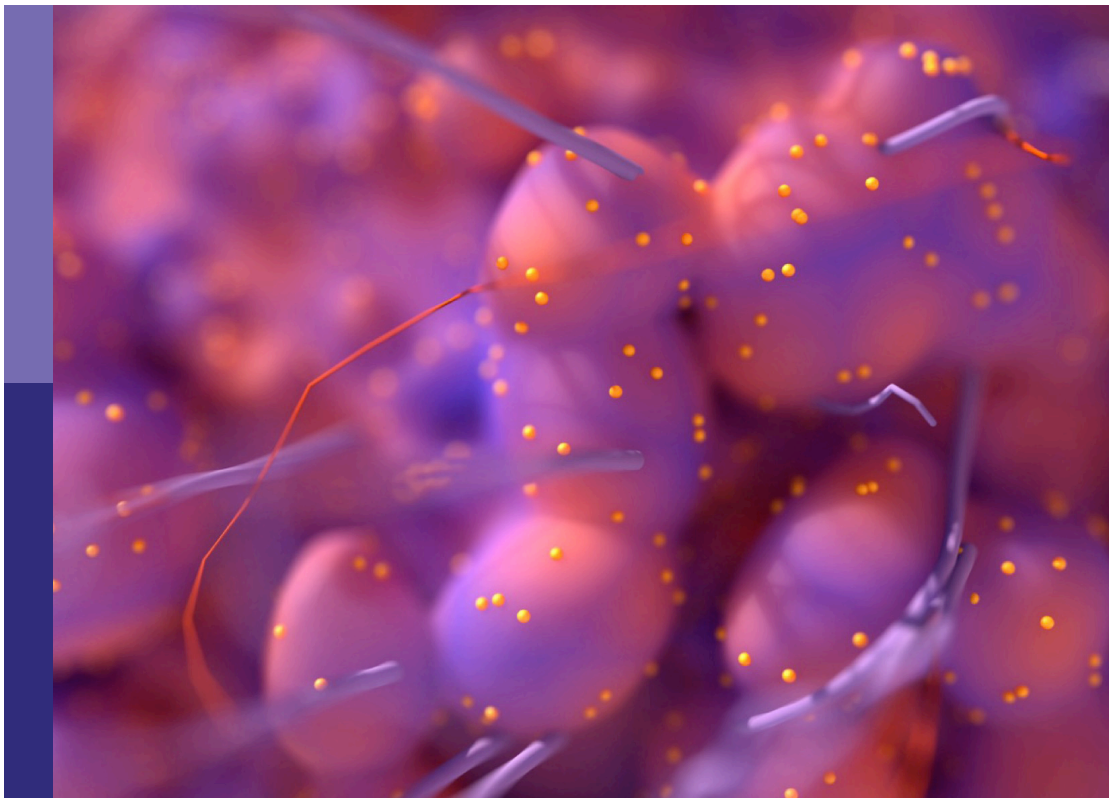

ISSN 1664-8714
ISBN 978-2-8325-2503-6
DOI 10.3389/978-2-8325-2503-6

About Frontiers

Frontiers is more than just an open access publisher of scholarly articles: it is a pioneering approach to the world of academia, radically improving the way scholarly research is managed. The grand vision of Frontiers is a world where all people have an equal opportunity to seek, share and generate knowledge. Frontiers provides immediate and permanent online open access to all its publications, but this alone is not enough to realize our grand goals.

Frontiers journal series

The Frontiers journal series is a multi-tier and interdisciplinary set of open-access, online journals, promising a paradigm shift from the current review, selection and dissemination processes in academic publishing. All Frontiers journals are driven by researchers for researchers; therefore, they constitute a service to the scholarly community. At the same time, the *Frontiers journal series* operates on a revolutionary invention, the tiered publishing system, initially addressing specific communities of scholars, and gradually climbing up to broader public understanding, thus serving the interests of the lay society, too.

Dedication to quality

Each Frontiers article is a landmark of the highest quality, thanks to genuinely collaborative interactions between authors and review editors, who include some of the world's best academicians. Research must be certified by peers before entering a stream of knowledge that may eventually reach the public - and shape society; therefore, Frontiers only applies the most rigorous and unbiased reviews. Frontiers revolutionizes research publishing by freely delivering the most outstanding research, evaluated with no bias from both the academic and social point of view. By applying the most advanced information technologies, Frontiers is catapulting scholarly publishing into a new generation.

What are Frontiers Research Topics?

Frontiers Research Topics are very popular trademarks of the *Frontiers journals series*: they are collections of at least ten articles, all centered on a particular subject. With their unique mix of varied contributions from Original Research to Review Articles, Frontiers Research Topics unify the most influential researchers, the latest key findings and historical advances in a hot research area.

Find out more on how to host your own Frontiers Research Topic or contribute to one as an author by contacting the Frontiers editorial office: frontiersin.org/about/contact

Chordoma: Advances in biology and clinical management

Topic editors

Jiwei Bai — Capital Medical University, China
Sebastien Froelich — Assistance Publique Hopitaux De Paris, France
Paul Gardner — University of Pittsburgh Medical Center, United States
Xiaohong Rose Yang — National Institutes of Health (NIH), United States
Cheng Yang — Shanghai Changzheng Hospital, China

Topic coordinators

Yazhuo Zhang — Capital Medical University, China
Jianru Xiao — Second Military Medical University, China

Citation

Bai, J., Froelich, S., Gardner, P., Yang, X. R., Yang, C., eds. (2023). *Chordoma: Advances in biology and clinical management*. Lausanne: Frontiers Media SA. doi: 10.3389/978-2-8325-2503-6

Table of contents

frontiers | Frontiers in Oncology

TYPE Editorial
PUBLISHED 05 May 2023
DOI 10.3389/fonc.2023.1175683

OPEN ACCESS

EDITED AND REVIEWED BY
David D. Eisenstat,
Royal Children's Hospital, Australia

*CORRESPONDENCE
Paul Gardner
gardpa@upmc.edu

RECEIVED 27 February 2023
ACCEPTED 17 April 2023
PUBLISHED 05 May 2023

CITATION
Gardner P, Bai J, Froelich S, Yang XR and Yang C (2023) Editorial: Chordoma: advances in biology and clinical management. *Front. Oncol.* 13:1175683. doi: 10.3389/fonc.2023.1175683

Editorial: Chordoma: advances in biology and clinical management

Paul Gardner[1]*, Jiwei Bai[2], Sebastien Froelich[3], Xiaohong Rose Yang[4] and Cheng Yang[5]

[1]Department of Neurological Surgery, University of Pittsburgh Medical Center, Pittsburgh, PA, United States, [2]Department of Neurosurgery, Beijing Tiantan Hospital, Capital Medical University, Beijing, China, [3]Department of Neurological Surgery, Assistance Publique Hopitaux De Paris, Paris, France, [4]Division of Cancer Epidemiology and Genetics, National Cancer Institute, National Institutes of Health (NIH), Bethesda, MD, United States, [5]Department of Orthopedics, Shanghai General Hospital, Shanghai, China

KEYWORDS

chordoma, radiomics, biomarkers, tumor microenvironment, proton radiotherapy

Editorial on the Research Topic
Chordoma: advances in biology and clinical management

Perspective

Chordoma is a rare bony tumor, occurring across the neuraxis, most commonly in the sacrum or skull base. Generally considered to be a malignant tumor, new evidence has shown that it can have a wide range of clinical behavior (1). This range reflects the same kind of variable molecular underpinnings that impact prognosis of every tumor type, the study of which can help to unlock the drivers of oncogenesis with the hope of defining the key targets for treatment. Current advances in chordoma treatment have arisen from the development of new surgical techniques, application of logical immuno- and chemotherapy trials, refinement of high-dose radiation techniques and individual targeted therapies.

Much of the initial work and motivation which initiated the scientific creativity and surprisingly rapid progress in the understanding of chordoma came from the efforts of the Chordoma Foundation (2). An international patient and scientific community, this foundation has brought together and supported a network of physicians and researchers in an institutionally agnostic setting, encouraging rapid and free sharing of results, even before publication. This has allowed a large number of clinicians and researchers to learn rapidly from each other and drive understanding and progress in a logical and cohesive fashion.

Tumor research in neurosurgery has largely focused on glioblastoma (GBM). However, given the complexity and rapid transformation of this disease, these efforts have gone largely unrewarded with respect to impactful treatments. However, applying the same rigorous study and techniques to other tumors such as meningioma and chordoma have, at a minimum, led to a dramatic improvement in understanding of the genetic range that drives behavior and prognosis despite similar histology. This understanding is the first step in personalized treatment for patients and begins to unlock the changes within these tumors which may provide new and effective treatment options. It is likely that applying similar efforts to chordoma, as have been applied to GBM, will yield far greater success as it

has in head and neck surgery. It is with this hope that this Research Topic was assembled with each article providing a small step along this path. Covering topics from radiomics to circulating DNA and new drug targets, this article collection will hopefully serve as part of the foundation upon which future successful chordoma research efforts will be built.

Article summary

The articles cover every aspect of chordoma, from predicting prognosis to treatment options to molecular analysis and personalized medicine. For the first time, radiomics have been applied to chordoma. The article by Zhai et al. shows that radiomics can be used to correlate chordoma prognostic categories. This would potentially allow preoperative prediction of behavior to allow tailored surgery. It could also be useful in settings where advanced molecular techniques are not available or when the tumor sample is too small to fully classify the tumor. Adding to that, further work on prognostic biomarkers in a systematic review by Rubino et al. help identify which biomarkers may provide the best surrogate for prognosis. Furthermore, Xiong et al. describe PALB2 (Partner and Localizer of BRCA2) as a novel prognostic factor, solidifying the concept of grades of chordoma and allowing for refinement of future radiomics. New work revealing the potential role of the tumor microenvironment (TME) in chordoma progression identified a correlation between systemic inflammatory score and adverse outcome (Li et al.). On the opposite end of the spectrum, Lopez et al. evaluated the immune microenvironment using immunofluorescence techniques and revealed spatial immune composition in chordoma TME. As with any tumor, understanding potential immunotherapies could go a long way toward controlling disease.

This Research Topic also evaluates treatment options, from a comprehensive review of new options to a systematic review of proton radiotherapy for chordoma and chondrosarcoma, to a study on the role of Gamma Knife Radiosurgery. Seeking to ease the impact of surgery, Fu et al. looked at factors associated with postoperative airway retention in skull base chordoma. Research hotspots are evaluated using bibliometric criteria and other articles present novel concepts for treatment or monitoring and diagnosing disease. Passeri et al. show their work using xenograft models for preclinical testing of therapeutic options. Freed et al. evaluate drug repurposing *via* target discovery and Zhao et al. review techniques for developing new therapeutics. Finally, circulating DNA in chordoma shows significant promise to allow detection of recurrence or even confirmation of diagnosis at initial presentation without biopsy.

As editors of this Research Topic, we hope that it will demonstrate the progress made in the understanding and treatment of this rare tumor. We have all seen the devastation chordoma can cause once uncontrolled; many of us have dealt with the morbidity of our current treatment strategies. Over time, this creates a strong desire for better treatment, to improve our patients' lives and clarify the role of our treatments in order to limit their impact. This desire underlies all of the work presented herein and hopefully helps to slowly achieve these mutually inclusive goals.

Author contributions

PG made substantial contributions to the design of the work and drafted and revised it critically for important intellectual content. JB, SF, XRY and CY provided approval for publication of the content. PG agrees to be accountable for all aspects of the work in ensuring that questions related to the accuracy or integrity of any part of the work are appropriately investigated and resolved.

Conflict of interest

The authors declare that the research was conducted in the absence of any commercial or financial relationships that could be construed as a potential conflict of interest.

Publisher's note

References

1. Zenonos GA, Fernandez-Miranda JC, Mukherjee D, Chang YF, Panayidou K, Snyderman CH, et al. Prospective validation of a molecular prognostication panel for clival chordoma. *J Neurosurg* (2019) 130(5):1528–37. doi: 10.3171/2018.3.JNS172321

2. Available at: https://www.chordomafoundation.org.

frontiers | Frontiers in Oncology

TYPE Original Research
PUBLISHED 08 September 2022
DOI 10.3389/fonc.2022.996892

OPEN ACCESS

EDITED BY
Haotian Zhao,
New York Institute of Technology,
United States

REVIEWED BY
Yongyu Yang,
Southern Medical University, China
Zujian Xiong,
Central South University, China

*CORRESPONDENCE
Yazhuo Zhang
zhangyazhuo@ccmu.edu.cn

SPECIALTY SECTION
This article was submitted to Neuro-Oncology and Neurosurgical Oncology, a section of the journal Frontiers in Oncology

RECEIVED 18 July 2022
ACCEPTED 15 August 2022
PUBLISHED 08 September 2022

CITATION
Xiong Y, Li M, Shen Y, Ma T, Bai J and Zhang Y (2022) PALB2 as a factor to predict the prognosis of patients with skull base chordoma. *Front. Oncol.* 12:996892. doi: 10.3389/fonc.2022.996892

PALB2 as a factor to predict the prognosis of patients with skull base chordoma

Yujia Xiong[1], Mingxuan Li[1], Yutao Shen[1], Tianshun Ma[1], Jiwei Bai[2] and Yazhuo Zhang[1,2,3,4]*

[1]Beijing Neurosurgical Institute, Capital Medical University, Beijing, China, [2]Department of Neurosurgery, Beijing Tiantan Hospital, Capital Medical University, Beijing, China, [3]Beijing Institute for Brain Disorders Brain Tumor Center, Beijing, China, [4]China National Clinical Research Center for Neurological Diseases, Beijing, China

Objective: This study aimed to study the role of PALB2 on the prognosis of skull base chordoma patients and the proliferation, migration, and invasion of chordoma cells.

Methods: 187 patients with primary skull base chordoma were involved in the study. Immunohistochemical analysis was used to measure the PALB2 protein expression. Kaplan-Meier analysis, univariate and multivariate Cox analysis were used to evaluate the impact of PALB2 on patient prognosis. A nomogram was established for predicting the progression free survival of chordoma patients. Cell counting kit-8, colony formation, transwell migration, and invasion assays were used to assess the proliferation, migration, and invasion of chordoma cells with PALB2 knockdown. TIMER 2.0 was used to explore the expression and prognostic role of PALB2 in cancers.

Results: High PALB2 expression indicated an adverse prognosis in chordoma. A nomogram involved PALB2, degree of resection, pathology, and Al-mefty classification could accurately predict the progression free survival of chordoma patients. The proliferation, migration, and invasion of chordoma cells significantly decreased after PALB2 knockdown. Additionally, PALB2 showed high expression in various cancers and was associated with a poor prognosis.

Conclusion: In summary, our results reveal that high PALB2 expression indicates a poor prognosis of chordoma patients and promotes the malignant phenotypes of chordoma cells *in vitro*.

KEYWORDS

chordoma, PALB2, prognosis, immunohistochemistry, nomogram

Introduction

Chordomas are rare bone tumors located in the skull base and axial skeleton (1). The incidence of chordomas is approximately 5/1000,000 (2). So far, surgical resection combined with radiotherapy is still the preferred treatment for chordomas (3). There is no approved drug for the treatment of chordomas (4). Chordomas are often adjacent to important structures, so it is difficult to remove tumors completely, which makes chordomas prone to recurrent (5). It is important to identify effective prognostic markers and explore the underlying mechanism of chordoma.

Partner and Localizer of BRCA2(PALB2) is a protein-coding gene located in chromosome 16p12.2. Robust data demonstrates that PALB2 mainly participates in DNA homologous recombination repair by binding to BRCA2 (6, 7). Recent studies reveal that the pathogenic variants of PALB2 are associated with some cancers, such as breast, pancreatic, and ovarian cancers (8, 9). PALB2 mutations lead to increased susceptibility to these tumors. In addition, high PALB2 expression leads to a poor prognosis in advanced breast cancer (10). However, to date, the role of PALB2 in chordoma remains to be studied.

In our study, we investigated the potential prognostic role of PALB2 in skull base chordomas, and a nomogram was further constructed. Moreover, we explored the effect of PALB2 on chordoma cells using several cellular experiments *in vitro*. In addition, we analyzed the possible role of PALB2 in other tumors.

Methods

Patients

A total of 187 patients with primary skull base chordoma received surgical treatment in the Neurosurgery Department of Beijing Tiantan Hospital from January 2008 to December 2014 were included in the study. Patients were included according to the following criteria (1) the pathological diagnosis was chordoma (2), complete clinical information (3), the tumor was located at the skull base. Exclusion criteria (1) tumor was too few to build the tissue microarray (TMA) (2) patients had other malignant tumors (3) patients were lost to follow up.

Clinical information

Tumor volume was estimated based on preoperative and intraoperative findings (length × width × height/2). We divided chordomas into tree types using AL-Mefty classification (11). Type I: the tumor was confined to a single anatomic space at the skull base. Type II: the tumor invaded 2 or even more anatomic spaces at the skull base, but the tumor could be completely removed *via* one surgical approach. Type III: the tumor extensively invaded multiple anatomic spaces, and the tumor couldn't be completely removed through one surgical approach. Preoperative and postoperative imaging were compared to estimate the extent of surgical resection (12). Total resection (TR): postoperative imaging showed no residual tumor; subtotal resection (STR): residual tumor ≤5%; and partial resection (PR): postoperative imaging showed residual tumor >5%. Rich blood supply: tumor resection surface bled easily and was difficult to aspirate clearly; poor blood supply: tumor resection surface bled less and was easy to aspirate clearly.

Immunohistochemistry

Chordoma tissues from the 187 chordoma patients were fixed with formalin and embedded in paraffin for following TMA construction. After assayed by TMA using the Tissue Array MiniCore (ALPHELYS, Plaisir), the most representative parts of the tissue were selected to build the TMA. Then TMAs were cut into 4μm thick sections for further staining with Leica RM 2135 Rotary Microtome (Rankin, Wetzlar, Germany). Leica BOND III automated system was used to perform Immunohistochemical staining with primary antibody (anti-PALB2 antibody, ab-202970, abcam, 1:500) and Bond Polymer Refine Detection (Leica Biosystems, DS9800) including secondary antibody. Leica Aperio AT2 scanner was used to scan TMA images at 400× magnification. Three pathologists examined the slides independently. Then, we analyzed the images by Leica Aperio ImageScope software (version 12.3). The H-score was used to evaluate staining intensity. H-Score (12) = 1 × (percent of light staining cells) + 2 × (percent of moderate staining cells) + 3 × (percent of strong staining cells).

Cell culture, cell counting kit-8, cell migration and invasion, colony formation assays

MUG-Chor1 and UM-Chor1 chordoma cell lines, donated by the Chordoma Foundation (for MUG-Chor1) and purchased from ATCC (for UM-Chor1), were cultured in IMDM (Isocove's modified Dulbecco's medium)/1640-RPMI (4:1) with 10% fetal bovine serum in an incubator at 37°C and 5% CO_2.

The small interfering RNAs (siRNAs) (siPALB2-1: GCAGTG AACTTACTACTCA, siPALB2-2: GGACCTTATTGTTCTAC CA, siPALB2-3: GAACTCACCTACAATAACT), purchased from RiboBio Medical Biotechnology (Guangzhou, China), were used to silence PALB2 in chordoma cell lines with lipofectamine 3000 (Invitrogen). After seeding UM-Chor1 cells and MUG-Chor1 cells into plates, PALB2 siRNA (si-PALB2) or control siRNA (si-NC) was transfected to the cells (concentration: 50nM).

After culturing chordoma cells in the 96-well plate (MUG-Chor1:6×10^3) cells/well, UM-Chor1: 2.5×10^3 cells/well) for 24 hours, chordoma cells were treated with si-PALB2 or si-NC. The optical density (OD) values at 450 nm were measured at 24, 48, 72, 96 hours, respectively after 2 hours incubation of CCK-8 (Dojindo).

For migration and invasion assays, 1×10^5 MUG-Chor1 cells and 2.5×10^4 UM-Chor1 cells transfected with si-PALB2 or si-NC were added into the transwell chamber with (invasion) or without (migration) Matrigel. After 48 hours, the cells on the surface were fixed, then stained with 0.1% crystal violet.

For colony formation assay, 2×10^3 chordoma cells transfected with si-PALB2 or si-NC were incubated into 6-well plates and cultured at 37°C for 2 weeks. Cell colonies were fixed and stained with 0.1% crystal violet.

Western blot and quantitative reverse transcription polymerase chain reaction

After transfection for 2 days, chordoma cells were collected for proteins and RNA extraction. For western blot, we used 10% sodium dodecyl sulfate-polyacrylamide gel electrophoresis to separated protein samples (20 μg). Then, protein blots were transferred to polyvinylidene difluoride membranes. The bands were incubated overnight with anti-PALB2 (ab202970) and anti-GAPDH or anti-β-actin (ZSGB-BIO) antibodies at 4°C, followed by secondary antibodies. Chemiluminescence was performed by Amersham Imager 600 for blot visualization.

After RNA extraction, the SuperScript III First-Strand Synthesis System (Invitrogen) was used to synthesize cDNA. QRT-PCR was performed using the QuantStudio 5 (Applied Biosystems). The expression of PALB2 was normalized according to GAPDH. The primers were as follows: GAPDH: 5'-GGAGCGAGATCCCTCCAAAAT-3' (Forward) and 5'-GG CTGTTGTCATACTTCTCATGG-3' (Reverse), PALB2: 5'-AGGGAATACAGCAAGACACTAG-3' (Forward) and 5'-GATCCTGCTGAGACAAACAATC-3' (Reverse).

Pan-cancer analysis

TIMER 2.0 was used to analyze the difference in PALB2 expression between normal tissue and tumor tissue in 33 types of cancer. The Kaplan-Meier analysis was used to explore the impact of PALB2 on the prognosis of liver hepatocellular carcinoma (LIHC) and lower-grade glioma (LGG) patients *via* the GEPIA website. Chordoma RNA sequencing datasets were obtained from dbGaP phs002301.v1.p1. LIMMA R package was used to select genes associated with PALB2. The clusterProfiler R package and enrichplot R package were applied to perform the KEGG enrichment analysis.

Statistical analysis

Statistical analysis was performed using R software (version 3.6.3) and SPSS (version 22.0, IBM Corp). The relationship between PALB2 and clinical characters was analyzed using Wilcoxon Mann–Whitney test, $\chi 2$ test, and 2 independent samples t-test. Survival R package and survminer R package were used to perform Kaplan-Meier analysis, Proportional Hazard assumption, univariate and multivariate Cox analysis. The nomogram and calibration curve were drawn using R software with rm, Hmisc, lattice, survival, ormula, and ggplot2 packages. And survivalROC package was used to draw the ROC curve. P value <0.05 indicated statistical significance.

Results

Associations between PALB2 and clinical characters in chordoma

187 primary skull base chordoma patients were involved in this study (Table 1; Supplementary Table 1). Those patients were separated into 2 groups by the median of the H-score of PALB2 (101.0). In addition, we analyzed the correlations between PALB2 and clinical characteristics. There was no significant difference in the distribution of males and females in the two groups (P=0.83). The mean age of patients was 39 years (range 3-78 years) in the high PALB2 group and 41 years (range 8-76 years) in the other group (P=0.45). The course of the disease ranged from 1 month to 84 months (mean 13 months) in the high group and 1 month to 360 months (mean 27 months) in the low group (P=0.06). The mean tumor volume in the high group was 34.7 cm^3 (range 1.7-258.0 cm^3), while in the low group, the mean tumor volume was 28.7 cm^3 (range 2.5-152.0cm^3) (P=0.19). Interestingly, we found that there were more conventional chordomas in the high PALB2 group (P=0.02). The distribution of Al-Mefty classification in the two groups showed no difference (P=0.46). Moreover, there was no remarkable difference in the proportion of patients who underwent endoscopy or craniotomy between the two groups (P=0.14). 59/94 patients received TR/STR in the high PALB2 group and 66/93 patients in the low PALB2 group (P=0.28). For blood supply, the tumor blood supply was rich in 109 patients and poor in 78 patients, no significant difference was observed between the two groups (P=0.51). By the end of follow-up, 129 patients suffered tumor recurrence and 72 patients died.

High levels of PALB2 indicated an adverse prognosis

The expression of PALB2 in 187 human chordoma tissues was analyzed by immunohistochemical staining, and we found that PALB2 was variedly expressed between chordoma patients,

10.3389/fonc.2022.996892

TABLE 1 Patient characteristics.

Characteristic	Total	PALB2 expression		P value
		High	Low	
Gender				0.83
Male	98	50	48	
Female	89	44	45	
Age, mean (range), year	40 (3-78)	39 (3-78)	41 (8-76)	0.45
Course of disease, mean (range), month	20 (1-360)	13 (1-84)	27 (1-360)	0.06
Tumor volume in cm^3, mean (range)	31.7 (1.7-258.0)	34.7 (1.7-258.0)	28.7 (2.5-152.0)	0.19
Pathology				0.02
Conventional	126	71	55	
Chondroid	61	23	38	
AL-mefty				0.46
Type I	34	15	19	
Type II	89	43	46	
Type III	64	36	28	
Surgical approach				0.14
Endoscopic transsphenoidal	79	45	34	
Craniotomy	108	49	59	
Extent of resection				0.28
Total resection/Subtotal resection	125	59	66	
Partial resection	62	35	27	
Blood supply				0.51
Poor	78	37	41	
Rich	109	57	52	

with the H-scores range from 1.74 to 177.5 (Figure 1). Then, we performed the Kaplan-Meier survival analysis between the low and high PALB2 expression groups, and our data suggested that the progression-free survival (PFS) times of patients with a high level of PALB2 were significantly shorter than those of patients with low PALB2 (Figure 2A). However, PALB2 has no significant effect on OS (p=0.124, Figure 2B). In addition, we found that the extent of resection, pathology, tumor volume, blood supply of tumor, and AL-Mefty level could impact both the OS and PFS of patients (Figure 2C–F; Supplementary Figure 1). The course of the disease was correlated with OS but not PFS (Supplementary Figure 1). Age, gender, and tumor calcification were not associated with prognosis (Table 2).

Univariate Cox(All the variables satisfy the PH assumption) revealed that high PALB2, partial resection, conventional

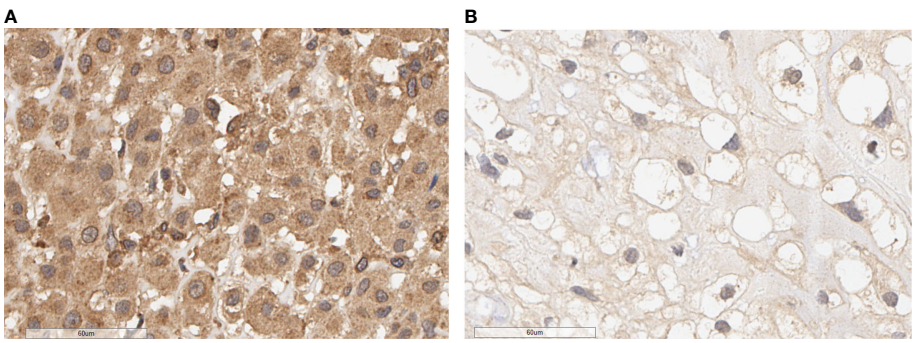

FIGURE 1
PALB2 immunohistochemical image of skull base chordoma (×400). **(A)** High expression of PALB2. **(B)** Low expression of PALB2.

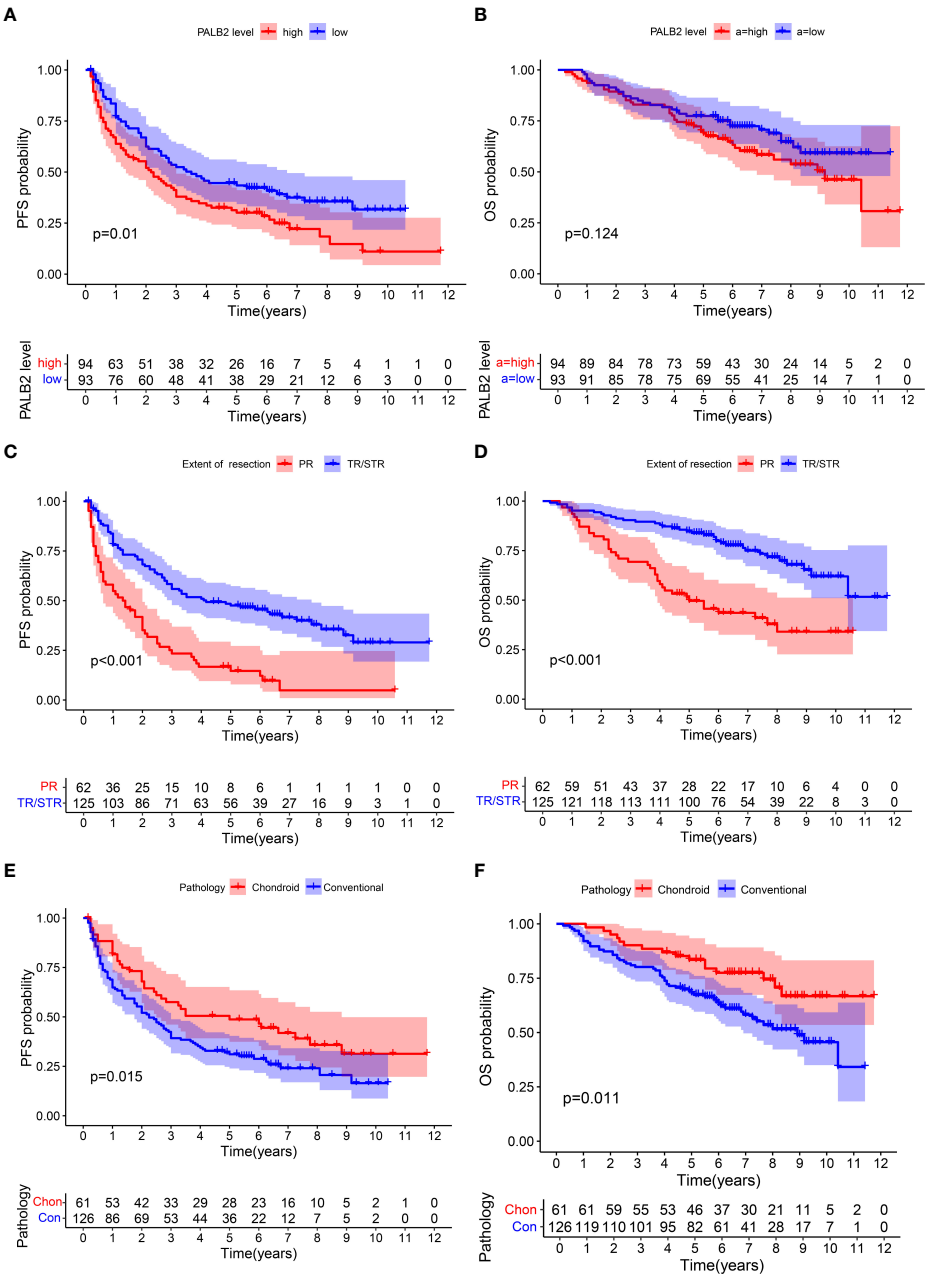

FIGURE 2
Kaplan–Meier survival curves of PFS and OS. PFS: **(A)** PALB2, **(C)** extent of resection, **(E)** pathology. OS: **(B)** PALB2, **(D)** extent of resection, **(F)** pathology.

chordoma, large tumor volume, the rich blood supply of the tumor, and high Al-mefty classification were risk factors for PFS (Figure 3A). And partial resection, conventional chordoma, the long course of the disease, large tumor volume, the rich blood supply, and high AL-mefty classification were risk factors for OS (Figure 3B). Moreover, multivariate Cox revealed that PALB2, the extent of resection, pathology, the course of the disease, and Al-mefty were independently associated with prognosis in skull base chordoma (Figures 3C, D).

A nomogram for individual PFS prediction in skull base chordoma

Based on the results of univariate Cox and multivariate Cox analysis, we selected PALB2, degree of resection, pathology, and AL-mefty classification to establish a nomogram model to predict the PFS of skull base chordoma patients (Figure 4A). The ROC curve revealed that the nomogram showed adequate performance in the 3-year (AUC=0.728) and 5-year

TABLE 2 Kaplan-Meier survival analysis of clinical characters.

Variables	P value	
	PFS	OS
PALB2	0.01	0.124
Extent of resection	<0.001	<0.001
pathology	0.015	0.011
tumor volume	0.002	0.044
blood supply	0.028	0.011
course of the disease	0.645	0.02
Age	0.485	0.708
gender	0.68	0.916
tumor calcification	0.687	0.332

(AUC=0.737) PFS prediction (Figure 4B). Moreover, patients were divided into two groups according to the median riskscore calculated by the nomogram. The PFS times of patients with high riskscore were shorter than those with low riskscore (Figure 4C). Then, bootstrap was used to select samples for verifying the accuracy of the nomogram model (62 samples/time, 1000 times). The calibration curve showed the model properly predicted 3-year PFS and 5-year PFS (Figures 4D, E).

Knockdown of PALB2 suppressed chordoma cells proliferation, migration, and invasion

The effect of PALB2 in chordoma cells was assessed in both UM-Chor1 and MUG-Chor1. We first confirmed reduced PALB2 expression after transfection of si-PALB2 using qRT-PCR and western blot (P<0.001, Figures 5A, B). CCK-8 was then used to measure cell viability. The proliferation of chordoma cells significantly reduced at 72 hours and 96 hours after si-PALB2 transfection compared to the si-NC group (Figure 5C). Colony formation experiments also showed that cells with PALB2 knockdown had fewer colonies (Figure 5D). The transwell assay revealed that the number of migrating and invading cells notably decreased after PALB2 knockdown (Figures 5E, F).

High PALB2 predicted poor prognosis in several cancers

To further explore the role of PALB2 in cancers, we performed a pan-cancer analysis of PALB2 in 33 types of cancers. Interestingly, the PALB2 expression level was higher in more than 10 types of cancers than that in the normal controls (Figure 6A). Moreover, we found that high expression of PALB2 indicated a poor prognosis in LIHC and LGG (Figures 6B, C). We then performed KEGG enrichment analysis and genes significantly correlated (cor>0.3, P<0.05) with PALB2 in LIHC and LGG were applied. The KEGG results showed PALB2 was associated with several cancer-associated pathways, including ubiquitin-mediated proteolysis, protein processing in the endoplasmic reticulum, autophagy, DNA replication, RNA transport, and cell cycle (Figures 6D, E). In addition, We perform KEGG enrichment analysis for genes significantly correlated (cor>0.3, P<0.05) with PALB2 in chordoma. Enrichment results showed that PALB2 may affect the Cell cycle and DNA replication in skull base chordoma, which is similar to LIHC and LGG. Interestingly, PALB2 may also

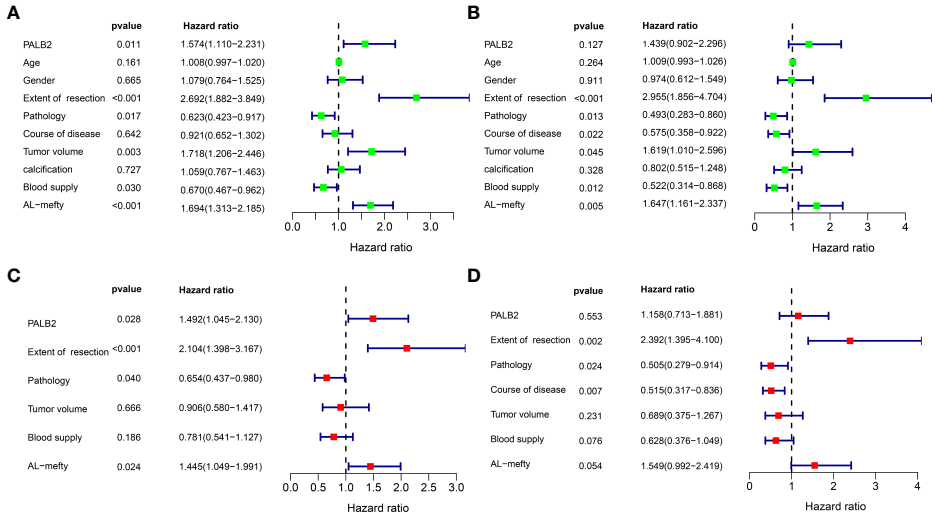

FIGURE 3
Univariate Cox and Multivariate Cox analysis of PFS and OS. **(A)** Univariate Cox analysis of PFS. **(B)** Univariate Cox analysis of OS. **(C)** Multivariate Cox analysis of PFS. **(D)** Multivariate Cox analysis of OS.

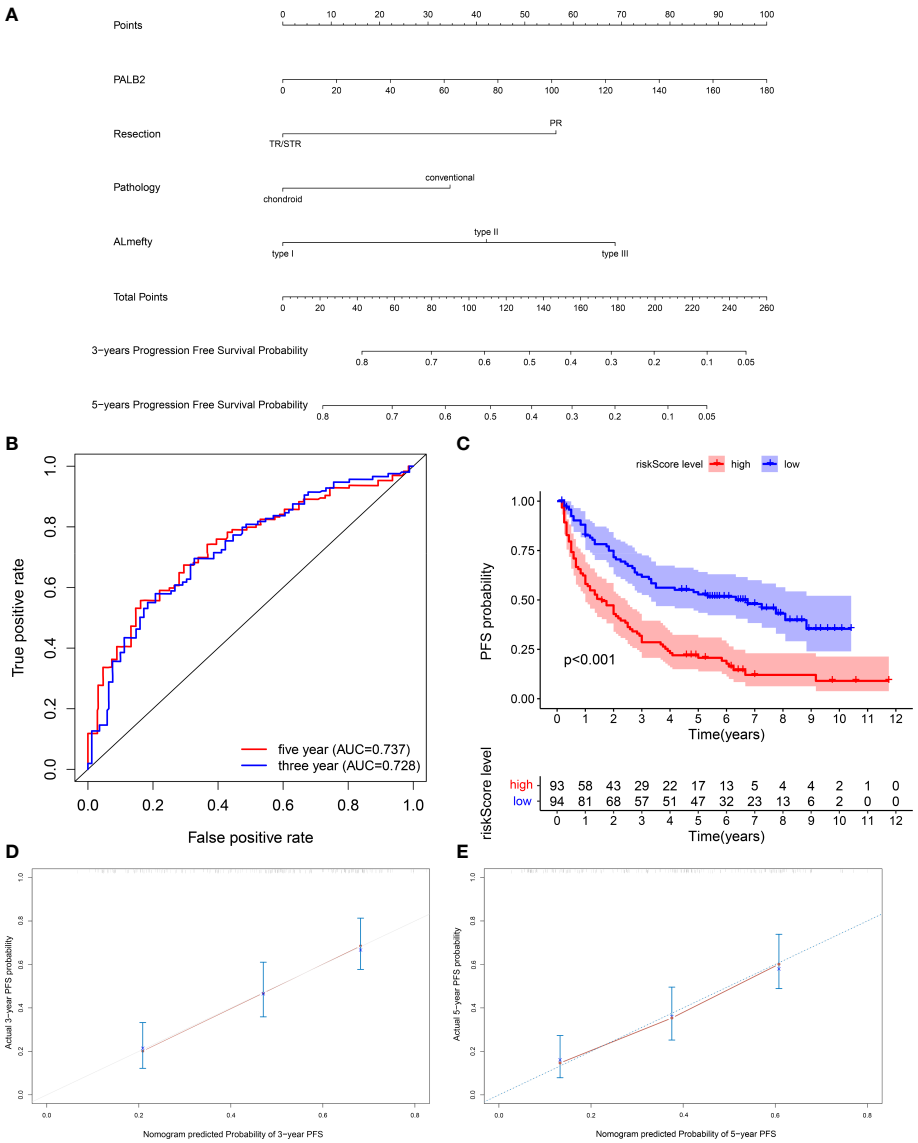

FIGURE 4
(A) Nomogram of 3-year and 5-year PFS in skull base chordoma patients. **(B)** ROC curves of the nomogram. **(C)** Kaplan–Meier survival curve of the patients separated by nomogram-predicted score. **(D)** Calibration curve of the nomogram prediction of 3-year PFS. **(E)** Calibration curve of the nomogram prediction of 5-year PFS.

affect many immune-related pathways, such as Th17 cell differentiation, the Chemokine signaling pathway, PD-L1 expression, PD-1 checkpoint pathway in cancer, and so on (Supplementary Figure 2).

Discussion

Chordoma is easy to relapse, with a 5-year recurrent rate of about 59.2% (13), leading to a poor prognosis of patients. Therefore, it is important to determine the factors affecting PFS in chordoma patients to better guide clinical treatment. AL-Mefty classification, the extent of resection, PDGFR-β, TGF-α, Ki-67, and SNF5 have been reported to affect the prognosis of chordoma patients (14–16). In addition, one previous study established a nomogram to predict the prognosis of chordoma patients according to the clinical characteristics and immunohistochemistry, including the extent of resection, E-cadherin, Ki-67, and VEGFA (12). However, the effect of PALB2 on the prognosis of chordomas has not been previously reported. Our study is the first to show that PALB2 expression is associated with chordoma recurrence, besides, we established a

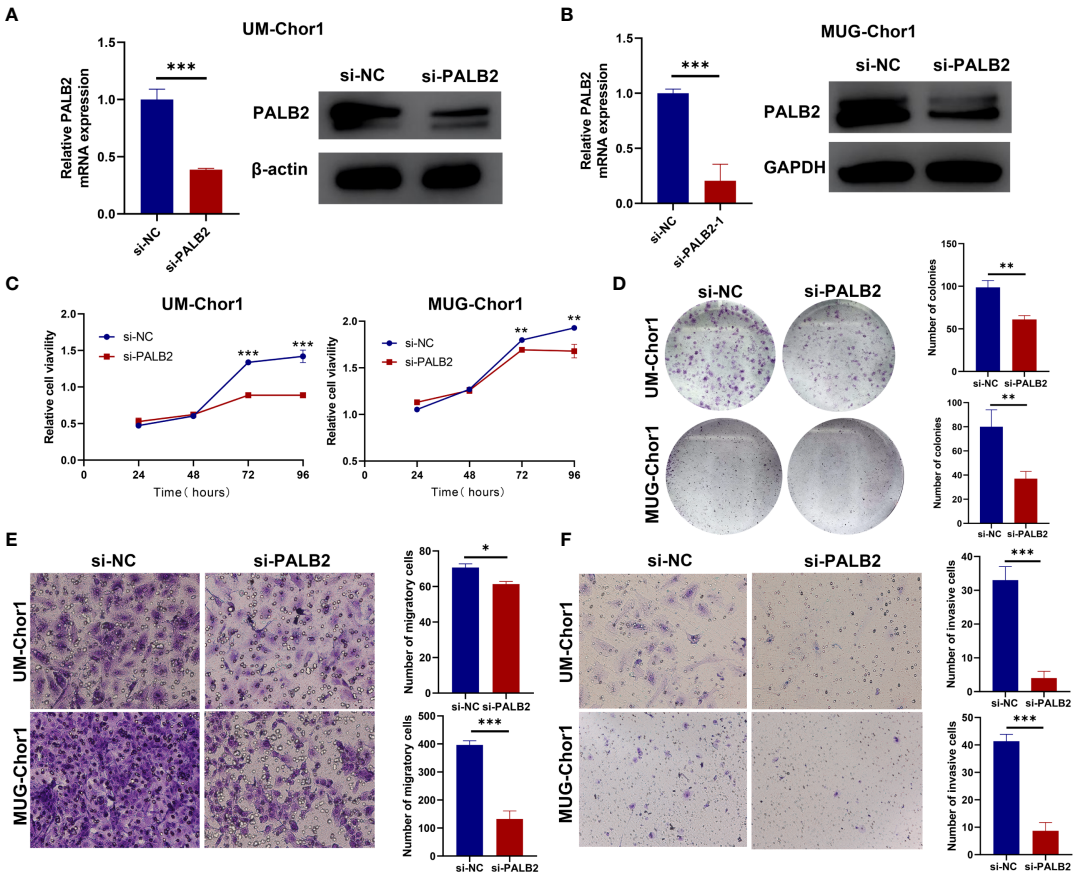

FIGURE 5
The function of PALB2 in chordoma cell lines. **(A)** QRT-PCR (left) and western blotting (right) analysis showed that the expression of PALB2 was decreased after being transfected with si-PALB2 in UM-Chor1. **(B)** QRT-PCR (left) and western blotting (right) analysis showed that the expression of PALB2 was decreased after transfected with si-PALB2 in MUG-Chor1. CCK8 assay **(C)** and Colony Formation Assays **(D)** indicated that the proliferation ability of chordoma cells (UM-Chor1 and MUG-Chor1) was decreased after being treated by si-PALB2. Transwell assay revealed that knockdown PALB2 inhibited the migration **(E)** and invasion **(F)** ability of UM-Chor1 and MUG-Chor1 chordoma cells. The results represent the mean ± s.d. of three independent experiments. Student's t test **(A–F)**. *p < 0.05, **p < 0.01, ***p < 0.001.

nomogram comprising PALB2 and clinical features for predicting the PFS of chordoma.

Our data confirmed that the extent of resection was significantly affecting the prognosis of patients, consistent with the previous studies (17). Moreover, we found that tumor pathology and Al-Mefty were correlated with PFS. Thus, in clinical management, for conventional chordoma patients with high PALB2 and high Al-Mefty classification, total resection and/or postoperative proton therapy, and close monitoring should be recommended to decrease the potential high recurrent rate. Intraoperative MRI and navigation may be helpful to achieve total resection (18).

Previous studies suggested that PALB2 served as a potential tumor suppressor gene, and its mutation led to increased susceptibility to breast cancer (19). However, our study found that high PALB2 expression patients had an adverse prognosis, and knockdown PALB2 inhibited the proliferation, migration, and invasion of chordoma cells. Previous studies of other tumors mainly focus on PALB2 mutations at the genome level rather than the expression of PALB2 (19, 20). However, few PALB2 mutations were found in large chordoma genome sequencing (21), suggesting that the role of PALB2 mutations reported in other tumors may not be applicable in chordomas. To further understand the effect of PALB2 expression on prognosis, we performed a pan-cancer analysis of the relationships between PALB mRNA level and prognosis in 33 tumor types. The results showed that PALB2 was highly expressed in various tumors and a high PALB2 level was associated with a poor prognosis, which supports our findings. In addition, KEGG enrichment analysis of PALB2-related genes revealed that PALB may promote tumor malignant phenotype *via* regulation of cell cycle, autophagy, and protein degradation.

The function of PALB2 in chordomas has not been reported. Our study is the first to propose high PALB2 indicates an

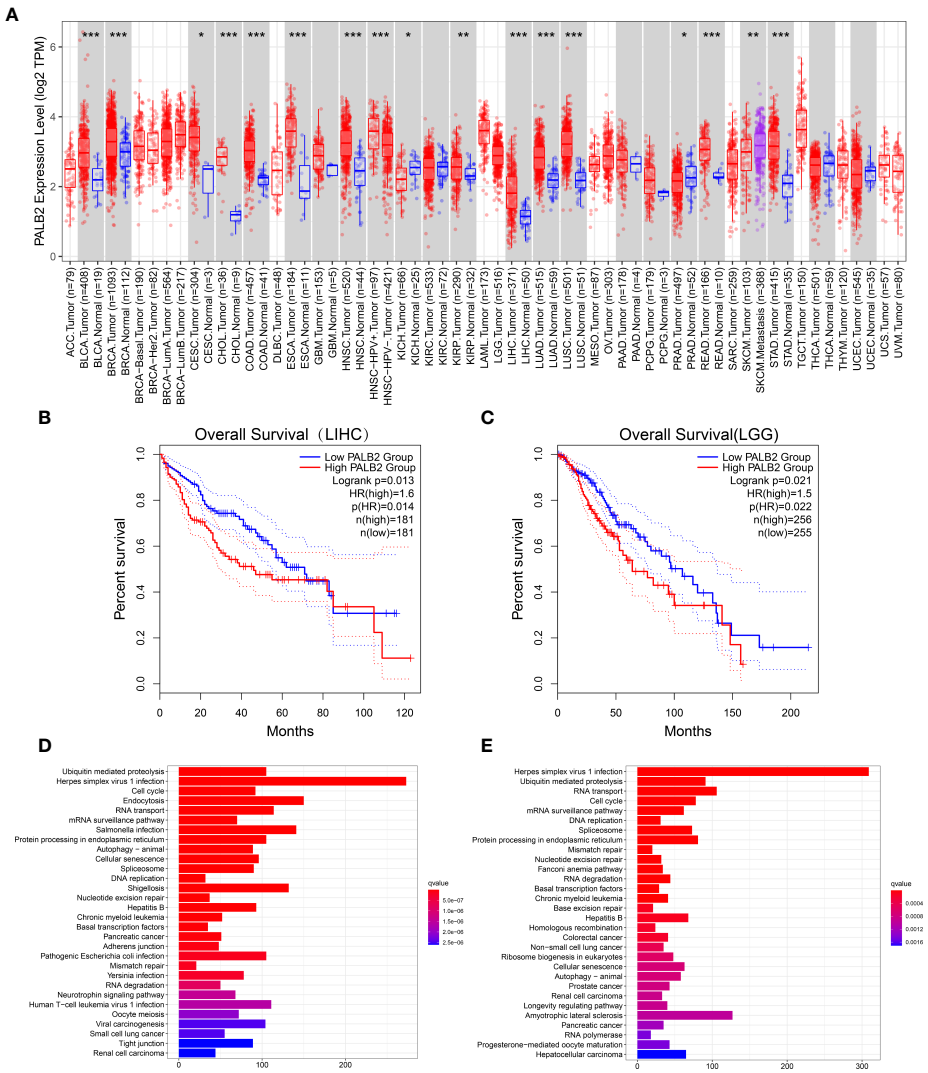

FIGURE 6
(A) Different PALB2 expression levels between tumor and normal tissue from TCGA. (adrenocortical carcinoma: ACC, bladder urothelial carcinoma: BLCA; breast invasive carcinoma: BRCA; cervical squamous cell carcinoma: CESC; cholangiocarcinoma: CHOL; colon adenocarcinoma: COAD; lymphoid neoplasm diffuse large B cell lymphoma: DLBC; esophageal carcinoma: ESCA; glioblastoma multiforme: GBM; brain lower grade glioma: LGG; head and neck squamous cell carcinoma: HNSC; kidney chromophobe: KICH; kidney renal clear cell carcinoma: KIRC; kidney renal papillary cell carcinoma: KIRP; acute myeloid leukemia: LAML; liver hepatocellular carcinoma: LIHC; lung adenocarcinoma: LUAD; lung squamous cell carcinoma: LUSC; mesothelioma: MESO; ovarian serous cystadenocarcinoma: OV; pancreatic adenocarcinoma: PAAD; pheochromocytoma and paraganglioma: PCPG; prostate adenocarcinoma: PRAD; rectum adenocarcinoma: READ; sarcoma: SARC; skin cutaneous melanoma: SKCM; stomach adenocarcinoma: STAD; testicular germ cell tumors: TGCT; thyroid carcinoma: THCA; thymoma: THYM; uterine corpus endometrial carcinoma: UCEC; uterine carcinosarcoma: UCS; and uveal melanoma: UVM). Kaplan–Meier survival curve showed that high PALB2 expression indicated a poor prognosis in LIHC **(B)** and LGG (**C**). KEGG pathways analysis of genes strongly associated with PALB2 in LIHC **(D)** and LGG **(E)**. *p < 0.05, **p < 0.01, ***p < 0.001.

adverse prognosis in chordoma. The mutation of PALB2 is mainly reported to influence DNA homologous recombination repair in other tumors, especially breast cancer (7). While few PALB2 mutations or copy number variation was found in whole-genome sequencing in chordoma (21). This suggested that PALB2 may function through different mechanisms in chordomas. According to previous reports, the homodimerization, phosphorylation, and ubiquitylation of different protein domains and modifications could regulate the PALB2 function (22, 23). Thus, the observed differences in PALB2 expression levels in chordoma might be due to the regulation of transcription and translation. As for the possible downstream mechanisms of PALB2 in chordomas, we hypothesize that PALB2 may influence cell cycle and

autophagy based on our analysis in other tumors. Interestingly, PALB2 was reported to restrict the homologous recombination in the S/G2 phase of cell cycle (24). We are currently verifying the above hypothesis and will explore the potential mechanism of PALB2 in chordoma using RNA sequencing.

Interestingly, one recent Phase III clinical trial of non-small cell lung cancer demonstrated that patients with high PALB2 expression were more sensitive to cisplatin - docetaxel chemotherapy (25), suggesting PALB2 as a promising biomarker for the identification of chemotherapy-sensitive patients. Given the high resistance of chordomas to chemotherapy, PALB2 may aid in identifying potential chemotherapy-sensitive chordomas, and further studies are highly needed.

In conclusion, our results reveal that high PALB2 expression indicates a poor prognosis of chordoma patients and promotes the malignant phenotype of chordoma cells *in vitro*.

Conclusion

In summary, our results reveal that high PALB2 expression indicates a poor prognosis of chordoma patients and promotes the malignant phenotypes of chordoma cells *in vitro*.

Data availability statement

The original contributions presented in the study are included in the article/Supplementary Material. Further inquiries can be directed to the corresponding author.

Ethics statement

The studies involving human participants were reviewed and approved by Ethics Committee of Beijing Tiantan Hospital. The patients/participants provided their written informed consent to participate in this study.

Author contributions

YX analyzed the data and carried out experiments. YX and ML wrote the main manuscript text. YS prepared Figures 1 and 2. TM and JB collected clinical information on patients. YZ designed and directed the entire study. All authors contributed to the article and approved the submitted version.

Funding

This research was funded by the National Natural Science Foundation of China (81771489).

Conflict of interest

The authors declare that the research was conducted in the absence of any commercial or financial relationships that could be construed as a potential conflict of interest.

Publisher's note

Supplementary material

The Supplementary Material for this article can be found online at: https://www.frontiersin.org/articles/10.3389/fonc.2022.996892/full#supplementary-material

References

1. Stacchiotti S, Gronchi A, Fossati P, Akiyama T, Alapetite C, Baumann M, et al. Best practices for the management of local-regional recurrent chordoma: a position paper by the chordoma global consensus group. *Ann Oncol* (2017) 28:1230–42. doi: 10.1093/annonc/mdx054

2. Zhou J, Sun J, Bai HX, Huang X, Zou Y, Tan X, et al. Prognostic factors in patients with spinal chordoma: An integrative analysis of 682 patients. *Neurosurgery* (2017) 81:812–23. doi: 10.1093/neuros/nyx081

3. Whelan JS, Davis LE. Osteosarcoma, chondrosarcoma, and chordoma. *J Clin Oncol Off J Am Soc Clin Oncol* (2018) 36:188–93. doi: 10.1200/jco.2017.75.1743

4. Sharifnia T, Wawer MJ, Chen T, Huang QY, Weir BA, Sizemore A, et al. Small-molecule targeting of brachyury transcription factor addiction in chordoma. *Nat Med* (2019) 25:292–300. doi: 10.1038/s41591-018-0312-3

5. van Wulfften Palthe ODR, Tromp I, Ferreira A, Fiore A, Bramer JAM, van Dijk NC, et al. Sacral chordoma: a clinical review of 101 cases with 30-year experience in a single institution. *Spine J Off J North Am Spine Soc* (2019) 19:869–79. doi: 10.1016/j.spinee.2018.11.002

6. Nepomuceno TC, Carvalho MA, Rodrigue A, Simard J, Masson JY, Monteiro ANA, et al. PALB2 variants: Protein domains and cancer susceptibility. *Trends Cancer* (2021) 7:188–97. doi: 10.1016/j.trecan.2020.10.002

7. Ducy M, Sesma-Sanz L, Guitton-Sert L, Lashgari A, Gao Y, Brahiti N, et al. The tumor suppressor PALB2: Inside out. *Trends Biochem Sci* (2019) 44:226–40. doi: 10.1016/j.tibs.2018.10.008

8. Yang X, Leslie G, Doroszuk A, Schneider S, Allen J, Decker B, et al. Cancer risks associated with germline PALB2 pathogenic variants: An international study of 524 families. *J Clin Oncol* (2020) 38:674–85. doi: 10.1200/jco.19.01907

9. Rantakari P, Nikkilä J, Jokela H, Ola R, Pylkäs K, Lagerbohm H, et al. Inactivation of Palb2 gene leads to mesoderm differentiation defect and early embryonic lethality in mice. *Hum Mol Genet* (2010) 19:3021–9. doi: 10.1093/hmg/ddq207

10. Li J, Li M, Chen P, Ba Q. High expression of PALB2 predicts poor prognosis in patients with advanced breast cancer. *FEBS Open Bio* (2018) 8:56–63. doi: 10.1002/2211-5463.12356

11. al-Mefty O, Borba LA. Skull base chordomas: a management challenge. *J Neurosurg* (1997) 86:182–9. doi: 10.3171/jns.1997.86.2.0182

12. Zhai Y, Bai J, Li M, Wang S, Li C, Wei X, et al. A nomogram to predict the progression-free survival of clival chordoma. *J Neurosurg* (2019), 1–9. doi: 10.3171/2019.10.JNS192414

13. Zou Y, Neale N, Sun J, Yang M, Bai HX, Tang L, et al. Prognostic factors in clival chordomas: An integrated analysis of 347 patients. *World Neurosurg* (2018) 118:e375–87. doi: 10.1016/j.wneu.2018.06.194

14. Li M, Zhai Y, Bai J, Wang S, Gao H, Li C, et al. SNF5 as a prognostic factor in skull base chordoma. *J Neurooncol* (2018) 137:139–46. doi: 10.1007/s11060-017-2706-3

15. Zhai Y, Bai J, Wang S, Gao H, Li M, Li C, et al. Analysis of clinical factors and PDGFR-beta in predicting prognosis of patients with clival chordoma. *J Neurosurg* (2018) 129:1429–37. doi: 10.3171/2017.6.JNS17562

16. Zhang S, Bai J, Li M, Zhai Y, Wang S, Liu Q, et al. Predictive value of transforming growth factor-alpha and ki-67 for the prognosis of skull base chordoma. *World Neurosurg* (2019) 129:e199–206. doi: 10.1016/j.wneu.2019.05.110

17. Lv GH, Zou MX, Liu FS, Zhang Y, Huang W, Ye A, et al. Clinicopathological and prognostic characteristics in extra-axial chordomas: An integrative analysis of 86 cases and comparison with axial chordomas. *Neurosurgery* (2019) 85:E527–e542. doi: 10.1093/neuros/nyz073

18. Konakondla S, Albers JA, Li X, Barber SM, Nakhla J, Houghton CE, et al. Maximizing sacral chordoma resection by precise 3-dimensional tumor modeling in the operating room using intraoperative computed tomography registration with preoperative magnetic resonance imaging fusion and intraoperative neuronavigation: A case series. *World Neurosurg* (2019) 125:e1125–31. doi: 10.1016/j.wneu.2019.01.257

19. Antoniou AC, Casadei S, Heikkinen T, Barrowdale D, Pylkäs K, Roberts J, et al. Breast-cancer risk in families with mutations in PALB2. *New Engl J Med* (2014) 371:497–506. doi: 10.1056/NEJMoa1400382

20. Velázquez C, Esteban-Cardeñosa EM, Lastra E, Abella LE, de la Cruz V, Lobatón CD, et al. A PALB2 truncating mutation: Implication in cancer prevention and therapy of hereditary breast and ovarian cancer. *Breast (Edinburgh Scotland)* (2019) 43:91–6. doi: 10.1016/j.breast.2018.11.010

21. Bai J, Shi J, Li C, Wang S, Zhang T, Hua X, et al. Whole genome sequencing of skull-base chordoma reveals genomic alterations associated with recurrence and chordoma-specific survival. *Nat Commun* (2021) 12:757. doi: 10.1038/s41467-021-21026-5

22. Ahlskog JK, Larsen BD, Achanta K, Sørensen CS. ATM/ATR-mediated phosphorylation of PALB2 promotes RAD51 function. *EMBO Rep* (2016) 17:671–81. doi: 10.15252/embr.201541455

23. Buisson R, Niraj J, Rodrigue A, Ho CK, Kreuzer J, Foo TK, et al. Coupling of homologous recombination and the checkpoint by ATR. *Mol Cell* (2017) 65:336–46. doi: 10.1016/j.molcel.2016.12.007

24. Orthwein A, Noordermeer SM, Wilson MD, Landry S, Enchev RI, Sherker A, et al. A mechanism for the suppression of homologous recombination in G1 cells. *Nature* (2015) 528:422–6. doi: 10.1038/nature16142

25. Karachaliou N, Bracht JWP, Fernandez Bruno M, Drozdowskyj A, Gimenez Capitan A, Moran T, et al. Association of PALB2 messenger RNA expression with platinum-docetaxel efficacy in advanced non-small cell lung cancer. *J Thorac Oncol* (2019) 14:304–10. doi: 10.1016/j.jtho.2018.10.168

frontiers | Frontiers in Neurology

TYPE Original Research
PUBLISHED 09 September 2022
DOI 10.3389/fneur.2022.992308

OPEN ACCESS

EDITED BY
Shaan M. Raza,
University of Texas MD Anderson Cancer Center, United States

REVIEWED BY
Ziya Levent Gokaslan,
Brown University, United States
Yongyu Yang,
Southern Medical University, China

*CORRESPONDENCE
Ruquan Han
ruquan.han@ccmu.edu.cn

†These authors have contributed equally to this work

SPECIALTY SECTION
This article was submitted to Neuro-Oncology and Neurosurgical Oncology, a section of the journal Frontiers in Neurology

RECEIVED 12 July 2022
ACCEPTED 23 August 2022
PUBLISHED 09 September 2022

CITATION
Fu Y, Yu Y, Cui Y, Wang J, Ma B, Jian M, Yao J, Jing L, Bai J and Han R (2022) Factors associated with artificial airway retention after skull base chordoma resection: A retrospective cohort study. *Front. Neurol.* 13:992308. doi: 10.3389/fneur.2022.992308

Factors associated with artificial airway retention after skull base chordoma resection: A retrospective cohort study

Yuxuan Fu[1†], Yun Yu[1†], Yidan Cui[1], Jing Wang[1], Bo Ma[1], Minyu Jian[1], Jingxin Yao[1], Longnian Jing[1], Jiwei Bai[2] and Ruquan Han[1*]

[1]Department of Anesthesiology, Beijing Tiantan Hospital, Capital Medical University, Beijing, China, [2]Department of Neurosurgery, Beijing Tiantan Hospital, Capital Medical University, Beijing, China

Background: Chordoma is a malignant bone and soft tissue tumor derived from embryonic notochord remnants, and skull base chordoma accounts for ~1/3 of all chordoma cases. Skull base chordoma is closely related to the brainstem and cranial nerves and has a high recurrence rate. The purpose of this study was to investigate the influence of the timing of tracheal extubation on perioperative pulmonary complications. We also aimed to explore predictors of postoperative artificial airway (AA) retention in patients with skull base chordoma.

Methods: This was a single-center, retrospective cohort study. The study population included all skull base chordoma patients undergoing surgical treatment between January 2019 and December 2021 at Beijing Tiantan Hospital. The primary outcome was the incidence of postoperative pulmonary complications. Several patient characteristics were evaluated for potential associations with AA retention.

Results: A total of 310 patients with skull base chordoma were enrolled. The frequency of AA retention after surgery for skull base chordoma was 30.97%. The incidence of postoperative pulmonary complications was much lower in those without AA retention (3.74 vs. 39.58%, $P < 0.001$). Factors with the highest point estimates for the odds of AA retention included body mass index, cranial nerve involvement, maximum tumor diameter, operative method, hemorrhage volume, operative duration and intraoperative mechanical ventilation duration.

Conclusions: In this retrospective cohort study, most of the factors associated with postoperative airway retention were closely related to the patient's tumor characteristics. These data demonstrate that respiratory management in patients with skull base chordoma remains an ongoing concern.

KEYWORDS

chordoma, artificial airway, postoperative pulmonary complications, anesthesiology, perioperative

Introduction

Chordoma is a rare malignant bone and soft tissue tumor derived from embryonic notochord remnants. The incidence of chordoma has been reported as 0.08 per 100,000, with skull base chordoma accounting for ∼1/3 of all chordoma cases (1, 2). Skull base chordoma is closely related to the brainstem and cranial nerves and has a high recurrence rate. The 5-year survival rate is only 60–70% (3). Chordoma is not sensitive to conventional low-dose radiation, and high-dose radiation may damage surrounding brain tissue and nerves (2, 4). Treatment of chordoma has been based on surgical resection and radiotherapy. A growing body of evidence to support the particles-ion radiotherapy is an effective treatment.

The growth rate of skull base chordoma tumors is slow, and the clinical manifestations are mainly mass effect and compression symptoms. Compression of cranial nerves by the tumor can result in preoperative neurological dysfunction, with clinical manifestations including dysphagia, choking on water, and decreased pharyngeal reflex. There are 9–12 pairs of posterior cranial nerves, including the glossopharyngeal nerve, vagus nerve, accessory nerve, and hypoglossal nerve. La Corte et al. conducted a retrospective study of 59 skull base chordoma patients and found that the preoperative clinical symptoms, tumor resection degree, surgeon's experience, and postoperative complications were significant factors affecting the prognosis (5). Additionally, long-term artificial airway (AA) retention may lead to pulmonary complications such as respiratory infection. However, in the case of damage to the posterior cranial nerves, early active extubation can lead to aspiration pneumonia due to the weakened protective airway reflex and increase the incidence of perioperative pulmonary complications. Therefore, choosing the appropriate endotracheal extubation time is particularly important. To date, there have been no studies on predictors of postoperative AA retention in patients with skull base chordoma.

This study aimed to explore predictors of postoperative AA retention in patients with skull base chordoma using retrospective observational data from Beijing Tiantan Hospital. We also aimed to investigate the influence of the timing of tracheal extubation on perioperative pulmonary complications.

Materials and methods

This was a single-center, retrospective cohort study conducted at Beijing Tiantan Hospital. The trial protocol was approved by the Clinical Research Ethics Committee of Beijing Tiantan Hospital (approval no. KY2021-112-02), and the requirement for informed consent was waived.

Participants

The study population included all skull base chordoma patients undergoing surgical treatment between January 2019 and December 2021 at Beijing Tiantan Hospital. Patients younger than 18 years of age and patients without anesthesia records were excluded.

Data collection and outcome assessment

All patients underwent standardized preoperative preparation according to our hospital. Anticoagulants and antiplatelet drugs were discontinued for a specified period of time and heparin bridging therapy was performed as needed. Baseline data included demographic characteristics, preoperative comorbidities, smoking and alcohol history, and laboratory test results. Intraoperative data included the types and doses of anesthetics/medications, vital signs, fluid balance and blood transfusions, intraoperative mechanical ventilation duration, and operative duration. In addition, unplanned secondary endotracheal intubation and unplanned secondary operations were recorded. The patients were divided into two groups according to whether the AA was retained postoperatively: patients with AA retention (AA group) and without AA retention (WOAA group). AAs included those present after oral endotracheal intubation, nasal endotracheal intubation, and tracheotomy. Tumor diameter was measured by a senior professional radiologist based on enhanced magnetic resonance imaging of the head.

The primary outcome was the incidence of postoperative pulmonary complications. The definition of perioperative pulmonary complications included respiratory infection, respiratory failure, pleural effusion, atelectasis, pneumothorax, bronchospasm, and aspiration pneumonia. The Clavien–Dindo classification was used to categorize pulmonary lesions. Complications of grade II or above were used to calculate the incidence rate (6). Secondary outcomes included the incidence of extrapulmonary complications, postoperative length of hospital stay, postoperative length of intensive care unit (ICU) stay, and rate of unplanned secondary endotracheal intubation. Postoperative extrapulmonary complications were defined as new events outside the respiratory system, including neurovascular complications (stroke, transient ischemic accident), cardiovascular complications (acute coronary syndrome, circulatory insufficiency, congestive heart failure, new-onset arrhythmia), thromboembolic complications (pulmonary embolism, deep venous thrombosis), gastrointestinal complications (gastrointestinal hemorrhage, acute pancreatitis, ileus), surgical complications (surgical-site infection, surgical bleeding), infectious complications (sepsis, septic shock), and liver and kidney complications (acute hepatic injury, acute kidney

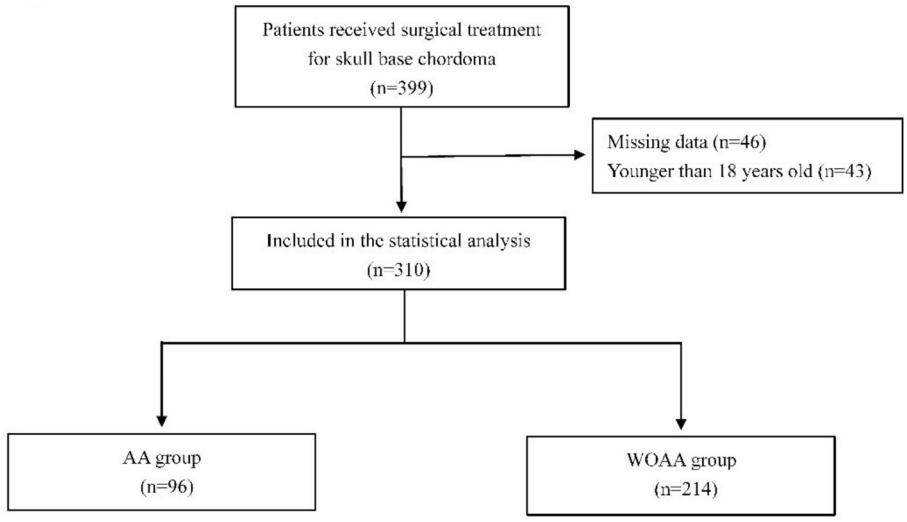

FIGURE 1
Patient flow chart.

injury) (6). The diagnosis of all postoperative complications was confirmed by two senior specialists. Surgical site infection is defined as infection related to an operative procedure, occurred at or near the surgical incision within 30 days of the procedure or cerebrospinal fluid tests confirm an intracranial infection (6). A poor prognosis was defined as death during hospitalization or Glasgow score of eight or less at discharge.

Statistical analysis

EmpowerStats software and R software (R version 4.2.0) were used for statistical analysis. The Kolmogorov–Smirnov test was applied for continuous variables with a normal distribution. Data conforming to a normal distribution are represented as the mean ± standard deviation (SD). Nonnormally distributed data are expressed as medians and interquartile ranges. The independent *T*-test or Mann–Whitney U test was performed according to the data distribution. Classification variables are expressed as a percentage and were analyzed using the chi-square test or Fisher's exact test. Based on the univariate logistic regression analysis, possible factors influencing postoperative pulmonary complications were found, and variables with a $P < 0.05$ were included in the multiple regression analysis. By logistic regression, odds ratios (ORs) and 95% confidence intervals (CIs) were calculated to evaluate the factors associated with postoperative AA retention. According to the multivariate analysis, continuous variables related to postoperative AA retention were selected to draw receiver operating characteristic (ROC) curves. $P < 0.05$ was considered statistically significant.

Results

From January 2019 to December 2021, 399 patients underwent surgical treatment for skull base chordoma at Beijing Tiantan Hospital. Among them, 43 patients were younger than 18 years, and anesthesia data were unavailable for 46 patients. Thus, a total of 310 patients were included in the statistical analysis (Figure 1).

Patient characteristics

The baseline characteristics of the patients in the two groups are shown in Table 1. There were no significant differences between the two groups in terms of smoking history, diabetes mellitus, hypertension, stroke history, heart disease, respiratory disease, recurrence, or maintenance of anesthesia. The operative duration, intraoperative mechanical ventilation duration, maximum tumor diameter, and hemorrhage volume were significantly greater in those with than those without AA retention. In addition, there were significant differences in age, body mass index (BMI), sex, posterior cranial nerve involvement, ASA physical status and the operative method between the two groups.

Postoperative outcomes

In this study, we found that the rate of AA retention after surgery for skull base chordoma was 30.97%; buccal endotracheal intubation was maintained in 55 patients, nasal

TABLE 1 Patient characteristics.

	Total	WOAA group	AA group	*P-value*
No. of cases	310	214 (69.03%)	96 (30.97%)	
Age (yr)	50.0 (37.0–59.0)	52.0 (39.8–60.0)	48.0 (34.0–56.0)	0.018
BMI (kg/m^2)	24.1 ± 3.7	24.6 ± 3.5	23.2 ± 4.0	0.002
Sex				<0.001
Male	186 (60.00%)	142 (66.36%)	44 (45.83%)	
Female	124 (40.00%)	72 (33.64%)	52 (54.17%)	
Smoking history	42 (13.55%)	31 (14.49%)	11 (11.46%)	0.471
Diabetes mellitus	12 (3.87%)	10 (4.67%)	2 (2.08%)	0.274
Hypertension	44 (14.19%)	35 (16.36%)	9 (9.38%)	0.103
Stroke	4 (1.29%)	3 (1.40%)	1 (1.04%)	0.795
Heart disease	9 (2.90%)	7 (3.27%)	2 (2.08%)	0.565
Respiratory disease	4 (1.29%)	4 (1.87%)	0 (0.00%)	0.178
Relapse	170 (54.84%)	115 (53.74%)	55 (57.29%)	0.561
Cranial nerve involvement	59 (19.03%)	17 (7.94%)	42 (43.75%)	<0.001
ASA physical status	310			0.008
I	18 (5.8%)	13 (6.1%)	5 (5.2%)	
II	255 (82.3%)	184 (86.0%)	71 (74.0%)	
III	35 (11.3%)	17 (7.9%)	18 (18.8%)	
IV	1 (0.3%)	0 (0%)	1 (1.0%)	
V	1 (0.3%)	0 (0%)	1 (1.0%)	
Operative method				<0.001
Endoscopy	230 (74.19%)	184 (85.98%)	46 (47.92%)	
Craniotomy	80 (25.81%)	30 (14.02%)	50 (52.08%)	
Maintenance of anesthesia				0.169
TIVA	18 (5.81%)	15 (7.01%)	3 (3.12%)	
Combined intravenous–inhalation anesthesia	279 (90.00%)	188 (87.85%)	91 (94.79%)	
Inhalation	13 (4.19%)	11 (5.14%)	2 (2.08%)	
Tranexamic acid	17 (5.48%)	10 (4.67%)	7 (7.29%)	0.349
Maximum tumor diameter (mm)	40.0 (32.0–50.0)	38.0 (30.0–48.5)	45.0 (37.0–58.0)	<0.001
Hemorrhage volume (ml)	400.00 (200.00–800.00)	300.00 (200.00–600.00)	600.00 (300.00–1000.00)	<0.001
Hemorrhage volume (ml/kg)	5.76 (3.33–11.67)	4.76 (2.87–8.60)	10.00 (4.98–17.94)	<0.001
Operative duration (min)	235.00 (160.00–340.00)	194.00 (140.00–255.00)	375.00 (300.00–466.25)	<0.001
Intraoperative mechanical ventilation duration (min)	287.50 (210.00–418.75)	250.00 (185.75–315.00)	447.50 (363.75–547.50)	<0.001

AA, with a retained artificial airway; BMI, body mass index; TIVA, total intravenous anesthesia; WOAA, without a retained artificial airway; ASA, American Society of Anesthesiologists.

endotracheal intubation in 22 patients, and tracheotomy in 19 patients.

The outcomes of the patients are shown in Table 2. In this study, 46 patients developed perioperative pulmonary complications, including 38 patients with AA retention and eight without AA retention. The incidence of postoperative pulmonary complications was much lower in those without AA retention (3.74 vs. 39.58%, $P < 0.001$). The incidence of postoperative extrapulmonary complications was 32.29 and 19.63% in those with and without AA retention, respectively ($P = 0.015$). Both the length of postoperative hospital stay and the length of ICU stay were extended in the AA group ($P < 0.001$). There were two patients (0.93%) with an unfavorable prognosis in the WOAA group and 23 patients (23.96%) in the AA group ($P < 0.001$).

There was no significant difference between the two groups in terms of unplanned secondary endotracheal intubation and unplanned secondary surgery. Six patients in the AA group underwent secondary endotracheal intubation; causes of secondary endotracheal intubation included dyspnea, poor cough reflex, and respiratory infection. Eleven patients in the WOAA group underwent secondary endotracheal intubation; reasons for endotracheal intubation included the need for a second operation, postoperative local cerebral edema, reflux aspiration, and pulmonary infection. Of the 17 patients who underwent secondary endotracheal intubation, one died, and

TABLE 2 Outcome variables, stratified by AA retention.

	Total	WOAA group	AA group	*P-value*
No. of cases	310	214	96	
Pulmonary complication	46 (14.84%)	8 (3.74%)	38 (39.58%)	<0.001
Respiratory infection	40 (12.90%)	7 (3.27%)	33 (34.38%)	<0.001
Extrapulmonary complications	73 (23.55%)	42 (19.63%)	31 (32.29%)	0.015
Unplanned secondaryendotracheal intubation	17 (5.48%)	11 (5.14%)	6 (6.25%)	0.691
Unplanned secondary operation	16 (5.16%)	9 (4.21%)	7 (7.29%)	0.256
Postoperative hospital stay (day)	8.00 (6.00–13.00)	7.00 (5.00–9.00)	12.00 (8.00–16.00)	<0.001
Postoperative ICU stay (day)	0.00 (0.00–1.00)	0.00 (0.00–1.00)	1.00 (1.00–4.25)	<0.001
Discharged				<0.001
Home	285 (91.94%)	212 (99.07%)	73 (76.04%)	
Rehabilitation hospital	21 (6.77%)	2 (0.93%)	19 (19.79%)	
Death	4 (1.29%)	0 (0.00%)	4 (4.17%)	
Poor prognosis	25 (8.06%)	2 (0.93%)	23 (23.96%)	<0.001

AA, with a retained artificial airway; ICU, intensive care unit; WOAA, without a retained artificial airway.

seven had a poor prognosis and required continued treatment in the rehabilitation hospital.

The artificial airway was retained for 20 h (15–219 h) after operation. The patients who retained the artificial airway after operation were divided into two groups: those who retained the artificial airway for < 24 h after operation were in the short-term group, and the others were in the long-term group. There were 50 people in the short-term group and 46 people in the long-term group. Short-term group of postoperative artificial airway retention time is 15.5 h (13.0–17.0 h), long-term group is 230.0 h (144.8–321.0 h).

Predictors associated with postoperative AA retention

Univariate analysis showed that women were more likely than men to require AA retention postoperatively (OR = 2.33, 95% CI: 1.43–3.81; $P = 0.0007$). Patients with cranial nerve involvement were also more likely to require AA retention postoperatively (OR = 9.01, 95% CI: 4.76–17.07; $P < 0.0001$). Compared with endoscopic surgery, patients who underwent craniotomy had a higher risk of postoperative AA retention (OR = 6.67, 95% CI: 3.82–11.63; $P < 0.0001$) (Table 3). In addition, the maximum tumor diameter, intraoperative hemorrhage volume, operative duration, and intraoperative mechanical ventilation duration were related to postoperative AA retention.

Two multifactor analysis models were established (Table 4). Model one was adjusted for sex and age, while model two was adjusted for sex, age, and smoking history. After adjusting for potential confounding factors, the multivariate analysis showed that BMI (OR = 0.91, 95% CI: 0.85–0.97; $P = 0.0077$), cranial nerve involvement (OR = 10.12, 95% CI: 5.11–20.05; $P < 0.0001$), maximum tumor diameter (OR = 1.05, 95% CI: 1.03–1.07; $P < 0.0001$), operative method (OR = 6.85, 95% CI: 3.84–12.21; $P < 0.0001$), hemorrhage volume (OR = 1.06, 95% CI: 1.03–1.09; $P < 0.0001$), operative duration (OR = 1.01, 95% CI: 1.01–1.02; $P < 0.0001$), and intraoperative mechanical ventilation duration (OR = 1.01, 95% CI: 1.01–1.02; $P < 0.0001$) were all associated with postoperative AA retention.

According to the multivariate analysis, continuous variables related to AA retention were selected for ROC curve analysis, and the results are shown in Figure 2. The area under the ROC curve (AUC) of the BMI was 0.61 (95% CI: 0.54–0.67). When the optimal threshold was 22.64, the specificity was 0.74, and the sensitivity was 0.49. The AUC of the maximum tumor diameter was 0.66 (95% CI: 0.59–0.73), with a specificity and sensitivity of 0.68 and 0.63, respectively, when the optimal threshold was 43.50 mm. The AUC of the operative duration was 0.85 (95% CI: 0.81–0.89), with a specificity and sensitivity of 0.83 and 0.83, respectively, when the optimal threshold was 282.50 min. The AUC of the intraoperative mechanical ventilation duration was 0.86 (95% CI: 0.82–0.91), with a specificity and sensitivity of 0.83 and 0.85, respectively, when the optimal threshold was 343.50 min. The AUC of the hemorrhage volume was 0.71 (95% CI: 0.64–0.77), when the optimal cutoff point was 8.63 ml/kg, with a specificity of 0.75 and sensitivity of 0.58.

Discussion

Chordoma is a rare malignant and aggressive tumor with a poor prognosis. Skull base chordomas are often more complex than other chordomas (7, 8). This study retrospectively analyzed the incidence of postoperative pulmonary complications in patients with skull base chordoma

TABLE 3 Univariate analysis for risk factors associated with retained artificial airways.

	Statistics	Retained artificial airways	*P*-value
Sex			0.0007
Male	186 (60.00%)	1.0	
Female	124 (40.00%)	2.33 (1.43, 3.81)	
Age (yr)	48.3 ± 13.7	0.98 (0.96, 1.00)	0.0155
Relapse	170 (54.84%)	1.15 (0.71, 1.88)	0.5612
Smoking history	42 (13.55%)	0.76 (0.37, 1.59)	0.4724
Cranial nerve involvement	59 (19.03%)	9.01 (4.76, 17.07)	<0.0001
BMI (kg/m^2)	24.1 ± 3.7	0.90 (0.84, 0.96)	0.0024
Maximum tumor diameter (mm)	42.22 ± 14.19	1.04 (1.02, 1.07)	<0.0001
Hemorrhage volume (ml)	400.0 (200.0–800.0)	1.00 (1.00, 1.00)	0.0001
Hemorrhage volume (ml/kg)	5.76 (3.33–11.67)	1.07 (1.04, 1.09)	<0.0001
Operative duration (min)	235.0 (160.0–340.0)	1.01 (1.01, 1.02)	<0.0001
Intraoperative mechanical ventilation duration (min)	287.50 (210.00–418.75)	1.01 (1.01, 1.02)	<0.0001
Maintenance of anesthesia			
TIVA	18 (5.81%)	1.0	
Combined intravenous–inhalation anesthesia	279 (90.00%)	2.42 (0.68, 8.57)	0.1707
Inhalation	13 (4.19%)	0.91 (0.13, 6.40)	0.9237
Operative method			
Endoscopy	230 (74.19%)	1.0	
Craniotomy	80 (25.81%)	6.67 (3.82, 11.63)	<0.0001

BMI, body mass index; TIVA, total intravenous anesthesia.

TABLE 4 Multifactorial regression for risk factors associated with retained artificial airways.

Exposure	Adjust I	*P*-value	Adjust II	*P*-value
Relapse	1.19 (0.72, 1.96)	0.5073	1.18 (0.71, 1.96)	0.5133
Cranial nerve involvement	9.58 (4.90, 18.73)	<0.0001	10.12 (5.11, 20.05)	<0.0001
Maximum tumor diameter (mm)	1.05 (1.02, 1.07)	<0.0001	1.05 (1.03, 1.07)	<0.0001
Operative method				
Endoscopy	1.0		1.0	
Craniotomy	6.85 (3.84, 12.23)	<0.0001	6.83 (3.83, 12.21)	<0.0001
Maintenance of anesthesia				
TIVA	1.0		1.0	
Combined intravenous–inhalation anesthesia	2.25 (0.62, 8.15)	0.2169	2.30 (0.63, 8.32)	0.2055
Inhalation	0.99 (0.14, 7.22)	0.9913	1.03 (0.14, 7.56)	0.9766
Hemorrhage volume (ml)	1.00 (1.00, 1.00)	0.0001	1.00 (1.00, 1.00)	0.0001
Hemorrhage volume (ml/kg)	1.06 (1.03, 1.09)	<0.0001	1.06 (1.03, 1.09)	<0.0001
Operative duration (min)	1.01 (1.01, 1.02)	<0.0001	1.01 (1.01, 1.02)	<0.0001
Intraoperative mechanical ventilation duration (min)	1.01 (1.01, 1.02)	<0.0001	1.01 (1.01, 1.02)	<0.0001
BMI (kg/m^2)	0.91 (0.85, 0.98)	0.0083	0.91 (0.85, 0.97)	0.0077

Adjust I model adjust for: sex; age.
Adjust II model adjust for: sex; age; smoke.
BMI, body mass index; TIVA, total intravenous anesthesia.

and explored the risk factors for postoperative AA retention. Among them, 30.97% of patients required postoperative AA retention, which was found to be associated with an increased frequency of pulmonary complications and a poor prognosis. The results of this study are consistent with those of studies of nonneurosurgical patients (9–12). Prolonged AA retention can lead to complications, including lung infection, glottis narrowing, and difficulty swallowing (13).

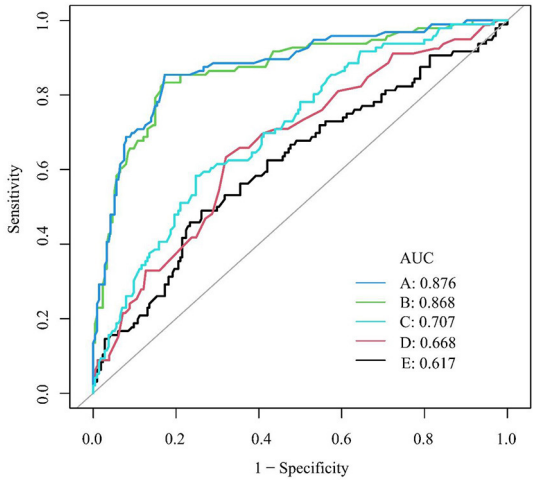

FIGURE 2
ROC curve for AA retention. **(A)** Duration of intraoperative mechanical ventilation (min); **(B)** operative duration (min); **(C)** hemorrhage volume (ml/kg); **(D)** maximum tumor diameter (mm); **(E)** BMI (kg/m^2). AUC, area under the ROC curve; BMI, body mass index; ROC, receiver operating characteristic.

Postoperative pulmonary complications are also associated with an increased mortality rate, length of hospital stay, and cost of hospitalization (14–19).

In neurosurgical patients, prolonged surgery, substantial hemorrhage, diabetes mellitus, chronic obstructive pulmonary disease, preoperative leukocytosis, ASA≥3 classification, and skull base occupation are risk factors for postoperative pneumonia (20). Additionally, symptoms of cranial nerve involvement, prolonged surgery, long-term mechanical ventilation, decreased postoperative consciousness, and skull base surgery increase the incidence of pulmonary complications in neurosurgical patients during the perioperative period (21, 22). Furthermore, postoperative blood transfusions, posterior cranial nerve compression, prolonged ICU stay, and tracheotomy are independent predictors of postoperative pulmonary complications in skull base surgery (20). Furthermore, postoperative pulmonary complications are significantly associated with a poorer prognosis, including higher rates of secondary surgery, readmission, mortality, and extended hospitalization, after craniocerebral tumor surgery (20).

Retained AAs and mechanical ventilation can provide direct access to the lungs for pathogens and reduce the immune barrier function of the mucosa, which may increase the risk of postoperative pulmonary complications (10). We identified several risk factors for perioperative AA retention, and the possibility of AA retention is considerable for patients with specific characteristics. Posterior cranial nerve involvement, craniotomy for chordoma resection, BMI > 22.64 kg/m^2, maximum tumor diameter > 43.5 mm, operative duration > 282.50 min, intraoperative mechanical ventilation duration > 343.50 min, and hemorrhage volume > 8.63 ml/kg were all independent risk factors for postoperative AA retention. Considering that most factors related to AA retention are tumor characteristics, few factors can be actively addressed. Therefore, clinical work may focus on reducing the incidence of pulmonary complications in high-risk patients who require AA retention. A meta-analysis of 178 randomized controlled studies found that exercise interventions and inspiratory muscle training reduced perioperative pulmonary complications in patients undergoing elective major surgery (23). Laurent et al. found that preoperative ventilator endurance training could improve respiratory muscle endurance and reduce the incidence of postoperative pulmonary complications (24).

More than 20% of complications in respiratory management occur during extubation, with severe consequences, including hypoxia and death (13). Although many guidelines focus on endotracheal intubation, there is limited literature on endotracheal extubation at the end of surgery. At the end of the surgery, endotracheal extubation or AA retention is necessary according to the patient's specific situation. In patients with skull base chordoma, cranial nerve involvement results in impaired cranial nerve function and poor protective airway reflexes. Therefore, caution is needed when considering whether to retain AAs. In addition, surgeons should minimize the operative duration and hemorrhage volume, and anesthetists should refine perioperative airway management methods. There are some limitations to this study. First, this was a single-center, retrospective study, and we could only determine the patient's condition through medical records. In addition, we could not collect intraoperative mechanical ventilation parameters, including the tidal volume, respiratory rate, airway pressure, and other data. Previous randomized controlled studies have found no significant difference in the incidence of pulmonary complications 7 days after surgery between adults patients ventilated with a low intraoperative tidal volume and those ventilated with a conventional tidal volume (25). There were significant differences in maximum tumor diameter, hemorrhage volume, operative duration, and intraoperative mechanical ventilation duration between the two groups. The above factors will affect the postoperative status of patients, making patients more sensitive to infection and other complications. It is difficult to draw a firm line between these factors as direct causes of poor prognosis or as reasons for the preservation of the artificial airway after surgery. However, the results of this study need to be validated by large prospective studies.

Conclusion

Postoperative AA retention in patients with skull base chordoma is associated with an increased incidence of pulmonary complications in the perioperative period. BMI, tumor compression of posterior cranial nerves, maximum tumor diameter, operative method, intraoperative hemorrhage volume, operative duration, and intraoperative mechanical ventilation duration are independent predictors of postoperative AA retention.

Data availability statement

The raw data supporting the conclusions of this article will be made available by the authors, without undue reservation.

Author contributions

All authors listed have made a substantial, direct, and intellectual contribution to the work and approved it for publication.

Funding

This study was supported by funding from Special Funding Support for Clinical Medicine Development (ZYLX201708 and DFL20180502) and the Beijing Municipal Science and Technology Commission (Z19110700660000).

Conflict of interest

The authors declare that the research was conducted in the absence of any commercial or financial relationships that could be construed as a potential conflict of interest.

Publisher's note

All claims expressed in this article are solely those of the authors and do not necessarily represent those of their affiliated organizations, or those of the publisher, the editors and the reviewers. Any product that may be evaluated in this article, or claim that may be made by its manufacturer, is not guaranteed or endorsed by the publisher.

References

1. Bai J, Li M, Shi J, Jing L, Zhai Y, Zhang S, et al. Mid-term follow-up surgical results in 284 cases of clival chordomas: the risk factors for outcome and tumor recurrence. *Neurosurg Rev.* (2022) 45:1451–62. doi: 10.1007/s10143-021-01576-4

2. Teng C, Yang Q, Xiong Z, Ye N, Li X. Multivariate analysis and validation of the prognostic factors for skull base chordoma. *Front Surg.* (2021) 8:764329. doi: 10.3389/fsurg.2021.764329

3. Snyderman CH, Gardner PA. Current opinion in otolaryngology and head and neck surgery: clival chordoma and its management. *Curr Opin Otolaryngol Head Neck Surg.* (2020) 28:118–21. doi: 10.1097/MOO.0000000000000614

4. Li M, Shen Y, Xiong Y, Wang S, Li C, Bai J, et al. Loss of SMARCB1 promotes autophagy and facilitates tumour progression in chordoma by transcriptionally activating ATG5. *Cell Prolif.* (2021) 54:e13136. doi: 10.1111/cpr.13136

5. La Corte E, Broggi M, Raggi A, Schiavolin S, Acerbi F, Danesi G, et al. Peri-operative prognostic factors for primary skull base chordomas: results from a single-center cohort. *Acta Neurochir.* (2021) 163:689–97. doi: 10.1007/s00701-020-04219-7

6. Yan T, Liang XQ, Wang GJ, Wang T, Li WO, Liu Y, et al. Prophylactic penehyclidine inhalation for prevention of postoperative pulmonary complications in high-risk patients: a double-blind randomized trial. *Anesthesiology.* (2022) 136:551–66. doi: 10.1097/ALN.0000000000004159

7. Tian K, Zhang H, Ma J, Wang K, Ru X, Du J, et al. Factors for overall survival in patients with skull base chordoma: a retrospective analysis of 225 patients. *World Neurosurg.* (2017) 97:39–48. doi: 10.1016/j.wneu.2016.09.055

8. Rock AK, Opalak CF, Workman KG, Broaddus WC. Safety outcomes following spine and cranial neurosurgery: evidence from the national surgical quality improvement program. *J Neurosurg Anesthesiol.* (2018) 30:328–36. doi: 10.1097/ANA.0000000000000474

9. Gal J, Hunter S, Reich D, Franz E, DeMaria S, Neifert S, et al. Delayed extubation in spine surgery is associated with increased postoperative complications and hospital episode-based resource utilization. *J Clin Anesth.* (2022) 77:110636. doi: 10.1016/j.jclinane.2021.110636

10. Xu Y, Zuo Y, Zhou L, Hao X, Xiao X, Ye M, et al. Extubation in the operating room results in fewer composite mechanical ventilation-related adverse outcomes in patients after liver transplantation: a retrospective cohort study. *BMC Anesthesiol.* (2021) 21:286. doi: 10.1186/s12871-021-01508-1

11. McCarthy C, Fletcher N. Early extubation in enhanced recovery from cardiac surgery. *Crit Care Clin.* (2020) 36:663–74. doi: 10.1016/j.ccc.2020.06.005

12. Harris KC, Holowachuk S, Pitfield S, Sanatani S, Froese N, Potts JE, et al. Should early extubation be the goal for children after congenital cardiac surgery? *J Thorac Cardiovasc Surg.* (2014) 148:2642–7. doi: 10.1016/j.jtcvs.2014.06.093

13. Anastasian ZH, Kim M, Heyer EJ, Wang S, Berman MF. Attending handoff is correlated with the decision to delay extubation after surgery. *Anesth Analg.* (2016) 122:758–64. doi: 10.1213/ANE.0000000000001069

14. Fernandez-Bustamante A, Frendl G, Sprung J, Kor DJ, Subramaniam B, Ruiz RM, et al. Postoperative pulmonary complications, early mortality, and hospital stay following noncardiothoracic surgery: a multicenter study by the perioperative research network investigators. *JAMA Surg.* (2017) 152:157–66. doi: 10.1001/jamasurg.2016.4065

15. Shander A, Fleisher LA, Barie PS, Bigatello LM, Sladen RN, Watson CB. Clinical and economic burden of postoperative pulmonary complications: patient safety summit on definition, risk-reducing interventions, and preventive strategies. *Crit Care Med.* (2011) 39:2163–72. doi: 10.1097/CCM.0b013e31821f0522

16. Marseu K, Slinger P. Peri-operative pulmonary dysfunction and protection. *Anaesthesia.* (2016) 71 Suppl 1:46–50. doi: 10.1111/anae.13311

17. Boden I, Skinner EH, Browning L, Reeve J, Anderson L, Hill C, et al. Preoperative physiotherapy for the prevention of respiratory complications after upper abdominal surgery: pragmatic, double blinded, multicentre randomised controlled trial. *BMJ.* (2018) 360:j5916. doi: 10.1136/bmj.j5916

18. Numata T, Nakayama K, Fujii S, Yumino Y, Saito N, Yoshida M, et al. Risk factors of postoperative pulmonary complications in patients with asthma and COPD. *BMC Pulm Med.* (2018) 18:4. doi: 10.1186/s12890-017-0570-8

19. Longo M, Agarwal V. Postoperative pulmonary complications following brain tumor resection: a national database analysis. *World Neurosurg.* (2019) 126:e1147–54. doi: 10.1016/j.wneu.2019.03.058

20. Zhao DW, Zhao FC, Zhang XY, Wei KY, Jiang YB, Liu D, et al. Association between postoperative hypoalbuminemia and postoperative pulmonary imaging abnormalities patients undergoing craniotomy for brain tumors: a retrospective cohort study. *Sci Rep.* (2022) 12:64. doi: 10.1038/s41598-021-00261-2

21. Zhang L, Xiong W, Peng Y, Zhang W, Han R. The effect of an intraoperative, lung-protective ventilation strategy in neurosurgical patients

undergoing craniotomy: study protocol for a randomized controlled trial. *Trials.* (2018) 19:85. doi: 10.1186/s13063-018-2447-4

22. Sogame LC, Vidotto MC, Jardim JR, Faresin SM. Incidence and risk factors for postoperative pulmonary complications in elective intracranial surgery. *J Neurosurg.* (2008) 109:222–7. doi: 10.3171/JNS/2008/109/8/0222

23. Perry R, Herbert G, Atkinson C, England C, Northstone K, Baos S, et al. Pre-admission interventions (prehabilitation) to improve outcome after major elective surgery: a systematic review and meta-analysis. *BMJ Open.* (2021) 11:e050806. doi: 10.1136/bmjopen-2021-050806

24. Laurent H, Aubreton S, Galvaing G, Pereira B, Merle P, Richard R, et al. Preoperative respiratory muscle endurance training improves ventilatory capacity and prevents pulmonary postoperative complications after lung surgery. *Eur J Phys Rehabil Med.* (2020) 56:73–81. doi: 10.23736/S1973-9087.19.05781-2

25. Karalapillai D, Weinberg L, Peyton P, Ellard L, Hu R, Pearce B, et al. Effect of intraoperative low tidal volume vs conventional tidal volume on postoperative pulmonary complications in patients undergoing major surgery: a randomized clinical trial. *JAMA.* (2020) 324:848–58. doi: 10.1001/jama.2020.12866

frontiers | Frontiers in Oncology

TYPE Original Research
PUBLISHED 16 September 2022
DOI 10.3389/fonc.2022.946597

OPEN ACCESS

EDITED BY
Jiwei Bai,
Beijing Tiantan Hospital, Capital Medical University, China

REVIEWED BY
Shuyu Hao,
Beijing Tiantan Hospital, Capital Medical University, China
Zhang Shuheng,
Anshan Central Hospital, China

*CORRESPONDENCE
Tong Meng
mengtong@medmail.com.cn
Dianwen Song
osongdianwen@126.com

†These authors have contributed equally to this work

SPECIALTY SECTION
This article was submitted to Neuro-Oncology and Neurosurgical Oncology, a section of the journal Frontiers in Oncology

RECEIVED 17 May 2022
ACCEPTED 29 August 2022
PUBLISHED 16 September 2022

CITATION
Gao J, Huang R, Yin H, Song D and Meng T (2022) Research hotspots and trends of chordoma: A bibliometric analysis.
Front. Oncol. 12:946597.
doi: 10.3389/fonc.2022.946597

Research hotspots and trends of chordoma: A bibliometric analysis

Jianxuan Gao[1,2†], Runzhi Huang[3†], Huabin Yin[1], Dianwen Song[1*] and Tong Meng[1,2*]

[1]Department of Spine Surgery, Shanghai General Hospital, School of Medicine, Shanghai Jiaotong University, Shanghai, China, [2]Tongji University Cancer Center, Shanghai Tenth People's Hospital, School of Medicine, Tongji University, Shanghai, China, [3]Department of Spine Surgery, Tongji Hospital, Tongji University School of Medicine, Tongji University, Shanghai, China

Background: Chordoma is a type of mesenchymal malignancy with a high recurrence rate and poor prognosis. Due to its rarity, the tumorigenic mechanism and optimal therapeutic strategy are not well known.

Methods: All relevant articles of chordoma research from 1 January 2000 to 26 April 2022 were obtained from Web of Science Core Collection database. Blibliometrix was used to acquire basic publication data. Visualization and data table of collaboration network, dynamic analysis, trend topics, thematic map, and factorial analysis were acquired using Blibliometrix package. VOSviewer was used to generate a visualization map of co-citation analysis and co-occurrence.

Results: A total of 2,285 articles related to chordoma were identified. The most influential and productive country/region was the United States, and Capital Medical University has published the most articles. Among all high-impact authors, Adrienne M. Flanagan had the highest average citation rate. Neurosurgery was the important periodical for chordoma research with the highest total/average citation rate. We focused on four hotspots in recent chordoma research. The research on surgical treatment and radiotherapy was relatively mature. The molecular signaling pathway, targeted therapy and immunotherapy for chordoma are not yet mature, which will be the future trends of chordoma research.

Conclusion: This study indicates that chordoma studies are increasing. Surgery and radiotherapy are well reported and always play fundamental roles in chordoma treatment. The molecular signaling pathway, targeted therapy, and immunotherapy of chordoma are the latest research hotspots.

KEYWORDS

chordoma, bibliometric analysis, hotspots, treatment, tumorigenesis

Introduction

Chordoma is a relatively rare malignancy characterized by local invasion (1). To reduce the risk of recurrence and improve the prognosis of patients, the en-bloc tumor resection with wide margins is recommended (2). Due to the notochord origination, chordoma is normally located in the axial skeleton, such as the skull base and sacrum (3). These specific anatomical structures compromise the application of en-bloc methods, leading to a high relapse rate (4, 5) . In addition, the chemo-/radiotherapy resistance features also challenge the management of chordoma (6). To improve the prognosis of chordoma patients, exploring the tumorigenic mechanisms and optimizing therapeutic strategies are pressing needs.

Pathologically, chordoma is derived from notochord remnants with the impacts of carcinogenic factors. Therefore, the identification of tumorigenic biomarkers may provide therapeutic targets for chordoma (7). Receptor tyrosine kinases (RTKs), which are crucial regulators of chordoma, can activate signaling cascades, leading to the dysfunction of various essential proteins. Thus, tyrosine kinase inhibitors (TKIs) are widely used in clinical practice for chordoma, such as imatinib, sunitinib, and apatinib (8, 9). Besides targeted therapies, novel techniques in adjuvant radiotherapies like proton and carbon ion therapy have been applied in chordoma with promising therapeutic effects (10, 11). Thus, recent progresses of basic and clinical research optimize chordoma treatment and improve patients' prognosis.

Due to the rarity of chordoma, studies focused on this malignancy are still limited. Given this limitation, it would be useful to summarize the current hotspots and future trends of chordoma research. Bibliometrics, a quantitative and qualitative analysis, can assist researchers in refining current research hotspots and future development trends by co-word and co-citation (12). Recently, bibliometrics and visualization have been used to analyze various fields of research, such as coronavirus disease 2019 (COVID-19) and breast cancer, whereas none focus on chordoma (13–15). In this study, we collected and collated the publications on chordoma in the twenty-first century from the Web of Science (Wos) database. By analyzing the current research hotspots and knowledge framework in chordoma field, we point out its research emphases and future trends.

Methods

Data sources and retrieval strategies

This study was approved by our Institutional Review Board (IRB). Data were obtained from the Wos Core Collection and analyzed by bibliometric analysis software. Publications were selected from SSCI and SCIE indexes, excluding other databases, such as Scopus. The retrieval strategy was as follows: subject words= chordoma or chordomas, literature type= article, language= English, date= 1 January 2000–26 April 2022. A total of 2,285 studies were retrieved. All records and references were downloaded in a TXT format, and all literature retrievals and data extractions were introduced into VOSviewer software (version 1.6.18) and R software version 4.1.0 using Bibliometrix R package (version 3.2.1) and Biblioshiny for further analysis.

Data and statistical analysis

Biblimetrix package is an open-source tool to analyze publications by qualitative and quantitative method (16). Biblimetrix package could convert and output simplify bibliographic information and complete data analysis and visualization, including annual scientific production, collaboration network, dynamic analysis, trend topics, thematic map, and factorial analysis. The institution impact or author impact was mainly determined by h-index, which was used to quantify the certain institutions and authors scientific influence by statistics of publication number and citation frequency (17).

Vosviewer was used to analyze bibliographic data on countries, institutions, authors, citations, and keywords and construct network maps of co-authorship, co-citation, and co-occurrence (18). In addition, VOSviewer could output three different visualization maps by setting thresholds: network visualization, overlay visualization, and density visualization.

Results

Annual publication analysis

A total of 2,285 articles were published in the chordoma field with a total citation frequency of 42,808 times (Table 1). The fitting curve of annual publication growth trend was $y \frac{102{,}808.8}{1+\left(\frac{x}{981.7}\right)^{-1.738}}$ +46.20=(R2= 0.9244), consistent with the current research trend of chordoma, so was the curve of annual cited frequency growth trend (Figure 1; Supplementary Figure S1). Since the twenty-first century, more scientific issues have been focused on chordoma. The research progress of chordoma has emerged endlessly, and the annual numbers of articles are also increasing year by year, indicating that chordoma is attracting more attention, and chordoma research has great clinical significance and development potential.

Most productive countries/regions and institutions

Since 2000, 68 countries/regions participated in chordoma research, of which the top 10 cumulative publication frequency

TABLE 1 Main information of publications.

Description	Results
Timespan	2000.01.01-2022.04.26
Sources (journals, books, etc)	594
Documents (articles)	2,285
Times Cited	42,808
References	31,268
Countries	68
Institutions	2,267
Funds	781
Authors	9,716
All Keywords	6,070
Author Keywords	3,691

was 1,880. Google Earth mapped the country/region distribution based on the number of publications (Figure 2A). Three countries published more than 1,000 articles, namely, the United States (N=703), China (N=306), and Japan (N=210) (Supplementary Table S1). Regarding the regional distribution of chordoma incidence rate, Asian/Pacific Islander (0.096; 95% CI 0.082–0.111) and White (0.093; 95%CI 0.093–0.096) individuals were relatively high, while American Indian/Alaskan Native (0.049; 95%CI 0.029–0.077) and Black (0.042; 95%CI 0.036–0.048) were correspondingly low (1). Thus, regional incidence distribution might be associated with country-related chordoma publications. Centrality is often used to evaluate the importance of nodes in the network. The United States had the highest centrality, indicating its prolificacy and influence in chordoma research. The United States paid the best attention to regional cooperation among countries, especially China, which promotes the rapid construction of knowledge framework (Figure 2B). In addition, high-impact institutions/authors in various countries cooperated with those in the United States inordinately (Supplementary Figures S2A, B). Collectively, we supposed that besides the incidence rate of chordoma, regional cooperation is another crucial driving force for chordoma research development.

A total of 2,098 institutions were involved in chordoma research (Supplementary Table S2), in which Capital Medical University has published the most articles (N=126), followed by University of Pittsburgh (N=124) and Massachusetts General Hospital (N=122). Among the top 10 institutions with the most article productions, seven are from the United States, publishing 666 articles with an average citation frequency of 23.9 times. The other three are from China (N=126, TC=696), Austria (N=87, TC=510), and Canada (N=66, TC=1,029), respectively. In recent years, Chinese institutions ranked high in total publication volume, whereas the h-index and average citations were lower than most institutions in the United States.

Fund is an important driving force for institutions to carry out research progress. Since 2000, 781 different types of funds financially aided chordoma research worldwide. Projects funded by US National Institutes of Health and United States Department of Health and Human Services produced the same number of articles (N=142), followed by National Natural Science Foundation of China (N=112). In the top 10 funds, four are from the United States, with three from China, two from Japan, and one from Europe (Supplementary Table S3). Based on these 10 funds, 625 articles were published, accounting for 27.4% of all studies. In addition, Chordoma Foundation, a non-profit organization, also

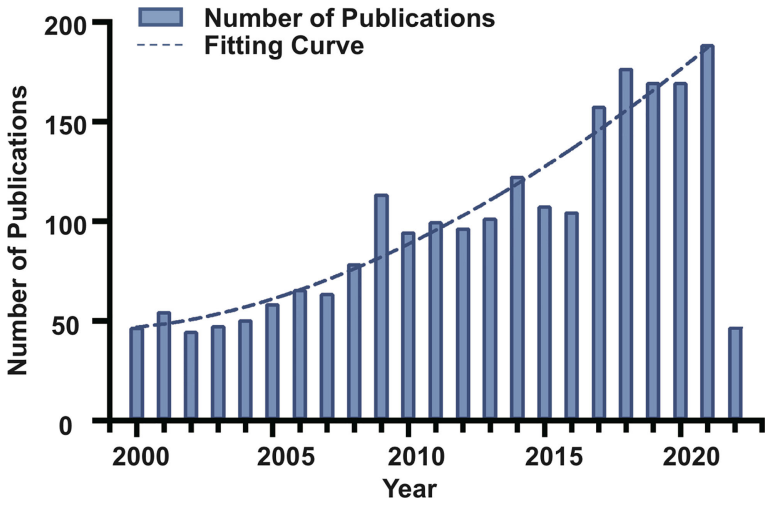

FIGURE 1
Trend of annual publication numbers and fitting curve for chordoma research in the twenty-first century.

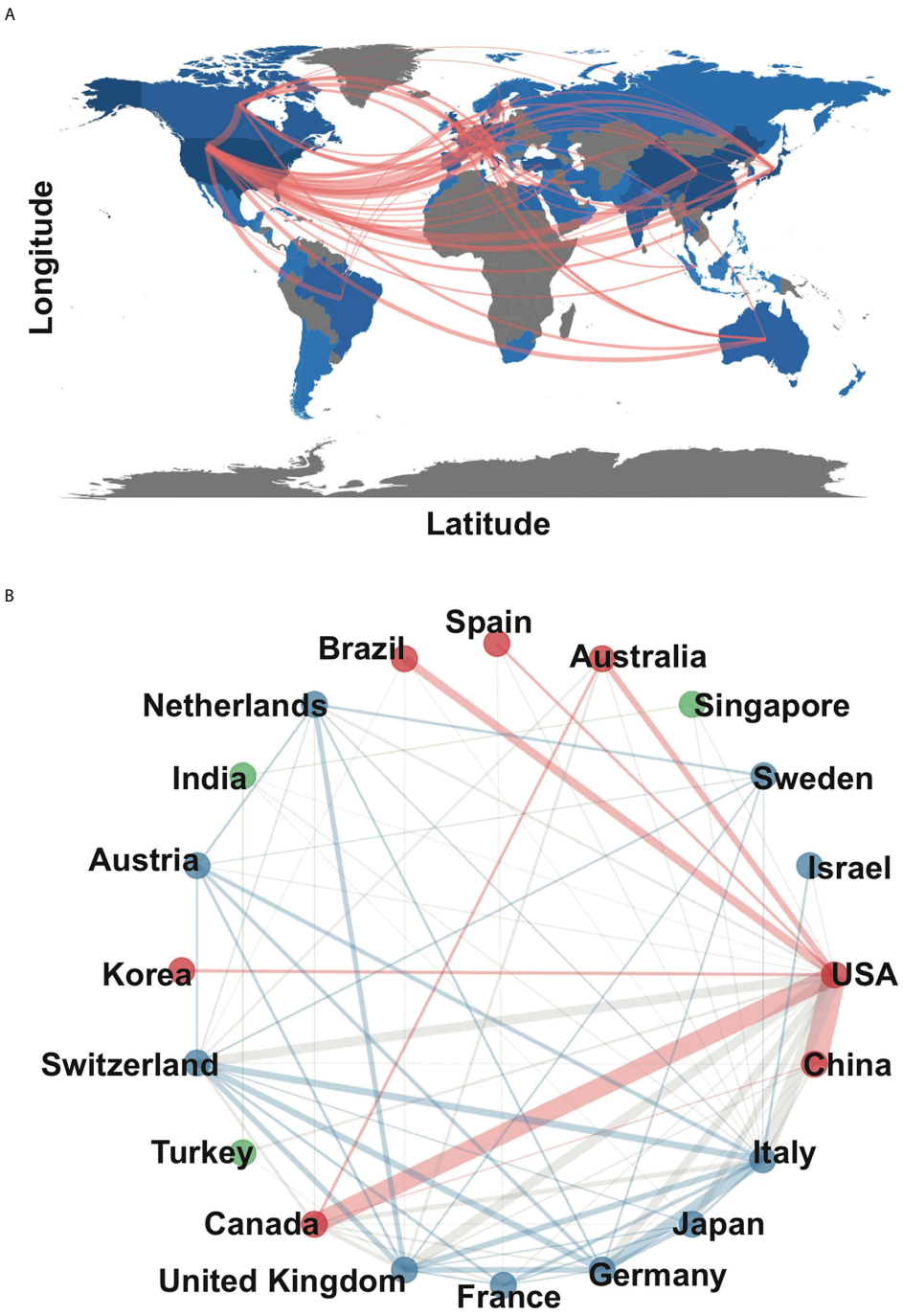

FIGURE 2
Main countries/regions of chordoma research and collaboration. **(A)** Countries/regions distribution of chordoma research and collaboration map; **(B)** collaboration network of 20 countries/regions in chordoma research.

plays a pivotal role in advancing chordoma research. Composed of more than 400 chordoma specialists worldwide, Chordoma Foundation provides trusted resources and assistance to thousands of researchers and patients around the world. By 2022, Chordoma Foundation has funded 28 studies and supported 73 chordoma-related studies in various forms. Therefore, institutions' prolificacy and high impact were related to the national and fund support for chordoma research.

Most productive and influential journal and author analysis

Journal analysis

We identified 594 journals publishing articles focused on chordoma. The top 10 published 551 articles accounted for 24.1% of all articles. World Neurosurgery, Journal of Neurosurgery, Neurosurgery, Spine, and Journal of Neurosurgery-Spine are the top 5 productive journals with Nature Medicine, Nature Genetics, European Urology, Acta Neuropathologica, and Journal of the American Chemical Society as top 5 high-impact journals (Table 2; Supplementary Table S4).

Total/average citations indicate the quality and impact, in which Neurosurgery ranked the first place. Its research topics of chordoma ranged from surgical options to combined treatment of surgery and adjuvant therapy. The recent topics are multi-dimensional therapeutic strategies including targeted therapy and immunotherapy, while scholars paid more attention to recurrent chordoma treatment. Chordoma articles in high-impact journals are mostly associated with multi-omics sequencing and clinical trials to identify tumorigenic signaling pathways, therapeutic targets, and novel treatment strategy.

Currently, the research system of the chordoma field is relatively mature, and the distribution and number of core journals accord with law of Bradford. The number of articles published in these journals shows an upward trend year by year (Figures 3A, B). As different journals have preferences for specific research fields, to grasp the hotspots of chordoma, we compared the changes in journals focusing on chordoma. The results revealed that studies of novel surgery and radiotherapy options, immune microenvironment, and tumorigenic signaling pathways are gradually expanding.

Most productive and influential authors

A total of 9,716 authors published articles in the chordoma field. As the first/corresponding author, Junting Zhang (N=21), Huilin Yang (N=20), and Yazhuo Zhang (N=19) are the top 3 high-yield authors (Supplementary Table S5). H-index of articles from Huilin Yang was 10, which ranked first among these authors. In addition to productivity, the average citation rate also optimizes the assessment of scientific influence. The average citation rate of Adrienne M. Flanagan was as high as 80.36. Adrienne M. Flanagan made significant contributions to the histopathology, tumorigenic mechanism of chordoma, and identification of potential therapeutic targets. Based on the law of Lotka, a relatively stable author-cooperation group has formed in chordoma fields, which cultivated several well-known scholars to promote the development of chordoma research (Supplementary Figures S3A, B).

Research hotspots and trends

Co-citation analysis

Citation is a useful method to evaluate the impact and recognition in the scientific community. Thus, identification of highly cited articles assists in recognizing the hotspots and future trends. All articles cited in chordoma publications were identified by co-citation analysis of VOSviewer (Figure 4A). Based on their intrinsic relevance, articles are divided into three color-coded clusters, in which the topics of blue cluster are oncogenic mechanism and targeted therapy; red and green are radiotherapy and surgery, respectively. The red/green nodes are distributed densely, while blue nodes are less. In the hotspots of chordoma research, the field of surgery and radiotherapy are relatively mature, while tumorigenic mechanism and targeted therapy are still in the development stage (Figure 4B).

In view of time-accumulating factors, the average citation rate per year was also adopted. The top 100 most-cited articles on average by year were analyzed, and the top 20 ones were described in Supplementary Table S6. The most cited article was an epidemiological survey published by McMaster et al., which was also the largest case series of chordoma in the United States before publication (3). This study analyzed and interpreted data

TABLE 2 Top 10 most productive journals in chordoma field.

Rank	Journal	Records	Proportion (%)	Total Citations	Citations per item	h-index
1	World Neurosurgery	98	4.29	885	9.03	18
2	Journal of Neurosurgery	77	3.37	2,251	29.23	27
3	Neurosurgery	66	2.89	3,818	57.85	33
4	Spine	60	2.63	2,028	33.80	24
5	Journal of Neurosurgery-Spine	52	2.28	1,477	28.40	21
6	International Journal of Radiation Oncology Biology Physics	47	2.06	2,450	52.13	29
7	Acta Neurochirurgica	46	2.04	644	14	15
8	European Spine Journal	41	1.79	804	19.61	18
9	Chordomas and Chondrosarcomas of the Skull Base and Spine	33	1.44	11	0.33	1
10	Journal of Clinical Neuroscience	31	1.37	333	10.74	11

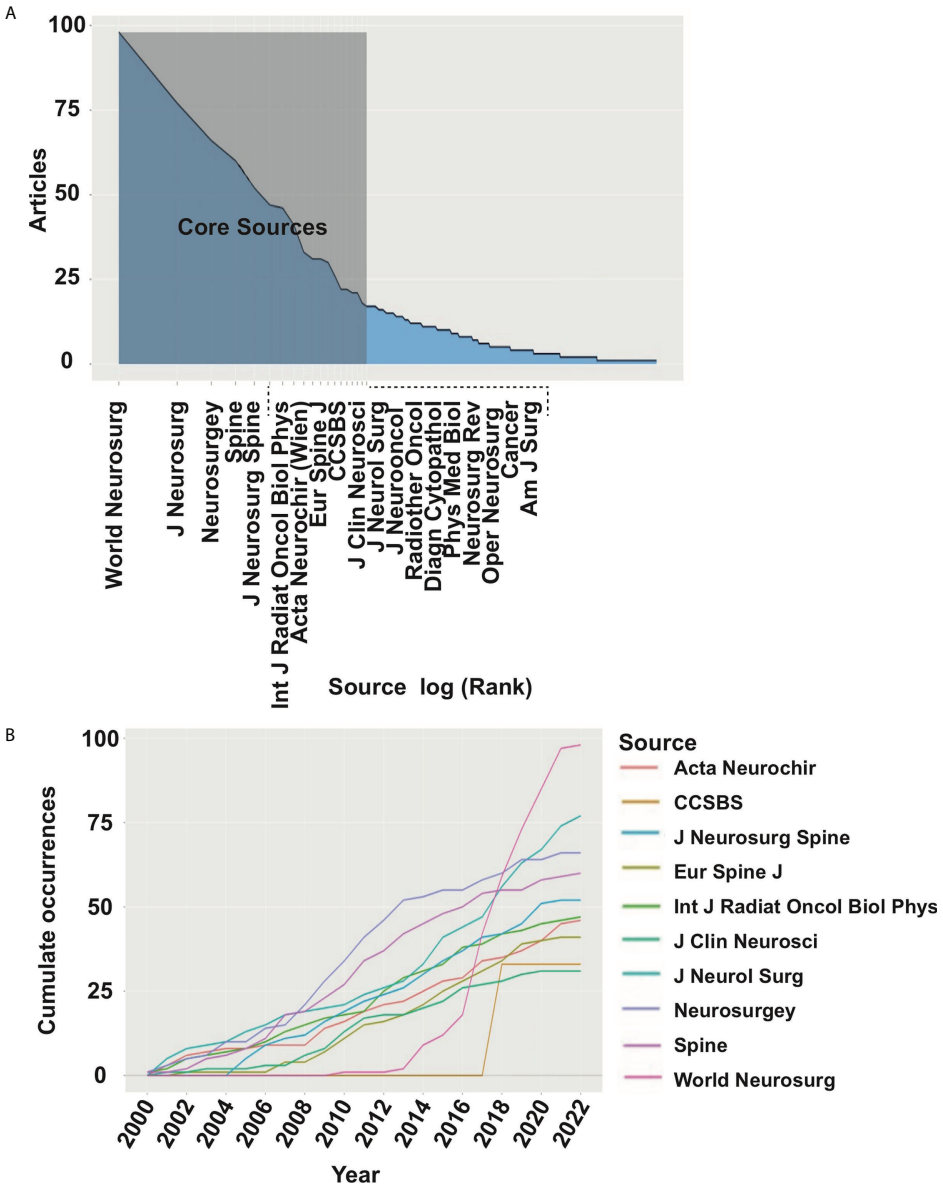

FIGURE 3
Core journals in chordoma research. **(A)** Identification of 19 core journals of chordoma field by law of Bradford; **(B)** publication numbers of top 10 core journal dynamic trend.

on incidence, treatment, and survival patterns chordoma from 1973 to 1995 based on the Surveillance, Epidemiology, and End Results (SEER) program of the National Cancer Institute. Among them, surgical treatment and radiotherapy remained the hottest topics. To grasp the future trends, we ranked the 100 high-impact articles according to the publication date. In the past 5 years, most publications focused on tumorigenic signaling pathways, immune microenvironments, and targeted therapy for chordoma (Supplementary Figure S4), consistent with the above co-citation analysis. As the similar features of chordoma and chondrosarcoma, their treatment therapy and tumorigenic mechanism were discussed together previously. Currently, the multi-omics sequencing specific for chordoma has been performed, and several signaling pathways has been identified as candidate therapeutic targets.

Co-word analysis

Co-word analysis can effectively identify the high-frequency keywords and reveal the specific research topics, hotspots, and future trends. After literature search (chordoma-related

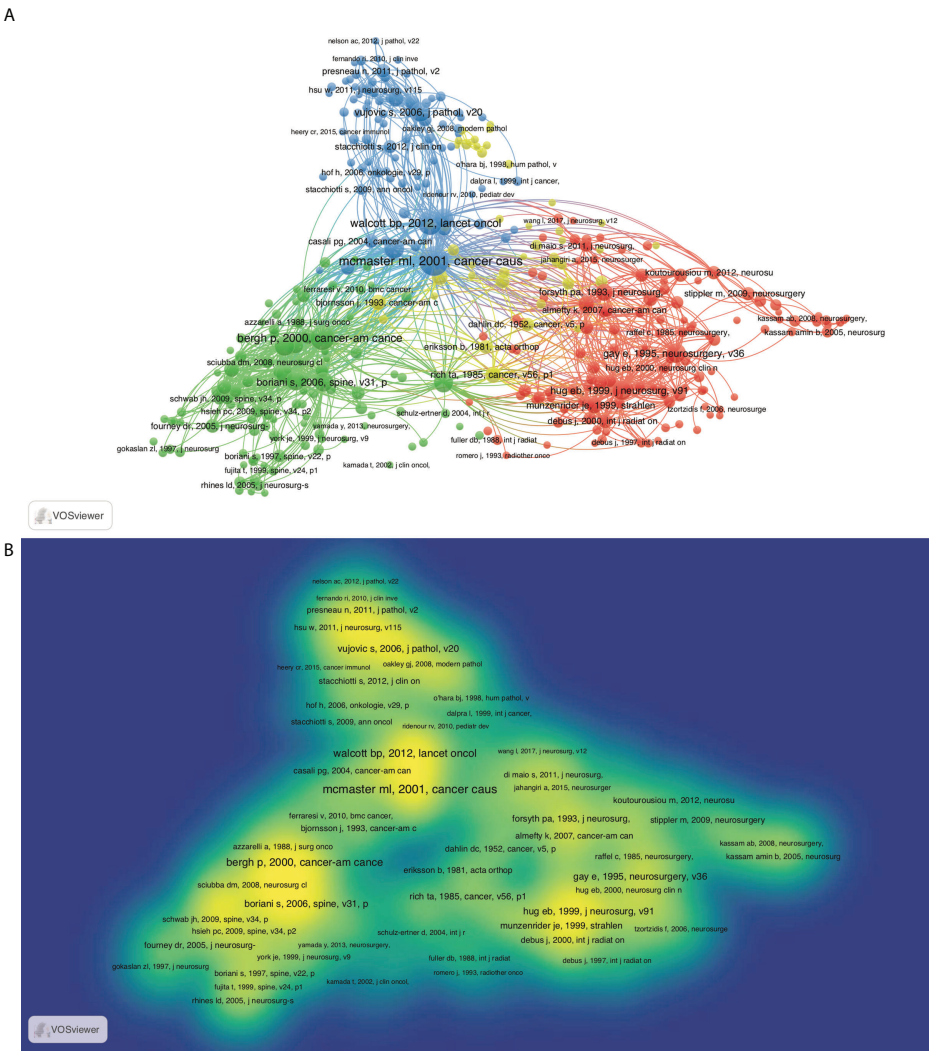

FIGURE 4
Co-citation map based on VOSviewer in chordoma field. **(A)** Network visualization; **(B)** density visualization.

publications, N=2,285; keywords, N=6,070), we analyzed the keywords provided by original authors and WoS using VOSviewer. Based on the frequency and ranking of keywords, we classified the 50 high-frequency keywords through co-occurrence network and Blibliometrix (Figure 5A; Supplementary Figures S5A, B). Based on the top 15 high-frequency keywords, surgery and radiotherapy are the focus of chordoma research. Recently, tumorigenic mechanism and molecular signaling pathway presented an upward trend (Figures 5B, C). Based on the strategic diagram analysis, we calculated four cluster's centrality and density (Figure 5D). The cluster of surgery, located in the first quadrant, had high centrality and density. Thus, this topic is relatively mature and crucial for chordoma research. Besides, radiotherapy is also a mature research topic. Although the research of tumorigenic mechanism was in the central position of the chordoma field, the current research was still insufficient.

Discussion

Chordoma is a relatively rare disease with a high relapse rate and poor prognosis. The tumorigenic mechanism and optimal therapeutic strategy are still unclear. In this article, we used bibliometrics to analyze the publications of chordoma since the twenty-first century. By 26 April 2022, a total of 2,285 articles in the field of chordoma have been published, with the citation times of 42,808. The most influential and productive country/region was the United States, followed by China and Japan. A total of 2,267 institutions participated in chordoma research, in

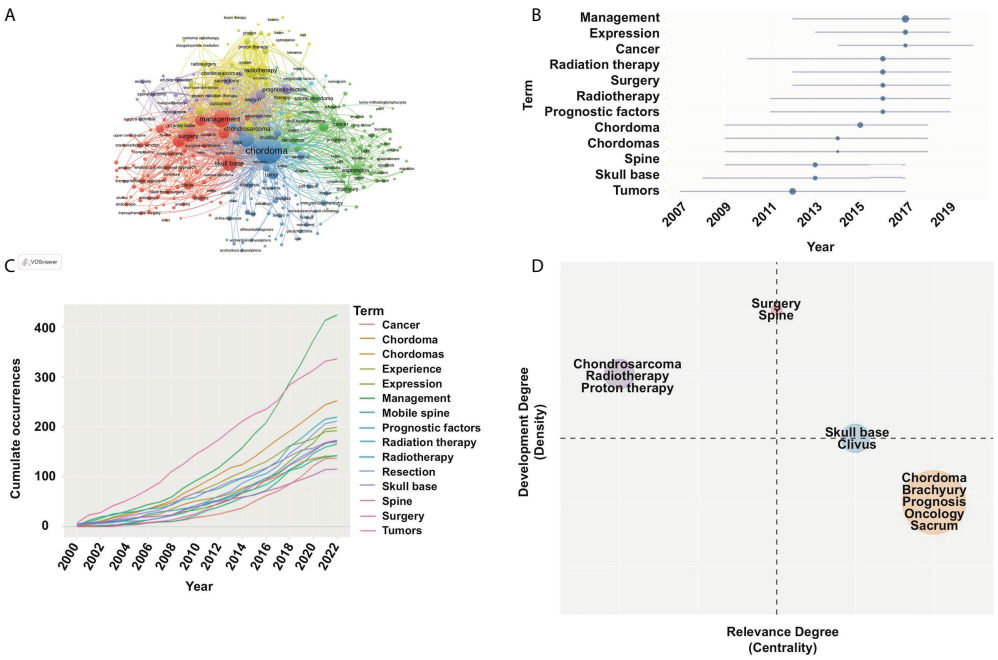

FIGURE 5
Keyword co-occurrence map with an occurrence frequency of more than 5 based on VOSviewer and Blibliometrix. **(A)** Network visualization; **(B)** topic trend of high-frequency keyword in chordoma filed; **(C)** high-frequency keyword dynamics; **(D)** strategic diagram in chordoma research.

which Capital Medical University published the most articles, followed by University of Pittsburgh and Massachusetts General Hospital. Among all high-impact authors, Huilin Yang had the highest h-index and Adrienne M. Flanagan had the highest citation rate and average citation rate. World Neurosurgery, Journal of Neurosurgery, Neurosurgery, Spine, and Journal of Neurosurgery-Spine were the first five periodicals with maximum publications in chordoma research. Among them, the highest total and average citation rate was Neurosurgery. Moreover, we also identified four hotspots by analyzing the topic of highly cited articles and co-word in the chordoma field: (1) molecular signaling pathway and targeted therapy of chordoma; (2) surgical treatment of chordoma; (3) optimization of radiotherapy; and (4) immunotherapy of chordoma.

Molecular signaling pathway and targeted therapy of chordoma

Facing the treatment dilemma of chordoma, exploring the tumorigenic mechanisms and the corresponding molecular signaling pathways are important. TBXT gene is a transcription factor for notochord development, and its duplication confers major susceptibility to familial chordoma (19). Its encoding protein, brachyury, is highly expressed in chordomas, which are associated with progression-free survival of chordoma patients (5, 20, 21). Besides, other gene mutations have also been identified in chordoma, such as CDKN2A, TP53, and LYST (22). CDK4 and p53, which function in the G1 phase cell cycle, are related to overall survival (OS) of chordoma patients (23, 24). In an integrated multi-omics analysis, CA2 and THNSL2 were identified in the switched compartments, cell-specific boundaries, and loops, indicating their tumorigenic roles in chordoma (25). Based on their key roles in chordoma tumorigenesis, targeting them provides potential therapeutic options. CDK7/12/13 inhibitor and the CA2 inhibitor, Dorzolamide, have been found to inhibit chordoma *in vitro* and *in vivo* (20, 25).

RTKs, such as platelet-derived growth factor receptor (PDGFR), epidermal growth factor receptor (EGFR), fibroblast growth factor receptor (FGFR), and vascular endothelial growth factor receptor (VEGFR), are also important oncogenic regulators of chordoma (26–28). They continuously translate extracellular stimuli into intracellular signaling cascades, such as PI3K-Akt-mTOR, and promote cell growth and tumorigenicity (29–31). Imatinib, an inhibitor of PDGFR, was used in six patients with advanced chordoma, and patients' prognoses were improved with more than 1 year follow-up (32). Gefitinib and afatinib, EGFR inhibitors, were also effective in chordoma patients (33, 34). With the treatment of apatinib, a potent inhibitor of VEGFR, one in seven patients achieved objective response according to RECIST and Choi criteria in 27 advanced

chordoma patients (9). In addition, targeting PI3K-Akt-mTOR pathway worked well in TKI-resistant chordoma, and the combination of sirolimus plus imatinib significantly reduced the tumor size in imatinib-resistant chordoma patients (8, 35).

Chordoma in different locations also has variable biological behaviors and molecular features. Poorly differentiated chordoma is mainly found in the clivus/cervix location (36). Histologically, skull base chordoma had more abundant chondroid matrix and diffuse growth pattern, whereas sacral/spinal chordoma had non-chondroid, myxoid matrix, and a lobulating pattern (37). As for transcriptome biomarkers, LMX1A is dominant in skull base chordoma, and SALL3 is unique to spine chordoma (38). Additionally, compared to clival chordoma, higher cMET dependence was found in sacral chordoma, indicating that cMET inhibitors alone or in combination with other drugs might particularly benefit patients with sacral chordoma (27).

Surgical treatment of chordoma

Surgical resection has always been a research hotspot in chordoma field and cornerstone of therapeutic strategy. The possible reasons for surgery as a key hotspot are as follows: (1) the complicated anatomical structures of axial skeleton and local invasiveness nature of chordoma increase the difficulty of resection (39, 40); (2) the surgical method is altered according to different locations (41–43); (3) the reconstruction is needed after tumor resection, and biomaterials with novel technologies, such as 3D printing, may provide optimized fixation (44); (4) the improvement of postoperative adjuvant therapy is beneficial to improve the survival outcomes of chordoma patients (45–47).

Chordoma-specific factors (volume, location, and pathological subtype) are associated with the surgical consideration, such as surgical method, approach, and scope. Take tumor location for example; skull base chordoma has a high recurrence rate because it infiltrates the skeleton and is closed to vital structures including brainstem and vital arteries. Thus, radical surgery combined with adjuvant radiotherapy is preferred for long-term survival (48). As for mobile spine and sacral chordoma, marginal resection or gross total resection is recommended (41). Based on single- and multi-center case series of chordoma, Meng et al. reported the glorious local control with the treatment of en-bloc spondylectomy (49, 50). However, more than 1 cm margin in three planes is hard to achieve even when performed by experienced surgeons (51). Therefore, accurate marginal excision is crucial, which promotes the application of computer navigation in tumor resection (52).

Bone stability maintenance is also a focus of tumor resection, and advanced biomaterials are widely used. Currently, custom-made prostheses have been successfully used, while 3D printing may have more benefits (44, 53). 3D-printed prostheses based on computer simulation can fit perfectly to defective sites and achieve personalized treatment (44, 54). Additionally, the bone contact surface of 3D-printed prosthesis can be made porous, inducing bone ingrowth to increase long-term stability (55). Other advanced biomaterial technologies, such as carbon-fiber-reinforced polyetheretherketone (CFR-PEEK) composite implants also improved the prognosis and decreased the risk of local recurrence (45).

Optimization of radiotherapy

Conventional radiotherapy is almost ineffective for chordoma either alone or combined with surgery (56–58). As the specific anatomical structure of peritumoral spinal cord, nerve root, and vessels, the methods, timing and complications of radiotherapy have always been the research focus (56). Currently, proton and carbon ion therapies that relied on Bragg peak effects are the preferred radiotherapy in most quaternary centers. Proton and carbon ion radiotherapies have little damage to normal tissue and target chordoma site for maximum dose of radiation therapy (10, 11). Thus, they are effective treatment options for chordoma with acceptable radiation toxicity (59, 60). Timing of these high-dose radiotherapy is also taken into consideration. DeLaney et al. confirmed that survival outcome of chordoma patients was significantly improved with preoperative radiotherapy (61). However, the preoperative high-dose radiotherapy may increase the complication of wound healing, and primary resection combined with postoperative proton or carbon ion therapy was recommended by many researchers (62–64).

The duration, dosage, and adjuvant materials [e.g., phosphorus-32 (P32), yttrium] of proton or carbon ion therapy are also key points. Due to the radioresistant characteristic of chordoma, local control rate of low-dose radiotherapy is often poor. Therefore, proton or carbon ion therapy, whether as a radical therapy or adjuvant option, has high-dose requirements. Several studies reported that current dose of radiotherapy strategies typically exceeded 70 Gy, and multi-cycles therapy was necessary (56, 65, 66). The local recurrence rate could remain low under high-dose radiotherapy, but the radiotoxicity still needs further discussion. Folkert et al. reported dural plaques as an auxiliary mean of external irradiation could increase radiotherapy dose delivery in radiation-resistant chordoma and improve local control rates with less toxic risk (45, 67). Increasing radiotherapy sensitivity is another option to reduce the radiation resistance and complication. In a preclinical research, Hao Shuyu et al. identified a protein phosphatase 2A (PP2A) inhibitor LB100, which could serve as a supplement for radiation to effectively enhance DNA damage-induced chordoma cell death and delay tumor growth *in vivo* (68).

Immunotherapy of chordoma

Immune checkpoint can attenuate the tumor killing ability of T lymphocytes. Recently, immune checkpoint inhibitors worked well in the treatment of chordoma (69). Programmed cell death protein-1 (PD-1) and programmed cell death ligand-1 (PD-L1) are highly expressed in chordoma (70–72). Nivolumab, an anti-PD-1 monoclonal antibody, showed effectivity against chordoma *in vivo* and is currently evaluated in clinical trials for chordomas (73, 74). In addition, avelumab could inhibit the chordoma cell proliferation by targeting PD-L1, while further clinical evidence is still needed for chordoma (75).

As brachyury is highly expressed in chordoma, it may serve as a target of current immunotherapy. Brachyury vaccines have been produced. GI-6301, which delivers antigens through dendritic cells, specifically activates $CD4^+$ and $CD8^+$ cell and has a lethal effect on brachyury-expressing tumor cells (76, 77). Additionally, modified vaccinia Ankara (MVA) poxviral vaccine vector encodes human brachyury, and adenovirus serotype 5 (Ad5) has been developed and applied in clinical trials (5, 78). Thus, immunotherapy is regarded as one future trend in the basic research and clinical treatment of chordoma.

Conclusion

This study indicates that chordoma studies are increasing. Surgery and radiotherapy are well reported and always play fundamental roles in chordoma treatment. The molecule signaling pathway, targeted therapy, and immunotherapy of chordoma are the latest research hotspots.

Data availability statement

The original contributions presented in the study are included in the article/Supplementary Material. Further inquiries can be directed to the corresponding authors.

Author contributions

TM conceived the project. JG, RH performed bioinformatics analysis. HY, DS and TM interpreted and analyzed data. JG and TM wrote the manuscript with comments from all authors. All authors contributed to the article and approved the submitted version.

Funding

This work was supported in part by the National Natural Science Foundation of China (82173168), Postdoctoral Research Foundation of China (2021M702485), Shanghai Rising-Star Program (21QA1407500).

Conflict of interest

The authors declare that the research was conducted in the absence of any commercial or financial relationships that could be construed as a potential conflict of interest.

Publisher's note

Supplementary material

The Supplementary Material for this article can be found online at: https://www.frontiersin.org/articles/10.3389/fonc.2022.946597/full#supplementary-material

References

1. Das P, Soni P, Jones J, Habboub G, Barnholtz-Sloan JS, Recinos PF, et al. Descriptive epidemiology of chordomas in the united states. *J Neurooncol* (2020) 148:173–8. doi: 10.1007/s11060-020-03511-x

2. Burke JF, Chan AK, Mayer RR, Garcia JH, Pennicooke B, Mann M, et al. Clamshell thoracotomy for en bloc resection of a 3-level thoracic chordoma: technical note and operative video. *Neurosurg Focus* (2020) 49:E16. doi: 10.3171/2020.6.FOCUS20382

3. McMaster ML, Goldstein AM, Bromley CM, Ishibe N, Parry DM. Chordoma: incidence and survival patterns in the united states, 1973-1995. *Cancer Causes Control CCC* (2001) 12:1–11. doi: 10.1023/A:1008947301735

4. Koga T, Shin M, Saito N. Treatment with high marginal dose is mandatory to achieve long-term control of skull base chordomas and chondrosarcomas by means of stereotactic radiosurgery. *J Neuro-Oncol* (2010) 98:233–8. doi: 10.1007/s11060-010-0184-y

5. Barber SM, Sadrameli SS, Lee JJ, Fridley JS, Teh BS, Oyelese AA, et al. Chordoma-current understanding and modern treatment paradigms. *J Clin Med* (2021) 10:1054. doi: 10.3390/jcm10051054

6. Stacchiotti S, Gronchi A, Fossati P, Akiyama T, Alapetite C, Baumann M, et al. Best practices for the management of local-regional recurrent chordoma: a position paper by the chordoma global consensus group. *Ann Oncol Off J Eur Soc Med Oncol* (2017) 28:1230–42. doi: 10.1093/annonc/mdx054

7. Arain A, Hornicek FJ, Schwab JH, Chebib I, Damron TA. Chordoma arising from benign multifocal notochordal tumors. *Skeletal Radiol* (2017) 46:1745–52. doi: 10.1007/s00256-017-2727-1

8. Meng T, Jin J, Jiang C, Huang R, Yin H, Song D, et al. Molecular targeted therapy in the treatment of chordoma: A systematic review. *Front Oncol* (2019) 9:30. doi: 10.3389/fonc.2019.00030

9. Liu C, Jia Q, Wei H, Yang X, Liu T, Zhao J, et al. Apatinib in patients with advanced chordoma: a single-arm, single-centre, phase 2 study. *Lancet Oncol* (2020) 21:1244–52. doi: 10.1016/S1470-2045(20)30466-6

10. Demizu Y, Imai R, Kiyohara H, Matsunobu A, Okamoto M, Okimoto T, et al. Carbon ion radiotherapy for sacral chordoma: A retrospective nationwide multicentre study in Japan. *Radiother Oncol* (2021) 154:1–5. doi: 10.1016/j.radonc.2020.09.018

11. Mohan R, Grosshans D. Proton therapy - present and future. *Adv Drug Deliv Rev* (2017) 109:26–44. doi: 10.1016/j.addr.2016.11.006

12. Jafari Roodbandi AS, Choobineh A, Barahmand N, Sadeghi M. Research outputs in ergonomics and human factors engineering: a bibliometric and co-word analysis of content and contributions. *Int J Occup Saf Ergon* (2021) 2021:1–12. doi: 10.1080/10803548.2021.1955495

13. Hao KJ, Jia X, Dai WT, Huo ZM, Zhang HQ, Liu JW, et al. Mapping intellectual structures and research hotspots of triple negative breast cancer: A bibliometric analysis. *Front Oncol* (2021) 11:689553. doi: 10.3389/fonc.2021.689553

14. Murillo J, Villegas LM, Ulloa-Murillo LM, Rodríguez AR. Recent trends on omics and bioinformatics approaches to study SARS-CoV-2: A bibliometric analysis and mini-review. *Comput Biol Med* (2021) 128:104162. doi: 10.1016/j.compbiomed.2020.104162

15. Zhu S, Liu Y, Gu Z, Zhao Y. A bibliometric analysis of advanced healthcare materials: Research trends of biomaterials in healthcare application. *Adv Healthc Mater* (2021) 10:e2002222. doi: 10.1002/adhm.202002222

16. Aria M, Alterisio A, Scandurra A, Pinelli C, D'Aniello B. The scholar's best friend: research trends in dog cognitive and behavioral studies. *Anim Cognit* (2021) 24:541–53. doi: 10.1007/s10071-020-01448-2

17. Hirsch JE. An index to quantify an individual's scientific research output. *Proc Natl Acad Sci USA* (2005) 102:16569–72. doi: 10.1073/pnas.0507655102

18. van Eck NJ, Waltman L. Software survey: VOSviewer, a computer program for bibliometric mapping. *Scientometrics* (2010) 84:523–38. doi: 10.1007/s11192-009-0146-3

19. Yang XR, Ng D, Alcorta DA, Liebsch NJ, Sheridan E, Li S, et al. T (brachyury) gene duplication confers major susceptibility to familial chordoma. *Nat Genet* (2009) 41:1176–8. doi: 10.1038/ng.454

20. Sharifnia T, Wawer MJ, Chen T, Huang QY, Weir BA, Sizemore A, et al. Small-molecule targeting of brachyury transcription factor addiction in chordoma. *Nat Med* (2019) 25:292–300. doi: 10.1038/s41591-018-0312-3

21. Otani R, Mukasa A, Shin M, Omata M, Takayanagi S, Tanaka S, et al. Brachyury gene copy number gain and activation of the PI3K/Akt pathway: association with upregulation of oncogenic brachyury expression in skull base chordoma. *J Neurosurg* (2018) 128:1428–37. doi: 10.3171/2016.12.JNS161444

22. Tarpey PS, Behjati S, Young MD, Martincorena I, Alexandrov LB, Farndon SJ, et al. The driver landscape of sporadic chordoma. *Nat Commun* (2017) 8:890. doi: 10.1038/s41467-017-01026-0

23. Yadav R, Sharma MC, Malgulwar PB, Pathak P, Sigamani E, Suri V, et al. Prognostic value of MIB-1, p53, epidermal growth factor receptor, and INI1 in childhood chordomas. *Neuro-oncology* (2014) 16:372–81. doi: 10.1093/neuonc/not228

24. Anderson E, Havener TM, Zorn KM, Foil DH, Lane TR, Capuzzi SJ, et al. Synergistic drug combinations and machine learning for drug repurposing in chordoma. *Sci Rep* (2020) 10:12982. doi: 10.1038/s41598-020-70026-w

25. Meng T, Huang R, Jin J, Gao J, Liu F, Wei Z, et al. A comparative integrated multi-omics analysis identifies CA2 as a novel target for chordoma. *Neuro-oncology* (2021) 23:1709–22. doi: 10.1093/neuonc/noab156

26. Liang C, Ma Y, Yong L, Yang C, Wang P, Liu X, et al. Y-box binding protein-1 promotes tumorigenesis and progression *via* the epidermal growth factor receptor/AKT pathway in spinal chordoma. *Cancer Sci* (2019) 110:166–79. doi: 10.1111/cas.13875

27. Lohberger B, Scheipl S, Heitzer E, Quehenberger F, de Jong D, Szuhai K, et al. Higher cMET dependence of sacral compared to clival chordoma cells: contributing to a better understanding of cMET in chordoma. *Sci Rep* (2021) 11:12466. doi: 10.1038/s41598-021-92018-0

28. Zhai Y, Bai J, Wang S, Du J, Wang J, Li C, et al. Differences in dural penetration of clival chordomas are associated with different prognosis and expression of platelet-derived growth factor receptor-β. *World Neurosurg* (2017) 98:288–95. doi: 10.1016/j.wneu.2016.07.096

29. Fasig JH, Dupont WD, LaFleur BJ, Olson SJ, Cates JM. Immunohistochemical analysis of receptor tyrosine kinase signal transduction activity in chordoma. *Neuropathol Appl Neurobiol* (2008) 34:95–104. doi: 10.1111/j.1365-2990.2007.00873.x

30. Du Z, Lovly CM. Mechanisms of receptor tyrosine kinase activation in cancer. *Mol Cancer* (2018) 17:58. doi: 10.1186/s12943-018-0782-4

31. Presneau N, Shalaby A, Idowu B, Gikas P, Cannon SR, Gout I, et al. Potential therapeutic targets for chordoma: PI3K/AKT/TSC1/TSC2/mTOR pathway. *Br J Cancer* (2009) 100:1406–14. doi: 10.1038/sj.bjc.6605019

32. Casali PG, Messina A, Stacchiotti S, Tamborini E, Crippa F, Gronchi A, et al. Imatinib mesylate in chordoma. *Cancer* (2004) 101:2086–97. doi: 10.1002/cncr.20618

33. Scheipl S, Barnard M, Cottone L, Jorgensen M, Drewry DH, Zuercher WJ, et al. EGFR inhibitors identified as a potential treatment for chordoma in a focused compound screen. *J Pathol* (2016) 239:320–34. doi: 10.1002/path.4729

34. Magnaghi P, Salom B, Cozzi L, Amboldi N, Ballinari D, Tamborini E, et al. Afatinib is a new therapeutic approach in chordoma with a unique ability to target EGFR and brachyury. *Mol Cancer Ther* (2018) 17:603–13. doi: 10.1158/1535-7163.MCT-17-0324

35. Stacchiotti S, Marrari A, Tamborini E, Palassini E, Virdis E, Messina A, et al. Response to imatinib plus sirolimus in advanced chordoma. *Ann Oncol Off J Eur Soc Med Oncol* (2009) 20:1886–94. doi: 10.1093/annonc/mdp210

36. Yeter HG, Kosemehmetoglu K, Soylemezoglu F. Poorly differentiated chordoma: review of 53 cases. *APMIS Acta Pathol Microbiol Immunol Scandinavica* (2019) 127:607–15. doi: 10.1111/apm.12978

37. Cha YJ, Suh YL. Chordomas: Histopathological study in view of anatomical location. *J Korean Med Sci* (2019) 34:e107. doi: 10.3346/jkms.2019.34.e107

38. Bell AH, DeMonte F, Raza SM, Rhines LD, Tatsui CE, Prieto VG, et al. Transcriptome comparison identifies potential biomarkers of spine and skull base chordomas. *Virchows Archiv Int J Pathol* (2018) 472:489–97. doi: 10.1007/s00428-017-2224-x

39. Heery CR. Chordoma: The quest for better treatment options. *Oncol Ther* (2016) 4:35–51. doi: 10.1007/s40487-016-0016-0

40. Al Shihabi A, Davarifar A, Nguyen HTL, Tavanaie N, Nelson SD, Yanagawa J, et al. Personalized chordoma organoids for drug discovery studies. *Sci Adv* (2022) 8:eabl3674. doi: 10.1126/sciadv.abl3674

41. Wang L, Wu Z, Tian K, Wang K, Li D, Ma J, et al. Clinical features and surgical outcomes of patients with skull base chordoma: a retrospective analysis of 238 patients. *J Neurosurg* (2017) 127:1257–67. doi: 10.3171/2016.9.JNS16559

42. Clarke MJ, Dasenbrock H, Bydon A, Sciubba DM, McGirt MJ, Hsieh PC, et al. Posterior-only approach for en bloc sacrectomy: clinical outcomes in 36 consecutive patients. *Neurosurgery* (2012) 71:357–64. doi: 10.1227/NEU.0b013e31825d01d4

43. Gokaslan ZL, Zadnik PL, Sciubba DM, Germscheid N, Goodwin CR, Wolinsky JP, et al. Mobile spine chordoma: results of 166 patients from the AOSpine knowledge forum tumor database. *J Neurosurg Spine* (2016) 24:644–51. doi: 10.3171/2015.7.SPINE15201

44. Wei R, Guo W, Ji T, Zhang Y, Liang H. One-step reconstruction with a 3D-printed, custom-made prosthesis after total en bloc sacrectomy: a technical note. *Eur Spine J Off Publ Eur Spine Society Eur Spinal Deform Society Eur Section Cervical Spine Res Soc* (2017) 26:1902–9. doi: 10.1007/s00586-016-4871-z

45. Boriani S, Tedesco G, Ming L, Ghermandi R, Amichetti M, Fossati P, et al. Carbon-fiber-reinforced PEEK fixation system in the treatment of spine tumors: a preliminary report. *Eur Spine J* (2018) 27:874–81. doi: 10.1007/s00586-017-5258-5

46. Cavallo LM, Mazzatenta D, d'Avella E, Catapano D, Fontanella MM, Locatelli D, et al. The management of clival chordomas: an Italian multicentric study. *J Neurosurg* (2020) 135(1):1–10. doi: 10.3171/2020.5.JNS20925

47. Biermann JS, Chow W, Reed DR, Lucas D, Adkins DR, Agulnik M, et al. NCCN guidelines insights: Bone cancer, version 2.2017. *J Natl Compr Cancer Netw JNCCN* (2017) 15:155–67. doi: 10.6004/jnccn.2017.0017

48. Ouyang T, Zhang N, Zhang Y, Jiao J, Ren J, Huang T, et al. Clinical characteristics, immunohistochemistry, and outcomes of 77 patients with skull base chordomas. *World Neurosurg* (2014) 81:790–7. doi: 10.1016/j.wneu.2013.01.010

49. Meng T, Yin H, Li B, Li Z, Xu W, Zhou W, et al. Clinical features and prognostic factors of patients with chordoma in the spine: a retrospective analysis of 153 patients in a single center. *Neuro-oncology* (2015) 17:725–32. doi: 10.1093/neuonc/nou331

50. Meng T, Huang R, Hu P, Yin H, Lin S, Qiao S, et al. Novel nomograms as aids for predicting recurrence and survival in chordoma patients: A retrospective multicenter study in mainland China. *Spine (Phila Pa 1976)* (2021) 46:E37-e47. doi: 10.1097/BRS.0000000000003716

51. Cartiaux O, Docquier PL, Paul L, Francq BG, Cornu OH, Delloye C, et al. Surgical inaccuracy of tumor resection and reconstruction within the pelvis: an experimental study. *Acta Orthop* (2008) 79:695–702. doi: 10.1080/17453670810016731

52. Ozaki T, Flege S, Kevric M, indner N, Maas R, Delling G, et al. Osteosarcoma of the pelvis: experience of the cooperative osteosarcoma study group. *J Clin Oncol* (2003) 21:334–41. doi: 10.1200/JCO.2003.01.142

53. Wuisman P, Lieshout O, van Dijk M, van Diest P. Reconstruction after total en bloc sacrectomy for osteosarcoma using a custom-made prosthesis: a technical note. *Spine (Phila Pa 1976)* (2001) 26:431–9. doi: 10.1097/00007632-200102150-00021

54. Xu N, Wei F, Liu X, Jiang L, Cai H, Li Z, et al. Reconstruction of the upper cervical spine using a personalized 3D-printed vertebral body in an adolescent with Ewing sarcoma. *Spine (Phila Pa 1976)* (2016) 41:E50–4. doi: 10.1097/BRS.0000000000001179

55. Shah FA, Snis A, Matic A, Thomsen P, Palmquist A. 3D printed Ti6Al4V implant surface promotes bone maturation and retains a higher density of less aged osteocytes at the bone-implant interface. *Acta Biomater* (2016) 30:357–67. doi: 10.1016/j.actbio.2015.11.013

56. Chen X, Lo SL, Bettegowda C, Ryan DM, Gross JM, Hu C, et al. High-dose hypofractionated stereotactic body radiotherapy for spinal chordoma. *J Neurosurg Spine* (2021) 35:674–83. doi: 10.3171/2021.2.SPINE202199

57. Tu K, Lee S, Roy S, Sawant A, Shukla H. Dysregulated epigenetics of chordoma: Prognostic markers and therapeutic targets. *Curr Cancer Drug Targets* (2022) 22:678–90. doi: 10.2174/1568009622666220419122716

58. Kitamura Y, Sasaki H, Yoshida K, Adams J, Dean S, Yeap BY. Genetic aberrations and molecular biology of skull base chordoma and chondrosarcoma. *Brain Tumor Pathol* (2017) 34:78–90. doi: 10.1007/s10014-017-0283-y

59. DeLaney TF, Liebsch NJ, Pedlow FX, Adams J, Dean S, Yeap BY, et al. Phase II study of high-dose photon/proton radiotherapy in the management of spine sarcomas. *Int J Radiat Oncol Biol Phys* (2009) 74:732–9. doi: 10.1016/j.ijrobp.2008.08.058

60. Jin CJ, Berry-Candelario J, Reiner AS, Laufer I, Higginson DS, Schmitt AM, et al. Long-term outcomes of high-dose single-fraction radiosurgery for chordomas of the spine and sacrum. *J Neurosurg Spine* (2019) 32:79–88. doi: 10.1093/neuros/nyz310_177

61. Rotondo RL, Folkert W, Liebsch NJ, Chen YL, Pedlow FX, Schwab JH, et al. High-dose proton-based radiation therapy in the management of spine chordomas: outcomes and clinicopathological prognostic factors. *J Neurosurg Spine* (2015) 23:788–97. doi: 10.3171/2015.3.SPINE14716

62. Park L, Delaney TF, Liebsch NJ, Hornicek FJ, Goldberg S, Mankin H, et al. Sacral chordomas: Impact of high-dose proton/photon-beam radiation therapy combined with or without surgery for primary versus recurrent tumor. *Int J Radiat Oncol Biol Phys* (2006) 65:1514–21. doi: 10.1016/j.ijrobp.2006.02.059

63. Dial BL, Kerr DL, Lazarides AL, Catanzano AA, Green CL, Risoli T, et al. The role of radiotherapy for chordoma patients managed with surgery: Analysis of the national cancer database. *Spine* (2020) 45:E742-e51. doi: 10.1097/BRS.0000000000003406

64. Fujiwara T, Tsuda Y, Stevenson J, Parry M, Jeys L. Sacral chordoma: do the width of surgical margin and the use of photon/proton radiotherapy affect local disease control? *Int Orthop* (2020) 44:381–9. doi: 10.1007/s00264-019-04460-5

65. Trifiletti DM, Brown PD. Proton and carbon ion therapy for skull base chordomas. *Neuro Oncol* (2020) 22:1241–2. doi: 10.1093/neuonc/noaa169

66. Basler L, Poel R, Schröder C, Bolsi A, Lomax A, Tanadini-Lang S, et al. Dosimetric analysis of local failures in skull-base chordoma and chondrosarcoma following pencil beam scanning proton therapy. *Radiat Oncol* (2020) 15:266. doi: 10.1186/s13014-020-01711-3

67. Folkert MR, Bilsky MH, Cohen GN, Zaider M, Dauer LT, Cox BW, et al. Intraoperative 32P high-dose rate brachytherapy of the dura for recurrent primary and metastatic intracranial and spinal tumors. *Neurosurgery* (2012) 71:1003–10. doi: 10.1227/NEU.0b013e31826d5ac1

68. Hao S, Song H, Zhang W, Seldomridge A, Jung J, Giles AJ, et al. Protein phosphatase 2A inhibition enhances radiation sensitivity and reduces tumor growth in chordoma. *Neuro-oncology* (2018) 20:799–809. doi: 10.1093/neuonc/nox241

69. Zou MX, Guo KM, Lv GH, Huang W, Li J, Wang XB, et al. Clinicopathologic implications of CD8(+)/Foxp3(+) ratio and miR-574-3p/PD-L1 axis in spinal chordoma patients. *Cancer Immunol Immunother CII* (2018) 67:209–24. doi: 10.1007/s00262-017-2080-1

70. Scognamiglio G, De Chiara A, Parafioriti A, Armiraglio E, Fazioli F, Gallo M, et al. Patient-derived organoids as a potential model to predict response to PD-1/PD-L1 checkpoint inhibitors. *Br J Cancer* (2019) 121:979–82. doi: 10.1038/s41416-019-0616-1

71. Kushlinskii NE, Alferov AA, Timofeev YS, Gershtein ES, Bulycheva IV, Bondarev AV, et al. Key immune checkpoint PD-1/PD-L1 signaling pathway components in the blood serum from patients with bone tumors. *Bull Exp Biol Med* (2020) 170:64–8. doi: 10.1007/s10517-020-05005-2

72. Mathios D, Ruzevick J, Jackson CM, Xu H, Shah SR, Taube JM, et al. PD-1, PD-L1, PD-L2 expression in the chordoma microenvironment. *J Neuro-Oncol* (2015) 121:251–9. doi: 10.1007/s11060-014-1637-5

73. Migliorini D, Mach N, Aguiar D, Vernet R, Landis BN, Becker M, et al. First report of clinical responses to immunotherapy in 3 relapsing cases of chordoma after failure of standard therapies. *Oncoimmunology* (2017) 6:e1338235. doi: 10.1080/2162402X.2017.1338235

74. Williamson LM, Rive CM, Di Francesco D, Titmuss E, Chun HE, Brown SD, et al. Clinical response to nivolumab in an INI1-deficient pediatric chordoma correlates with immunogenic recognition of brachyury. *NPJ Precis Oncol* (2021) 5:103. doi: 10.1038/s41698-021-00238-4

75. Fujii R, Friedman ER, Richards J, Tsang KY, Heery CR, Schlom J, et al. Enhanced killing of chordoma cells by antibody-dependent cell-mediated cytotoxicity employing the novel anti-PD-L1 antibody avelumab. *Oncotarget* (2016) 7:33498–511. doi: 10.18632/oncotarget.9256

76. Heery CR, Singh BH, Rauckhorst M, Marte JL, Donahue RN, Grenga I, et al. Phase I trial of a yeast-based therapeutic cancer vaccine (GI-6301) targeting the transcription factor brachyury. *Cancer Immunol Res* (2015) 3:1248–56. doi: 10.1158/2326-6066.CIR-15-0119

77. DeMaria PJ, Bilusic M, Park DM, Heery CR, Donahue RN, Madan RA, et al. Randomized, double-blind, placebo-controlled phase II study of yeast-brachyury vaccine (GI-6301) in combination with standard-of-Care radiotherapy in locally advanced, unresectable chordoma. *Oncologist* (2021) 26:e847-e58. doi: 10.1002/onco.13720

78. DeMaria PJ, Lee-Wisdom K, Donahue RN, Madan RA, Karzai F, Schwab A, et al. Phase 1 open-label trial of intravenous administration of MVA-BN-brachyury-TRICOM vaccine in patients with advanced cancer. *J Immunother Cancer* (2021) 9:e003238. doi: 10.1136/jitc-2021-003238

frontiers | Frontiers in Oncology

TYPE Systematic Review
PUBLISHED 29 September 2022
DOI 10.3389/fonc.2022.997506

OPEN ACCESS

EDITED BY
Sebastien Froelich,
Assistance Publique Hopitaux De Paris, France

REVIEWED BY
Johannes Wach,
University Hospital Bonn, Germany
Joao Paulo Almeida,
Mayo Clinic Florida, United States

*CORRESPONDENCE
Shaan M. Raza
smraza@mdanderson.org

SPECIALTY SECTION
This article was submitted to Neuro-Oncology and Neurosurgical Oncology, a section of the journal Frontiers in Oncology

RECEIVED 19 July 2022
ACCEPTED 12 September 2022
PUBLISHED 29 September 2022

CITATION
Rubino F, Alvarez-Breckenridge C, Akdemir K, Conley AP, Bishop AJ, Wang W-L, Lazar AJ, Rhines LD, DeMonte F and Raza SM (2022) Prognostic molecular biomarkers in chordomas: A systematic review and identification of clinically usable biomarker panels.
Front. Oncol. 12:997506.
doi: 10.3389/fonc.2022.997506

Prognostic molecular biomarkers in chordomas: A systematic review and identification of clinically usable biomarker panels

Franco Rubino[1], Christopher Alvarez-Breckenridge[1], Kadir Akdemir[1], Anthony P. Conley[2], Andrew J. Bishop[3], Wei-Lien Wang[4], Alexander J. Lazar[4], Laurence D. Rhines[1], Franco DeMonte[1] and Shaan M. Raza[1]*

[1]Department of Neurosurgery, Division of surgery, The University of Texas MD Anderson Cancer Center, University of Texas, Houston, TX, United States, [2]Department of Sarcoma Medical Oncology, Division of Cancer Medicine,The University of Texas MD Anderson Cancer Center, University of Texas, Houston, TX, United States, [3]Department of Radiation Oncology, Division of Radiation Oncology, The University of Texas MD Anderson Cancer Center, University of Texas, Houston, TX, United States, [4]Department of Pathology, Division of Pathology-Lab Medicine Division, The University of Texas MD Anderson Cancer Center, University of Texas, Houston, TX, United States

Introduction and objective: Despite the improvements in management and treatment of chordomas over time, the risk of disease recurrence remains high. Consequently, there is a push to develop effective systemic therapeutics for newly diagnosed and recurrent disease. In order to tailor treatment for individual chordoma patients and develop effective surveillance strategies, suitable clinical biomarkers need to be identified. The objective of this study was to systematically review all prognostic biomarkers for chordomas reported to date in order to classify them according to localization, study design and statistical analysis.

Methods: Using the Preferred Reporting Items for Systematic Reviews and Meta-Analyses (PRISMA) guidelines, we systematically reviewed published studies reporting biomarkers that correlated with clinical outcomes. We included time-to-event studies that evaluated biomarkers in skull base or spine chordomas. To be included in our review, the study must have analyzed the outcomes with univariate and/or multivariate methods (log-rank test or a Cox-regression model).

Results: We included 68 studies, of which only 5 were prospective studies. Overall, 103 biomarkers were analyzed in 3183 patients. According to FDA classification, 85 were molecular biomarkers (82.5%) mainly located in nucleus and cytoplasm (48% and 27%, respectively). Thirty-four studies analyzed biomarkers with Cox-regression model. Within these studies, 32 biomarkers (31%) and 22 biomarkers (21%) were independent prognostic factors for PFS and OS, respectively.

10.3389/fonc.2022.997506

Conclusion: Our analysis identified a list of 13 biomarkers correlating with tumor control rates and survival. The future point will be gathering all these results to guide the clinical validation for a chordoma biomarker panel. Our identified biomarkers have strengths and weaknesses according to FDA's guidelines, some are affordable, have a low-invasive collection method and can be easily measured in any health care setting (RDW and D-dimer), but others molecular biomarkers need specialized assay techniques (microRNAs, PD-1 pathway markers, CDKs and somatic chromosome deletions were more chordoma-specific). A focused list of biomarkers that correlate with local recurrence, metastatic spread and survival might be a cornerstone to determine the need of adjuvant therapies.

KEYWORDS

Chordoma, prognostic biomarkers, molecular, skull base, spine, systematic review, multivariate analysis

Introduction

Chordomas are malignant bone tumors, of possible embryologic origin, arising anywhere along the neuroaxis (1), that are prone to both local recurrence and systemic relapse. Successful treatment of chordomas requires an experienced multidisciplinary team. The median overall survival of patients with chordoma is between 6.3 and 7.7 years (1, 2) with a 5-year overall survival around 70% in most series (2–4). For newly diagnosed patients, primary treatment consists of radical but safe resection; importantly, the extent of resection directly impacts outcomes in patients with skull base and spine chordomas. Over time, treatment of newly diagnosed chordomas has also evolved to incorporate adjuvant radiation, commonly with particle therapy (carbon-ion or proton-ion), particularly for skull base chordomas (5–8). While outcomes have improved over time, the rates of both local recurrence and distant metastases remain high. Ultimately, it is widely accepted that chordoma behaves across a biological spectrum – ranging from an indolent to a more aggressive phenotype with poorer survival and increased risk of local recurrence and metastatic disease. Unfortunately, there is still an unmet clinical need to develop effective systemic therapeutic agents that can be incorporated into the treatment paradigm for newly diagnosed and recurrent disease. To this end, clinical biomarkers that can be used to better tailor treatment and implement surveillance strategies for patients with chordoma are needed.

To meet this need for clinical biomarkers, several molecular studies have been conducted to identify therapeutic targets and prognostic markers in order to predict outcome (9–12). While many of the identified biomarkers have been validated in the research laboratory setting, the challenge lies in creating a biomarker panel that can be used in the clinical setting to guide real-time decision-making (13, 14). According to the US Food and Drug Administration (FDA), a biomarker is defined as a measurable characteristic that serves as an indicator of normal or pathological biological processes or responses to an exposure or intervention. Additionally, biomarkers can include molecular, histologic, radiographic or physiologic features (15). To be clinically utilized, there are certain critical features that any biomarker should include: 1) it should be non-invasive, easily measured, affordable, and produce rapid results; 2) it should be accessible from readily available sources, such as blood or urine; 3) it should have high sensitivity to allow early detection and have a high specificity in diseased samples; 4) the expression level of the biomarker should aid in risk stratification and possess prognostic value in terms of clinical outcomes; and 5) the biomarker should provide insight into the underlying disease mechanism (16). Specifically, a prognostic biomarker identifies the likelihood of a clinical event, disease recurrence, or progression in patients who have a medical condition of interest (17).

The objective of the present study was to review all prognostic biomarkers reported to date for chordomas in order to classify them according to localization, clinical utility, study design and statistical analysis.

Abbreviations: PRISMA, Preferred Reporting Items for Systematic Reviews and Meta-Analyses; FDA ,Food and Drug Administrations; PFS, Progression Free Survival; OS, Overall Survival; PD-1, programmed cell death protein 1; CDK, cyclin dependent kinases.

Methods

Study design

The current systematic review was performed according to the Preferred Reporting Items for Systematic Reviews and Meta-Analyses (PRISMA) guidelines (18). Studies were classified according to their design as *prospective* or *retrospective*. The level of evidence of each study was determined according to Oxford Centre for Evidence-Based Medicine (OCEBM) guidelines (19, 20). A systematic search was conducted in the PubMed/Medline and Google Scholar databases using the following terms: "chordoma", "biomarker", "overall survival", "progression free survival", "prognosis" and "biological marker". Any discrepancies were resolved through consensus. The search strategy utilized is reported in Figure 1. Inclusion criteria were as follows: i) the study must have been a prospective clinical trial or a retrospective case-control/cross sectional study published in English with no start date restriction and until February 2022 (when analyses for this review were performed); ii) the studies had to have reported chordomas confirmed by pathology (either in the skull base, mobile spine or sacrum); iii) the studies must have been *time-to-event studies*, which determined Progression Free Survival (PFS), and/or Overall Survival (OS); iv) the outcomes must have been analyzed by employing Kaplan-Meier (K-M) analysis with log-rank test or a Cox proportional hazards analysis (Cox model); v) the study must have included a full biomarker description including the brand name of the assay used, the source/matrix, the measurement technique and the assay technology used; vi) studies must not have had overlapping patients.

Studies using other biomarker categories, such as susceptibility/risk, diagnostic, monitoring, predictive, pharmacodynamic/response or safety were excluded.

Data abstraction

The extracted variables of each study include the following: Type of study, number of patients, localization of the primary tumor (skull base, mobile spine and/or sacrum), localization of the biomarker (cellular [nuclear, cytoplasm or cell membrane] or extracellular [blood or extracellular matrix]), assay technique for measurement, prognostic variable analyzed, non-parametric statistical approach, level of significance (p-value), and study design (prospective or retrospective). For classification purposes, we divide the biomarker as 'positive' or 'negative', according to its correlation with PFS or OS.

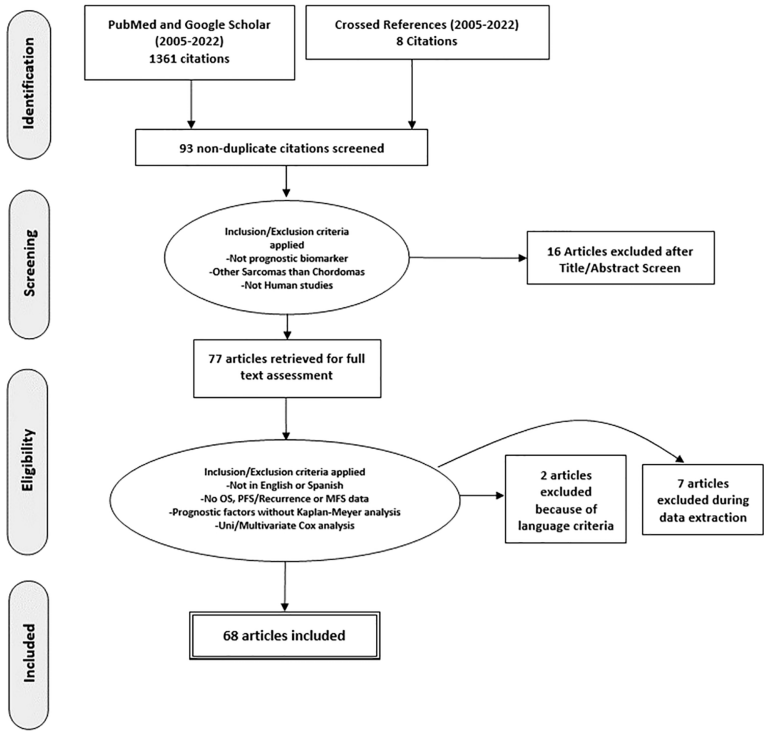

FIGURE 1
PRISMA-based flow chart of the study.

Statistical analysis

The primary goal was to determine whether there was significant correlation between the biomarker and prognostic variable analyzed, either using Log-rank univariate analysis or Cox regression multivariate analysis. All statistical analyses were performed using Microsoft Excel 365 (Microsoft, Washington, USA) and GraphPad Prism 9.0 statistical software package (La Jolla, California, USA). Descriptive statistics was the main statistical technique. Categorical variables are presented as proportions and the continuous variables are presented with mean and standard deviation or median and interquartile range.

Results

Literature review

Sixty-eight studies met predetermined eligibility criteria and were included for data abstraction (Figure 1). Fourteen studies used the same cohort of patients with different biomarkers, so a total number of 1263 patients are duplicated (21–33). Two studies were multicenter, which includes different populations, increasing the strength of the study (21, 34). With regard to study design, 5 studies were prospective (7.3%) (26, 35–38) and 63 studies were retrospective (92.7%) (21–25, 27–34, 39–87).

Identification of pertinent biomarkers

Data for a total of 3183 patients (not duplicated) were analyzed using different prognostic biomarkers. We excluded data from patients that was collected from the same hospital and in the same time frame. Of these, 3150 cases were adult patients (99%) and 33 were pediatric patients (1%); there were 1595 (50%) skull base chordomas, 1165 (36.6%) sacrococcygeal chordomas and 423 (13.4%) chordomas in mobile spine segments. A total of 103 biomarkers were analyzed in the 68 studies included in our analysis. Using the FDA classification system (15) we divided the biomarkers into 4 groups: molecular (82.5%; n=85), physiological (9.7%; n=10), histological (6.8%; n=7) and radiographic biomarkers (1%; n=1) (82).

Localization for each biomarker was different. A total of 40% were located in the nucleus (n=41), 22% in the cytoplasm (n=23), 14% in the cellular membrane (n=14), 7% in the extracellular matrix (n=7), and 16% from blood samples (n=17). The most common detection technique used was immunohistochemistry (IHC) in 66% of the studies (n=45) followed by polymerase chain reaction (PCR), serum protein analysis, and DNA sequencing in 20% (n=14), 9% (n=6) and 5% (n=3), respectively.

Three studies did not consider the expression of individual biomarkers, but instead they described a score using a group of biomarkers. One study describes an "miRNA-score", which measures the nuclear concentration of different microRNAs (miR-1290; miR-574-3p; miR-1; miR-1237-3p; miR-155; miR-140-3p) using PCR-based techniques (42). Another study describes a "Systemic Inflammatory Index" (SII), which is obtained by multiplying blood platelet count and neutrophil count and dividing by lymphocyte blood counts (*P x N/L*) (41), and the last study describes an "Immunoscore" based on the expression of CD3+ and CD8+ cells in the tumor specimen, using IHC (58).

Correlation of biomarkers with clinical outcomes

The clinical outcomes commonly evaluated in the selected studies were Progression free survival (PFS) and overall survival (OS). Only those biomarkers that demonstrated significant correlation with clinical outcomes in non-parametric tests were considered. Significant correlation of biomarkers with OS, PFS, or both, appeared in 35% (n=24), 23% (n=16) and 40% (n=27) of the studies, respectively. One study found that the lack of 1p36 LOH correlates with improved OS and PFS but did not report the HR and/or the CI (60). Because of this, we did not include their results in the following figures and analysis. Ultimately, 82 biomarkers were demonstrated to have statistical correlation in PFS and/or OS.

Elevated expression of 15 biomarkers was found to be associated with improved PFS and/or OS in chordoma patients (23, 24, 30, 31, 39, 55, 58, 62, 69, 76, 78, 84, 88). Among them, five biomarkers correlated with improved OS (elevated CD8+/Foxp3+ ratio, H-TERT promoter mutations, and high expression of SNF5 protein, c-MET receptor, and miRNA-1), eight biomarkers correlated with improved PFS (high *Immunoscore*, elevated PD1+ Tumor-Infiltrating Lymphocytes (TIL), high expression of PHLPP1 protein, Raf-1 and ERK proteins, elevated MMP-9/RECK protein ratio, and the high nuclear expression of miRNA-1290 and mi-RNA-1237-3p) and, 2 biomarkers were linked with both PFS and OS (elevated PD-L1+ TIL and high preoperative serum albumin level).

Increased expression of the remaining biomarkers (82%, n=67) correlated with poorer PFS and/or OS outcomes. Among them, the Ki-67 Level Index (LI) was the most frequent biomarker analyzed across the collection of studies (n=7, 10.3%). A high Ki-67 LI correlated with a shorter OS or PFS (even on COX regression analysis) (27, 33, 56).

Thirty-four studies analyzed the correlation between biomarkers and clinical outcomes using Cox multivariate regression and found that 35 biomarkers (43%) and 22 biomarkers (27%) were independent prognostic factors for PFS and OS, respectively. Although these biomarkers demonstrated a *p-value* less than 0.05, the confidence intervals (95% CI) varied greatly, partly due to limited sample sizes. To mention some

examples, in one study, high *Brachyury* gene expression or increased number of alterations in chromosome 2p (CNA 2p) correlated with improved PFS in a sample of 37 patients, but the CI of both is wide and include the value 1 (45). Furthermore, other biomarkers like VEGFA and E-cadherin had a CI of almost 1 in a sample size of 151 patients (27).

Forest plots in Figures 2 and 3, help to clearly differentiate those studies with more statistical strength. Overall, 13 biomarkers (19%) had significant correlation with both clinical outcomes (Table 1).

Discussion

There is increasing recognition of the need for predictive biomarkers to assist in the management of chordomas. To the best of our knowledge, this is the first comprehensive review that summarizes prognostic biomarkers in chordoma that have been reported to date. The mainstay of treatment for localized chordomas is extensive resection with negative margins, but local recurrence and systemic metastases are common. Clinically reliable prognostic biomarkers that could aid in determining whether a particular chordoma is likely to recur would impact clinical decision-making, particularly with regard to the need for adjuvant therapy, the early incorporation of systemic therapy agents, and surveillance strategies.

PFS is a surrogate for OS (89). However, OS in diseases with more than 12 months of survival after disease progression/recurrence (like chordomas) is not a reliable endpoint, and a very large number of patients is required to power studies to detect statistically significant differences in solely in OS (90). Therefore, we focused on studies of biomarkers with a significant correlation for both endpoints. Because most of these studies are retrospective, potential confounders must be unmasked and multivariate analysis is an effective method of ranking various prognostic factors (91, 92). We found 13 biomarkers which are independently prognostic for both PFS and OS with statistical significance (Table 1). In each case, we compared the Hazard ratio (HR) and the Confidence Interval (CI). As a rule, the width of the CI correlates inversely with the precision of the biomarker. In other words, some biomarkers have a significant *p-value*, but the CI could be wide or includes the value of 1 (Figures 2 and 3). This situation decreases the precision of the biomarker when compared with others and is therefore an important consideration. We further discuss some of the 13 biomarkers below.

The expression of Programmed Death-1 (PD-1) receptor, its ligand, and the immune microenvironment in chordoma have been widely studied (30, 58). The PD-1/PD-L1 pathway is

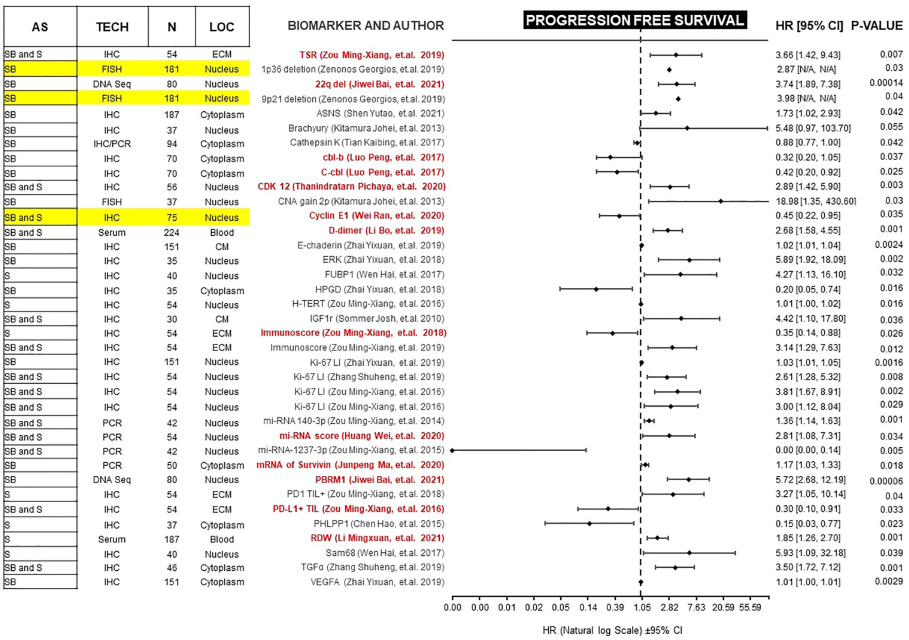

FIGURE 2
Forest plot showing biomarkers associated with PFS benefit on multivariate analysis. Those biomarkers with benefit in PFS and OS are marked in red. Prospective studies are marked in yellow. AS (Anatomic Site), TECH (Assay technique used), N (number of patients), LOC (Biomarker localization), SB (Skull base), S (Spine), IHC (Immunohistochemistry), PCR (Polymerase chain reaction), DNA Seq (DNA sequencing), FISH (fluorescence *in situ* hybridization), ECM (extracellular matrix), CM (Cell Membrane), TSR (Tissue-stroma ratio), PD-L1 TIL (Programmed death ligand 1, Tumor infiltrating lymphocytes), CDK (Cyclin-dependent kinase), TGFα (Tumor Growth Factor α), RDW (Red cell distribution width), CNA (copy number alterations), N/A (Not available).

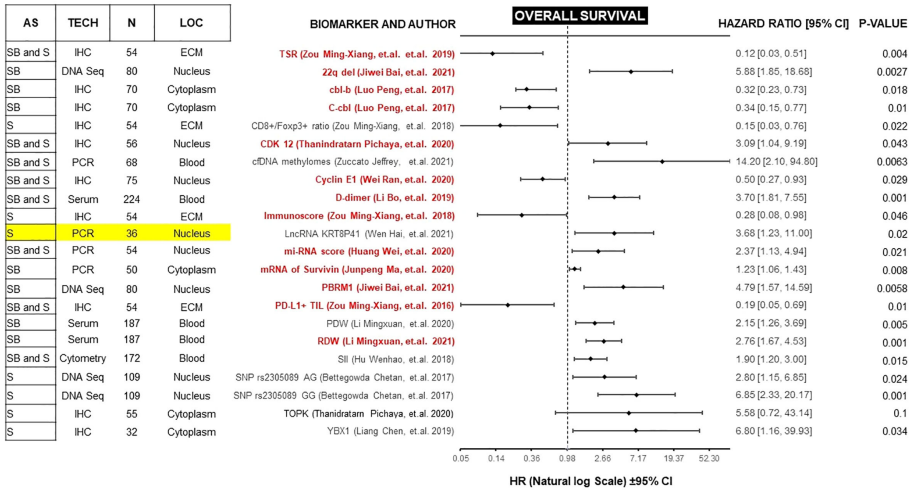

FIGURE 3
Forest plot showing biomarkers associated with OS benefit on multivariate analysis. Those biomarkers with benefit in PFS and OS are marked in red. Prospective studies are marked in yellow. AS (Anatomic Site), TECH (Assay technique used), N (number of patients), LOC (Biomarker localization), SB (Skull base), S (Spine), IHC (Immunohistochemistry), PCR (Polymerase chain reaction), DNA Seq (DNA sequencing), FISH (fluorescence *in situ* hybridization), ECM (extracellular matrix), CM (Cell Membrane), TSR (Tissue-stroma ratio), PD-L1 TIL (Programmed death ligand 1, Tumor infiltrating lymphocytes), RDW (Red cell distribution width), PDW (Platelet distribution width), LncRNA (Long non coding RNA).

responsible for modulating T-cell activation (anti-tumor response) and exhaustion in cancer (93). Tumor cells express PD-L1 as an adaptive immune mechanism to escape this anti-tumor environment with a high number of CD8+ cells (Immunoscore) (58) or a high CD8+/Foxp3 ratio (30), consistently analyzed in our review. The blockade of this immune checkpoint signal has the potential clinical benefit of increasing the sensitivity of chordoma cells to T-cell mediated lysis. In this sense, PD-L1+ is currently a prognostic and therapeutic biomarker (10, 94). FDA-approved monoclonal

TABLE 1 List of reported biomarkers with independent prognostic impact in PFS and OS (with Cox multivariate analysis).

Biomarker	Level of evidence	N	Localization	Assay Technique	HR os	OS 95% CI	p-value OS	HR PFS	PFS 95% CI	p-value PFS
22q del	IIb	80	Nucleus	DNA sequencing	5.88	1.85-18.68	***0.046***	3.74	1.89-7.38	***0.0024***
Cbl-B	IIb	70	Cytoplasm	IHC	0.32	0.234-0.734	***0.018***	0.32	0.20-1.054	***0.037***
C-Cbl	IIb	70	Cytoplasm	IHC	0.34	0.153-0.771	***0.01***	0.42	0.20-0.92	***0.025***
CDK-12	IIb	56	Nucleus	IHC	3.09	1.04-9.19	***0.043***	2.89	1.42-5.9	***0.003***
Ciclin E1	Ib	75	Nucleus	IHC	0.5	0.27-0.93	***0.029***	0.45	0.22-0.95	***0.035***
Immunoscore (Cd3+/Cd8+)	IIb	54	Extracellular matrix	IHC	0.28	0.08-0.98	***0.046***	0.35	0.14-0.88	***0.026***
mi-RNA Score	IIb	54	Nucleus	PCR	2.37	1.13-4.94	***0.021***	2.81	1.08-7.31	***0.034***
PBRM1	IIb	80	Nucleus	DNA sequencing	4.79	1.57-14.59	***0.006***	5.72	2.68-12.19	***0.00006***
PD-L1+ TIL	IIb	54	Extracelullar matrix	IHC	0.188	0.051-0.69	***0.01***	0.3	0.10-0.91	***0.033***
RDW	IIb	187	Blood sample	Hemocytometry	2.757	1.67-4.53	***0.001***	1.85	1.26-2.7	***0.001***
Survivin (mRNA)	IIb	50	Nucleus	PCR	1.23	1.06-1.43	***0.008***	1.17	1.03-1.33	***0.018***
Tissue-Stroma Ratio	IIb	54	Extracellular matrix	IHC	0.12	0.03-0.51	***0.004***	3.66	1.42-9.43	***0.007***
D-Dimer	IIb	224	Serum sample	Serum analysis	3.7	1.81-7.55	***0.001***	2.68	1.58-4.55	***0.001***

Le (Level of evidence); N (Number of Patients); PCR (Polymerase Chain Reaction); ihc (Immunohistochemistry); RDW (Red Cell Distribution Width); CDK (Cyclin-Dependent Kinase). Bold letters mean statistical significance.

antibodies currently used to block the PD-1/PD-L1 pathway include Pembrolizumab, Nivolumab, and Avelumab. Additionally, Nivolumab is currently being evaluated amongst rare CNS cancers including chordoma in 3 open clinical trials (NCT03173950, NCT02989636, NCT03623854). Even though the PD-1/PD-L1 pathway appears to be a very promising therapeutic and prognostic marker, the clones of anti-mouse PD-1 antibodies used are not consistent, and validation of them is needed to reach a wide reproducibility.

MicroRNA are small noncoding RNAs that play important roles in transcriptional gene regulation. Different miRNAs have been implicated in several cancers, including chordomas (30, 31, 42, 69, 88). Multiple proteins are involved in chordomagenesis, therefore it is unlikely that a single miRNA would provide optimal information regarding prognosis. Rather than focusing on a single miRNA, Huang et al. identified 6 prognostic miRNAs and developed a miRNA score (miRscore) based on integrated data. Using this approach, the miRscore was able to predict clinical outcome in chordoma (42). However, the main limitation of using this biomarker in clinical practice is the affordability along with ease and consistency of measurement using RT-PCR. An alternative approach is miRNA-seq but that is also hampered by technical complications limiting broad adoption (95).

Survivin is an apoptosis inhibitor protein widely expressed in tumors and non-terminally differentiated tissues (96). Ma et al. evaluated the expression of survivin in primary versus recurrent chordomas and demonstrated that survivin expression is elevated in recurrent tumors. Additionally, they found survivin levels were increased in recurrent tumors collected from the same patient, and expression of survivin was found to be an independent prognostic factor for progression (44). However, the lab technique used to quantify survivin expression was quantitative RT-PCR which is not practical assay from a clinical testing standpoint, although the use of survivin as a biomarker offers the advantage of measuring a single molecule as compared with the use of miRscore which measures 6 different miRNAs (42).

The Cyclin-dependent kinases (CDKs) are serine/threonine nuclear protein kinases involved in DNA transcription and cell cycle progression. In chordoma, CDK overexpression induces migration of tumor cells, proliferation, and tumor growth. In particular, the CDKN2A/p16INK4a/CDK4-6/RB pathway is a well-known cascade involved in tumor cell proliferation across multiple cancer types (97). The CDKN2A gene, and its protein product p16INK4a, have an inhibitory role over CDK4 and 6, decreasing cell proliferation. Mutations in CDKN2A gene have been studied as a prognostic biomarker in independent studies (38, 43, 50), but none have found a significant correlation with clinical outcomes. Only Sommer et al. (50) found that CDKN2A gene expression level correlated with a higher PFS *(p=.03)*; however, this correlation was not significant in multivariate analysis. CDK4 expression was found to be significantly associated with OS in a study by Yakkioui et al. (83), however, this was only in univariate analysis *(p=.021)*. These data suggest that this pathway has an unclear prognostic role in chordoma PFS or OS. Despite these uncertain results, the pathway is currently being evaluated for chordoma therapy. For example, palbociclib is an approved CDK4/6 inhibitor for chordomas with CDKN2A gene loss (98) and is currently being evaluated in a clinical trial (NCT03110744).

CDK12 overexpression increases the phosphorylation of antiapoptotic proteins, including Survivin and MCL-1 and correlates with shorter overall survival in breast cancer, ovarian cancer and gastric cancer (99, 100). Pichaya et al. measured the expression of CDK12 in tumor tissue in a cohort of 56 spine chordoma patients using immunohistochemistry, and grouped chordomas as those with low CDK-12 expression (less than 75% of the cells with positive nuclear staining) and those with high CDK-12 expression (more than 75% of the cells with positive nuclear staining) (52). The statistical analysis demonstrated a negative effect of this CDK in prognosis, however the results need to be interpreted with caution because the wide CI indicates lack of precision and little knowledge about the effect. While a study with a larger sample is required, the strength of this biomarker lies in the relatively easy assay technique, affordability and it resides upstream of other biomarkers implicated in poor clinical outcomes.

Somatic chromosome deletions have been studied as a type of genomic driver event in chordomas. Bai et al. conducted whole-genome sequencing of 80 skull base chordomas and evaluated the prognostic value of 17 somatic chromosomal events including gains of chromosomes 1q, 7p, and 7q, and deletions of 1p, 3, 4, 9, 10, 13q, 14q, 18, and 22q (43). Of these, the hemizygous deletion of 22q, where SMARCB1 gene is located, demonstrated a strong association with clinical outcomes. The homozygous deletion of SMARCB1 is a hallmark of poorly differentiated chordoma (101), but this finding suggests that even partial inactivation of SMARCB1 in conventional chordoma could be used as a prognostic biomarker. Nevertheless, the wide CI in this study highlights the need for validation with a larger sample. Although genome sequencing is an expensive and highly specialized assay technique, chromosomal deletion can be assessed with Fluorescence *in situ* hybridization (FISH) or spectral karyotyping (SKY) (102). In this regard, it is worth mentioning that Zenonos et al. present one of the few prospective studies with a strong statistical design (36). Using FISH, they found that skull base chordoma patients with a threshold percentage of cells with 1p36 and 9p21 deletions (more than 15% for 1p36 and more than 4% for 9p21) have a shorter PFS. Despite being a prospective study with thorough statistical design and promising HR, we did not include in Table 1 because the study did not include OS and CIs in the analysis.

The last two biomarkers were assessed in blood samples and are the most promising in terms of affordability, limited invasiveness, reproducibility, assay technique, and required sample size (22, 46). Other studies have reported that increased levels of RDW or D-dimer are observed in many

types of cancers and act as useful markers of adverse prognosis (103–106). In chordoma patients, a preoperative measurement above the cut-off values of 12.7 for RDW (in a spine chordoma population) and 840 µg/L for D-dimer (in a skull base chordoma population) were associated with a poor prognosis. However, these biomarkers do not provide an insight about the underlying disease mechanism, and they lack specificity (106–108).

After analyzing all of the available information gathered for this review, Table 1 presents a set of biomarkers that have been demonstrated to correlate with both PFS and OS. While additional studies are needed to validate a narrower list of biomarkers with the strongest prognostic value, this proposed panel serves as a starting point. Given the techniques employed and the already available testing, there are biomarkers that can be readily incorporated into routine clinical setting. For example, preoperative D-dimer can be readily integrated as a potential prognostic biomarker due to its low-invasiveness, accessible measurement technique, and affordability. Also, the D-dimer study collected a significant cohort of patients (n=224) when compared with other biomarker studies and reported results using multivariate analysis with narrow CI (PFS, HR 2.68 [1.58, 4.55], p=.001; OS, 3.70 [1.81, 7.55], p=.001).

Furthermore, our inferential statistical analysis of the data has limitations because chordoma has intrinsic low incidence. Most of the studies report a limited patient cohort, making it difficult to assess the multivariate analysis of each biomarker. It is worth mentioning that none of the biomarkers met all the criteria mentioned in the introduction of this manuscript. They need to be validated in prospective studies with a larger sample size, and across multiple institutions. Affordability is one of the most important factors to consider for a biomarker that can be tested ubiquitously. The less expensive techniques used were serum protein analysis or hemocytometry, followed by immunohistochemistry and finally, some of the studies used expensive measurement techniques such as DNA sequencing (21, 43, 62), DNA microarrays (60, 86) and FISH (36, 45, 74). Also, when the lab technique is expensive or difficult to use, the studies are concentrated among the same centers, resulting in limited widespread integration. In order to use biomarker information to evaluate chordoma patients and enable clinical decision-making, high-quality prospective studies to evaluate the known potential biomarkers with strong biological underpinnings in chordomas are warranted. While retrospective studies remain useful in identifying potential new biomarkers, prospective trials with larger cohorts are essential for the eventual clinical translation of biomarkers.

Conclusion

In this study we gathered all the prognostic biomarker studies reported to date according to PRISMA guidelines. More than a hundred biomarkers have been analyzed. The information is assorted, heterogenous, and lacks consistency in terms of markers used and tests performed. There is an increasing need to gather all these results to guide future validation studies to determine its clinical utility. A comprehensive understanding of this information can eventually help determine adjuvant treatments and surveillance strategies for patients with the worst prognosis. Further work is needed to validate a narrower list of biomarkers that correlate with overall survival, local recurrence, and metastatic spread with the strongest significance. Taken collectively, we encourage the comprehensive centers that evaluate and treat chordoma patients to collaboratively work to create a panel of prognostic biomarkers that can then be applied universally.

Data availability statement

The original contributions presented in the study are included in the article/supplementary material. Further inquiries can be directed to the corresponding author.

Author contributions

The authors confirm contribution to the paper as follows:

Study conception and design: FR and SR. Data collection: FR and SR. Analysis and interpretation of results: FR, CA-B, AC, AB, W-LW, AL, LR, FD, and SR. Draft manuscript preparation: FR, CA-B, KA, LR, FD, and SR. All authors reviewed the results and approved the final version of the manuscript.

Acknowledgments

We thank Preeti Ramadoss, PhD for her editorial assistance in preparing this publication.

Conflict of interest

The authors declare that the research was conducted in the absence of any commercial or financial relationships that could be construed as a potential conflict of interest.

Publisher's note

References

1. Ulici V, Hart J. Chordoma. *Arch Pathol Lab Med* (2022) 146(3):386–95. doi: 10.5858/arpa.2020-0258-RA

2. Smoll NR, Gautschi OP, Radovanovic I, Schaller K, Weber DC. Incidence and relative survival of chordomas: The standardized mortality ratio and the impact of chordomas on a population. *Cancer* (2013) 119(11):2029–37. doi: 10.1002/cncr.28032

3. Jones PS, Aghi MK, Muzikansky A, Shih HA, Barker FG2nd, Curry WT. Outcomes and patterns of care in adult skull base chordomas from the surveillance, epidemiology, and end results (SEER) database. *J Clin Neurosci* (2014) 21(9):1490–6. doi: 10.1016/j.jocn.2014.02.008

4. Scampa M, Tessitore E, Dominguez DE, Hannouche D, Buchs NC, Kalbermatten DF, et al. Sacral chordoma: A population-based analysis of epidemiology and survival outcomes. *Anticancer Res* (2022) 42(2):929.LP–37. doi: 10.21873/anticanres.15552

5. Takahashi S, Kawase T, Yoshida K, Hasegawa A, Mizoe J-E. Skull base chordomas: Efficacy of surgery followed by carbon ion radiotherapy. *Acta Neurochirurgica* (2009) 151(7):759–69. doi: 10.1007/s00701-009-0383-5

6. Bugoci DM, Girvigian MR, Chen JCT, Miller MM, Rahimian J. Photon-based fractionated stereotactic radiotherapy for postoperative treatment of skull base chordomas. *Am J Clin Oncol* (2013) 36(4):404–10. doi: 10.1097/COC.0b013e318248dc6f

7. Yu E, Koffer PP, DiPetrillo TA, Kinsella TJ. Incidence, treatment, and survival patterns for sacral chordoma in the united states, 1974-2011. *Front Oncol* (2016) 6:203–. doi: 10.3389/fonc.2016.00203

8. Chambers KJ, Lin DT, Meier J, Remenschneider A, Herr M, Gray ST. Incidence and survival patterns of cranial chordoma in the united states. *Laryngoscope* (2014) 124(5):1097–102. doi: 10.1002/lary.24420

9. Liu T, Shen JK, Choy E, Zhang Y, Mankin HJ, Hornicek FJ, et al. CDK4 expression in chordoma: A potential therapeutic target. *J Orthopaedic Res* (2018) 36(6):1581–9. doi: 10.1002/jor.23819

10. Fujii R, Friedman ER, Richards J, Tsang KY, Heery CR, Schlom J, et al. Enhanced killing of chordoma cells by antibody-dependent cell-mediated cytotoxicity employing the novel anti-PD-L1 antibody avelumab. *Oncotarget* (2016) 7(23):33498–511. doi: 10.18632/oncotarget.9256

11. Stacchiotti S, Tamborini E, Lo Vullo S, Bozzi F, Messina A, Morosi C, et al. Phase II study on lapatinib in advanced EGFR-positive chordoma. *Ann Oncol* (2013) 24(7):1931–6. doi: 10.1093/annonc/mdt117

12. Houessinon A, Boone M, Constans J-M, Toussaint P, Chauffert B. Sustained response of a clivus chordoma to erlotinib after imatinib failure. *Case Rep Oncol* (2015) 8:25–9. doi: 10.1159/000371843

13. Romeo S, Hogendoorn PCW. Brachyury and chordoma: the chondroid-chordoid dilemma resolved? *J Pathol* (2006) 209(2):143–6. doi: 10.1002/path.1987

14. Vujovic S, Henderson S, Presneau N, Odell E, Jacques TS, Tirabosco R, et al. Brachyury, a crucial regulator of notochordal development, is a novel biomarker for chordomas. *J Pathol* (2006) 209(2):157–65. doi: 10.1002/path.1969

15. FDA-NIH Biomarker Working Group.. *BEST (Biomarkers, EndpointS, and other Tools) Resource [Internet]*. (US: Silver Spring (MD): Food and Drug Administration) (2016).

16. Group BDW. Biomarkers and surrogate endpoints: preferred definitions and conceptual framework. *Clin Pharmacol Ther* (2001) 69(3):89–95. doi: 10.1067/mcp.2001.113989

17. Oldenhuis CNAM, Oosting SF, Gietema JA, de Vries EGE. Prognostic versus predictive value of biomarkers in oncology. *Eur J Cancer (Oxford England: 1990)*. (2008) 44(7):946–53. doi: 10.1016/j.ejca.2008.03.006

18. Moher D, Liberati A, Tetzlaff J, Altman DG. Preferred reporting items for systematic reviews and meta-analyses: the PRISMA statement. *J Clin Epidemiol* (2009) 21:6(7). doi: 10.1371/journal.pmed.1000097

19. Richards D. GRADING – levels of evidence. *Evidence-Based Dentistry* (2009) 10(1):24–5. doi: 10.1038/sj.ebd.6400636

20. OCEBM Levels of Evidence Working Group. *The 2011 Oxford levels of evidence*. (UK: University of Oxford) (2011). Available at: http://www.cebm.net/index.aspx?o=5653.

21. Bettegowda C, Yip S, Lo S-FL, Fisher CG, Boriani S, Rhines LD, et al. Spinal column chordoma: prognostic significance of clinical variables and T (brachyury) gene SNP rs2305089 for local recurrence and overall survival. *Neuro-Oncology* (2017) 19(3):405–13. doi: 10.1093/neuonc/now156

22. Li M, Shen Y, Xiong Y, Bai J, Wang S, Li C, et al. High red cell distribution width independently predicts adverse survival in patients with newly diagnosed skull base chordoma. *OncoTargets Ther* (2021) 14:5435. doi: 10.2147/OTT.S335454

23. Li M, Bai J, Wang S, Zhai Y, Zhang S, Li C, et al. Prognostic value of cumulative score based on preoperative fibrinogen and albumin level in skull base chordoma. *OncoTargets Ther* (2020) 13:8337. doi: 10.2147/OTT.S257779

24. Li M, Zhai Y, Bai J, Wang S, Gao H, Li C, et al. SNF5 as a prognostic factor in skull base chordoma. *J Neuro-Oncol* (2018) 137(1):139–46. doi: 10.1007/s11060-017-2706-3

25. Thanindratarn P, Dean DC, Nelson SD, Hornicek FJ, Duan Z. T-LAK cell-originated protein kinase (TOPK) is a novel prognostic and therapeutic target in chordoma. *Cell Proliferation* (2020) 53(10):e12901–e. doi: 10.1111/cpr.12901

26. Wen H, Fu Y, Zhu Y, Tao S, Shang X, Li Z, et al. Long non-coding RNA KRT8P41/miR-193a-3p/FUBP1 axis modulates the proliferation and invasion of chordoma cells. *J Bone Oncol* (2021) 31:100392–. doi: 10.1016/j.jbo.2021.100392

27. Zhai Y, Bai J, Li M, Wang S, Li C, Wei X, et al. A nomogram to predict the progression-free survival of clival chordoma. *J Neurosurg* (2019) 134(1):144–52. doi: 10.3171/2019.10.JNS192414

28. Zhai Y, Bai J, Gao H, Wang S, Li M, Gui S, et al. Clinical features and prognostic factors of children and adolescents with clival chordomas. *World Neurosurg* (2017) 98:323–8. doi: 10.1016/j.wneu.2016.11.015

29. Zhang K, Chen H, Wu G, Chen K, Yang H. High expression of SPHK1 in sacral chordoma and association with patients' poor prognosis. *Med Oncol* (2014) 31(11):1–5. doi: 10.1007/s12032-014-0247-6

30. Zou M-X, Guo K-M, Lv G-H, Huang W, Li J, Wang X-B, et al. Clinicopathologic implications of CD8+/Foxp3+ ratio and miR-574-3p/PD-L1 axis in spinal chordoma patients. *Cancer Immunol Immunother* (2018) 67(2):209–24. doi: 10.1007/s00262-017-2080-1

31. Zou M-X, Huang W, Wang X-b, Li J, Lv G-H, Wang B, et al. Reduced expression of miRNA-1237-3p associated with poor survival of spinal chordoma patients. *Eur Spine J* (2015) 24(8):1738–46. doi: 10.1007/s00586-015-3927-9

32. Zou M-X, Huang W, Wang X-B, Lv G-H, Li J, Deng Y-W. Identification of miR-140-3p as a marker associated with poor prognosis in spinal chordoma. *Int J Clin Exp Pathol* (2014) 7(8):4877.

33. Zou M-X, Lv G-H, Li J, She X-L, Jiang Y. Upregulated human telomerase reverse transcriptase (hTERT) expression is associated with spinal chordoma growth, invasion and poor prognosis. *Am J Trans Res* (2016) 8(2):516.

34. Zuccato JA, Patil V, Mansouri S, Liu JC, Nassiri F, Mamatjan Y, et al. DNA Methylation based prognostic subtypes of chordoma tumors in tissue and plasma. *Neuro-Oncology* (2021) 24(3):442–54. doi: 10.1093/neuonc/noab235

35. Wei R, Dean DC, Thanindratarn P, Hornicek FJ, Guo W, Duan Z. Prognostic significance of cyclin E1 expression in patients with chordoma: A clinicopathological and immunohistochemical study. *Frontiers Oncology* (2020) 10:596330. doi: 10.3389/fonc.2020.596330

36. Zenonos GA, Fernandez-Miranda JC, Mukherjee D, Chang Y-F, Panayidou K, Snyderman CH, et al. Prospective validation of a molecular prognostication panel for clival chordoma. *J Neurosurg* (2018) 130(5):1528–37. doi: 10.3171/2018.3.JNS172321

37. Lebellec L, Bertucci F, Tresch-Bruneel E, Bompas E, Toiron Y, Camoin L, et al. Circulating vascular endothelial growth factor (VEGF) as predictive factor of progression-free survival in patients with advanced chordoma receiving sorafenib: an analysis from a phase II trial of the french sarcoma group (GSF/GETO). *Oncotarget* (2016) 7(45):73984–94. doi: 10.18632/oncotarget.12172

38. Yang C, Sun J, Yong L, Liang C, Liu T, Xu Y, et al. Deficiency of PTEN and CDKN2A Tumor-suppressor genes in conventional and chondroid chordomas: Molecular characteristics and clinical relevance. *OncoTargets Ther* (2020) 13:4649. doi: 10.2147/OTT.S252990

39. Chen H, Zhang K, Wu G, Song D, Chen K, Yang H. Low expression of PHLPP1 in sacral chordoma and its association with poor prognosis. *Int J Clin Exp Pathol* (2015) 8(11):14741–. doi: 10.1007/s12032-014-0247-6

40. Wen H, Li P, Ma H, Zheng J, Yu Y, Lv G. High expression of Sam68 in sacral chordomas is associated with worse clinical outcomes. *OncoTargets Therapy* (2017) 10:4691–700. doi: 10.2147/OTT.S147446.

41. Hu W, Yu J, Huang Y, Hu F, Zhang X, Wang Y. Lymphocyte-related inflammation and immune-based scores predict prognosis of chordoma patients after radical resection. *Trans Oncol* (2018) 11(2):444–9. doi: 10.1016/j.tranon.2018.01.010

42. Huang W, Yan Y-G, Wang W-J, Ouyang Z-H, Li X-L, Zhang T-L, et al. Development and validation of a 6-miRNA prognostic signature in spinal chordoma. *Front Oncol* (2020) 10:2298–. doi: 10.3389/fonc.2020.556902

43. Bai J, Shi J, Li C, Wang S, Zhang T, Hua X, et al. Whole genome sequencing of skull-base chordoma reveals genomic alterations associated with recurrence and

chordoma-specific survival. *Nature Communications* (2021) 12(1):757. doi: 10.1038/s41467-021-21026-5

44. Ma J, Tian K, Du J, Wu Z, Wang L, Zhang J. High expression of survivin independently correlates with tumor progression and mortality in patients with skull base chordomas. *J Neurosurg* (2020) 132(1):140–9. doi: 10.3171/2018.8.JNS181580

45. Kitamura Y, Sasaki H, Kimura T, Miwa T, Takahashi S, Kawase T, et al. Molecular and clinical risk factors for recurrence of skull base chordomas: Gain on chromosome 2p, expression of brachyury, and lack of irradiation negatively correlate with patient prognosis. *J Neuropathol Exp Neurol* (2013) 72(9):814–21. doi: 10.1093/jnen/72.9.814

46. Li B, Zhang H, Zhou P, Yang J, Wei H, Yang X, et al. Prognostic significance of pretreatment plasma d-dimer levels in patients with spinal chordoma: A retrospective cohort study. *Eur Spine J* (2019) 28(6):1480–90. doi: 10.1007/s00586-018-05872-4

47. Li M, Bai J, Wang S, Zhai Y, Zhang S, Li C, et al. Mean platelet volume and platelet distribution width serve as prognostic biomarkers in skull base chordoma: A retrospective study. *BMC Cancer* (2020) 20(1):988. doi: 10.1186/s12885-020-07497-7

48. Liang CA-O, Ma Y, Yong L, Yang C, Wang P, Liu X, et al. Y-box binding protein-1 promotes tumorigenesis and progression via the epidermal growth factor receptor/AKT pathway in spinal chordoma *Cancer Science* (2019) 110(1):166–79. doi: 10.1111/cas.13875

49. Luo P, Wang X, Zhou J, Li L, Jing Z. C-cbl and cbl-b expression in skull base chordomas is associated with tumor progression and poor prognosis. *Human Pathology* (2018) 74:129–34. doi: 10.1016/j.humpath.2017.12.019

50. Sommer J, Itani DM, Homlar KC, Keedy VL, Halpern JL, Holt GE, et al. Methylthioadenosine phosphorylase and activated insulin-like growth factor-1 receptor/insulin receptor: Potential therapeutic targets in chordoma. *J Pathol* (2010) 220(5):608–17. doi: 10.1002/path.2679

51. Shen Y, Li M, Xiong Y, Gui S, Bai J, Zhang Y, et al. *Proteomics analysis identified ASNS as a novel biomarker for predicting recurrence of skull base chordoma*. Frontiers in oncology (Switzerland). (2021) 2234–943X.

52. Thanindratarn P, Dean DC, Feng W, Wei R, Nelson SD, Hornicek FJ, et al. Cyclin-dependent kinase 12 (CDK12) in chordoma: Prognostic and therapeutic value. *Eur Spine J* (2020) 29(12):3214–28. doi: 10.1007/s00586-020-06543-z

53. Tian K, Ma J, Wang L, Wang K, Li D, Hao S, et al. *Expression of cathepsin K in skull base chordoma*. (US: World Neurosurgery) (2017) 1878–8769.

54. Wen H, Ma H, Li P, Zheng J, Yu Y, Lv G. Expression of far upstream element-binding protein 1 correlates with c-myc expression in sacral chordomas and is associated with tumor progression and poor prognosis. *Biochem Biophys Res Commun* (2017) 491(4):1047–54. doi: 10.1016/j.bbrc.2017.08.008

55. Zhai Y, Bai J, Wang S, Li M, Wang F, Li C, et al. Aberrant expression of extracellular signal-regulated kinase and 15-hydroxyprostaglandin dehydrogenase indicates radiation resistance and poor prognosis for patients with clival chordomas. *World Neurosurg* (2018) 115:e146–e51. doi: 10.1016/j.wneu.2018.03.216

56. Zhang S, Bai J, Li M, Zhai Y, Wang S, Liu Q, et al. Predictive value of transforming growth factor-α and ki-67 for the prognosis of skull base chordoma. *World Neurosurg* (2019) 129:e199–206. doi: 10.1016/j.wneu.2019.05.110

57. Zou MX, Peng AB, Lv GH, Wang XB, Li J, She XL, et al. Expression of programmed death-1 ligand (PD-L1) in tumor-infiltrating lymphocytes is associated with favorable spinal chordoma prognosis. *American J Translational Res* (2016) 8(7):3274–87.

58. Zou M-X, Zheng B-W, Liu F-S, Wang X-B, Hu J-R, Huang W, et al. The relationship between tumor-stroma ratio, the immune microenvironment, and survival in patients with spinal chordoma. *Neurosurgery* (2019) 85(6):E1095–E110. doi: 10.1093/neuros/nyz333

59. Zou MX, Lv GH, Wang XB, Huang W, Li J, Jiang Y, et al. Clinical impact of the immune microenvironment in spinal chordoma: Immunoscore as an independent favorable prognostic factor. *Neurosurgery* (2019) 84(6):E318–33. doi: 10.1093/neuros/nyy274

60. Longoni M, Orzan F, Stroppi M, Boari N, Mortini P, Riva P. Evaluation of 1p36 markers and clinical outcome in a skull base chordoma study. *Neuro-Oncology* (2008) 10(1):52–60. doi: 10.1215/15228517-2007-048

61. Akhavan-Sigari R, Gaab Mr Fau - Rohde V, Rohde V Fau - Abili M, Abili M Fau - Ostertag H, Ostertag H. Prognostic significance of immunohistochemical expression of VEGFR2 and iNOS in spinal chordoma. *European Spine J* (2014) 23 (11):2416–22. doi: 10.1007/s00586-014-3417-5

62. Bettegowda C, Yip S, Jiang B, Wang W-L, Clarke MJ, Lazary A, et al. Prognostic significance of human telomerase reverse transcriptase promoter region mutations C228T and C250T for overall survival in spinal chordomas. *Neuro-Oncology* (2019) 21(8):1005–15. doi: 10.1093/neuonc/noz066

63. Boari N, Gagliardi F, Cavalli A, Gemma M, Ferrari L, Riva P, et al. Skull base chordomas: Clinical outcome in a consecutive series of 45 patients with long-term follow-up and evaluation of clinical and biological prognostic factors. *J Neurosurg*, (2016) 125(2):450–60. doi: 10.3171/2015.6.JNS142370

64. Chen C, Yang Hl Fau - Chen K-W, Chen Kw Fau - Wang G-L, Wang Gl Fau - Lu J, Lu J Fau - Yuan Q, Yuan Q Fau - Gu Y-P, et al. High expression of survivin in sacral chordoma. *Medical oncology (Northwood, London, England)*, (2013) 30 (2):529. doi: 10.1007/s12032-013-0529-4.

65. Chen H, Garbutt CC, Spentzos D, Choy E, Hornicek FJ, Duan Z. Expression and therapeutic potential of SOX9 in chordoma. *Clinical cancer research: An official journal of the American Association for Cancer Research (US)*. (2017); pp. 1557–3265.

66. Chen KW, Yang Hl Fau - Lu J, Lu J Fau - Wang G-L, Wang Gl Fau - Ji Y-M, Ji Ym Fau - Wu G-Z, Wu Gz Fau - Zhu L-F, et al. Expression of vascular endothelial growth factor and matrix metalloproteinase-9 in sacral chordoma. *J Neuro-Oncology*, (2011) 101(3):357–63. doi: 10.1007/s11060-010-0263-0.

67. de Castro CV, Guimaraes G, Aguiar SJr, Aguiar SJr, Lopes A, Lopes A, et al. Tyrosine kinase receptor expression in chordomas: phosphorylated AKT correlates inversely with outcome. *Human Pathology* (2013) 44(9):1747–55. doi: 10.1016/j.humpath.2012.11.024

68. Ding Y, Bui MM, Wang Q, Sun X, Zhang M, Niu X, et al. *ADAM10 is a potential novel prognostic biomarker for sacral chordoma*. Annals of clinical and laboratory science (US). (2019) pp. 1550–8080.

69. Duan Z, Shen J, Yang X, Yang P, Osaka E, Choy E, et al. Prognostic significance of miRNA-1 (miR-1) expression in patients with chordoma. *J Orthopaedic Res* (2014) 32(5):695–701. doi: 10.1002/jor.22589

70. Tauziéde-Espariat A, Bresson D, Bresson D, Polivka M, Polivka M, Bouazza S, et al. Prognostic and therapeutic markers in chordomas: A study of 287 tumors. *Journal of neuropathology and experimental neurology* (2016) 75(2):111–20. doi: 10.1093/jnen/nlv010

71. Feng Y, Zhang Q, Wang Z, Yan B, Wei W, Li P. Overexpression of the BMP4/SMAD signaling pathway in skull base chordomas is associated with poor prognosis. *International J Clin E Pathol* (2015) 8(7):8268–75.

72. Gulluoglu S, Tuysuz EC, Sahin M, Yaltirik CK, Kuskucu A, Ozkan F, et al. The role of TNF-α in chordoma progression and inflammatory pathways. *Cellular Oncology (Dordrecht)* (2019) 42(5):663–77. doi: 10.1007/s13402-019-00454-y

73. Hobusch GM, Bodner F, Walzer S, Marculescu R, Funovics PT, Sulzbacher I, et al. C-reactive protein as a prognostic factor in patients with chordoma of lumbar spine and sacrum–a single center pilot study. *World J Surgical Oncology* (2016) 14:111. doi: 10.1186/s12957-016-0875-8

74. Horbinski C, Oakley GJ, Cieply K, Mantha GS, Nikiforova MN, Dacic S, et al. The prognostic value of ki-67, p53, epidermal growth factor receptor, 1p36, 9p21, 10q23, and 17p13 in skull base chordomas. *Arch Pathol Lab Med* (2010) 134 (8):1170–6. doi: 10.5858/2009-0380-OA.1

75. Morimoto Y, Tamura R, Ohara K, Kosugi K, Oishi Y, Kuranari Y, et al. Prognostic significance of VEGF receptors expression on the tumor cells in skull base chordoma. *J Neuro-Oncology* (2019) 144(1):65–77. doi: 10.1007/s11060-019-03221-z

76. Naka T, Kuester D, Boltze C, Scheil-Bertram S, Samii A, Herold C, et al. Expression of hepatocyte growth factor and c-MET in skull base chordoma. *Cancer: Interdiscip Int J Am Cancer Society* (2008) 112(1):104–10. doi: 10.1002/cncr.23141

77. Otani R, Mukasa A, Shin M, Omata M, Takayanagi S, Tanaka S, et al. Brachyury gene copy number gain and activation of the PI3K/Akt pathway: Association with upregulation of oncogenic brachyury expression in skull base chordoma. *J Neurosurg* (2018) 128(5):1428–37. doi: 10.3171/2016.12.JNS161444

78. Rahmah NN, Sakai K, Nakayama J, Hongo K. Reversion-inducing cysteine-rich protein with kazal motifs and matrix metalloproteinase-9 are prognostic markers in skull base chordomas. *Neurosurg review* (2010) 33(2):167–73. doi: 10.1007/s10143-009-0228-y

79. Saad AG, Collins MH. Prognostic value of MIB-1, e-cadherin, and CD44 in pediatric chordomas. *Pediatric Developmental Pathology* (2005) 8(3):362–368. doi: 10.1007/s10024-005-1127-z

80. Tosuner Z, Bozkurt Su Fau - Kiliç T, Kiliç T Fau - Yilmaz B, Yilmaz B. The role of EGFR, hepatocyte growth factor receptor (c-met), c-ErbB2 (HER2-neu) and clinicopathological parameters in the pathogenesis and prognosis of chordoma. *Turk Patoloji Dergisi* (2017) 33(2):112–20. doi: 10.5146/tjpath.2016.01378

81. Wang B, Zhang K, Chen H, Lu J, Wu G, Yang H, et al. miR-1290 inhibits chordoma cell proliferation and invasion by targeting Robo1. *Translational Cancer Res* (2019) 8(2):542–51. doi: 10.21037/tcr.2019.03.13

82. Wei W, Wang K, Liu Z, Tian K, Wang L, Du J, et al. Radiomic signature: A novel magnetic resonance imaging-based prognostic biomarker in patients with skull base chordoma. *Radiother Oncol* (2019) 141:239–46. doi: 10.1016/j.radonc.2019.10.002

83. Yakkioui Y, Temel Y, Creytens D, Jahanshahi A, Fleischeuer R, Santegoeds RGC, et al. A comparison of cell-cycle markers in skull base and sacral chordomas. *World Neurosurg* (2014) 82(1-2):e311–e8. doi: 10.1016/j.wneu.2013.01.131

84. Zhang K, Chen H, Zhang B, Sun J, Lu J, Chen K, et al. Overexpression of raf-1 and ERK1/2 in sacral chordoma and association with tumor recurrence. *Int J Clin Exp Pathol* (2015) 8(1):608.

85. Zhou M, Chen K Fau - Yang H, Yang H Fau - Wang G, Wang G Fau - Lu J, Lu J Fau - Ji Y, Ji Y Fau - Wu C, et al. Expression of insulin-like growth factor II mRNA-binding protein 3 (IMP3) in sacral chordoma. *J Neuro-Oncology* (2014) 116 (1):77–82. doi: 10.1007/s11060-013-1274-4

86. Zhu GG, Ramirez D, Chen W, Lu C, Wang L, Frosina D, et al. Chromosome 3p loss of heterozygosity and reduced expression of H3K36me3 correlate with longer relapse-free survival in sacral conventional chordoma. *Hum Pathol* (2020) 104:73–83. doi: 10.1016/j.humpath.2020.07.002

87. Li Z, Lv T, Lv T, Liu Y, Liu Y, Huang X, et al. *PARP1 is a novel independent prognostic factor for the poor prognosis of chordoma*. Cancer biomarkers: Section A of Disease markers (US). (2016) pp. 1875–8592.

88. Wang Y, Chen K, Chen H, Zhang K, Lu J, Mao H, et al. Low expression of miRNA-1290 associated with local invasion and recurrence in sacral chordoma. *Int J Clin Exp Pathol* (2017) 10(11):10934.

89. Miksad RA, Zietemann V, Gothe R, Schwarzer R, Conrads-Frank A, Schnell-Inderst P, et al. Progression-free survival as a surrogate endpoint in advanced breast cancer. *Int J Technol Assess Health Care* (2008) 24(04):371–83. doi: 10.1017/S0266462308080495

90. Broglio KR, Berry DA. Detecting an overall survival benefit that is derived from progression-free survival. *JNCI: J Natl Cancer Inst* (2009) 101(23):1642–9. doi: 10.1093/jnci/djp369

91. Randolph KA, Myers LL. *Basic statistics in multivariate analysis*. (USA: Oxford University Press) (2013).

92. Hortobagyi GN, Smith TL, Legha SS, Swenerton KD, Gehan EA, Yap HY, et al. Multivariate analysis of prognostic factors in metastatic breast cancer. *J Clin Oncol* (1983) 1(12):776–86. doi: 10.1200/JCO.1983.1.12.776

93. Han Y, Liu D, Li L. PD-1/PD-L1 pathway: current researches in cancer. *Am J Cancer Res* (2020) 10(3):727–42.

94. Gill CM, Fowkes M, Shrivastava RK. Emerging therapeutic targets in chordomas: A review of the literature in the genomic era. *Clin Neurosurg: Oxford Univ Press* (2020) p:E118–E23. doi: 10.1093/neuros/nyz342

95. Potla P, Ali SA, Kapoor M. A bioinformatics approach to microRNA-sequencing analysis. *Osteoarthritis Cartilage Open* (2021) 3(1):100131. doi: 10.1016/j.ocarto.2020.100131

96. Li F, Yang J Fau - Ramnath N, Ramnath N Fau - Javle MM, Javle Mm Fau - Tan D, Tan D. Nuclear or cytoplasmic expression of survivin: what is the significance. *International J Cancer (US)*. (2005) pp. 0020–7136.

97. Barber SM, Sadrameli SS, Lee JJ, Fridley JS, Teh BS, Oyelese AA, et al. Chordoma-current understanding and modern treatment paradigms. *J Clin Med* (2021) 10(5):1054. doi: 10.3390/jcm10051054

98. Von Witzleben A, Goerttler LT, Marienfeld R, Barth H, Lechel A, Mellert K, et al. Preclinical characterization of novel chordoma cell systems and their targeting by pharmocological inhibitors of the CDK4/6 cell-cycle pathway. *Cancer Res* (2015) 75(18):3823–31. doi: 10.1158/0008-5472.CAN-14-3270

99. Ekumi KM, Paculova H, Lenasi T, Pospichalova V, Bösken CA, Rybarikova J, et al. Ovarian carcinoma CDK12 mutations misregulate expression of DNA repair genes *via* deficient formation and function of the Cdk12/CycK complex. *Nucleic Acids Res* (2015) 43(5):2575–89. doi: 10.1093/nar/gkv101

100. Naidoo K, Wai PT, Maguire SL, Daley F, Haider S, Kriplani D, et al. Evaluation of CDK12 protein expression as a potential novel biomarker for DNA damage response-targeted therapies in breast cancer. *Mol Cancer Ther* (2018) 17 (1):306–15. doi: 10.1158/1535-7163.MCT-17-0760

101. Mobley BC, McKenney Jk, Bangs CD, Bangs Cd, Callahan K, Callahan K, et al. Loss of SMARCB1/INI1 expression in poorly differentiated chordomas. *Acta Neuropathologica (Germany)* (2010) pp. 1432–0533.

102. Song Q, Peng M, Chu Y, Huang S. Techniques for detecting chromosomal aberrations in myelodysplastic syndromes. *Oncotarget* (2017) 8(37):62716–29. doi: 10.18632/oncotarget.17698

103. Chen Y, Yu H, Wu C, Li J, Jiao S, Hu Y, et al. Prognostic value of plasma d-dimer levels in patients with small-cell lung cancer. *Biomed Pharmacother = Biomed Pharmacother* (2016) 81:210–7. doi: 10.1016/j.biopha.2016.02.030

104. Kilic M, Yoldas O, Keskek M, Ertan T, Tez M, Gocmen E, et al. Prognostic value of plasma d-dimer levels in patients with colorectal cancer. *Colorectal Dis* (2008) 10(3):238–41. doi: 10.1111/j.1463-1318.2007.01374.x

105. Hu L, Li M, Ding Y, Pu L, Liu J, Xie J, et al. Prognostic value of RDW in cancers: A systematic review and meta-analysis. *Oncotarget* (2017) 8(9):16027–35. doi: 10.18632/oncotarget.13784

106. Furtado S, Dunogué B, Jourdi G, Chaigne B, Chibah A, Legendre P, et al. High d-dimer plasma concentration in systemic sclerosis patients: Prevalence and association with vascular complications. *J Scleroderma Related Disord* (2021) 6 (2):178–86. doi: 10.1177/2397198320957558

107. He Q, Ding J, He S, Yu Y, Chen X, Li D, et al. The predictive value of procalcitonin combined with c-reactive protein and d dimer in moderately severe and severe acute pancreatitis. *Eur J Gastroenterol Hepatol* (2022) 34(7):744–50. doi: 10.1097/MEG.0000000000002376

108. Chen P-C, Sung F-C, Chien K-L, Hsu H-C, Su T-C, Lee Y-T. Red blood cell distribution width and risk of cardiovascular events and mortality in a community cohort in Taiwan. *Am J Epidemiol* (2010) 171(2):214–20. doi: 10.1093/aje/kwp360

frontiers | Frontiers in Oncology

TYPE Original Research
PUBLISHED 14 October 2022
DOI 10.3389/fonc.2022.1046093

OPEN ACCESS

EDITED BY
Hailiang Tang,
Fudan University, China

REVIEWED BY
Paolo Palmisciano,
University of Cincinnati, United States
Li Cai,
CHI St Vincent, United States

*CORRESPONDENCE
Yazhuo Zhang
zyz2004520@yeah.net

SPECIALTY SECTION
This article was submitted to Neuro-Oncology and Neurosurgical Oncology, a section of the journal Frontiers in Oncology

RECEIVED 16 September 2022
ACCEPTED 29 September 2022
PUBLISHED 14 October 2022

CITATION
Li M, Bai J, Xiong Y, Shen Y, Wang S, Li C and Zhang Y (2022) High systemic inflammation score is associated with adverse survival in skull base chordoma. *Front. Oncol.* 12:1046093. doi: 10.3389/fonc.2022.1046093

High systemic inflammation score is associated with adverse survival in skull base chordoma

Mingxuan Li[1,2], Jiwei Bai[1], Yujia Xiong[2], Yutao Shen[2], Shuai Wang[2], Chuzhong Li[2] and Yazhuo Zhang[1,2,3,4,5]*

[1]Department of Neurosurgery, Beijing Tiantan Hospital, Capital Medical University, Beijing, China, [2]Beijing Neurosurgical Institute, Capital Medical University, Beijing, China, [3]Beijing Institute for Brain Disorders Brain Tumor Center, Beijing, China, [4]China National Clinical Research Center for Neurological Diseases, Beijing, China, [5]Key Laboratory of Central Nervous System Injury Research, Capital Medical University, Beijing, China

Background: The systemic inflammation score (SIS), based on preoperative lymphocyte to monocyte ratio (LMR) and albumin (ALB), was recently developed and is demonstrated to be a novel prognostic indicator in several cancers. However, data discussing the utility of SIS in chordoma are lacking. We aimed to investigate the distribution and the prognostic role of SIS in primary skull base chordoma patients undergoing surgery.

Material and methods: Preoperative SIS was retrospectively collected from 183 skull base chordoma patients between 2008 and 2014 in a single center. Its associations with clinical features and overall survival (OS) were further analyzed. The SIS-based nomogram was developed and evaluated by the concordance index (C-index), time-dependent receiver operating characteristic (ROC) curve, calibration curve, and decision curve analysis (DCA).

Results: The numbers of patients in the SIS 2, 1, and 0 group were 29 (15.8%), 60 (32.8%), 94 (51.4%), respectively. High SIS was associated with older age (p = 0.008), brainstem involvement of tumors (p = 0.039), and adverse OS (p < 0.001). Importantly, multivariate Cox analysis showed that high SIS independently predicts adverse OS. Furthermore, the nomogram based on SIS and clinical variables showed eligible performance for OS prediction in both training and validation cohorts.

Conclusions: The SIS is a promising, simple prognostic biomarker, and the SIS-based nomogram serves as a potential risk stratification tool for outcome in skull base chordoma patients.

KEYWORDS

systemic inflammation score, skull base chordoma, prognosis, biomarker, nomogram

Abbreviations: LMR, lymphocyte to monocyte ratio; ALB, albumin; SIS, systemic inflammation score; OS, overall survival; HR, hazard ratio; CI, confidence interval; C-index, concordance index; ROC, receiver operating characteristic; DCA, decision curve analysis.

Introduction

Chordoma accounts for 1-4% of primary bone neoplasm, and previous studies recognized that chordoma originates from the remnant of notochord (1, 2). Chordoma is largely found in the axial skeleton, about 30-40% of which is located at the skull base (clivus) (2, 3). To date, surgery with the help of radiotherapy is the main treatment for chordoma patients. However, the commonly large tumor burden and the involvement of critical neurovascular tissues make chordoma difficult to eradicate, especially for skull base chordoma (4). In addition, studies showed no significant value of classical chemotherapy. Despite the development of surgical technology, such as endoscopic surgery and intraoperative navigation, and the effort on targeted therapy, skull base chordoma patients had a high recurrent rate and sequent mortality (2, 5, 6). Improvement of the survival of chordoma patients requires the identification of reliable biomarkers and effective patient risk stratification.

Inflammation has been widely recognized as a prevalent characteristic of cancer since Virchow first promoted a potential association between inflammation and cancer (7). Cancer patients can present both local inflammatory symptoms and systemic inflammation, such as changes in the peripheral blood cell count (8). Moreover, increasing studies show that systemic inflammation plays an essential role in cancer patient outcomes *via* several aspects, including tumor oncogenesis, progression, and metastasis (9, 10). Consequently, several pretreatment inflammatory biomarkers based on blood cells, including neutrophil to lymphocyte ratio (NLR), prognostic nutritional index (PNI), lymphocyte to monocyte ratio (LMR), platelet to lymphocyte ratio (PLR), and Glasgow prognostic score (GPS), are developed in recent studies; and these biomarkers can act as prognostic indicators in various cancers (11–14). In addition, accumulating studies identify preoperative level of serum albumin (ALB) as a prognostic factor for cancer (15). However, there are currently few studies investigating the establishment of a scoring system that combines these inflammatory indicators for prognostic prediction in skull base chordoma patients (16).

More recently, a promising prognostic score based on levels of ALB and LMR, known as the systemic inflammation score (SIS), is proposed, and is highly associated with outcomes in colorectal cancer, oral cavity squamous cell carcinoma, and clear cell renal cell carcinoma (17–19). Until now, the role of SIS in predicting the prognosis of skull base chordoma patients remains to be elucidated. Thus, in this study, we evaluated the distribution of SIS in a relatively large cohort of skull base chordoma patients undergoing surgery and investigated the associations of SIS with patient characteristics. We also examined the prognostic impact of SIS on overall survival (OS) in skull base chordoma patients, and a nomogram including SIS and clinical variables was further developed and validated for survival prediction.

Material and methods

Patient population

This retrospective study enrolled 183 skull base chordoma patients undergoing surgery between January 2008 and September 2014 in our institute. This cohort has been previously described in our studies (20). The following inclusion criteria were applied: 1) patients were histopathologically diagnosed as chordoma and the tumor located at the skull base. 2) patients with detailed medical records, routine blood tests before surgery, and follow-up data. Exclusion criteria were as follows: 1) patients with an unclear diagnosis or tumors located at the cervical vertebra alone were not included; 2) patients who received adjuvant radiotherapy and/or chemotherapy, cancer-related operation including biopsy before their first surgery at our institute were excluded; 3) unavailable clinical/laboratory data; 4) patients with infection, inflammatory disease, hemopathy, liver/kidney disorder, other malignant diseases were excluded.

Follow-up investigation and survival analysis

Patients were recommended to follow up with physical examination, magnetic resonance imaging, and/or computed tomography every 3-6 months for the first 2 years and annually thereafter. For patients unable to come to our hospital for a check, telephone, or email was applied. The follow-up investigation was terminated in October 2019. The primary endpoint, OS, was defined as the time from operation to death or censored at the last follow-up.

For survival analysis and the development of the nomogram, 183 patients were divided into training and validation groups with a ratio of 2:1.

Data extraction

For each participant, clinical and pathological data and blood tests were gathered, including age at surgery, sex, pathological type, degree of resection, tumor size, tumor texture, tumor blood supply, brainstem involvement, preoperative complete blood cell count, and ALB level (g/L). Pathological types of chordoma were confirmed by a professional pathologist and recorded as classical, chondroid, or dedifferentiated types (2). The degree of resection was recorded as total/subtotal resection (≤ 5% residual tumor) and partial resection (> 5% residual tumor) according to the postoperative images (21).

Definition of SIS

Given the contiguous features of preoperative LMR and ALB, the optimal cutoff values, determined by the "surv_cutpoint" function of R package "survminer", were used to transfer LMR and ALB into categorical variables (high level, > the cutoff value; and low level, ≤ the cutoff value). The threshold point was defined as the value with the maximally selected log-rank test statistics (22). The SIS was then defined based on ALB and LMR levels as previously described: score 0, patients with a high LMR and a high ALB; score 1, patients with either low LMR or low ALB; and score 2, patients with both low ALB and low LMR (17, 19).

Statistical analysis

The analysis was performed with SPSS for Windows version 19.0 (IBM Corp, Armonk, NY, USA), and R software version 4.0.2 (R Foundation for Statistical Computing, Vienna, Austria). Continuous variables were shown as median with interquartile range (IQR). Correlations between SIS, LMR, and categorical variables were analyzed by the chi-squared test, and their correlations to continuous variables were analyzed using the Kruskal-Wallis test or Wilcoxon rank-sum test. The Kaplan-Meier survival curve and log-rank test were applied to find the difference in OS between groups. Univariate and multivariate Cox proportional hazard regression model was also performed, and variables with $P < 0.05$ in the univariate analysis were included in the multivariate analysis. A nomogram was developed based on our multivariate analysis and previously reported prognostic-related variables (2, 4, 23). The concordance index (C-index), time-dependent receiver operating characteristic (ROC) curve, and the calibration curve were used to assess the predictive performance and accuracy of the nomogram. Decision curve analysis (DCA) was performed to evaluate the clinical value of the nomogram. A two-sided *P* value less than 0.05 was considered to indicate statistical significance.

Results

Patient characteristics

In total, 183 patients were included in this study. Supplementary Table S1 showed the clinicopathological characteristics of enrolled patients. There were 96 (52.5%) males and 87 (47.5%) females. The median age at admission was 41 years (IQR, 29-51 years). Respectively, 125 (68.3%), 58 (31.7%), 0 (0%) patients had classical, chondroid, and dedifferentiated chordoma. Based on the longest diameters of the coronal, sagittal, and axial axes, the median tumor size was 21.0 cm^3 (IQR, 11.9-38.8 cm^3). The median value of preoperative LMR was 5.35 (IQR, 4.17-6.75), and the median level of preoperative ALB was 45.8 g/L (IQR, 43.9-48.2 g/L). The excellent cutoff value of LMR was 4.75, and 44.5 g/L for ALB in the training cohort (Supplementary Figure S1). According to the above definition of SIS, the distribution of SIS in our cohort was 29 (15.8%) patients in the SIS 2 group, 60 (32.8%) patients with an SIS of 1, and 94 (51.4%) patients with an SIS of 0.

Correlations between SIS and clinicopathological findings

Relationships between SIS and clinicopathological variables were detailed in Table 1. Higher SIS was significantly correlated with older patient age ($p = 0.008$). In addition, patient with brainstem involvement was associated with a higher SIS ($p = 0.039$). Patients with higher SIS tended to have tumors with a rich blood supply, although the difference was not significant ($p = 0.096$). No significant differences in gender, tumor size, tumor texture, and pathology types were observed between different SIS groups (all $p > 0.05$). Additionally, we observed that low ALB was associated with older age ($p < 0.001$), though no significant difference between low LMR and old age was found ($p = 0.316$) (20). Decreased ALB was also correlated with

TABLE 1 Association between SIS and clinicopathological features in skull base chordoma.

Variables	SIS			
	0	1	2	*P* value
Cases	94	60	29	
Age, years				0.008
Median	37.0	43.5	47.0	
Gender				0.889
Male	48	33	15	
Female	46	27	14	
Tumor size				0.814
≤20cm^3	45	31	13	
>20cm^3	49	29	16	
Texture				0.992
Soft	28	18	9	
Others (hard or moderate)	66	42	20	
Blood supply				0.096
Rich	50	35	22	
Others (poor or moderate)	44	25	7	
Pathology				0.634
Classical	63	40	22	
Chondroid	31	20	7	
Brainstem involvement				0.039
Absent	30	30	8	
Present	64	30	21	

SIS, systemic inflammation score.

soft tumors and chondroid chordoma types ($p = 0.023$ and 0.026, respectively) (20), while LMR was not associated with tumor texture ($p = 0.094$) or pathological type ($p = 0.311$).

Survival analysis

The median follow-up period was 74 months (IQR, 53-96 months; range, 3-141 months). During the follow-up period, 72 (39.3%) patients died and the 5-year OS rate was 67.8% for the whole cohort. In the training cohort, Kaplan-Meier curves indicated that decreased LMR was associated with shorter OS time (median OS time, 87 months vs 125 months; 5-year OS rate, 61.9% vs 85.0%; $p = 0.004$) (Figure 1A). Similarly, patients with low ALB had adverse OS than that of patients with high ALB (median OS time, 73 months vs not reached; 5-year OS rate, 61.1% vs 83.7%; $p < 0.001$, Figure 1B) (20). Moreover, we found that patients with higher SIS were correlated with worse OS ($p < 0.001$, Figure 1C). Specifically, significant differences of OS were observed between SIS = 2 group and SIS = 1 group (median OS time, 47 months vs 110 months; 5-year OS rate, 38.9% vs 81.0%; $p = 0.001$) or SIS = 0 group (median OS time, 47 months vs 125 months; 5-year OS rate, 38.9% vs 85.5%; $p < 0.001$). In the validation cohort, we also observed that low LMR was correlated with shorter OS time (median OS time, 59 months vs 107 months; 5-year OS rate, 52.4% vs 77.2%; $p = 0.024$) (Figure 2A). Additionally, low ALB was associated with decreased 5-year OS rate (median OS time, 49 months vs not reached; 5-year OS rate, 36.1% vs 78.1%; $p = 0.001$) (Figure 2B). Importantly, patients with higher SIS were correlated with worse OS outcome (median OS time, 38 months, 59 months, and not reached, respectively; 5-year OS rate, 87.5%, 42.8%, and 24.2%, respectively; $p = 0.003$) (Figure 2C).

We also performed a subgroup analysis of LMR, ALB, and SIS stratified by degree of resection. For patients with total/subtotal resection, decreased ALB ($p < 0.001$ in the training cohort and $p = 0.003$ in the validation cohort) and high SIS ($p < 0.001$ in the training cohort and $p = 0.024$ in the validation cohort) were associated with unfavorable OS, low LMR tended to correlate with poor OS ($p = 0.197$ in the training cohort and $p = 0.107$ in the validation cohort) (Figure 3). For patients with partial resection, we also confirmed the potential prognostic value of LMR ($p = 0.011$ in the training cohort), ALB ($p = 0.052$ in the training cohort and $p = 0.006$ in the validation cohort), and SIS ($p = 0.024$ in the training cohort and $p = 0.071$ in the validation cohort) (Figure 4).

In the univariate Cox analysis of the training cohort, LMR, ALB, and SIS were associated with OS as well as age at admission, tumor pathology, degree of resection, and lymphocyte count. Moreover, multivariate analysis including these variables revealed that SIS was an independent prognostic indicator for OS (Table 2). Consistently, in the validation cohort, higher SIS was independently associated with adverse survival (Table 3).

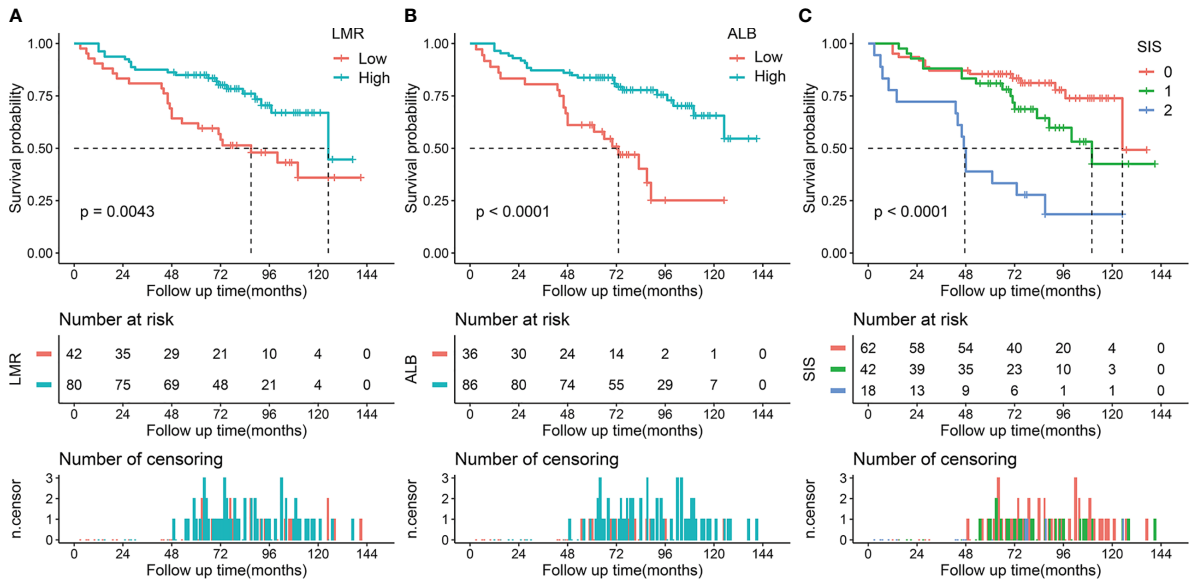

FIGURE 1
Kaplan-Meier survival analysis of LMR, ALB, and SIS in the training cohort. **(A)** Low LMR correlated with a poor OS. **(B)** Low ALB correlated with an adverse OS. **(C)** High SIS was associated with a poor OS. LMR, lymphocyte to monocyte ratio; ALB, albumin; SIS, systemic inflammation score; OS, overall survival.

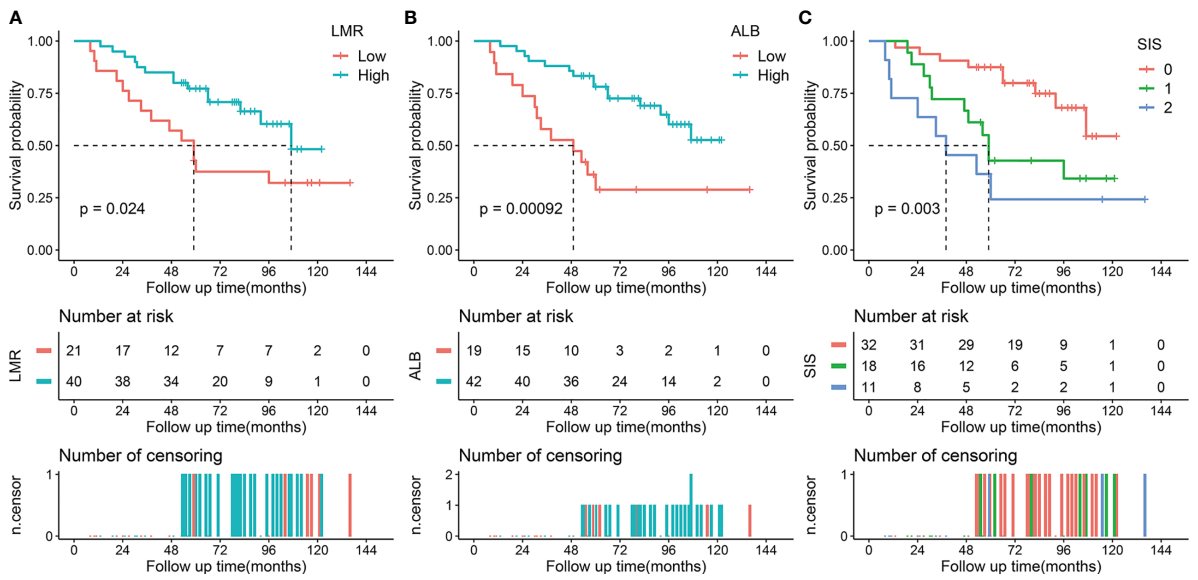

FIGURE 2
Kaplan-Meier survival analysis of LMR, ALB, and SIS in the validation cohort. **(A)** Low LMR correlated with a poor OS. **(B)** Low ALB correlated with an adverse OS. **(C)** High SIS was associated with a poor OS. LMR, lymphocyte to monocyte ratio; ALB, albumin; SIS, systemic inflammation score; OS, overall survival.

Prognostic nomogram for OS

We then developed the nomogram integrating SIS and significant clinical variables for clinical OS prediction (Figure 5A). The C-indexes of the nomogram were 0.791 (95% CI, 0.720-0.861) in the training cohort and 0.798 (95% CI, 0.727-0.868) in validation cohort. Time-dependent ROC also revealed the satisfying prediction performance of the SIS-based nomogram during the follow-up time (Figure 5B). Moreover, calibration curves for 3-year, 5-year, and 8-year OS suggested favorable agreements between the nomogram and actual observation in both training and validation cohorts (Figure 6A). Importantly, DCA, a tool to assess the clinical values of models, showed that the SIS-based nomogram had higher net benefits (Figure 6B).

Discussion

In the current study, we described the distribution of SIS in newly diagnosed skull base chordoma and investigated its associations with the clinical features of patients. To our knowledge, the current study was the first report to characterize the prognostic role of SIS in chordoma. Our results showed that higher SIS was correlated with older patient age and brainstem involvement of the tumor, and the multivariate analysis demonstrated that high SIS could independently predict adverse OS. Moreover, a nomogram including SIS and significant clinical variables showed a favorable prediction ability for OS. Our data highlighted the SIS-based nomogram may be of important value for clinical survival prediction, and further supported that drugs targeting inflammation may be a promising therapy for chordoma.

The role of inflammation, a prevalent characteristic of cancer, on tumor pathogenesis and progression has gained much attention in recent years (7, 24). Increasing research has indicated that inflammatory cytokines in tumors, including tumor-infiltrating lymphocyte and tumor-infiltrating neutrophils, play essential roles in tumor oncogenesis and patient outcome (25, 26). Moreover, tumor-associated macrophage was also correlated with poorer outcome and therapy resistance in cancer (27). In addition, the peripheral blood cells of cancer patients, such as neutrophil, monocyte, and lymphocyte, and further pretreatment NLR, PLR, and LMR showed effective prognostic values in various cancers (11, 13). Recently, one retrospective study by Hu et al. investigated the role of inflammatory indexes including NLR, PLR, and monocyte lymphocyte ratio (MLR) in 172 chordoma patients (16). However, the authors found that preoperative MLR was not correlated with patient OS, which is inconsistent with the finding in this study. Our result of Kaplan-Meier analyses showed that low LMR was associated with unfavorable OS in skull base chordoma ($p = 0.004$ in the training cohort and 0.024 in the validation cohort). Several differences exist in the current study compared to Hu's study, which may help explain the inconsistency. First, the study populations differed from each

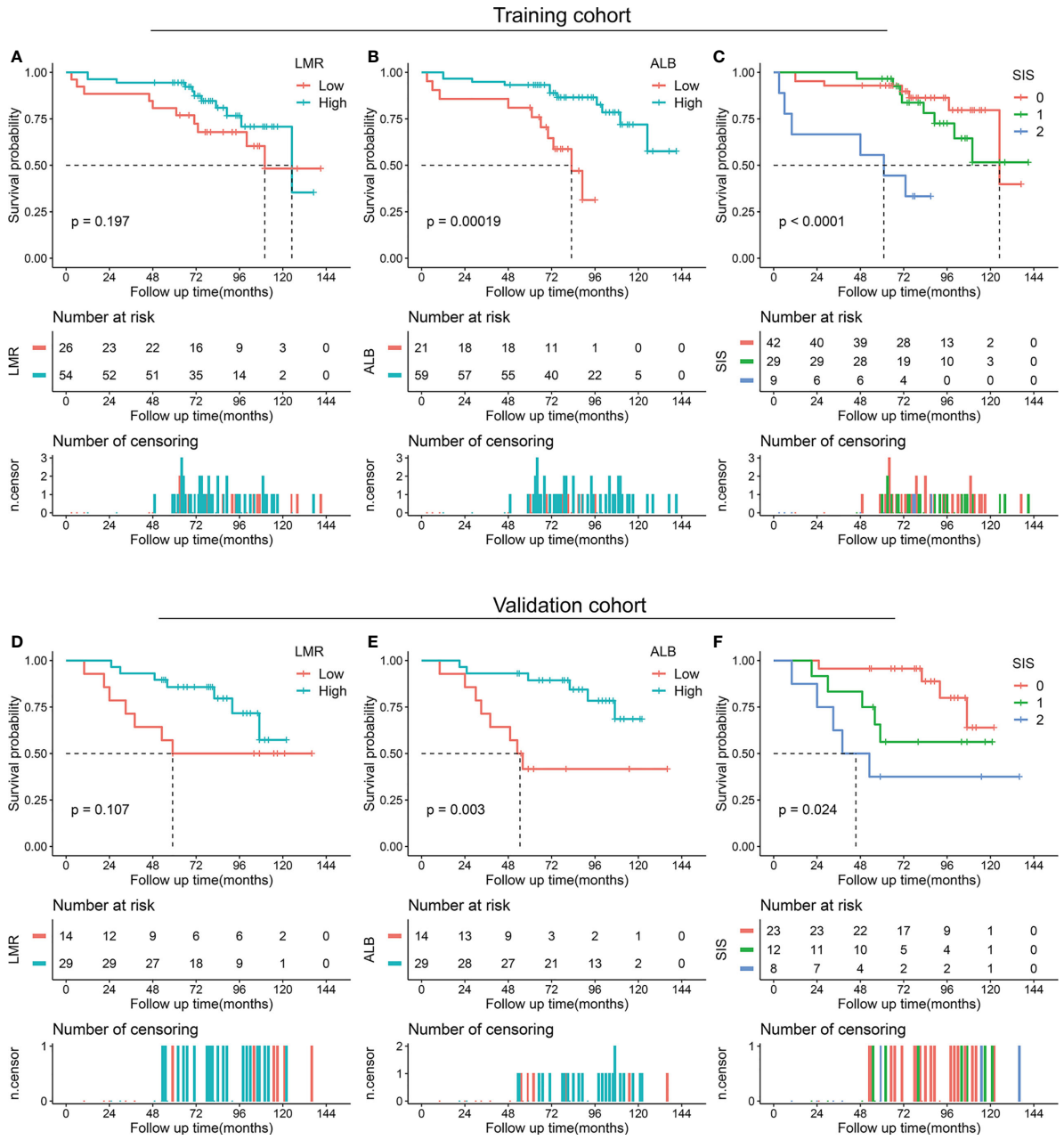

FIGURE 3
Kaplan-Meier survival analysis of LMR, ALB, and SIS in skull base chordoma with total or subtotal resection. **(A)** OS analysis of LMR in the training cohort. **(B)** OS analysis of ALB in the training cohort. **(C)** OS analysis of SIS in the training cohort. **(D)** OS analysis of LMR in the validation cohort. **(E)** OS analysis of ALB in the validation cohort. **(F)** OS analysis of SIS in the validation cohort. LMR, lymphocyte to monocyte ratio; ALB, albumin; SIS, systemic inflammation score; OS, overall survival.

other; in the study of Hu, 79 skull base chordoma, 43 spine chordoma, and 50 sacrum chordoma were enrolled while our study only involved skull base chordoma. Spine chordoma often correlated with metastasis while limited metastasis was reported in skull base chordoma patients, and metastasis was identified as a significant prognostic factor for outcome (2, 28). Given the potential differences between spine chordoma and skull base chordoma, the results may be biased by the analysis of the entire cohort without stratification by tumor location. Second, the cut-off values were not consistent; the cutoff value of MLR was 0.36 (LMR, 2.78) in the study of Hu, while the cutoff value of LMR in the current study was 4.75. Finally, methods determining cutoff

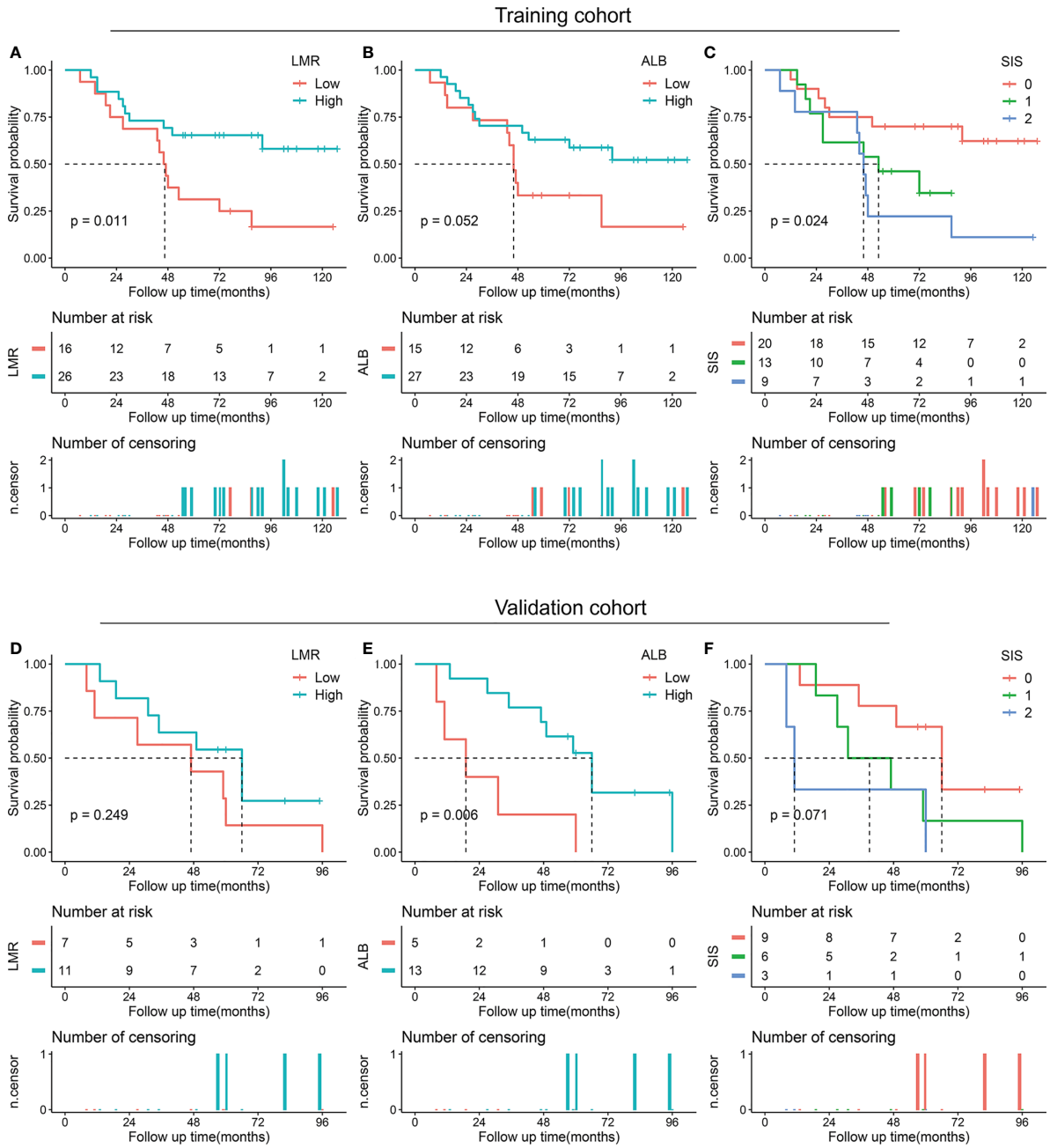

FIGURE 4
Kaplan-Meier survival analysis of LMR, ALB, and SIS in skull base chordoma with partial resection. **(A)** OS analysis of LMR in the training cohort. **(B)** OS analysis of ALB in the training cohort. **(C)** OS analysis of SIS in the training cohort. **(D)** OS analysis of LMR in the validation cohort. **(E)** OS analysis of ALB in the validation cohort. **(F)** OS analysis of SIS in the validation cohort. LMR, lymphocyte to monocyte ratio; ALB, albumin; SIS, systemic inflammation score; OS, overall survival.

values were not the same; R package "survminer" was used in the current study while ROC analysis was applied in Hu's study.

SIS attracts accumulating attention in recent studies for its integration of ALB and LMR, which may indicate the status of both nutrition and systemic inflammation in patients (17). Increasing studies have shown the prognostic value of SIS in cancer patients (19, 29). In our study, similar to previous studies, we found high SIS was correlated with older age and brainstem invasion, and SIS was independently associated with OS, identifying SIS as a novel risk stratification system for skull base chordoma. Given the difficulty and high risk of surgery involving the brainstem, patients with a high SIS may need a

TABLE 2 Univariate and multivariate Cox proportional analysis of OS in the training cohort.

Variables	Univariate analysis		Multivariate analysis	
	HR (95% CI)	*P* value	HR (95% CI)	*P* value
Age, years (>55 vs ≤55)	2.626 (1.345-5.128)	0.005	2.895 (1.412-5.935)	0.004
Gender (female vs male)	0.904 (0.500-1.634)	0.738		
Tumor size, cm^3(>20 vs ≤20)	1.593 (0.873-2.906)	0.129		
Texture (hard + moderate vs soft)	1.154 (0.603-2.207)	0.666		
Blood supply (poor + moderate vs rich)	0.536 (0.281-1.026)	0.060		
Pathology (chondroid vs classical)	0.303 (0.128-0.717)	0.007	0.385 (0.159-0.913)	0.034
Brainstem involvement (present vs absent)	0.938 (0.512-1.717)	0.835		
Degree of resection (partial vs total/subtotal)	2.696 (1.488-4.883)	<0.001	2.085 (1.123-3.870)	0.020
Postoperative radiotherapy (yes vs no)	0.880 (0.482-1.607)	0.678		
Neutrophil count (10^9/L) [a]	0.996 (0.798-1.242)	0.969		
Lymphocyte count (10^9/L) [a]	0.521 (0.305-0.891)	0.017	NA	
Monocyte count (10^9/L) [a]	0.244 (0.028-2.115)	0.200		
Platelet count (10^9/L) [a]	0.999 (0.994-1.004)	0.586		
LMR (≤4.75 vs >4.75)	2.309 (1.277-4.184)	0.006	NA	
ALB (≤44.5 vs >44.5)	3.370 (1.827-6.216)	<0.001	NA	
SIS				
0	Reference		Reference	
1	1.827 (0.891-3.749)	0.100	1.702 (0.799-3.626)	0.168
2	5.848 (2.756-12.406)	<0.001	4.626 (2.124-10.074)	<0.001

[a]analyzed as continuous variables; NA, not acquired; OS, overall survival; HR, hazard ratio; CI, confidence interval; LMR, lymphocyte to monocyte ratio; ALB, albumin; SIS, systemic inflammation score.

10.3389/fonc.2022.1046093

TABLE 3 Univariate and multivariate Cox proportional analysis of OS in the validation cohort.

Variables	Univariate analysis		Multivariate analysis	
	HR (95% CI)	*P* value	HR (95% CI)	*P* value
Age, years (>55 vs ≤55)	1.169 (0.443-3.085)	0.752		
Gender (female vs male)	1.204 (0.564-2.568)	0.632		
Tumor size, cm^3(>20 vs ≤20)	1.728 (0.793-3.765)	0.168		
Texture (hard + moderate vs soft)	2.711 (0.936-7.850)	0.066		
Blood supply (poor + moderate vs rich)	0.510 (0.223-1.167)	0.111		
Pathology (chondroid vs classical)	0.932 (0.430-2.019)	0.857		
Brainstem involvement (present vs absent)	1.245 (0.573-2.706)	0.580		
Degree of resection (partial vs total/subtotal)	3.907 (1.812-8.423)	0.001	4.193 (1.934-9.089)	<0.001
Postoperative radiotherapy (yes vs no)	0.581 (0.246-1.370)	0.215		
Neutrophil count (10^9/L) [a]	1.434 (1.146-1.793)	0.002	NA	
Lymphocyte count (10^9/L) [a]	1.253 (0.681-2.302)	0.468		
Monocyte count (10^9/L) [a]	3.357 (0.325-34.622)	0.309		
Platelet count (10^9/L) [a]	1.005 (1.001-1.010)	0.018	NA	
LMR (≤4.75 vs >4.75)	2.306 (1.093-4.865)	0.028	NA	
ALB (≤44.5 vs >44.5)	3.364 (1.573-7.195)	0.002	NA	
SIS				
0	Reference		Reference	
1	2.807 (1.158-6.808)	0.022	2.697 (1.108-6.564)	0.029
2	4.480 (1.712-11.720)	0.002	5.167 (1.962-13.610)	0.001

[a]analyzed as continuous variables; NA, not acquired; OS, overall survival; HR, hazard ratio; CI, confidence interval; LMR, lymphocyte to monocyte ratio; ALB, albumin; SIS, systemic inflammation score.

10.3389/fonc.2022.1046093

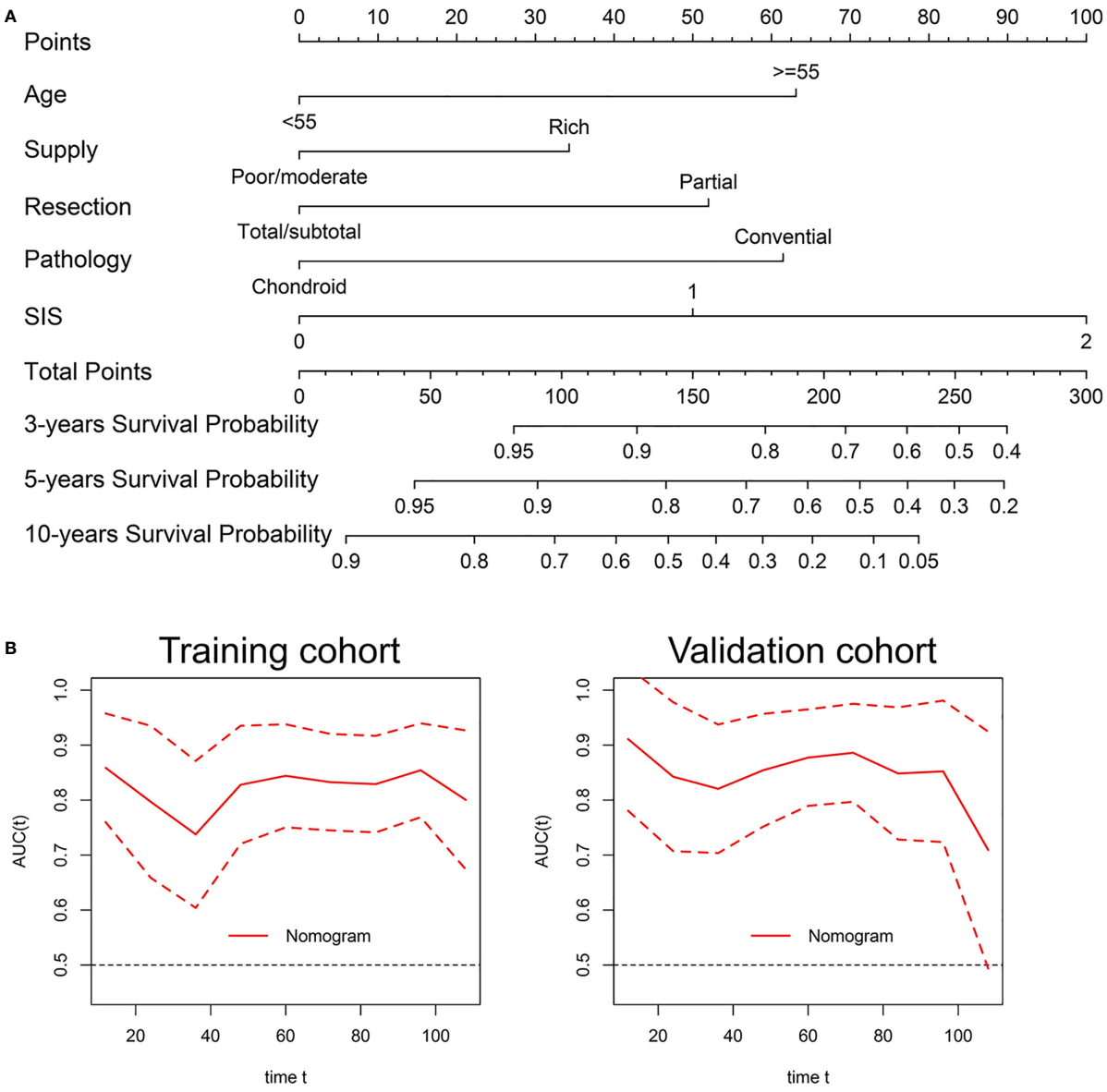

FIGURE 5
Development and validation of a nomogram for OS prediction in skull base chordoma. **(A)** Nomogram for OS prediction. **(B)** Time-dependent ROC curve of the nomogram. SIS, systemic inflammation score; OS, overall survival; ROC, receiver operating characteristic.

more careful preoperative preparation such as navigation-assisted operation, and electrophysiological monitoring, aiming for maximal safe resection and less possibility of recurrence. Moreover, patients with high SIS are recommended to receive closer monitoring after surgery and a more radical therapeutic option due to the increased risk of death (SIS = 1 vs SIS = 0, 1.702 times; SIS = 2 vs SIS = 0, 4.626 times in the training cohort).

The reason for the prognostic role of SIS in cancer is largely unclear, and previous studies proposed that it may be elucidated by the role of lymphocyte, monocyte, and ALB. The lymphocyte is recognized as an essential component of the immune system and it contributes to immune surveillance of cancer cells, inhibition of tumor cell growth, and metastasis *via* secreting various cytokines (30). A decrease in lymphocytes may lead to an insufficiency of the immune response to cancer, and it is correlated with poor outcomes in various cancers (31). In contrast, monocyte-derived tumor-associated macrophage in tumor tissues can act as a cancer-promoting role by enhancing tumor cell proliferation, increased angiogenesis, stroma remodeling, and inhibiting antitumor immunity (32). Moreover, monocyte count is correlated with survival in cancer patients (33). Therefore, the association between low LMR and adverse outcome is found in cancer

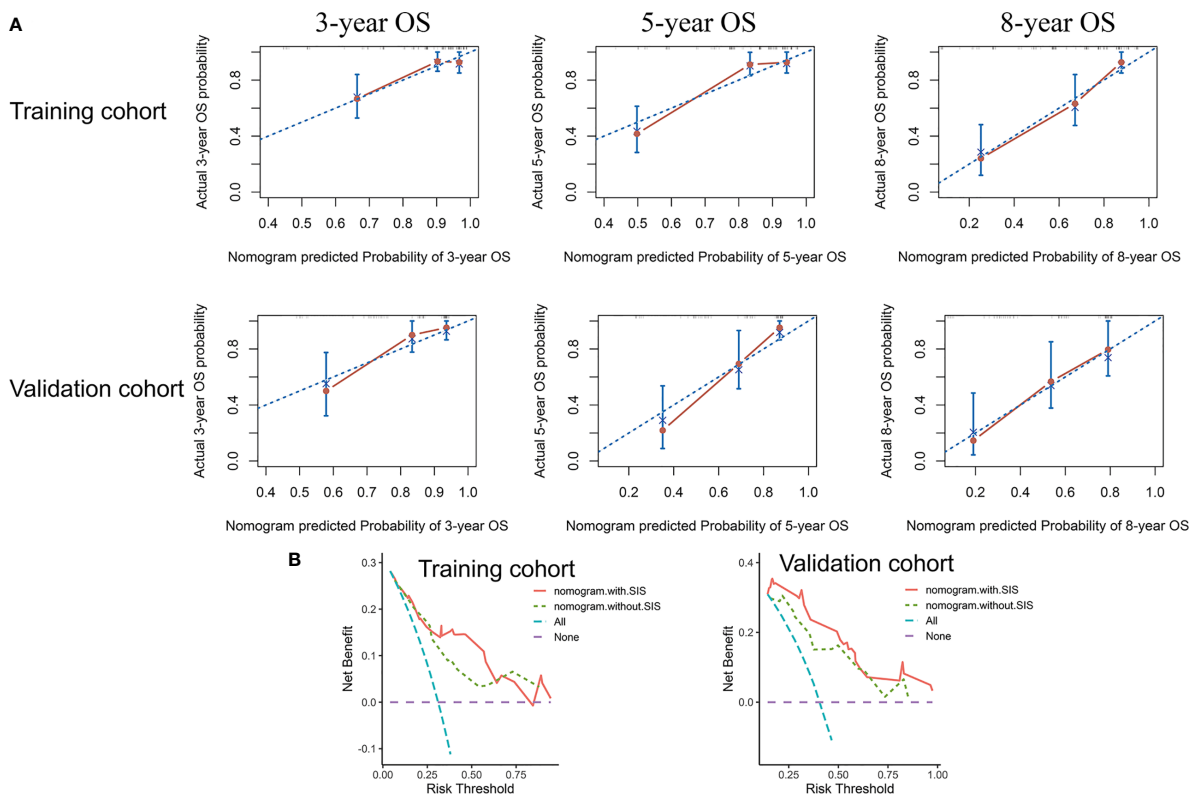

FIGURE 6
The nomogram showed satisfactory performance for OS prediction in the training and validation cohort. **(A)** 3-year, 5-year, and 8-year OS calibration curves of the nomogram. **(B)** Decision curve analysis of the nomogram for OS. OS, overall survival.

patients in recent studies (13). ALB, which is regarded as an index of nutrition, is also a negative acute phase protein involved in systemic inflammation response (10). Previous studies indicated the association between low ALB and poor prognosis, which may be explained by the abnormal response to surgical stress, insufficient immune defense, and increased risks of complications (34).

Several limitations existed in this study. First, retrospective nature may be subject to selection bias. The prognostic role of SIS in chordoma remains to be elucidated in future large-scale research. In addition, preoperative C-reactive protein and pretreatment GPS were not collected due to the not routine measurement in examinations; and their associations with SIS were not analyzed in this study, while the previous study showed the prognostic value of C-reactive protein in chordoma (35). Finally, the associations between SIS and inflammatory cells in tumor tissues such as tumor-infiltrating lymphocyte were not analyzed (36).

In summary, our results reveal that SIS is an independent prognostic indicator of OS in skull base chordoma, and the SIS-based nomogram can act as a clinically preoperative risk stratification tool for the decision-making of individualized therapy for skull base chordoma patients.

Data availability statement

The original contributions presented in the study are included in the article/Supplementary Material. Further inquiries can be directed to the corresponding author.

Ethics statement

The studies involving human participants were reviewed and approved by the Ethics Committee of Beijing Tiantan Hospital. The patients/participants provided their written informed consent to participate in this study.

Author contributions

ML, JB, and YZ contributed to the conception and design of the study. YX, YS, SW, and CL contributed to data collection, analysis and interpretation of data, and revision of the manuscript. ML wrote the manuscript. All authors read and approved the final manuscript.

Funding

This study was supported by the National Natural Science Foundation of China (82071559 and 82272939).

Acknowledgments

We are grateful for the support of all patients.

Conflict of interest

The authors declare that the research was conducted in the absence of any commercial or financial relationships that could be construed as a potential conflict of interest.

Publisher's note

Supplementary material

The Supplementary Material for this article can be found online at: https://www.frontiersin.org/articles/10.3389/fonc.2022.1046093/full#supplementary-material

References

1. Vujovic S, Henderson S, Presneau N, Odell E, Jacques T, Tirabosco R, et al. Brachyury, a crucial regulator of notochordal development, is a novel biomarker for chordomas. *J Pathology: A J Pathological Soc Great Britain Ireland* (2006) 209 (2):157–65. doi: 10.1002/path.1969

2. Walcott BP, Nahed BV, Mohyeldin A, Coumans J-V, Kahle KT, Ferreira MJ. Chordoma: Current concepts, management, and future directions. *Lancet Oncol* (2012) 13(2):e69–76. doi: 10.1016/s1470-2045(11)70337-0

3. Chambers KJ, Lin DT, Meier J, Remenschneider A, Herr M, Gray ST. Incidence and survival patterns of cranial chordoma in the united states. *Laryngoscope* (2014) 124(5):1097–102. doi: 10.1002/lary.24420

4. Brito da Silva H, Straus D, Barber JK, Rostomily RC, Ferreira MJr., Sekhar LN. Cranial chordoma: A new preoperative grading system. *Neurosurgery* (2018) 83(3):403–15. doi: 10.1093/neuros/nyx423

5. Stacchiotti S, Gronchi A, Fossati P, Akiyama T, Alapetite C, Baumann M, et al. Best practices for the management of local-regional recurrent chordoma: A position paper by the chordoma global consensus group. *Ann Oncol* (2017) 28 (6):1230–42. doi: 10.1093/annonc/mdx054

6. Stacchiotti S, Longhi A, Ferraresi V, Grignani G, Comandone A, Stupp R, et al. Phase ii study of imatinib in advanced chordoma. *J Clin Oncol* (2012) 30 (9):914–20. doi: 10.1200/JCO.2011.35.3656

7. Balkwill F, Mantovani A. Inflammation and cancer: Back to virchow? *Lancet (London England)* (2001) 357(9255):539–45. doi: 10.1016/s0140-6736(00)04046-0

8. Chechlinska M, Kowalewska M, Nowak R. Systemic inflammation as a confounding factor in cancer biomarker discovery and validation. *Nat Rev Cancer* (2010) 10(1):2–3. doi: 10.1038/nrc2782

9. Diakos CI, Charles KA, McMillan DC, Clarke SJ. Cancer-related inflammation and treatment effectiveness. *Lancet Oncol* (2014) 15(11):e493–503. doi: 10.1016/s1470-2045(14)70263-3

10. McMillan DC. Systemic inflammation, nutritional status and survival in patients with cancer. *Curr Opin Clin Nutr Metab Care* (2009) 12(3):223–6. doi: 10.1097/MCO.0b013e32832a7902

11. Yodying H, Matsuda A, Miyashita M, Matsumoto S, Sakurazawa N, Yamada M, et al. Prognostic significance of neutrophil-to-Lymphocyte ratio and platelet-to-Lymphocyte ratio in oncologic outcomes of esophageal cancer: A systematic review and meta-analysis. *Ann Surg Oncol* (2016) 23(2):646–54. doi: 10.1245/s10434-015-4869-5

12. Huang PY, Wang CC, Lin CC, Lu SN, Wang JH, Hung CH, et al. Predictive effects of inflammatory scores in patients with bclc 0-a hepatocellular carcinoma after hepatectomy. *J Clin Med* (2019) 8(10):1676. doi: 10.3390/jcm8101676

13. Nishijima TF, Muss HB, Shachar SS, Tamura K, Takamatsu Y. Prognostic value of lymphocyte-to-Monocyte ratio in patients with solid tumors: A systematic review and meta-analysis. *Cancer Treat Rev* (2015) 41(10):971–8. doi: 10.1016/j.ctrv.2015.10.003

14. McMillan DC. The systemic inflammation-based Glasgow prognostic score: A decade of experience in patients with cancer. *Cancer Treat Rev* (2013) 39(5):534–40. doi: 10.1016/j.ctrv.2012.08.003

15. Gupta D, Lis CG. Pretreatment serum albumin as a predictor of cancer survival: A systematic review of the epidemiological literature. *Nutr J.* (2010) 9:69. doi: 10.1186/1475-2891-9-69

16. Hu W, Yu J, Huang Y, Hu F, Zhang X, Wang Y. Lymphocyte-related inflammation and immune-based scores predict prognosis of chordoma patients after radical resection. *Transl Oncol* (2018) 11(2):444–9. doi: 10.1016/j.tranon.2018.01.010

17. Suzuki Y, Okabayashi K, Hasegawa H, Tsuruta M, Shigeta K, Kondo T, et al. Comparison of preoperative inflammation-based prognostic scores in patients with colorectal cancer. *Ann Surg* (2018) 267(3):527–31. doi: 10.1097/sla.0000000000002115

18. Eltohami YI, Kao HK, Lao WW, Huang Y, Abdelrahman M, Liao CT, et al. The prediction value of the systemic inflammation score for oral cavity squamous cell carcinoma. *Otolaryngology–head Neck Surg Off J Am Acad Otolaryngology-Head Neck Surg* (2018) 158(6):1042–50. doi: 10.1177/0194599817751678

19. Chang Y, An H, Xu L, Zhu Y, Yang Y, Lin Z, et al. Systemic inflammation score predicts postoperative prognosis of patients with clear-cell renal cell carcinoma. *Br J Cancer* (2015) 113(4):626–33. doi: 10.1038/bjc.2015.241

20. Li M, Bai J, Wang S, Zhai Y, Zhang S, Li C, et al. Prognostic value of cumulative score based on preoperative fibrinogen and albumin level in skull base chordoma. *Onco Targets Ther* (2020) 13:8337–46. doi: 10.2147/ott.s257779

21. Zhai Y, Bai J, Wang S, Gao H, Li M, Li C, et al. Analysis of clinical factors and pdgfr-beta in predicting prognosis of patients with clival chordoma. *J Neurosurg* (2018) 129(6):1429–37. doi: 10.3171/2017.6.JNS17562

22. Sun L, Ke X, Wang D, Yin H, Jin B, Xu H, et al. Prognostic value of the albumin-to-Γ-Glutamyltransferase ratio for gallbladder cancer patients and establishing a nomogram for overall survival. *J Cancer* (2021) 12(14):4172–82. doi: 10.7150/jca.49242

23. Zou MX, Lv GH, Zhang QS, Wang SF, Li J, Wang XB. Prognostic factors in skull base chordoma: A systematic literature review and meta-analysis. *World Neurosurg* (2018) 109:307–27. doi: 10.1016/j.wneu.2017.10.010

24. Elinav E, Nowarski R, Thaiss CA, Hu B, Jin C, Flavell RA. Inflammation-induced cancer: Crosstalk between tumours, immune cells and microorganisms. *Nat Rev Cancer* (2013) 13(11):759–71. doi: 10.1038/nrc3611

25. Zou MX. Expression of programmed death-1 ligand (Pd-L1) in tumor-infiltrating lymphocytes is associated with favorable spinal chordoma prognosis. *Am J Transl Res.* (2016) 8(7):3274–87. doi: 10.13140/RG.2.1.1007.0649

26. Zhou L, Xu L, Chen L, Fu Q, Liu Z, Chang Y, et al. Tumor-infiltrating neutrophils predict benefit from adjuvant chemotherapy in patients with muscle invasive bladder cancer. *Oncoimmunology* (2017) 6(4):e1293211. doi: 10.1080/2162402x.2017.1293211

27. Ruffell B, Coussens LM. Macrophages and therapeutic resistance in cancer. *Cancer Cell* (2015) 27(4):462–72. doi: 10.1016/j.ccell.2015.02.015

28. Zhou J, Sun J, Bai HX, Huang X, Zou Y, Tan X, et al. Prognostic factors in patients with spinal chordoma: An integrative analysis of 682 patients. *Neurosurgery* (2017) 81(5):812–23. doi: 10.1093/neuros/nyx081

29. Lin JX, Lin JP, Xie JW, Wang JB, Lu J, Chen QY, et al. Prognostic importance of the preoperative modified systemic inflammation score for patients with gastric cancer. *Gastric Cancer Off J Int Gastric Cancer Assoc Japanese Gastric Cancer Assoc* (2019) 22(2):403–12. doi: 10.1007/s10120-018-0854-6

30. Dunn GP, Old LJ, Schreiber RD. The immunobiology of cancer immunosurveillance and immunoediting. *Immunity* (2004) 21(2):137–48. doi: 10.1016/j.immuni.2004.07.017

31. Johnson ME, Zhu F, Li T, Wu H, Galloway TJ, Farma JM, et al. Absolute lymphocyte count: A potential prognostic factor for merkel cell carcinoma. *J Am Acad Dermatol* (2014) 70(6):1028–35. doi: 10.1016/j.jaad.2014.01.890

32. Qian BZ, Pollard JW. Macrophage diversity enhances tumor progression and metastasis. *Cell* (2010) 141(1):39–51. doi: 10.1016/j.cell.2010.03.014

33. Kumagai S, Marumo S, Shoji T, Sakuramoto M, Hirai T, Nishimura T, et al. Prognostic impact of preoperative monocyte counts in patients with resected lung adenocarcinoma. *Lung Cancer* (2014) 85(3):457–64. doi: 10.1016/j.lungcan.2014.06.015

34. Ryan AM, Power DG, Daly L, Cushen SJ, Ni Bhuachalla E, Prado CM. Cancer-associated malnutrition, cachexia and sarcopenia: The skeleton in the hospital closet 40 years later. *Proc Nutr Soc* (2016) 75(2):199–211. doi: 10.1017/s002966511500419x

35. Hobusch GM, Bodner F, Walzer S, Marculescu R, Funovics PT, Sulzbacher I, et al. C-reactive protein as a prognostic factor in patients with chordoma of lumbar spine and sacrum–a single center pilot study. *World J Surg Oncol* (2016) 14:111. doi: 10.1186/s12957-016-0875-8

36. Zhou J, Jiang Y, Zhang H, Chen L, Luo P, Li L, et al. Clinicopathological implications of Tim3(+) tumor-infiltrating lymphocytes and the mir-455-5p/Galectin-9 axis in skull base chordoma patients. *Cancer Immunol Immunother* (2019) 68(7):1157–69. doi: 10.1007/s00262-019-02349-1

frontiers | Frontiers in Oncology

TYPE Mini Review
PUBLISHED 20 October 2022
DOI 10.3389/fonc.2022.1016385

OPEN ACCESS

EDITED BY
Gerardo Caruso,
University Hospital of Policlinico G. Martino, Italy

REVIEWED BY
Junpeng Ma,
Beijing Tiantan Hospital, Capital Medical University, China

*CORRESPONDENCE
Georgios A. Zenonos
zenonosg2@upmc.edu

SPECIALTY SECTION
This article was submitted to Neuro-Oncology and Neurosurgical Oncology, a section of the journal Frontiers in Oncology

RECEIVED 10 August 2022
ACCEPTED 30 September 2022
PUBLISHED 20 October 2022

CITATION
Frederico SC, Darling C, Zhang X, Huq S, Agnihotri S, Gardner PA, Snyderman CH, Wang EW and Zenonos GA (2022) Circulating tumor DNA – A potential aid in the management of chordomas. *Front. Oncol.* 12:1016385. doi: 10.3389/fonc.2022.1016385

Circulating tumor DNA – A potential aid in the management of chordomas

Stephen C. Frederico[1,2], Corbin Darling[1,2], Xiaoran Zhang[2], Sakibul Huq[2], Sameer Agnihotri[2], Paul A. Gardner[2], Carl H. Snyderman[2,3], Eric W. Wang[3] and Georgios A. Zenonos[2*]

[1]School of Medicine, University of Pittsburgh, Pittsburgh, PA, United States, [2]Department of Neurological Surgery, University of Pittsburgh, Pittsburgh, PA, United States, [3]Department of Otolaryngology, University of Pittsburgh, Pittsburgh, PA, United States

Chordomas are a locally invasive, low-grade, CNS malignancy that are primarily found in the skull base, spine, and sacrum. They are thought to be derived from notochordal remnants and remain a significant clinical challenge due to their local invasiveness, resistance to chemoradiation, and difficulty in achieving a complete resection. Adjuvant therapy such as proton beam therapy is critical in preventing recurrence in patients who are at high risk, however this treatment is associated with increased risk of complication. Currently, intraoperative observation and imaging findings are used to determine recurrence and success of gross total resection. These methods can be unreliable due to limited operative view, bony and soft tissue involvement, and complex post-operative changes on MRI. Earlier detection of incomplete resection or recurrence will allow for earlier ability to intervene and potentially improve patient outcomes. Circulating-tumor DNA (ctDNA) is cell-free DNA that is released by tumor cells as they undergo cellular turn-over. Monitoring ctDNA has been shown to be more sensitive at predicting residual tumor than imaging in numerous solid malignancies. Furthermore, ctDNA could be detected earlier in peripheral blood as opposed to imaging changes, allowing for earlier intervention. In this review, we intend to give a brief overview of the current state of molecular diagnosis for skull base chordomas. We will then discuss current advances in the utilization of ctDNA for the management of CNS pathologies such as glioblastoma (GBM) and brain metastases. We will also discuss the role ctDNA has in the management of non-CNS pathologies such as osteosarcoma and Ewing sarcoma (EWS). Finally, we will discuss potential implications of ctDNA monitoring for chordoma management.

KEYWORDS

clivus, ctDNA, DNA, tumor, skull base, chordoma

Introduction

Chordomas are low grade tumors that reside primarily in the sacral region, skull base, or within the vertebral bodies. Known to primarily affect patients that are 40-75 years of age, this tumor accounts for approximately 3% of all bone tumors, and roughly 300 new cases of chordoma are diagnosed in the United States each year (1, 2).

Derived from remnants of the notochord, these tumors are very slow growing yet locally invasive, enabling this tumor to have a higher recurrence rate compared to other low grade CNS tumors. Specific genes that are known to contribute to the formation of chordomas include the mTOR signaling pathway, a deficiency in the PTEN pathway, and the brachyury gene, among others (3–5). Deletions of 1p36 and 9p21 (p16/CDKN2A) have been shown to be strongly predictive of outcomes and have recently been incorporated into treatment paradigms allowing for the individualization of treatment (6–8).

The centerpiece of treatment for skull base chordomas is surgical resection, however, total en bloc resection of this tumor is often challenging as it is often difficult to achieve negative margins. Surgical outcomes for this disease are difficult to determine as outcomes are often determined through intra-operative observation as well as post-operative imaging, however these methods of assessment are often inaccurate due to both the presence of unresected microscopic disease, as well as the presence of significant post-operative changes.

While patients can undergo adjuvant radiation therapy for this disease, this treatment modality is associated with significant risks (9). Studies by Abdallah and colleagues highlighted how genetic information can be helpful in determining whether skull base chordoma patients should undergo radiation therapy. Specifically, the results from this study suggested that skull base chordomas with genetic profiles that were deemed "low risk" (based on the presence of 1p36 and 9p21 deletions) could forgo radiation therapy as these patients experienced minimal benefit from this treatment which carries significant risks of complication. The phenotype for tumors with low-risk genetic profiles was defined by the authors as tumors that were smaller, less invasive, asymptomatic when discovered, and more often discovered in younger patients. While genetically profiling chordomas is helpful in determining whether to administer radiation therapy following initial surgical resection, new methods must be created to aid in determining the true extent of surgical resection and the presence of microscopic disease, as well as in determining whether patients are experiencing a recurrence so that they can be more closely monitored. ctDNA could aid in addressing these areas of concern as this technology is being used in cancers outside the CNS to monitor for tumor recurrence as well as to glean genomic information about CNS and non-CNS cancers.

Cell-free DNA (cfDNA) are DNA fragments that can be found in the blood, CSF, or other bodily fluids, that are derived from different cell populations within the body. A subtype of cfDNA is circulating-tumor DNA (ctDNA) which are DNA fragments that have been released into the blood stream from a tumor. It has been well established that tumors are often highly vascularized as tumors need an increased blood supply to continue their growth and proliferation. As tumors grow, their cells undergo apoptosis/necrosis and these cells release their DNA into the blood stream which is often adjacent to the lesion (10). This ctDNA can then be detected *via* liquid biopsy and analyzed to determine whether a tumor is recurring, as well as to establish a mutational profile for the lesion which can be exploited *via* targeted therapies.

In this review, we intend to highlight how ctDNA technology is currently being used in clinical studies to monitor for tumor recurrence in patients diagnosed with brain metastases, glioblastoma (GBM), as well as osteosarcoma and Ewing sarcoma (EWS). In addition to highlighting whether this monitoring of recurrence improved patient outcomes, we will also highlight genomic findings that were gleaned from these studies. Finally, we will share our reasons for why we believe the field should consider incorporating ctDNA monitoring into the management of patients diagnosed with skull base chordomas.

Current molecular methods for diagnosing skull base chordomas

The current methods used for diagnosing skull base chordomas are quite limited as fine-needle aspiration or core needle biopsy are the preferred methods of diagnosis prior to surgical resection. However, these methods pose a concern for tumor seeding (11). Until recently, chordomas were diagnosed by examining their histopathological features as well as their immunoreactivity for S-100 and the presence of epithelial markers such as cytokeratins (12). However, while these methods were useful in diagnosing chordomas, it was quite difficult to differentiate between chordoma and chondrosarcoma which are managed quite differently and bear different prognoses. Recently, brachyury has been recognized as a biomarker capable of distinguishing between chordomas and other chondroid tumors. A study by Oakley and colleagues found that in tissue microarray analysis of 103 chondroid tumors residing within the skull base and other regions within the head and neck, brachyury and cytokeratin staining had a specificity and sensitivity for detecting chordomas of nearly 100% (13). Additionally, histopathologic features such as mitotic figures and a Ki-67 labeling index of greater than 6% are used as measures predictive of chordoma recurrence (14).

Given the risks associated with needle biopsy, the time is now to develop a minimally invasive molecular method for diagnosing and monitoring skull base chordomas. ctDNA analysis is a promising molecular method in the management of skull base chordomas as it has been shown that ctDNA

harbors tumor specific somatic mutations, which can potentially be therapeutically exploited, and many tumors will release ctDNA into the bloodstream (15–17). Additionally, it has been shown that ctDNA can be utilized to detect microscopic disease burden up to six months before disease is able to be observed *via* conventional imaging studies (15, 16, 18). This finding highlights how blood based ctDNA monitoring may be incredibly useful in chordoma management as chordomas are often slow growing and can recur years after initial resection. Early detection of recurrence may allow for therapy to be administered earlier in a patient's recurrence, which could lead to a potential improvement in patient outcomes.

While studies assessing the value of ctDNA analysis in chordoma management are few, one study by Mattox and colleagues found that 87.1% of patients with spinal chordomas were ctDNA positive at the time of their initial blood draw, which was prior to initial surgical resection (18). Additionally, the authors note that follow up blood draws in twenty of the thirty-two patients enrolled in this study suggested that ctDNA levels may reflect clinical status of disease however, these results were not statistically significant due to small sample size (18). Finally, the authors observed that patients who had positive ctDNA levels had greater mutant allele frequencies and were more likely to undergo radiation therapy (18). While not statistically significant, findings from this study suggest that the presence of ctDNA may be correlated with systemic response to chemotherapy and/or recurrence of disease (18).

Currently, little if any studies are present in the literature that assess whether ctDNA analysis is valuable for managing skull base chordomas. Therefore, in addition to discussing the few studies showing how ctDNA has been used in the management of chordomas, we will also discuss how this promising technology is being used in the management of brain metastases, GBM, EWS and osteosarcoma, as we hope to create a narrative for why this technology may be useful in the management of skull base chordomas.

Brain metastases

Brain metastases are the most common neurological complications of systemic cancer, with most neurological metastases frequently found within the brain parenchyma, cranium, dura, and leptomeninges (19). Among all cancer types, lung cancer, breast cancer, and melanoma are the most frequent to metastasize to the brain (20). In many instances, patients with established diagnosis or primary malignancy don't undergo biopsies for metastatic lesions due to the procedure's invasiveness. Additionally, the tissue biopsy approach for brain lesion sampling is dependent upon access to the tumor, and is subject to sampling bias due to tumor heterogeneity (19). Within recent years, peripheral blood cell-free circulating tumor DNA (ctDNA) has been used to characterize and monitor various types of cancer (21, 22). Research suggests that ctDNA is not only an extremely effective method of disease assessment more so than CT imaging, but it can be used to determine response to treatment, differentiating pseudo progression from true tumor progression, and track levels of residual disease (23).

ctDNA, also referred to as liquid biopsy, carries specific gene mutations, and has been used to analyze somatic sequence alterations in various cancers through next-generation sequencing (NGS) or droplet digital polymerase chain reaction (ddPCR) (24). With the promising emergence of this biomarker, several studies have demonstrated its use in the monitoring of intracranial and extracranial brain metastases (16, 25, 26). In a large-case series that sought to determine the predictive value and limitations of peripheral blood-derived ctDNA at baseline and during treatment in patients with melanoma with brain metastases receiving PD-1 inhibitor-based therapy, ctDNA reflected extracranial melanoma activity (27). However, it was not an accurate biomarker of intracranial activity. Intracranial and extracranial disease volume was evaluated in 57 of 72 (79%) patients *via* CT and MRI at baseline. Of those evaluated, 19% had intracranial metastases only, while 81% had intracranial and concurrent extracranial metastases. ctDNA at baseline was undetectable in all patients with intracranial metastases only, while the concurrent group had a ctDNA detection rate of 70%. Intracranial disease response was evaluable in all patients, with ctDNA detectable in 53%, 0% of which were intracranial responses and 64% of which were extracranial, supporting the conclusion that ctDNA is associated with extracranial response, but not intracranial response.

Despite the either absent or extremely low levels of plasma-derived ctDNA associated with exclusive intracranial lesions, it has been shown that ctDNA is present in cerebrospinal fluid (CSF) of brain tumor patients (28). Given CSF's intimate contact with tumor cells of the CNS derived from primary or metastatic lesions and its routine use in cytology examinations for patients with brain lesions (19), there is substantial clinical relevance in its analysis for CNS malignancies. In a recent case report published by Huang W.T. et al, ctDNA was analyzed and used to tailor the treatment of a patient with brain metastases. In a 35-year-old woman who presented with hydrocephalus due to leptomeningeal metastases and a focal mass in the spinal cord adjacent to the cerebellum, the large spinal tumor was excised with histopathological examination confirming adenocarcinoma. The patient was then given several adjuvant immunotherapeutic regimens and chemotherapy drugs, with only anti-HER2 therapy resulting in any clinical benefit. ctDNA analysis was then performed which revealed amplifications of HER2 and MPL, as well as mutations in the PIK3CA, CDKN2A and TP53 genes. Given the ctDNA mutation profile, ado-trastuzumab emtansine was added to a combination regimen of intrathecal trastuzumab and oral lapatinib. Within two weeks of the new anti-HER2 regimen combination, neurological signs increased dramatically and a significant decrease in tumor markers CEA and CA19-9

were noted. Not only does this highlight ctDNA's ability to monitor the effectiveness of ongoing treatment, but its ability to provide insight to the tailoring of personalized treatment.

A prospective study of 21 consecutive patients with non-small cell lung cancer (NSCLC) and brain metastasis also confirmed the specificity of CSF-derived ctDNA over plasma-derived ctDNA in detecting genetic abnormalities specific to brain metastases (29). The study found that mutations were detected in the CSF ctDNA of 20 (95.2%) patients, with a detection rate of epidermal growth factor receptor (EGFR) mutations of 57.1% in CSF ctDNA versus only 23.8% in peripheral blood ctDNA and plasma circulating tumor cells (CTCs). EGFR mutations were found in the CSF of 81.8% of patients with leptomeningeal metastases, as compared with 30% of patients with brain parenchymal metastases. Additionally, the status of EGFR and TP53 mutations was consistent between CSF ctDNA and brain lesion tissue in all patients. As this study further confirms the ability of CSF ctDNA to assist in improving the management of patients with brain metastases, in terms of EGFR-driven genes, the results supported prior studies by Li et al (30) who indicated that CSF was more representative of EGR mutation status in brain metastases than plasma-derived. Additionally, its specificity gives credence to the fact that CSF ctDNA may also reveal uncommon EGFR mutations that could be targeted with specific treatments (31, 32), a consequential tool in molecular brain metastases surveillance.

Another case in a HER2-positive metastatic breast cancer patient with brain metastases also confirms CSF-derived ctDNA's ability to harbor clinically relevant genomic alterations in patients with CNS metastases, making it an effective tool in tracking tumor evolution (33). Baseline CSF-derived ctDNA analysis revealed TP53 and PIK3CA mutations as well as ERBB2 and cMYC amplification. Post treatment ctDNA analysis showed decreased marker levels in plasma, consistent with extra-CNS disease control, while increased in the CSF, confirmed poor treatment benefit in the CNS. Consequently, these results are a positive indicator that CSF ctDNA is more suitable than plasma in revealing the mutational profile of CNS metastases, enabling the characterization of genomic complexity (23) as we seek to create optimized management and treatments for patients with known and unknown brain metastases.

Glioblastoma (GBM)

GBM is one of the most common primary brain tumors and boasts an average life expectancy of just 15-18 months after initial diagnosis. The standard of care for GBM includes maximal surgical resection and chemoradiation therapy, however, despite these measures, patient survival remains poor. One of the major challenges associated with GBM management is monitoring for tumor recurrence as patients often undergo radiation therapy following surgical resection and it is often difficult to differentiate between tumor recurrence and radiation necrosis. This often requires patients to undergo a tumor biopsy which is highly invasive.

ctDNA has been a useful tool in the management of patients with GBM as it has enabled physicians to establish a mutational profile for one's tumor. A study by Bettegowda and colleagues, was able to use ctDNA to detect IDH1, EGFR, TP53 and PTEN mutations in a subset of patients diagnosed with high- and low-grade gliomas (16). However, the authors note that only 10% of patients with gliomas enrolled in the study were able to have ctDNA detected whereas 100% of patients with cancer residing outside the CNS (bladder, colorectal, gastroesphogeal and ovarian) were able to have ctDNA detected. Studies performed since this have had higher ctDNA detection rates in GBM as one study by Piccioni and colleagues detected ctDNA in 50% of patients diagnosed with GBM (34). The results from this study suggest that the ability to detect ctDNA in patients diagnosed with GBM may be correlated with tumor grade and histopathology. Other studies have successfully used ctDNA to detect mutations in the TP53, EGFR, MET, PIK3CA and NOTCH1 genes, as well as the NF1, APC and PDGFRA genes in GBM (34, 35).

ctDNA monitoring has also been used to predict patient outcome in patients diagnosed with GBM that had MGMT methylation. Specifically, it was observed that patients with MGMT methylation detected *via* ctDNA analysis had an improved response and time till progression following treatment with alkylating agents (36). An additional study by Chen and colleagues found that GBM patients whose ctDNA demonstrated Alu methylation had an improved survival when compared to control (37). Studies that seek to use ctDNA as a means to monitor for GBM recurrence are few as GBMs are typically far removed from areas of the brain where CSF abounds, leaving blood as the most viable means to detect GBM ctDNA.

Ewing sarcoma and osteosarcoma

While skull base chordomas reside within the intracranial compartment, unlike brain metastases and primary brain tumors, these bone tumors are outside of the BBB. Additionally, like other bone tumors, chordomas are considered slow growing.

Osteosarcoma is the most common primary bone tumor that primarily affects individuals between the ages of 10 and 30 years old (38). Treatment for osteosarcoma includes surgery which can be targeted to removing just the cancer or removing the affected limb (amputation) if the cancer is too widespread (39). Following surgery, patients undergo chemo-radiation therapy (39). The National Cancer Institute reports in the SEER database that if an osteosarcoma is considered "localized" the five-year survival rate is 77%. However, if this tumor has spread beyond the bone regionally or distantly, the five-year survival reduces to 65% and 26% respectively.

Ewing sarcoma (EWS) are the second most common type of primary bone cancer and are rarely found in individuals over the age of 30 (40). In contrast to treatment for osteosarcoma, patients diagnosed with EWS typically receive chemotherapy prior to surgical resection as this tumor is known to respond well to chemotherapy (41). Following chemotherapy, patients will undergo surgical resection or radiation therapy to remove any remaining disease (41). The National Cancer Institute reports in the SEER database that if the tumor is considered localized the five-year survival rate is 81%. However, if this tumor has spread beyond the bone regionally or distantly, the five-year survival reduces to 67% and 38% respectively.

ctDNA has proven to be a valuable tool in the management of patients diagnosed with osteosarcoma or EWS. In a study by Shulman and colleagues, ctDNA was detected in 53% and 57% of plasma samples from patients with newly diagnosed EWS and osteosarcoma respectively (42). In patients diagnosed with localized EWS detection of ctDNA was correlated with an inferior 3-year event free survival of 48.6% compared to a 3-year event free survival of 82.1% for those without detectable ctDNA (42). The risk of event and death increased in patients diagnosed with EWS or osteosarcoma as the levels of ctDNA increased (42). These findings are supported by Shah and colleagues whose work highlights that EWS and osteosarcoma patients with high ctDNA levels have a significantly increased risk of disease-related death and that a rise in ctDNA levels is predictive of patient relapse (43).

In a study by Krumbholz and colleagues, the authors demonstrate that ctDNA levels in treatment naïve patients are correlated with event-free and OS in patients diagnosed with EWS (44). Like Shah and colleagues, the authors observed that patients experience a reduction in ctDNA levels following treatment with chemotherapy (44). However, the authors also highlight that persistent ctDNA presence following two blocks of treatment with vincristine, ifosfamide, doxorubicin and etoposide is a strong predictor of poor survival (44).

In addition to serving as a valuable predictor of patient survival and highlighting patient response to treatment, ctDNA can reveal complex chromosomal rearrangements. In the study by Shah and colleagues, the research team was able to identify a novel EWSR1-PKNOX2 translocation in a EWS patient's plasma at the time of their relapse (43). This translocation has not been previously described in the literature. While the impact this translocation has on patient survival is unknown, it has been well established that translocations can lead to gene fusions which have been shown to impact disease course (45). Incorporating ctDNA into the management of CNS and non-CNS cancers may allow for the detection of other translocations and gene fusions, allowing the field to develop a further understanding of how tumors progress, as well as better understand how these events impact patient outcomes.

Discussion

In this review we have highlighted cancers of the CNS where ctDNA technology has demonstrated success in determining disease recurrence and/or allowed for the further understanding of tumor genetics (Table 1). It is important to note that ctDNA technology has been valuable in patient care for those diagnosed with non-CNS cancers as well (Table 1). In patients with breast cancer, ctDNA has become a valuable biomarker and enabled physicians to better determine overall patient prognosis (46, 47). Additionally, in patients diagnosed with non-small cell lung

TABLE 1 Clinical trials that have used ctDNA in the management of breast cancer, non-small cell lung cancer, melanoma, brain metastases, glioblastoma, osteosarcoma, EWS, and chordoma.

Trial #	Tumor Type	Detection Method Used	Collection Time	ctDNA Measurement	Trial Status
NCT04353557	Stage I - III Breast Cancer	liquid biopsy (blood)	1-month post-surgery	Determine ctDNA presence at first post-operative timepoint	Recruiting
NCT04768426	Triple-negative Breast Cancer (TNBC)	liquid biopsy (blood)	1. At initial standard adjuvant treatment 2. 6 months after standard adjuvant treatment	Characterize the ctDNA profile of TNBC in participants with residual disease after standard neoadjuvant chemotherapy receiving standard-of-care adjuvant capecitabine	Recruiting
NCT05079074	Late-stage Metastatic Breast Cancer	liquid biopsy (blood)	1. Before treatment 2. After two medication cycles 3. After disease progression	Determine the progression free survival ctDNA change index (12 months)	Completed
NCT04906369	Stage IV Breast Cancer	liquid biopsy (blood)	1. Baseline 2. 2 weeks after start of treatment 3. Beginning of each new treatment cycle	Identify patients with high ctDNA fractions in an effort to detect treatment failure (1 year)	Recruiting
NCT03881384	Breast Neoplasms	liquid biopsy (blood)	Prior to every chemotherapy session until first documented disease progression (up to 100 months)	Determine the concentration of ctDNA	Recruiting

(Continued)

TABLE 1 Continued

Trial #	Tumor Type	Detection Method Used	Collection Time	ctDNA Measurement	Trial Status
NCT05382052	Stage IIIA Non-small Cell Lung Cancer	liquid biopsy (blood) (QIAamp Circulating Nucleic Acid Kit)	1. Before starting neoadjuvant treatment 2. At the end of the neoadjuvant treatment & before surgery 3. After surgery 4. 6 months after surgery 5. At first disease progression (if occurs within 24 months after surgery	Assess the association between the baseline ctDNA and ctDNA clearance with each one of three outcomes: after neoadjuvant treatment, before surgery and PFS	Recruiting
NCT03465241	Stage II-IIIA Non-small Cell Lung Cancer	liquid biopsy (blood) (Secondary Gene Sequencing -NGS)	1. Day before surgery 2. 3rd to 7th day after surgery 3. 3-4 weeks after adjuvant chemotherapy 4. 6-month intervals in following 2 years	To detect ctDNA in patients using the second generation of high-throughput gene sequencing (NGS)	Completed
NCT04791215	Non-Small Cell Lung Cancer	liquid biopsy (blood) (WES)	1. Baseline 2. With routine clinical blood draw	Verify radiologic response to immune checkpoint blockade (ICB) by clonal dynamics of serial ctDNA	Recruiting
NCT04761783	Melanoma Non-small Cell Lung Cancer	liquid biopsy (blood) (SIGNATERA)	1. Baseline 2. During routine care	To use ctDNA to determine patient PFS and OS as well as response rate and duration of response	Recruiting
NCT03808441	Stage III/IV Melanoma	liquid biopsy (blood)	2 to 3 months throughout study completion (an average of 1 year)	To assess decrease in ctDNA levels of mutant BRAF by >80% as an appropriate cut off for changing to immune therapy	Recruiting
NCT05079113	Stage III Melanoma Stage IV Cutaneous Melanoma	liquid biopsy (blood)	1. baseline 2. 3, 6, 18 months	To use ctDNA to identify genetic alterations correlating with the development of disease recurrence	Recruiting
NCT02251314	BRAF Mutant Melanoma	liquid biopsy (blood)	Pre-mortem - 3x 1-30 days apart (1st blood draw during 1st visit) Post-mortem - 48-72 hours from when death expected	Determine the percentage correlation between ctDNA and metastatic sites	Completed
NCT02875652	Choroidal Melanoma	liquid biopsy (blood)	1. Before treatment 2. 1 month after local treatment 3. 7 months 4. Every 6 months up to 3 years	Assess change of ctDNA from baseline to 3 years	Completed
NCT02071056	Leptomeningeal CNS Metastasis	cerebrospinal fluid	During clinically indicated procedures throughout study	To determine whether circulating tumor DNA can be identified in the CSF of patients prior to cytological evidence of leptomeningeal metastasis in patients with history of visceral cancer	Completed
NCT04112238	Diffuse Large B Cell Lymphoma CNS Metastasis	cerebrospinal fluid	1. At time of diagnosis 2. At time of relapse	Determine CSF tumor cfDNA and metabolite detectability and cytological/flow cytometric confirmation of CNS lymphoma at the time of diagnosis and relapse	Recruiting
NCT05480644	Primary Brain Tumor Brain Metastases	liquid biopsy (blood)	6 weeks post radiation therapy	To create a repository of blood samples with number of circulating immune cells and ctDNA in peripheral blood to associate with radiation therapy outcomes	Not yet recruiting
NCT04109131	CNS Metastases	liquid biopsy (blood) cerebrospinal fluid	Pre-diagnosis: 1. TNBC/HER2+ BC: once a year 2. NSCLC/SCLC: every 4 months 3. Melanoma: every 6 months At 1st CNS diagnosis: As close to diagnosis of CNS metastases and no later than 6 weeks after Post diagnosis: Every 3 months (+/- 1 month)	To use ctDNA to better understand the epidemiology and biology of CNS metastases derived from solid tumors	Recruiting
NCT02060890	Glioblastoma	liquid biopsy (blood)	1. Before surgery 2. After surgery 3. 2-month intervals (post-op)	To use ctDNA to help guide treatment plan in adults with recurrent/progressive disease	Completed
NCT05281731	Glioblastoma	liquid biopsy (blood)	1. 10 minutes prior to ultrasound sonication	Determine the feasibility of sonobiopsy as measured by change in ctDNA level	Recruiting

(Continued)

TABLE 1 Continued

Trial #	Tumor Type	Detection Method Used	Collection Time	ctDNA Measurement	Trial Status
			2. 10 minutes after ultrasound sonication 3. 30 or 60 minutes after ultrasound sonication		
NCT04776980	Glioblastoma	liquid biopsy (blood)	During surgical biopsy	Determine proportion of mutations identified by biopsy that are correctly identified in samples of plasma ctDNA	Recruiting
NCT03496402	Osteosarcoma and Ewing Sarcoma	liquid biopsy (blood) cerebrospinal fluid	1. At time of diagnosis 2. During treatment 2. At time of relapse	Compare between genetic variations identified at diagnosis and those identified on ctDNA during treatment, FU and/or relapse	Recruiting
NCT02736565	Ewing Sarcoma	liquid biopsy (blood)	1. Chemotherapy Cycle 1 Week 1 Day 1 2. Chemotherapy Cycle 1 Week 3 Day 1 3. Chemotherapy Cycle 2 Week 1 Day 1 Prior to product infusion and every even cycle thereafter at week 1 day 1 prior to product infusion	Assess ctDNA (EWSR-FLI1) levels and compare to tumor burden and disease response prior to and following pbi-shRNA EWS/FLI1 Type 1 lipoplex administration	Active, not recruiting
NCT02306161	Ewing Sarcoma	liquid biopsy (blood)	Unknown	Determine the proportion of patients that have change in translocation result associated with ctDNA testing over different time periods	Active, not recruiting
NCT02180867	Osteosarcoma	liquid biopsy (blood)	At time of diagnosis	Determine the prevalence of ctDNA at the time of diagnosis	Active, not recruiting
NCT03083678	Chordoma	liquid biopsy (blood)	1. Baseline 2. Cycle 4 - Day 1 3. Cycle 7 - Day 1 4. End of Treatment (within 30 days of last dose)	To gather ctDNA at baseline, during treatment and at the end of treatment for patients treated with afatinib	Active, not recruiting

cancer, ctDNA has been shown to predict overall survival in patients treated with PD-L1 blockade or with chemotherapy, in addition to revealing valuable tumor genetic information (48).

Few studies have utilized ctDNA in the management of chordoma, however, a study by Zuccato and colleagues revealed that chordomas have different subtypes based on their DNA methylation profiles (49). The research team found that different methylation profiles had a strong impact on clinical outcome (49). Additionally, the study found that cell-free DNA methylomes can be used to distinguish chordomas from meningiomas and spinal metastases (49).

There are many potential benefits ctDNA may provide should it be incorporated into the management of those diagnosed with chordomas. In CNS and non-CNS cancers discussed throughout this manuscript, ctDNA has been used to glean valuable tumor genetic information. Given that tumor genetics impacts chordoma invasiveness and risk of recurrence, analysis of genetic information from ctDNA may aid in determining whether patients should undergo radiation therapy, which has risks of complication (7). Additionally, genetic information gleaned from ctDNA analysis may inform patient prognosis as well as aid in understanding tumor subtype.

There are major challenges in determining chordoma recurrence *via* conventional imaging studies due to anatomical changes following surgical resection as well as the slow growing nature of chordomas (50). ctDNA has been used in determining recurrence for tumors residing outside the CNS and may be of value in determining chordoma recurrence as this tumor resides outside the BBB, allowing for the release of ctDNA into the bloodstream and subsequent detection *via* peripheral biopsy.

Author contributions

SF performed a review of the literature, wrote the manuscript, and is the first author. CD contributed to the writing of the manuscript and created the table included in the manuscript. XZ, SH, SA, PG, CS, EW, and GZ provided their expertise on the clinical aspects of the manuscript. GZ supervised the writing of the manuscript. All authors contributed to the article and approved the submitted version.

Conflict of interest

The authors declare that the research was conducted in the absence of any commercial or financial relationships that could be construed as a potential conflict of interest.

Publisher's note

References

1. Phang ZH, Saw XY, Nor N, Ahmad ZB, Ibrahim SB. Rare case of neglected large sacral chordoma in a young female treated by wide en bloc resection and sacrectomy. *BMC Cancer* (2018) 18(1):1112. doi: 10.1186/s12885-018-5012-3

2. Heery CR. Chordoma: The quest for better treatment options. *Oncol Ther* (2016) 4(1):35–51. doi: 10.1007/s40487-016-0016-0

3. Presneau N, Shalaby A, Idowu B, Gikas P, S, Cannon R, Gout I, et al. Potential therapeutic targets for chordoma: PI3K/AKT/TSC1/TSC2/mTOR pathway. *Br J Cancer* (2009) 100(9):1406–14. doi: 10.1038/sj.bjc.6605019

4. Yang C, Sun J, Yong L, Liang C, Liu T, Xu Y, et al. Deficiency of PTEN and CDKN2A Tumor-suppressor genes in conventional and chondroid chordomas: Molecular characteristics and clinical relevance. *Onco Targets Ther* (2020) 13:4649–63. doi: 10.2147/OTT.S252990

5. Sharifnia T, Wawer MJ, Chen T, Huang QY, Weir BA, Sizemore A, et al. Small-molecule targeting of brachyury transcription factor addiction in chordoma. *Nat Med* (2019) 25(2):292–300. doi: 10.1038/s41591-018-0312-3

6. Abdallah HM, Gersey ZC, Muthiah N, McDowell MM, Costacou T, Snyderman CH, et al. An integrated management paradigm for skull base chordoma based on clinical and molecular characteristics. *J Neurol Surg B Skull Base* (2021) 82(6):601–7. doi: 10.1055/s-0041-1725263

7. Zenonos GA, Fernandez-Miranda JC, Mukherjee D, Chang YF, Panayidou K, Snyderman CH, et al. Prospective validation of a molecular prognostication panel for clival chordoma. *J Neurosurg* (2018) 2018:1–10. doi: 10.3171/2018.3.JNS172321

8. Fernandes Cabral DT, Zenonos GA, Fernandez-Miranda JC, Wang EW, Gardner PA. Iatrogenic seeding of skull base chordoma following endoscopic endonasal surgery. *J Neurosurg* (2018) 129(4):947–53. doi: 10.3171/2017.6.JNS17111

9. Alahmari M, Temel Y. Skull base chordoma treated with proton therapy: A systematic review. *Surg Neurol Int* (2019) 10:96. doi: 10.25259/SNI-213-2019

10. Papadopoulos N. Pathophysiology of ctDNA release into the circulation and its characteristics: What is important for clinical applications. *Recent Results Cancer Res* (2020) 215:163–80. doi: 10.1007/978-3-030-26439-0_9

11. Arnautović KI, Al-Mefty O. Surgical seeding of chordomas. *J Neurosurg* (2001) 95(5):798–803. doi: 10.3171/jns.2001.95.5.0798

12. Crapanzano JP, Ali SZ, Ginsberg MS, Zakowski MF. Chordoma. *Cancer Cytopathol* (2001) 93(1):40–51. doi: 10.1002/1097-0142(20010225)93:1<40::AID-CNCR9006>3.0.CO;2-D

13. Oakley GJ, Fuhrer K, Seethala RR. Brachyury, SOX-9, and podoplanin, new markers in the skull base chordoma vs chondrosarcoma differential: a tissue microarray-based comparative analysis. *Modern Pathol* (2008) 21(12):1461–9. doi: 10.1038/modpathol.2008.144

14. Holton JL, Steel T, Luxsuwong M, Crockard HA, Revesz T. Skull base chordomas: correlation of tumour doubling time with age, mitosis and Ki67 proliferation index. *Neuropathol Appl Neurobiol* (2000) 26(6):497–503. doi: 10.1046/j.1365-2990.2000.00280.x

15. Diehl F, Schmidt K, Choti MA, Romans K, Goodman S, Li M, et al. Circulating mutant DNA to assess tumor dynamics. *Nat Med* (2008) 14(9):985–90. doi: 10.1038/nm.1789

16. Bettegowda C, Sausen M, Leary RJ, Kinde I, Wang Y, Agrawal N, et al. Detection of circulating tumor DNA in early- and late-stage human malignancies. *Sci Transl Med* (2014) 6(224):224ra224. doi: 10.1126/scitranslmed.3007094

17. Wang Y, Springer S, Zhang M, McMahon KW, Kinde I, Dobbyn L, et al. Detection of tumor-derived DNA in cerebrospinal fluid of patients with primary tumors of the brain and spinal cord. *Proc Natl Acad Sci U S A* (2015) 112(31):9704–9. doi: 10.1073/pnas.1511694112

18. Mattox AK, Yang B, Douville C, Lo SF, Sciubba D, Wolinsky JP, et al. The mutational landscape of spinal chordomas and their sensitive detection using circulating tumor DNA. *Neurooncol Adv* (2021) 3(1):vdaa173. doi: 10.1093/noajnl/vdaa173

19. Huang WT, Lu NM, Hsu WY, Lo S, Sciubba D, Wolinsky J, et al. CSF-ctDNA SMSEQ analysis to tailor the treatment of a patient with brain metastases: A case report. *Case Rep Oncol* (2018) 11(1):68–74. doi: 10.1159/000486568

20. Gavrilovic IT, Posner JB. Brain metastases: epidemiology and pathophysiology. *J Neurooncol* (2005) 75(1):5–14. doi: 10.1007/s11060-004-8093-6

21. De Mattos-Arruda L, Weigelt B, Cortes J, Won HH, Ng CKY, Nuciforo P, et al. Capturing intra-tumor genetic heterogeneity by *de novo* mutation profiling of circulating cell-free tumor DNA: a proof-of-principle. *Ann Oncol* (2018) 29(11):2268. doi: 10.1093/annonc/mdu239

22. Murtaza M, Dawson SJ, Pogrebniak K, Rueda OM, Provenzano E, Grant J, et al. Multifocal clonal evolution characterized using circulating tumour DNA in a case of metastatic breast cancer. *Nat Commun* (2015) 6:8760. doi: 10.1038/ncomms9760

23. Escudero L, Martínez-Ricarte F, Seoane J. ctDNA-based liquid biopsy of cerebrospinal fluid in brain cancer. *Cancers (Basel)* (2021) 13(9). doi: 10.3390/cancers13091989

24. Diaz LA, Bardelli A. Liquid biopsies: genotyping circulating tumor DNA. *J Clin Oncol* (2014) 32(6):579–86. doi: 10.1200/JCO.2012.45.2011

25. McEvoy AC, Warburton L, Al-Ogaili Z, Celliers L, Calapre L, Pereira MR, et al. Correlation between circulating tumour DNA and metabolic tumour burden in metastatic melanoma patients. *BMC Cancer* (2018) 18(1):726. doi: 10.1186/s12885-018-4637-6

26. Wong SQ, Raleigh JM, Callahan J, Vergara IA, Ftouni S, Hatzimihalis A, et al. Circulating tumor DNA analysis and functional imaging provide complementary approaches for comprehensive disease monitoring in metastatic melanoma. *JCO Precis Oncol* (2017) 1:1–14. doi: 10.1200/PO.16.00009

27. Lee JH, Menzies AM, Carlino MS, McEvoy AC, Sandhu S, Weppler AM, et al. Longitudinal monitoring of ctDNA in patients with melanoma and brain metastases treated with immune checkpoint inhibitors. *Clin Cancer Res* (2020) 26(15):4064–71. doi: 10.1158/1078-0432.CCR-19-3926

28. Pan W, Gu W, Nagpal S, Gephart MH, Quake SR. Brain tumor mutations detected in cerebral spinal fluid. *Clin Chem* (2015) 61(3):514–22. doi: 10.1373/clinchem.2014.235457

29. Ma C, Yang X, Xing W, Yu H, Si T, Guo Z. Detection of circulating tumor DNA from non-small cell lung cancer brain metastasis in cerebrospinal fluid samples. *Thorac Cancer* (2020) 11(3):588–93. doi: 10.1111/1759-7714.13300

30. Li YS, Jiang BY, Yang JJ, Zhang XC, Zhang Z, Ye JY, et al. Unique genetic profiles from cerebrospinal fluid cell-free DNA in leptomeningeal metastases of EGFR-mutant non-small-cell lung cancer: a new medium of liquid biopsy. *Ann Oncol* (2018) 29(4):945–52. doi: 10.1093/annonc/mdy009

31. Tu HY, Ke EE, Yang JJ, Sun YL, Yan HH, Zheng MY, et al. A comprehensive review of uncommon EGFR mutations in patients with non-small cell lung cancer. *Lung Cancer* (2017) 114:96–102. doi: 10.1016/j.lungcan.2017.11.005

32. O'Kane GM, Bradbury PA, Feld R, Leighl NB, Liu G, Pisters KM, et al. Uncommon EGFR mutations in advanced non-small cell lung cancer. *Lung Cancer* (2017) 109:137–44. doi: 10.1016/j.lungcan.2017.04.016

33. Siravegna G, Geuna E, Mussolin B, Crisafulli G, Bartolini A, Galizia D, et al. Genotyping tumour DNA in cerebrospinal fluid and plasma of a HER2-positive breast cancer patient with brain metastases. *ESMO Open* (2017) 2(4):e000253. doi: 10.1136/esmoopen-2017-000253

34. Piccioni DE, Achrol AS, Kiedrowski LA, Banks KC, Boucher N, Barkhoudarian G, et al. Analysis of cell-free circulating tumor DNA in 419 patients with glioblastoma and other primary brain tumors. *CNS Oncol* (2019) 8(2):Cns34. doi: 10.2217/cns-2018-0015

35. Schwaederle M, Husain H, Fanta PT, Piccioni DE, Kesari S, Schwab RB, et al. Detection rate of actionable mutations in diverse cancers using a biopsy-free (blood) circulating tumor cell DNA assay. *Oncotarget* (2016) 7(9):9707–17. doi: 10.18632/oncotarget.7110

36. Balaña C, Ramirez JL, Taron M, Roussos Y, Ariza A, Ballester R, et al. O6-methyl-guanine-DNA methyltransferase methylation in serum and tumor DNA predicts response to 1,3-bis(2-chloroethyl)-1-nitrosourea but not to temozolamide plus cisplatin in glioblastoma multiforme. *Clin Cancer Res* (2003) 9(4):1461–8.

37. Chen J, Huan W, Zuo H, Zhao L, Huang C, Liu X, et al. Alu methylation serves as a biomarker for non-invasive diagnosis of glioma. *Oncotarget* (2016) 7(18):26099–106. doi: 10.18632/oncotarget.8318

38. Ottaviani G, Jaffe N. The epidemiology of osteosarcoma. *Cancer Treat Res* (2009) 152:3–13. doi: 10.1007/978-1-4419-0284-9_1

39. Isakoff MS, Bielack SS, Meltzer P, Gorlick R. Osteosarcoma: Current treatment and a collaborative pathway to success. *J Clin Oncol* (2015) 33 (27):3029–35. doi: 10.1200/JCO.2014.59.4895

40. Baldini EH, Demetri GD, Fletcher CD, Foran J, Marcus KC, Singer S. Adults with ewing's sarcoma/primitive neuroectodermal tumor: adverse effect of older age and primary extraosseous disease on outcome. *Ann Surg* (1999) 230(1):79–86. doi: 10.1097/00000658-199907000-00012

41. Biswas B, Bakhshi S. Management of Ewing sarcoma family of tumors: Current scenario and unmet need. *World J Orthop* (2016) 7(9):527–38. doi: 10.5312/wjo.v7.i9.527

42. Shulman DS, Klega K, Imamovic-Tuco A, Clapp A, Nag A, Thorner AR, et al. Detection of circulating tumour DNA is associated with inferior outcomes in Ewing sarcoma and osteosarcoma: a report from the children's oncology group. *Br J Cancer* (2018) 119(5):615–21. doi: 10.1038/s41416-018-0212-9

43. Shah AT, Azad TD, Breese MR, Chabon JJ, Hamilton EG, Straessler K, et al. A comprehensive circulating tumor DNA assay for detection of translocation and copy-number changes in pediatric sarcomas. *Mol Cancer Ther* (2021) 20(10):2016–25. doi: 10.1158/1535-7163.MCT-20-0987

44. Krumbholz M, Eiblwieser J, Ranft A, Zierk J, Schmidkonz C, Stütz AM, et al. Quantification of translocation-specific ctDNA provides an integrating parameter for early assessment of treatment response and risk stratification in Ewing sarcoma. *Clin Cancer Res* (2021) 27(21):5922–30. doi: 10.1158/1078-0432.CCR-21-1324

45. Bunting SF, Nussenzweig A. End-joining, translocations and cancer. *Nat Rev Cancer* (2013) 13(7):443–54. doi: 10.1038/nrc3537

46. Rohanizadegan M. Analysis of circulating tumor DNA in breast cancer as a diagnostic and prognostic biomarker. *Cancer Genet* (2018) 228-229:159–68. doi: 10.1016/j.cancergen.2018.02.002

47. Shang M, Chang C, Pei Y, Guan Y, Chang J, Li H. Potential management of circulating tumor DNA as a biomarker in triple-negative breast cancer. *J Cancer* (2018) 9(24):4627–34. doi: 10.7150/jca.28458

48. Zou W, Yaung SJ, Fuhlbrück F, Ballinger M, Peters E, Palma JF, et al. ctDNA predicts overall survival in patients with NSCLC treated with PD-L1 blockade or with chemotherapy. *JCO Precis Oncol* (2021) 5:827–38. doi: 10.1200/PO.21.00057

49. Zuccato JA, Patil V, Mansouri S, Liu JC, Nassiri F, Mamatjan Y, et al. DNA Methylation-based prognostic subtypes of chordoma tumors in tissue and plasma. *Neuro-Oncology* (2021) 24(3):442–54. doi: 10.1093/neuonc/noab235

50. al-Mefty O, Borba LA. Skull base chordomas: a management challenge. *J Neurosurg* (1997) 86(2):182–9. doi: 10.3171/jns.1997.86.2.0182

frontiers | Frontiers in Oncology

TYPE Original Research
PUBLISHED 21 October 2022
DOI 10.3389/fonc.2022.1012058

OPEN ACCESS

EDITED BY
Jiwei Bai,
Beijing Tiantan Hospital, Capital Medical University, China

REVIEWED BY
Fabio Stossi,
Baylor College of Medicine, United States
Xiaopeng Guo,
Peking Union Medical College Hospital (CAMS), China

*CORRESPONDENCE
Nyall R. London Jr.
nlondon2@jhmi.edu;
nyall.london@nih.gov

SPECIALTY SECTION
This article was submitted to Neuro-Oncology and Neurosurgical Oncology, a section of the journal Frontiers in Oncology

RECEIVED 05 August 2022
ACCEPTED 27 September 2022
PUBLISHED 21 October 2022

CITATION
Lopez DC, Robbins YL, Kowalczyk JT, Lassoued W, Gulley JL, Miettinen MM, Gallia GL, Allen CT, Hodge JW and London NR Jr (2022) Multi-spectral immunofluorescence evaluation of the myeloid, T cell, and natural killer cell tumor immune microenvironment in chordoma may guide immunotherapeutic strategies. *Front. Oncol.* 12:1012058. doi: 10.3389/fonc.2022.1012058

Multi-spectral immunofluorescence evaluation of the myeloid, T cell, and natural killer cell tumor immune microenvironment in chordoma may guide immunotherapeutic strategies

Diana C. Lopez[1,2], Yvette L. Robbins[3], Joshua T. Kowalczyk[4], Wiem Lassoued[4], James L. Gulley[4], Markku M. Miettinen[5], Gary L. Gallia[6,7], Clint T. Allen[3], James W. Hodge[4] and Nyall R. London Jr[1,6,7]*

[1]Sinonasal and Skull Base Tumor Program, National Institute on Deafness and Other Communication Disorders, National Institutes of Health, Bethesda, MD, United States, [2]Cleveland Clinic Lerner College of Medicine, Cleveland Clinic, Cleveland, OH, United States, [3]Section on Translational Tumor Immunology, National Institute on Deafness and Other Communication Disorders, National Institutes of Health, Bethesda, MD, United States, [4]Center for Immuno-Oncology, National Cancer Institute, Center for Cancer Research, National Institutes of Health (CCR, NIH), Bethesda, MD, United States, [5]Laboratory for Pathology, Center for Cancer Research, National Cancer Institute, Bethesda, MD, United States, [6]Department of Otolaryngology-Head and Neck Surgery, Johns Hopkins University School of Medicine, Baltimore, MD, United States, [7]Department of Neurosurgery, Johns Hopkins University School of Medicine, Baltimore, MD, United States

Background: Chordoma is a rare, invasive, and devastating bone malignancy of residual notochord tissue that arises at the skull base, sacrum, or spine. In order to maximize immunotherapeutic approaches as a potential treatment strategy in chordoma it is important to fully characterize the tumor immune microenvironment (TIME). Multispectral immunofluorescence (MIF) allows for comprehensive evaluation of tumor compartments, molecular co-expression, and immune cell spatial relationships. Here we implement MIF to define the myeloid, T cell, and natural killer (NK) cell compartments in an effort to guide rational design of immunotherapeutic strategies for chordoma.

Methods: Chordoma tumor tissue from 57 patients was evaluated using MIF. Three panels were validated to assess myeloid cell, T cell, and NK cell populations. Slides were stained using an automated system and HALO software objective analysis was utilized for quantitative immune cell density and spatial comparisons between tumor and stroma compartments.

Results: Chordoma TIME analysis revealed macrophage infiltration of the tumor parenchyma at a significantly higher density than stroma. In contrast,

helper T cells, cytotoxic T cells, and T regulatory cells were significantly more abundant in stroma versus tumor. T cell compartment infiltration more commonly demonstrated a tumor parenchymal exclusion pattern, most markedly among cytotoxic T cells. NK cells were sparsely found within the chordoma TIME and few were in an activated state. No immune composition differences were seen in chordomas originating from diverse anatomic sites or between those resected at primary versus advanced disease stage.

Conclusion: This is the first comprehensive evaluation of the chordoma TIME including myeloid, T cell, and NK cell appraisal using MIF. Our findings demonstrate that myeloid cells significantly infiltrate chordoma tumor parenchyma while T cells tend to be tumor parenchymal excluded with high stromal infiltration. On average, myeloid cells are found nearer to target tumor cells than T cells, potentially resulting in restriction of T effector cell function. This study suggests that future immunotherapy combinations for chordoma should be aimed at decreasing myeloid cell suppressive function while enhancing cytotoxic T cell and NK cell killing.

KEYWORDS

chordoma, tumor immune microenvironment (TIME), immunotherapy, myeloid cells, T cells, natural killer cells

Introduction

Chordoma is a rare, invasive, and devastating bone malignancy (1, 2). Chordomas arise from residual notochord tissue within the axial skeleton (1–3), and are therefore found in the clivus of the skull base, spine, or sacrum (1, 2). Prognosis is poor with reported five and ten-year survival rates of approximately 70% and 40%, respectively (3, 4). When feasible, standard treatment typically consists of surgical resection and radiotherapy. However, the tumor's invasive nature and close proximity to critical neurovascular structures makes a negative margin or gross total resection difficult (2, 3). Furthermore, chordoma's resistance to traditional chemotherapy and radiation is well established (5), and primary and adjuvant treatment strategies come with significant morbidity (1, 6). Thus, there is an unmet need for additional or targeted treatment options, and the role of immunotherapy for chordoma remains under investigation.

The study of the tumor microenvironment, consisting of tumor, immune, vascular, and fibroblast cells (7), has garnered increased recent attention due to advances in immunotherapeutic options. An understanding of the host immune antitumor response can be important in prognostication, tumor phenotyping, and optimization of targeted treatment (8). However, the characterization of chordoma's complex and heterogeneous tumor immune microenvironment continues to be preliminary (7, 9). Of particular interest in the TIME are the myeloid, T cell, and natural killer cell compartments (10–12). Myeloid cells include macrophages, monocytes, neutrophils, and other cell types that can have a broad array of immunomodulatory effects on the TIME (13). Furthermore, myeloid cells can differentiate into myeloid-derived suppressor cells (MDSC) which can have profound immunosuppressive disruption of T cell mediated tumor immunity (13, 14). Amongst T cells, $CD4^+$ helper and $CD8^+$ cytotoxic T cells enact immune surveillance, recognition, and destruction of tumor cells while regulatory T cells (T_{reg}) suppress anti-tumor immune responses (15). In contrast to T cells, natural killer (NK) cells do not depend on antigen presentation for their activity and can work in concerted effort with antibodies and T cells to enact tumor cell destruction (16).

Harnessing a patient's immune system to maximize therapeutic efficacy and limit treatment toxicity is a promising research direction for many treatment-resistant malignancies. Immune checkpoint blockade is one such method that may prove beneficial for chordoma (8). The programmed cell death receptor/programmed cell death ligand 1 (PD-1/PD-L1) axis is a known pathway exploited by neoplasms to evade immune surveillance (17, 18), inhibition of which has demonstrated clinical efficacy in melanoma and malignancies of the lung (19, 20). In chordoma specifically, tumor infiltrating lymphocyte (TIL) PD-1 expression has been associated with worsened local recurrence free survival (21). This notion substantiates a current phase II clinical trial underway for nivolumab, a monoclonal antibody against PD-1, in combination with relatlimab, another

immune checkpoint inhibitor, for the treatment of recurrent, advanced or metastatic chordoma (NCT03623854). Derivation of additional therapeutic targets for the treatment of chordoma must stem from a better understanding of its TIME. Future immunotherapeutic chordoma clinical trial design would also significantly benefit, as prior trials in breast cancer (22) and melanoma (23) have, from precise evaluation of pre- versus post-treatment tumor-host immune interactions.

Multispectral immunofluorescence (MIF) is an advanced technique that involves staining of tissue specimens with panels of multiple simultaneous antibody markers and allows for appraisal of the high-resolution images. Single cell analyses of these images enable cellular characterization by surface phenotype into tumor compartment (i.e. tumor and stroma), precise immune cell and tumor cell quantification, and evaluation of spatial arrangements among these. Herein, we describe the first comprehensive interrogation of the chordoma TIME including the myeloid cell, T cell, and NK cell compartments, using MIF. We hypothesized that myeloid, T cells, and NK cells would be identifiable within the chordoma TIME, and that effector cells may exhibit restricted tumor penetrance while cells with potentially immunosuppressive activity may be seen within closer proximity to chordoma cells.

Methods

Patient population

Ten chordoma specimens were obtained through a Johns Hopkins Institutional Review Board approved study (IRB00227737) and each patient provided written informed consent. Ten chordoma specimens were also obtained from the Chordoma Foundation Biobank and studied following National Institutes of Health Institutional Review Board exemption. Additionally, a tumor microarray (TMA) of 37 anonymized chordoma samples was obtained from the NIH Department of Pathology, totaling a sample size of 57 chordomas. Of these, clinical data could be acquired for the 20 patients from the Chordoma Foundation and Johns Hopkins University. A retrospective chart review of chordoma patients at Johns Hopkins University was conducted. Clinical variables collected included patient demographics (age, sex, race, and ethnicity), anatomic site of tumor origin (skull base, spine, sacrum/coccyx), disease stage, tumor resection extent, tumor grade, treatment regimen (chemotherapy and radiotherapy), and last documented clinical status.

Tissue preparation

Slides were first baked at 60°C for 30 minutes and soaked in Bond Dewax Solution (Leica Biosystems, #AR9222) at 72°C followed by rehydration with 100% ethanol. Leica BOND Rx autostainer (Leica Biosystems Melbourne Pty Ltd, Melbourne, Australia) was used for deparaffinization and staining of all tissue.

Panel validation

The dilution of each antibody specific to formalin fixed paraffin embedded (FFPE) chordoma tissue type was determined first using monoplex immunohistochemistry (IHC) and then monoplex immunofluorescence (IF). Staining strength and specificity for the marker of interest with IHC, carried out using chromogen 3'-3' diaminobenzidine tetrahydrochloride hydrate (DAB) detection (BOND Polymer Refine Detection, Leica Biosystems, New Castle Upon Tyne, UK; #DS9800), determined the dilution to be used as a starting point for IF optimization. IHC positive control tissue, either normal tonsil or normal lung tissue (4-5μm sections), was chosen based on previously identified protein of interest expression, as listed in the Human Protein Atlas (proteinatlas.org) (24). Unstained chordoma tissue (4-5μm sections) served as a negative control for all validation steps. Once optimal IF dilutions were established, multiple combinations of antibodies were tested to determine the most appropriate staining order for the final creation of each multispectral immunofluorescence (MIF) panel (Supplementary Table 1).

The myeloid cell panel was comprised of antibodies against CD15 (BD Biosciences [HI98], #555400; 1:1500), CD68 (Invitrogen [KP1], #MA5-13324; 1:1000), CD11b (Abcam [EPR1344], #ab133357; 1:5000), CD14 (Abcam [EPR3653], #ab133335; 1:1000), HLA-DR (Abcam [TAL 1B5], #ab20181; 1:1200), and cytokeratin (Santa Cruz [AE1/AE3], #sc-81714; 1:400). Staining was completed in this order. The myeloid panel allowed for the recognition of pan macrophages, monocytes, and polymorphonuclear (PMN) leukocytes. Cells highly positive for CD68 were categorized as pan macrophages. Tumor associated macrophages (TAMs) express a number of macrophage-specific markers, among these CD68, a heavily glycosylated type I transmembrane glycoprotein (25, 26). CD68 was chosen to identify pan macrophages in this study in keeping with prior investigations of TAMs for the purposes of generalizability and because CD68 has been shown as a good prognostic indicator of cancer patient survival (27–30). Monocyte phenotypes were $CD11b^+/CD14^+/CD15^-$/HLA-DR while PMN phenotypes were $CD11b^+/C14^-/CD15^+$/HLA-DR^-. In the literature, monocyte myeloid derived suppressor cells have been defined as $CD11b^+CD14^+$ $CD15^-$HLA-$DR^{-/}$lo. Conversely, PMN myeloid derived suppressor cells have been defined as $CD11b^+CD14^-CD15^+$ (31, 32). These established definitions served as the authors' rationale for identifying myeloid cell subtypes as described above. However, we acknowledge that in the absence of functional assays one cannot definitely determine

whether monocytes and PMNs meeting the phenotypic criteria direct a suppressive response.

The T cell panel consisted of antibodies against CD4 (Abcam [EPR6855], #ab133616; 1:1000), CD8 (Abcam [EPR10640(2)], #ab215041; 1:2000), FOXP3 (Invitrogen [SP97], #MA5-16365; 1:200), PD-1 (Abcam [EPR4877(2)], #ab137132; 1:750), Ki67 (Ventana [30-9], #790-4286; 1:1), and cytokeratin (Santa Cruz [AE1/AE3], #sc-81714; 1:400). Staining was completed in this order. This T cell panel revealed the presence of T-regulatory cells, $CD4^+$ T-helper cells, and $CD8^+$ cytotoxic T cells. T-regulatory cells were simultaneously positive for CD4 and FOXP3 markers, while non-T-regulatory cells were FOXP3 negative. $CD4^+$ T-helper cell phenotypes were $CD4^+$ and $CD8^-$/$FOXP3^-$, while $CD8^+$ cytotoxic T cell phenotypes were $CD8^+$ and $CD4^-$/$FOXP3^-$. Positive Ki67 staining denoted proliferating cells. PD-1 stain allowed for identification of PD-1^+ T cells.

The NK cell panel was comprised of antibodies against CD3 (Abcam [SP7], #ab16669; 1:300), CD56 (NCAM1) (Sigma Aldrich [MRQ-42], #156R-94; 1:250), CD16 (Abcam [SP175], #ab183354; 1:150), Granzyme B (Abcam [EPR8260], #ab134933; 1:200), and cytokeratin (Santa Cruz [AE1/AE3], #sc-81714; 1:400). Staining was completed in this order. $CD16^+$/$CD56^+$/$CD3^-$ and a decreased size threshold relative to tumor cells was the phenotype used to identify NK cells. Granzyme B positivity denoted activated NK cells.

Similar to the validation stages, positive and negative controls included normal human tonsil or lung tissue and unstained sections lacking primary antibody, respectively. All slides were counterstained with 4′,6-diamidino-2-phenylindole (DAPI) to identify cell nuclei. Cytokeratin distinguished chordoma tumor cells in all panels.

Staining and scanning

Standardized staining protocols (Perkin Elmer platform), using the Leica Bond Rx automated system described above, were completed with 4μm FFPE sections of chordoma tissue. Heat induced epitope retrieval (HIER) was executed for all antibodies except CD15 by heating slides to 95°C and treating with paired BOND Epitope Retrieval (ER) solutions, either citrate-based ER1 (Leica Biosystems, #AR9961) or EDTA-based ER2 (Leica Biosystems, #AR9640). Primary antibody was applied for 60 minutes, followed by secondary HRP-conjugated antibody for 30 minutes, and finalized by fluorescent signal amplification for every protein target. OPAL (Akoya Biosciences) multiplex kit consisting of OPAL-480, 520, 570, 620, 690, 780 conjugates allowed for the evaluation of up to six colors simultaneously. With the exception of Opal 780 made at 1:50 dilution, all opals were made at a 1:150 dilution. Opal 780 was combined with TSA-DIG at a 1:100 dilution. After staining, slides were cover slipped with the Leica CV5030 automated glass cover slipper (Leica Biosystems, Nussloch, Germany Ltd) and scanned at 40x magnification with suitable exposure times using PerkinElmer Vectra Polaris for the creation of high-resolution digital images. One slide stained with the myeloid panel was excluded due to technical issues with slide scanning and three tumors stained with the NK panel on the tumor microarray slide were excluded due to overexposure with scanning parameters best suited to the greatest number of tumors.

Image analysis

Images were analyzed using the HALO® (Indica Labs, Albuquerque, NM, USA) platform v3.3, which allows for diverse cell type quantification, identification of marker of interest co-localization, and cellular spatial relation analysis. First, slides were annotated into tumor core and stroma using the HALO® random forest classifier based on cytokeratin staining. Histologic areas of bone, bone marrow, and blood vessels, identified using hematoxylin and eosin (H&E) stains, along with auto fluorescent tissue subsections, were manually excluded for analysis. Cell size, nuclear to cytoplasmic ratio, nuclear segmentation, and individual biomarker fluorescence intensity thresholds were set to denote cells of each phenotype of interest. These were calibrated for each independent specimen to account for variability in staining uptake. Quantification analyses were run using the HALO® Highplex FL analysis algorithm v4.1.3. Nearest neighbor analyses, to determine the average distance and number of unique neighbors between two cell populations, and proximity analyses, for calculation of the number of cells within a 20μm or 100μm distance of a given cell of interest, were conducted. These were used to investigate distances of helper T cells, cytotoxic T cells, T-regulatory cells, pan macrophages, monocytes, and PMNs to chordoma cells. Spatial relationships between T-regulatory cells and cytotoxic T cells were also evaluated. HALO® density heat maps of all immune cell compartments were created to visually compare immune infiltrate patterns.

Statistical analysis

Immune cell densities and spatial relationships were represented with box and whisker plots and histograms, respectively. Wilcoxon signed rank tests were used to detect statistical differences between dependent groups of tumors versus stroma immune cell density. A Wilcoxon signed rank test was also used to evaluate the difference between T-regulatory cell distances to cytotoxic T cells by proliferation status. Two-way ANOVA analysis was used to compare immune cell densities among groups by anatomic site of origin and disease

stage. A p value significance threshold of <0.05 was employed in all cases. All statistics were conducted and graphs prepared using GraphPad Prism version 9.2.

Results

The presence of myeloid cells, particularly a myeloid-derived suppressor cell subset, within the tumor microenvironment has been associated with immunosuppression and a decreased clinical immunotherapy response (32–34). To identify myeloid cells within the chordoma tumor microenvironment, chordoma tissue sections were stained using an automated multispectral immunofluorescence system with antibodies against C11b, HLA-DR, CD14, CD15, CD68, and cytokeratin (CK) (Figure 1A) followed by digital scanning, image annotation, and cellular analysis (Supplementary Figure 1). Significant tumor parenchymal myeloid cell infiltration was noted. The highest expressing CD68 cells were classified as pan macrophages, and cytokeratin positive cells as chordoma tumor cells. Myeloid cell quantification analysis revealed that macrophages infiltrated the tumor parenchyma at a significantly higher density than stroma (median 43.60 cells per mm^2 in tumor, median 25.11 cells per mm^2 in stroma, p = 0.006) and made up the majority of myeloid cells found within the chordoma tumor microenvironment (Figure 1B). Co-localization of CD11b and CD14 in the absence of CD15 and with low HLA-DR identified monocytes. There was a slightly greater monocyte cell density identified in the stroma as compared to tumor (median 2.02 cells per mm^2 in tumor, median 3.87 cells per mm^2 in stroma, p = 0.036) (Figure 1B). Co-localization of CD11b and CD15 in the absence of CD14 and with low HLA-DR identified PMN-like cells. PMN-like cell density was comparable between tumor and stroma (median 1.79 cells per mm^2 in tumor, median 2.12 cells per mm^2 in stroma, p = 0.378) (Figure 1B). Myeloid cell density differences between tumor and stroma are graphed using mean ± standard error of the mean (SEM) in Supplementary Figure 2.

T cells are vital players to the antitumor response and represent some of the most important targets for immunotherapeutics to date (10). To identify T cells within the chordoma tumor immune microenvironment, tissue sections were stained with a panel of antibodies against CD4, CD8, FOXP3, Ki67, PD-1, and CK (Figure 2A). Staining with the validated T cell panel showed grossly appreciable T cell tumor parenchymal exclusion with restriction of most T cells to stromal

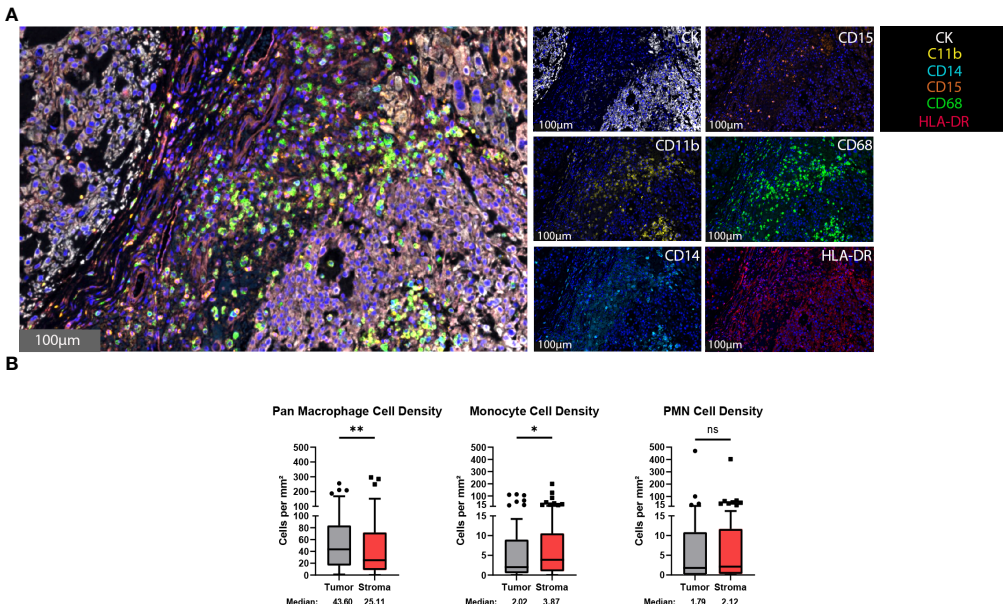

FIGURE 1
Myeloid cells are found within the chordoma tumor immune microenvironment. **(A)** Representative photomicrographs from one chordoma of merged and single-color immunofluorescence images assessing the presence of myeloid cells with a validated panel of six biomarkers, CD11b (yellow, Opal 570), HLA-DR (red, Opal 690), CD14 (turquoise, Opal 480), CD15 (orange, Opal 620), CD68 (green, Opal 520), and CK (white, Opal 780). Multispectral immunofluorescence images are counterstained with DAPI. High expression of CD68 identified pan macrophages. Co-localization of CD11b and CD14 without CD15 and HLA-DR identified monocytes. Co-localization of CD11b and CD15 without CD14 and HLA-DR identified PMNs. Expression of CK identified chordoma tumor cells. **(B)** Quantification of pan macrophages, monocytes, and PMNs per mm^2 in chordoma tumor and stroma (n = 56 individual tumors). Wilcoxon signed rank tests with p value threshold of <0.05 were used to compare tumor and stroma myeloid cell infiltrate. *$p \leq 0.05$, **$p \leq 0.01$, ns, non significant. CK, cytokeratin; DAPI, 4′,6-diamidino-2- phenylindole; PMN, polymorphonuclear cells.

tissue (Figure 2A). FOXP3 negative $CD4^+$ cells were identified as helper T cells, co-localization of CD4 and FOXP3 in the absence of CD8 identified T_{regs}, and $CD8^+$ cells were identified as T cells with potential cytotoxic activity against chordoma cells. T cell quantification analysis objectively revealed significantly more T cells per mm^2 in stroma as compared to tumor for all $CD4^+$ T cells (median 11.43 and 30.56 cells per mm^2 in tumor and stroma, respectively, $p < 0.0001$), $CD8^+$ T cells (median 10.11 and 36.71 cells per mm^2 in tumor and stroma, respectively, $p < 0.0001$), and T_{regs} (median 0.75 and 3.18 cells per mm^2 in tumor and stroma, respectively, p value < 0.0001) (Figure 2B). Proliferating $CD8^+$ T cells (median 1.17 and 1.75 cells per mm^2 in tumor and stroma, respectively, $p = 0.011$) and $PD1^+$ $CD8^+$ T cells (median 3.68 and 11.56 cells per mm^2 in tumor and stroma, respectively, $p = 0.0001$) were also significantly more abundant in chordoma stroma. Although proliferating $CD4^+$ T cells (median 1.24 and 1.00 cells per mm^2 in tumor and stroma, respectively, $p = 0.888$) and $PD1^+$ $CD4^+$ T cells (median 1.05 and 0.46 cells per mm^2 in tumor and stroma, respectively, $p = 0.180$) were slightly more abundant in the tumor parenchyma, these small differences failed to reach statistical significance. Only a minor subset of samples contained proliferating T_{regs} (median 0.00 cells per mm^2 in tumor and stroma) and $PD1^+$ T_{regs} (median 0.00 cells per mm^2 in tumor and stroma) (Figure 2B).

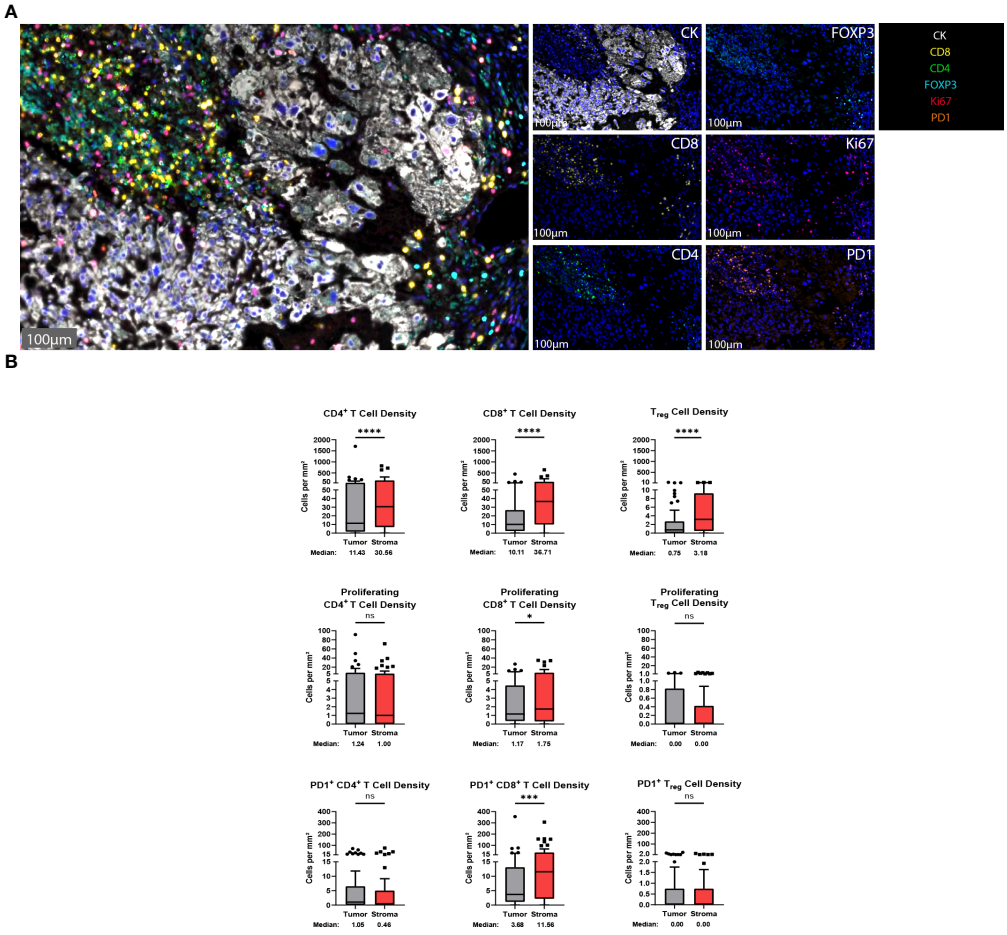

FIGURE 2
T cells are found in abundance within the chordoma tumor immune microenvironment, most often within the stroma. **(A)** Representative photomicrographs from one chordoma of merged and single-color immunofluorescence images assessing the presence of T cells with a validated panel of six biomarkers, CD8 (yellow, Opal 570), CD4 (green, Opal 520), FOXP3 (turquoise, Opal 480), Ki67 (red, Opal 690), PD1 (orange, Opal 620), and CK (white, Opal 780). Multispectral immunofluorescence images are counterstained with DAPI. Expression of CD4 without CD8 and FOXP3 identified $CD4^+$ T helper cells, while expression of CD8 without CD4 and FOXP3 identified $CD8^+$ cytotoxic effector T cells. Co-localization of CD4 and FOXP3 without CD8 identified T_{regs}. T cells with positive Ki67 nuclear expression were proliferating, and PD1 positivity denoted $PD1^+$ T cells. Expression of CK identified chordoma tumor cells. **(B)** Quantification of $CD4^+$ T cell, $CD8^+$ T cell, and T_{reg} cell density (per $mm^{2)}$, as well as proliferating and PD-1^+ subcategories of these are compared between chordoma tumor and stroma (n = 57 individual tumors). Wilcoxon signed rank tests with p value threshold of <0.05 were used to compare tumor and stroma T cell infiltrate. *$p \leq 0.05$, ***$p \leq 0.001$, ****$p \leq 0.0001$, ns, non significant. CK, cytokeratin; DAPI, 4′,6-diamidino-2- phenylindole; PD1, programmed cell death protein 1.

Similarly, Ki67$^+$, or proliferating CD4$^+$ and CD8$^+$ T cells, made up small proportions, less than 20%, of these cell types. Of note, the PD1$^+$ CD8$^+$ T cell subcategory represented over one third of cytotoxic T cells. T cell density differences between tumor and stroma are graphed using mean ± standard error of the mean (SEM) in Supplementary Figure 3.

The degree of tumor parenchymal T cell inclusion versus exclusion was assessed (Figures 3A, B). A ratio of >1.5 tumor to stroma T cell infiltrate defined substantial T cell inclusion whereas a ratio of >4.5 stroma to tumor T cell infiltrate defined substantial T cell exclusion. Figure 3A shows high parenchymal CD4$^+$ T cell inclusion in six samples, high CD8$^+$ T cell inclusion in three samples, and high T_{reg} inclusion in four samples. However, notable tumor parenchymal exclusion was seen at higher rates, with 13 samples meeting criteria for high CD4$^+$ T cell exclusion, 23 samples for high CD8$^+$ T cell exclusion, and 12 samples for high T_{reg} exclusion. Thus, chordoma T cell compartment inflammation more commonly takes on a tumor parenchymal exclusion pattern, most markedly among cytotoxic T cells.

Natural killer (NK) cells are viable therapeutic targets known to kill adjacent cells independently of antigen presentation and have been shown by our group to effectively act against chordoma tumor cells in an inducible fashion (11, 16). CD56, also known as neural cell adhesion molecule, is a common marker for NK cells. However, we found that a significant proportion of chordoma cells express CD56 as previously reported (35). We therefore defined NK cells by a decreased size threshold as compared to larger chordoma cells along with CD16, CD56 co-localization in the absence of CD3. Granzyme B positivity revealed active NK cells. NK cells were sparsely observed in chordoma tissue (Figure 4A). Quantification uncovered slightly greater, albeit non-significant, tumor NK cell infiltration (median 0.52 cells per mm^2 in tumor, median 0.11 cells per mm^2 in stroma, $p = 0.085$) with similar patterns detected by Granzyme B$^-$ subcategorization (median 0.30 cells per mm^2 in tumor, median 0.00 cells per mm^2, $p = 0.056$) (Figure 4B). Few NK cells expressed Granzyme B overall (median 0.00 cells per mm^2 in tumor and stroma), although a subset of five tumors were identified that expressed >2 Granzyme B$^+$ NK cells per mm^2 (Figure 4B).

Immune cell spatial analysis using the HALO® (Indica Labs) v3.3 platform allowed for a greater understanding of spatial relationships between immune cells and tumor cells within the chordoma tumor immune microenvironment (Figures 5A–C). The majority of myeloid cells and T cells were found within 30μm and 50μm of chordoma cells, respectively (Figure 5D). Myeloid cell mean distance to chordoma cells was comparable for all three cell types, pan macrophage: 36.55μm ± 25.70μm, PMN-like: 43.59μm ± 37.15

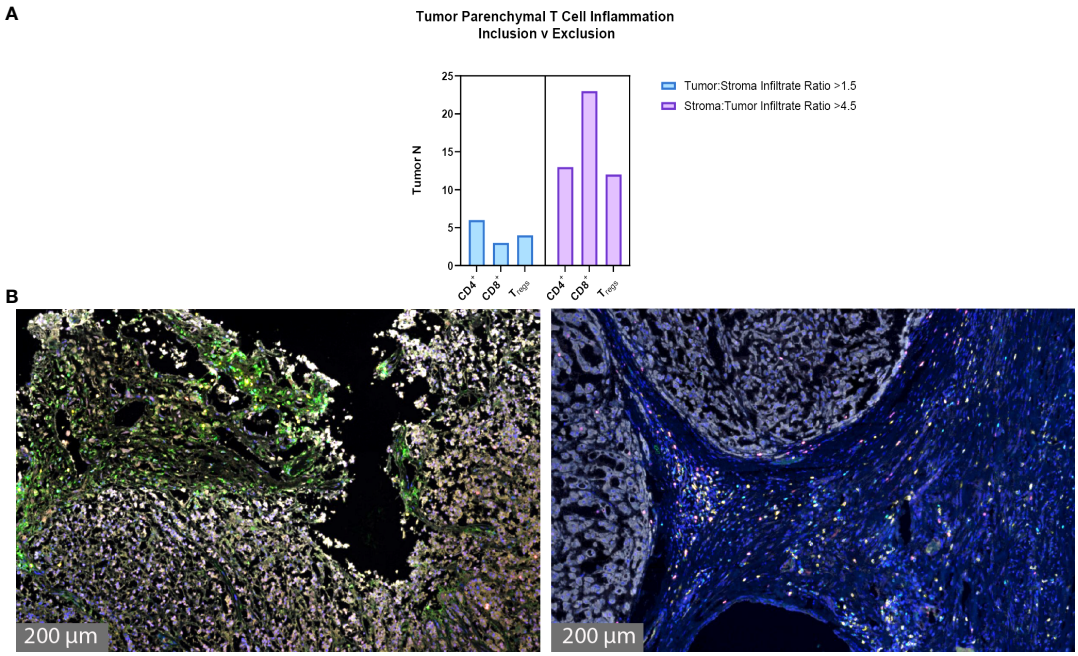

FIGURE 3
Chordoma tumor parenchymal T cell inclusion versus exclusion. T cell compartment inflammation in chordoma more commonly takes on a tumor parenchymal exclusion, rather than inclusion, pattern (n = 57 individual tumors). **(A)** A tumor:stroma T cell infiltrate ratio >1.5 defined substantial tumor parenchymal inclusion. A stroma:tumor T cell infiltrate ratio >4.5 defined substantial tumor parenchymal exclusion. **(B)** Representative chordoma samples with heavy tumoral infiltrate (left) versus heavy stromal infiltrate (right).

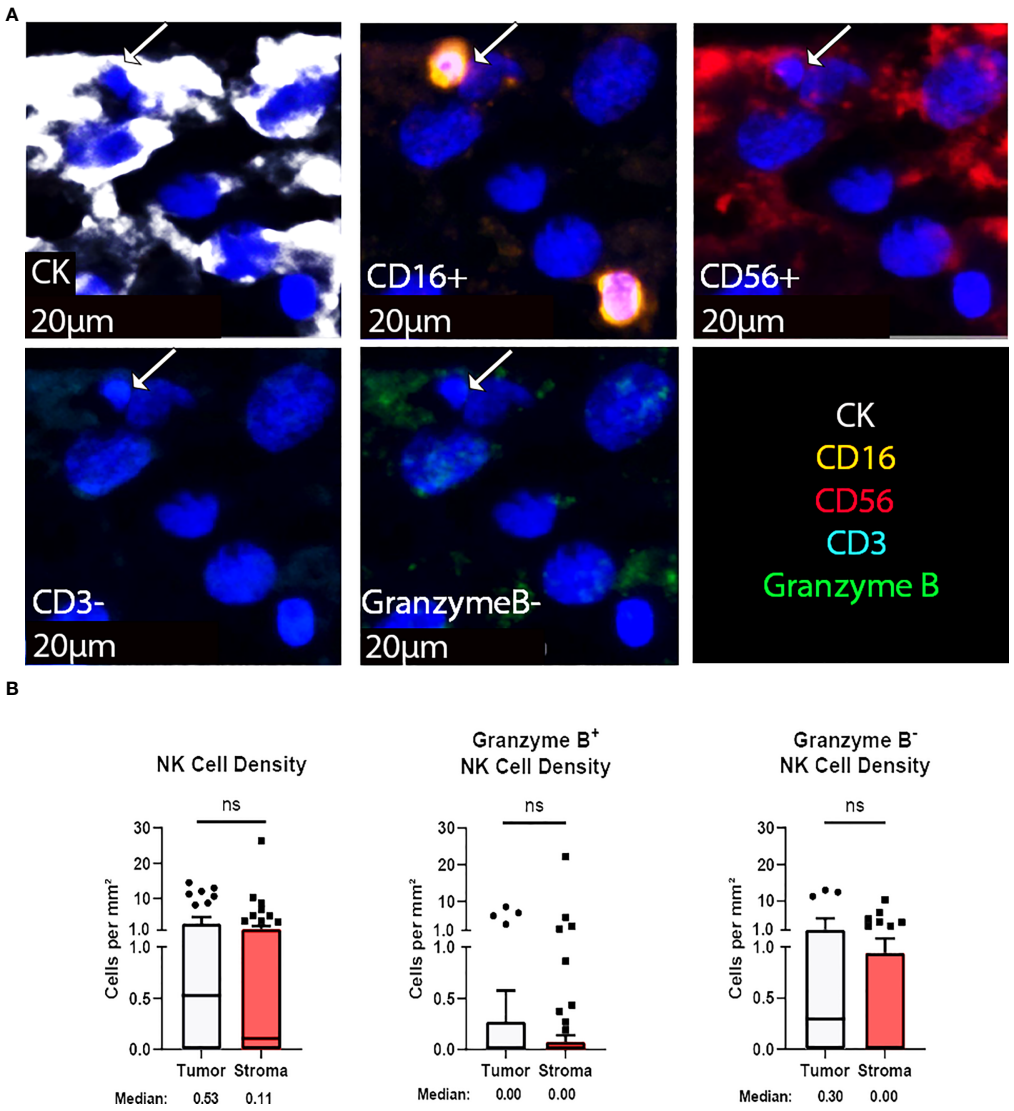

FIGURE 4
NK cells are sparsely found within the chordoma tumor immune microenvironment. **(A)** Representative photomicrographs from one chordoma of merged and single-color immunofluorescence images assessing the presence of NK cells with a validated panel of five biomarkers, CD16 (orange, Opal 620), CD56 (red, Opal 690), CD3 (turquoise, Opal 480), Granzyme B (green, Opal 520), and CK (white, Opal 780). Multispectral immunofluorescence images are counterstained with DAPI. Co-localization of CD16 and CD56 without CD3 and a decrease size threshold compared to tumor cells identified NK cells. Expression of Granzyme B identified Granzyme B^+ or Granzyme B^- NK cells. Expression of CK identified chordoma tumor cells. **(B)** Quantification of NK cells overall, Granzyme B^+, and Granzyme B^- NK cells per mm^2 in chordoma tumor and stroma (n = 54 individual tumors). Wilcoxon signed rank tests with p value threshold of <0.05 were used to compare tumor and stroma NK cell infiltrate. ns, non significant. NK cell, natural killer cell; CK, cytokeratin; DAPI, 4′,6-diamidino-2- phenylindole.

μm, monocyte: 50.67μm ± 45.54μm. Mean distance to chordoma cells was likewise similar among all T cells, $CD4^+$ T cells: 97.40μm ± 185.07μm, $CD8^+$ T cells: 92.52μm ± 167.04μm, and T_{regs}: 114.66μm ± 165.67μm. The distance between T cells and tumor cells was consistently greater than the distance between myeloid cells and tumor cells. Similarly, the mean percentage of myeloid cells identified within 100μm of chordoma cells (PMN: 90.68% ± 19.79%, monocyte: 86.66% ± 23.44%, pan macrophage: 93.34% ± 11.74%) was greater than the mean percentage of T cells identified within 100μm of chordoma cells ($CD4^+$ T cells: 81.40% ± 26.22%, $CD8^+$ T cells: 80.49% ± 26.65%, T_{regs}: 62.76% ± 33.15%). The T_{reg} phenotype is known to abrogate the $CD8^+$ T cell cytotoxic response and inhibit effector T cell expansion (36, 37). Thus, it is important to characterize the spatial relationship that exists between T_{regs} and effector cytotoxic T cells within the chordoma tumor immune microenvironment. The mean percentage of T_{regs} residing within 20μm of nonproliferating $CD8^+$ T cells (8.90

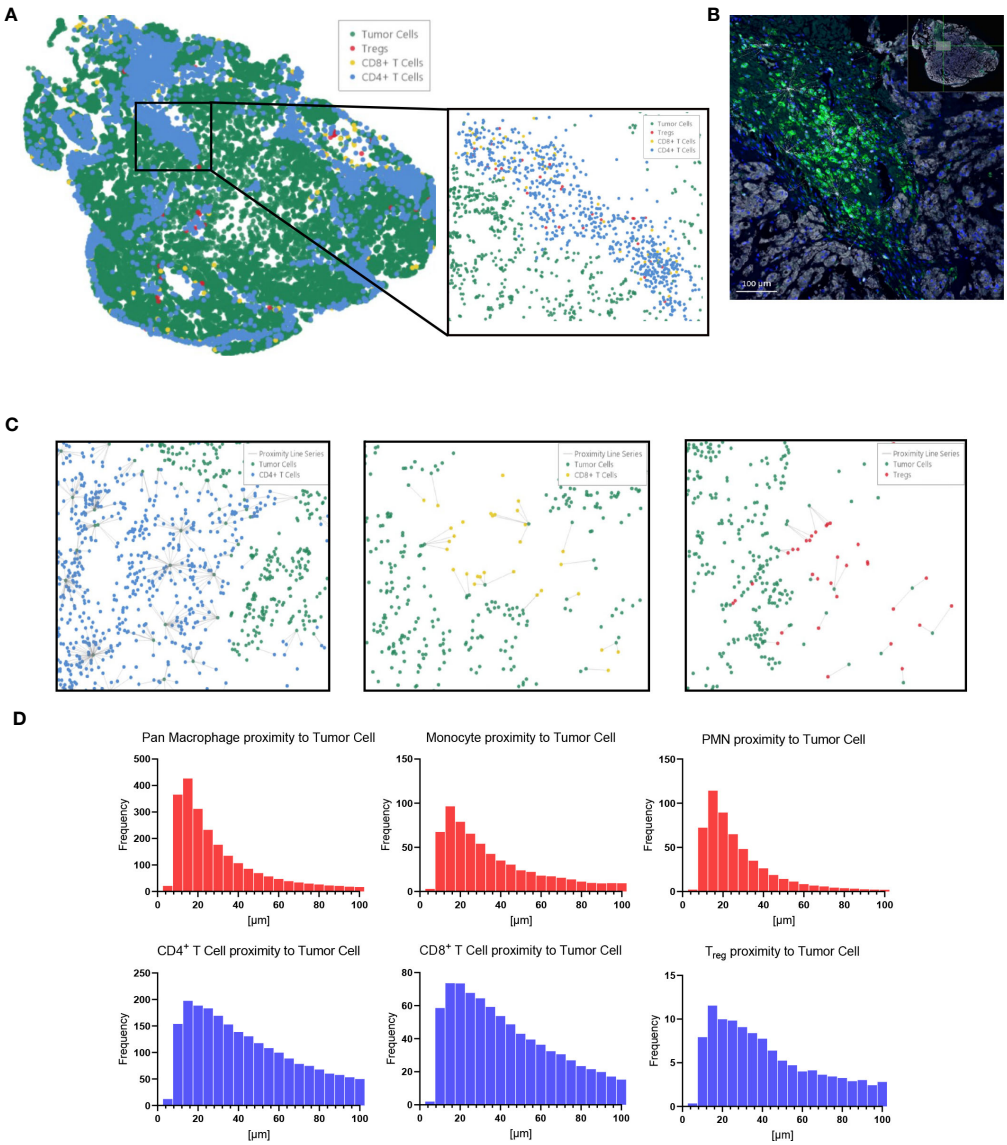

FIGURE 5
HALO® spatial proximity analyses of immune cells to chordoma cells demonstrate that T cells are nearer than myeloid cells to tumor cells. **(A)** Sacral chordoma specimen with three categories of T cells, $CD4^+$ T cells, $CD8^+$ T cells, and T_{regs} shown in blue, yellow, and red respectively. Tumor cells are shown in green. A segment of heavy T cell infiltrate is magnified. **(B)** Real time proximity analysis between $CD4^+$ T cells (green, Opal 520) and chordoma cells (white, Opal 780) with bars measuring distance between these superimposed on the image in white. **(C)** Proximity line series between T cells and chordoma tumor cells. **(D)** Proximity analysis histograms of myeloid cells (top row, red) and T cells (bottom row, blue) to chordoma tumor cells within a 100µm radius by progressive segments of 20µm bands (n = 56 individual tumors).

± 13.05) was significantly greater ($p < 0.0001$) than that residing within 20µm of proliferating $CD8^+$ T cells (1.34 ± 4.28) ($p < 0.001$) (Figure 6). These data indicate that T_{regs}, consistent with known immunosuppressive capacity in other solid tumor types, may be abrogating the proliferative capacity of cytotoxic T cells. Density heat maps of a representative chordoma specimen illustrated similar immune cell infiltration patterns among myeloid cells, T cells, and NK cells (Supplementary Figure 4).

Of 20 patients with available clinical data, 40% were of female sex, 94% of Caucasian race, and 15% of Hispanic ethnicity. The mean patient age was 49 ± 16 years. Patient clinical data is delineated in Table 1. Interestingly, myeloid cell, T cell, and NK cell density did not significantly differ among tumors originating from skull base, spine, or sacral anatomic subsites (Figure 7). No significant differences were appreciated in the quantity or character of chordoma immune infiltrate of patients with primary or locally advanced disease (Figure 7). No

10.3389/fonc.2022.1012058

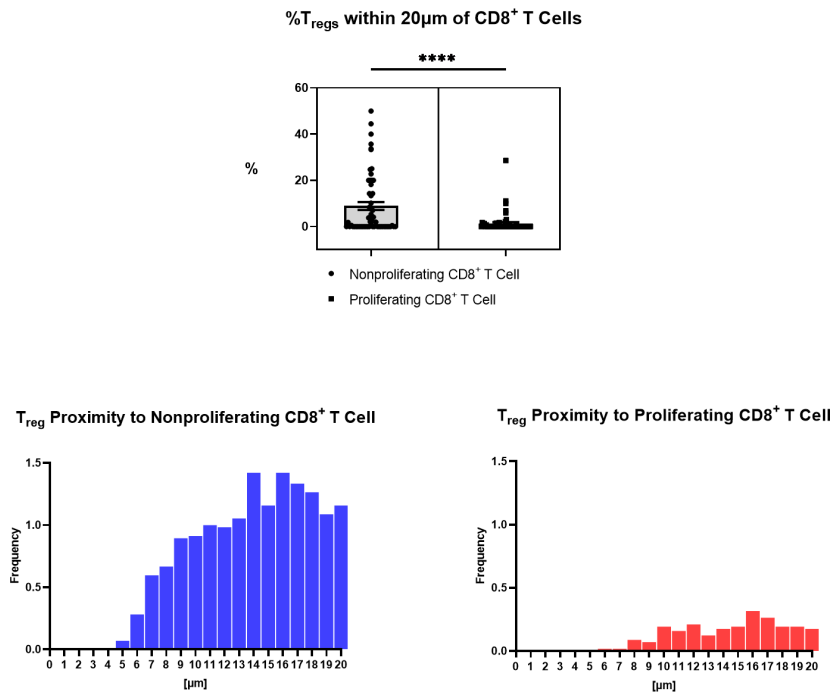

FIGURE 6
Spatial characterization of distance between Tregs to proliferating and nonproliferating CD8+ T cells in chordoma tumor slides (n = 57). Percentage of Tregs within 20µm of nonproliferating CD8+ T cells (mean 8.90 ± SEM 1.74) is significantly greater than that within 20µm of proliferating CD8+ T cells (mean 1.34 ± SEM 0.57) ($p < 0.0001$), shown above. A Wilcoxon signed rank test with a p value threshold of <0.05 was used. ****$p \leq 0.0001$. Proximity analysis histograms of Tregs within a 20µm radius of nonproliferating CD8+ T cells (left, blue) and proliferating CD8+ T cells (right, red) by progressive segments of 1µm bands, shown below.

TABLE 1 Patient Clinical Data.

	N (%)
Anatomic Site of Origin	
Skull Base	9 (45%)
Spine	3 (15%)
Sacral/Coccygeal	8 (40%)
Disease Stage	
Primary	9 (45%)
Advanced	9 (45%)
Recurrent	2 (10%)
Extent of Resection	
Gross Total/Near Gross Total	13 (65%)
Partial	1 (5%)
Unavailable	6 (30%)
Therapeutic Regimen	
Pre- or postoperative radiotherapy	11 (55%)
Chemotherapy	0 (0%)

Clinical data of patients diagnosed with chordoma included in the study (n = 20). Data is shown as n(%).

significant differences in immune cell infiltrate were appreciated in tumors arising from patients ≤ 35 years old compared to those of patients >35 years old (Supplementary Figure 5).

Discussion

Chordoma is a rare tumor of the skull base and axial skeleton with a well-established radiotherapy resistance and a strong propensity for recurrence for which immunotherapeutic strategies could play an important role. To adeptly set the stage for future immunotherapy investigations and clinical trial design, we appraised the myeloid, T cell, and NK cell compartments of the chordoma TIME using multispectral immunofluorescence. Our data demonstrated a strong myeloid tumor parenchymal infiltrate, a predominant T cell parenchymal exclusion profile, a spatial analysis suggestive of T_{reg} immunosuppression, and the presence of a small number of non-activated NK cells. Similar to extensively validated data in other solid tumor types, these results suggest that therapeutic strategies aimed at abrogating myeloid cell or T_{reg} tumor

10.3389/fonc.2022.1012058

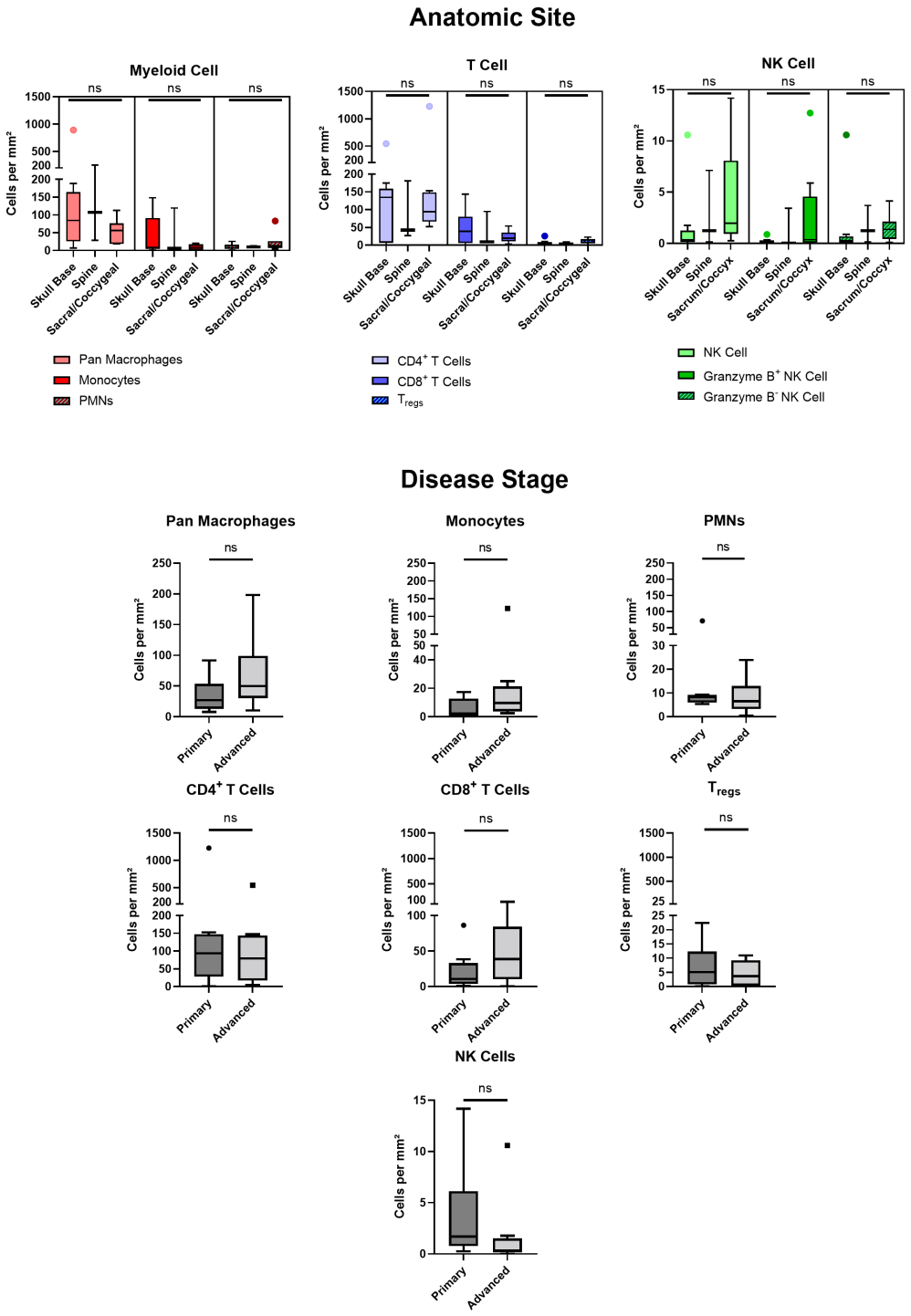

FIGURE 7
Chordoma myeloid, T cell, and NK cell density does not significantly differ by anatomic site. Immune infiltrate differences among chordomas (n = 20) originating from skull base (n = 9), spine (n = 3), or sacrum/coccyx (n = 8) were assessed with two-way ANOVA analysis using a p value threshold of <0.05. Chordoma myeloid, T cell, and NK cell density does not significantly differ by disease stage. Immune infiltrate differences between chordoma patients (n = 20) with primary and advanced disease were assessed with Mann Whitney tests using a p value threshold of <0.05. Advanced disease was defined as including cases of locally progressive and locally advanced, destructive disease. ns, non significant. NK cell, natural killer cell.

trafficking or immunosuppression in addition to direct activation of cytotoxic T cells may be warranted.

In this study, $CD68^+$ pan macrophages more significantly infiltrated chordoma tumor parenchyma than stroma, unlike trends appreciated in the T cell compartment, and all myeloid cell types identified were within notably closer proximity to chordoma tumor cells than T cells. Potent macrophage tumor penetrance and myeloid cell proximity to target cells points to a potential immunosuppressive myeloid cell role within the chordoma TIME. Myeloid-derived suppressor cells (MDSCs) are known to foster neoplasm escape of immune-mediated killing through inhibition of T cell and NK cell function (38). Monocytic-MDSCs have been defined as HLA-DR $^{low/-}$/$CD14^+$/$CD15^-$/$CD11b^+$ and have been associated with poor survival in non-small-cell lung carcinoma (NSCLC) (32). PMN-MDSC have been defined as HLA-DR $^{low/-}$/$CD14^-$/$CD15^+$/$CD11b^+$ (32). We employed these corresponding phenotypes to identify monocytes and PMN-like cells. Use of archived tissue for this analysis precluded the ability to functionally determine the suppressive capacity of these cells, but these phenotypes have been definitively linked to immunosuppressive capacity in other tumor solid types. In head and neck squamous cell carcinoma, the colony stimulating factor 2 (CSF-2) gene encoding granulocyte-macrophage colony-stimulating factor (GM-CSF) expression, linked to MDSC, was strongly associated with poor overall survival in anti-PD-1 treated recurrent and metastatic patients, and CD34, an MDSC marker, was increased in tumors without derived therapeutic benefit (34). Another study by Karpathiou et al., demonstrated that high levels of infiltrating tumor-associated-macrophages (TAMs) were linked to poor induction chemotherapy response, corroborated by Sugimura et al. in the study of esophageal cancer (39, 40). High TAM infiltrates have been correlated with worsened prognosis in a variety of cancers, including breast, urogenital, gastric, ovarian, thyroid, and prostate neoplasms (41). Sun et al. demonstrated in oral and lung squamous cell carcinoma that small molecule inhibition of C-X-C Motif Chemokine Receptor 2 (CXCR2), important to neutrophil chemotaxis, with SX-682 hindered tumor growth in the setting of PD-axis immune checkpoint inhibition and adoptive T cell transfer therapy (33). This substantiates the strategy of abrogation of myeloid cell trafficking into tumors to enhance T cell effector efficacy and T cell-based immunotherapy. Although further study of the chemokine profiles produced by chordoma cells that result in myeloid infiltration are needed, such strategies may be applied to chordoma in combination with T cell based immunotherapeutic approaches (13, 38).

In this study, we found that T cells were predominantly localized in the stroma and largely excluded from the tumor parenchyma (Figures 2, 3). As previous studies of the head and neck squamous cell carcinoma TIME have reported that high lymphocytic tumor infiltration carries favorable prognostic significance and is associated with positive predictive response to induction chemotherapy (39, 42), strategies to increase tumor parenchymal infiltration may be of benefit for chordoma. Additionally, T_{reg} cells were found in closer proximity to non-proliferating $CD8^+$ T cells, suggesting that T_{reg} cells may be playing a significant immunosuppressive role in chordoma (Figure 6). Thus, targeting T_{reg} cells may also aid in improving T cell activation and proliferation. Lastly, few NK cells were found in chordoma tissue and furthermore very few were in an activated state (Figure 4). This suggests that strategies to increase NK cell proliferation and activation such as with interleukin-15 superagonism, or adoptive NK cell therapies may be beneficial for chordoma as previously shown in *in vitro* studies (16). Collectively, this study suggests that future immunotherapy combinations for chordoma should be aimed at decreasing myeloid cell trafficking or suppressive function while enhancing cytotoxic T cell and NK cell killing. Importantly, this study also found a similar immune profile amongst chordoma from each anatomic subsite. A lack of distinct chordoma TIME composition amongst tumors of differing sub-sites and disease stage (Figure 7) suggests that chordoma may reasonably be treated with similar approaches and uniformly investigated in clinical trials independent of anatomic site of origin or diagnostic stage.

To our knowledge, this is the first application of multispectral immunofluorescence to skull base chordomas although spinal chordomas (43–45) and a single case of a sacral chordoma (46) have been analyzed with such techniques. Notable strengths of our study include the number of tumors studied and the capacity to study spatial immune cell relationships *in situ* in human tissue samples, obtaining nuance that *in vitro* studies cannot afford, and offering information previously undescribed in the literature. An ability to uniformly stain tumors with antibody panels with an automated staining system (PerkinElmer) controls for variation that accompanies staining by hand. Similarly, uniform analysis methods applied *via* HALO allow for high throughput, precise, and comparable results amongst assorted chordoma samples. Although chordomas are known to be heterogeneous with varying levels of expression of the markers we examined (7), a large sample size aided in achieving a more comprehensive idea of the chordoma TIME than what has previously been described, with the inclusion of myeloid and NK cell compartments.

This study is limited by its retrospective nature and, thus, by restricted access to patient data, particularly treatment regimen and outcome data, for chordoma tissue sections in the tumor microarray. Additionally, recurrent tumors comprised a minor proportion of the cohort available for clinical comparisons (10%, n=2). Due to low statistical power, the authors were unable to include recurrence as an independent category for TIME analysis. Similarly, no metastatic cases were available for inclusion. The study of recurrent and metastatic tumors remain of interest as these have previously been associated with inferior overall survival (47). Therefore, the field would

benefit from prospective studies in which differences due to recurrent or metastatic tumor status and the role of radiotherapy on the chordoma TIME and could be further investigated. A limitation of the analysis platform used is an inability to merge or superimpose images of distinct panels (i.e. myeloid cell panel, T cell panel, and NK cell panel) for a more extensive immune cell-to- immune cell spatial relationship analysis. Currently, each panel is restricted to a maximum of six antibodies due to the upper limit of six fluorescent channels of the platform, and thus, myeloid, T cell, and NK cell markers could not be combined within a single panel. These limitations could be overcome with emerging high-plex technologies such as spatial transcriptomics or proteomics. There are also limitations attributable to analysis of a tumor microarray with this method, including the ability to interrogate only a small portion of each individual tumor and an inability to set customized scanning exposure times for every tumor on the slide in efforts to account for varying levels of staining uptake amongst heterogeneous chordoma specimens.

Conclusion

This study characterizes the human chordoma TIME myeloid cell, T cell, and NK cell composition, making comparisons between tumoral and stromal infiltration and determining spatial relationships between immune cells and tumor cells. We conclude that the presence of myeloid cells, cytotoxic T cells, T_{regs}, and NK cells suggest chordoma's susceptibility to immunotherapeutic approaches. Given findings of increased proximity of myeloid cells to tumor cells in the setting of decreased tumor penetrance by effector T cells, and co-localization of T_{regs} and cytotoxic T cells in the stroma, treatment strategies aimed at restricting the trafficking and function of potentially immunosuppressive myeloid cells and T_{regs} may allow for greater T cell killing of target chordoma cells. The establishment of an optimized chordoma immunofluorescence protocol also affords scientists a powerful tool with which to compare TIME alterations in future immunotherapeutic studies with application to clinical trial design.

Data availability statement

The raw data supporting the conclusions of this article will be made available by the authors, without undue reservation.

Ethics statement

Ten chordoma specimens were obtained through a Johns Hopkins Institutional Review Board approved study (IRB00227737) and each patient provided written informed consent. Ten chordoma specimens were also obtained from the Chordoma Foundation Biobank and studied following National Institutes of Health Institutional Review Board exemption. Additionally, a tumor microarray (TMA) of 37 anonymized chordoma samples was obtained from the NIH Department of Pathology, totaling a sample size of 57 chordomas.

Author contributions

Conceptualization: DL, JG, GG, CA, JH, and NL. Methodology: DL, YR, JK, WL, JG, GG, CA, JH, and NL. Investigation: DL, YR, JK, WL, JG, MM, GG, CA, JH, and NL. Funding acquisition: JH and NL. Writing – original draft: DL, JH, and NL. Writing – review and editing: DL, YR, JK, WL, JG, MM, GG, CA, JH, and NL. All authors contributed to the article and approved the submitted version.

Funding

This research was supported (in part) by the Intramural Research Program of the NIH, NIDCD. This work was funded by a Translational Immunotherapy Award from the Chordoma Foundation to N. London. This research was made possible through the NIH Medical Research Scholars Program, a public-private partnership supported jointly by the NIH and contributions to the NIH from the Doris Duke Charitable Foundation (DDCF Grant #2014194), the American Association for Dental Research, the Colgate-Palmolive Company, Genentech, Elsevier, and other private donors.

Acknowledgments

We would like to thank Dr. Wade Chien and Dr. Michael Hoa for critical review of this manuscript.

Conflict of interest

NL receives research funding from Merck Sharp & Dohme, LLC regarding HPV related sinonasal carcinomas, holds stock in Navigen Pharmaceuticals and was a consultant for Cooltech Inc., none of which are relevant to the present manuscript.

The remaining authors declare that the research was conducted in the absence of any commercial or financial relationships that could be construed as a potential conflict of interest.

Publisher's note

Supplementary material

The Supplementary Material for this article can be found online at: https://www.frontiersin.org/articles/10.3389/fonc.2022.1012058/full#supplementary-material

SUPPLEMENTARY FIGURE 1
Chordoma tissue samples (n=57) were stained using the Leica BOND Rx automated system (PerkinElmer protocol), scanned with VectraPolaris, and analyzed using the HALO® (Indica Labs) v3.3 platform (first panel). For analysis, slides were digitally annotated based on cytokeratin stain (white, Opal 780), which distinguished CK^+ chordoma cells from surrounding CK^- stroma (third panel). Immune cell quantification, spatial analysis, and clinical comparisons were completed using the HALO® platform and GraphPad Prism version 9.2 (fourth panel).

SUPPLEMENTARY FIGURE 2
Myeloid cells are found within the chordoma tumor immune microenvironment. Quantification of pan macrophages, monocytes, and PMNs per mm2 in chordoma tumor and stroma (n= 56 individual tumors) presented in formatted here as mean ± standard error of the mean. Wilcoxon signed rank tests with p value threshold of <0.05 were used to compare tumor and stroma myeloid cell infiltrate. *p ≤ 0.05, **p ≤ 0.01,ns, non significant. CK, cytokeratin; DAPI, 4′,6-diamidino-2-phenylindole; PMN, polymorphonuclear cells.

SUPPLEMENTARY FIGURE 3
T cells are found in abundance within the chordoma tumor immune microenvironment, most often within the stroma. Quantification of $CD4^+$ T cell, $CD8^+$ T cell, and T_{reg} cell density (per $mm^{2)}$, as well as proliferating and PD-1^+ subcategories of these are compared between chordoma tumor and stroma (n= 57 individual tumors) presented in formatted here as mean ± standard error of the mean. Wilcoxon signed rank tests with p value threshold of <0.05 were used to compare tumor and stroma T cell infiltrate. *$p \leq 0.05$, ***$p \leq 0.001$, ****$p \leq 0.0001$, ns, non significant. CK, cytokeratin; DAPI, 4′,6-diamidino-2- phenylindole; PD1, programmed cell death protein 1.

SUPPLEMENTARY FIGURE 4
Representative density heat maps of pan macrophages, monocytes, PMNs, $CD4^+$ T cells, $CD8^+$ T cells, T_{regs}, and NK cells infiltrating a chordoma specimen. A large proportion of myeloid cells, T cells, and NK cells are concentrated along the superior and left tumor borders. Many myeloid cells also infiltrate its center. PMNs, polymorphonuclear cells; NK cells, natural killer cells.

SUPPLEMENTARY FIGURE 5
Chordoma myeloid, T cell, and NK cell density does not significantly differ by age. Immune infiltrate differences between chordoma patients ≤35 years old and >35 years old (n=20) were assessed with a Mann Whitney test using a p value threshold of <0.05. ns, non significant.NK cell, natural killer cell.

SUPPLEMENTARY FIGURE 6
HALO® spatial proximity analyses of immune cells to chordoma cells demonstrate that T cells are nearer than myeloid cells to tumor cells. (A) Sacral chordoma specimen with three categories of T cells, $CD4^+$ T cells, $CD8^+$ T cells, and T_{regs} shown in blue, yellow, and red respectively. Tumor cells are shown in green. A segment of heavy T cell infiltrate is magnified. (B) Real time proximity analysis between $CD4^+$ T cells (green, Opal 520) and chordoma cells (white, Opal 780) with bars measuring distance between these superimposed on the image in white. (C) Proximity line series between T cells and chordoma tumor cells. (D) Proximity analysis histograms of myeloid cells (top row, red) and T cells (bottom row, blue) to chordoma tumor cells within a 100μm radius by progressive segments of 20μm bands (n=56 individual tumors). Histogram y axes have been standardized for the direct comparison of immune cell phenotype frequencies.

References

1. Bakker SH, Jacobs WCH, Pondaag W, Gelderblom H, Nout RA, Dijkstra P, et al. Chordoma: a systematic review of the epidemiology and clinical prognostic factors predicting progression-free and overall survival - PubMed. *Eur Spine J* (2018) 27:3043–58. doi: 10.1007/s00586-018-5764-0

2. Walcott BP, Nahed BV, Mohyeldin A, Coumans J-V, Kahle KT, Ferreira MJ. Chordoma: current concepts, management, and future directions. *Lancet Oncol* (2012) 13(2):e69–76. doi: 10.1016/S1470-2045(11)70337-0

3. Fujii R, Friedman ER, Richards J, Tsang KY, Heery CR, Schlom J, et al. Enhanced killing of chordoma cells by antibody-dependent cell-mediated cytotoxicity employing the novel anti-PD-L1 antibody avelumab. *Oncotarget* (2016) 7(23):33498–511. doi: 10.18632/oncotarget.9256

4. Chugh R, Tawbi H, Lucas DR, Biermann JS, Schuetze SM, Baker LH. Chordoma: the nonsarcoma primary bone tumor. *Oncol* (2007) 12(11):1344–50. doi: 10.1634/theoncologist.12-11-1344

5. Stacchiotti S, Sommer JChordoma Global Consensus Group. Building a global consensus approach to chordoma: a position paper from the medical and patient community. *Lancet Oncol* (2015) 16(2):e71–83. doi: 10.1016/S1470-2045(14)71190-8

6. Takagi M, Demizu Y, Nagano F, Terashima K, Fujii O, Jin D, et al. Treatment outcomes of proton or carbon ion therapy for skull base chordoma: a retrospective study. *Radiat Oncol Lond Engl* (2018) 13(1):232. doi: 10.1186/s13014-018-1173-0

7. Duan W, Zhang B, Li X, Chen W, Jia S, Xin Z, et al. Single-cell transcriptome profiling reveals intra-tumoral heterogeneity in human chordomas. *Cancer Immunol Immunother* (2022) 71(9):2185–95. doi: 10.1007/s00262-022-03152-1

8. Patel SS, Schwab JH. Immunotherapy as a potential treatment for chordoma: a review. *Curr Oncol Rep* (2016) 18(9):55. doi: 10.1007/s11912-016-0543-8

9. Dridi M, Krebs-Drouot L, Meyronet D, Dumollard JM, Vassal F, Jouanneau E, et al. The immune microenvironment of chordomas: An immunohistochemical analysis. *Cancers* (2021) 13(13):3335. doi: 10.3390/cancers13133335

10. Waldman AD, Fritz JM, Lenardo MJ. A guide to cancer immunotherapy: from T cell basic science to clinical practice. *Nat Rev Immunol* (2020) 20(11):651–68. doi: 10.1038/s41577-020-0306-5

11. Shimasaki N, Jain A, Campana D. NK cells for cancer immunotherapy. *Nat Rev Drug Discovery* (2020) 19(3):200–18. doi: 10.1038/s41573-019-0052-1

12. Li T, Li X, Zamani A, Wang W, Lee CN, Li M, et al. C-rel is a myeloid checkpoint for cancer immunotherapy. *Nat Cancer* (2020) 1(5):507–17. doi: 10.1038/s43018-020-0061-3

13. Goswami S, Anandhan S, Raychaudhuri D, Sharma P. Myeloid cell-targeted therapies for solid tumours. *Nat Rev Immunol* (2022) Online ahead of print. doi: 10.1038/s41577-022-00737-w

14. Pramanik A, Bhattacharyya S. Myeloid derived suppressor cells and innate immune system interaction in tumor microenvironment. *Life Sci* (2022) 305:120755. doi: 10.1016/j.lfs.2022.120755

15. Wang J, Gong R, Zhao C, Lei K, Sun X, Ren H. Human FOXP3 and tumour microenvironment. *Immunology* (2022) Online ahead of print. doi: 10.1111/imm.13520

16. Hoke ATK, Padget MR, Fabian KP, Nandal A, Gallia G, Bilusic M, et al. Combinatorial natural killer cell–based immunotherapy approaches selectively target chordoma cancer stem cells. *Cancer Res Commun* (2021) 1(3):127–39. doi: 10.1158/2767-9764.CRC-21-0020

17. London NR, Rooper LM, Bishop JA, Xu H, Bernhardt L, Ishii M, et al. Expression of programmed cell death ligand 1 and associated lymphocyte infiltration in olfactory neuroblastoma. *World Neurosurg* (2020) 135:e187–93. doi: 10.1016/j.wneu.2019.11.112

18. Wang X, Teng F, Kong L, Yu J. PD-L1 expression in human cancers and its association with clinical outcomes. *OncoTargets Ther* (2016) 9:5023–39. doi: 10.2147/OTT.S105862

19. Franklin C, Livingstone E, Roesch A, Schilling B, Schadendorf D. Immunotherapy in melanoma: Recent advances and future directions. *Eur J Surg Oncol J Eur Soc Surg Oncol Br Assoc Surg Oncol* (2017) 43(3):604–11. doi: 10.1016/j.ejso.2016.07.145

20. Motta G, Vigneri P. Current strategies incorporating immune checkpoint inhibitors for the treatment of advanced or metastatic non-small-cell lung cancers. *Future Oncol Lond Engl* (2019) 15(27):3097–101. doi: 10.2217/fon-2018-0119

21. Zou M-X, Peng A-B, Lv G-H, Wang X-B, Li J, She X-L, et al. Expression of programmed death-1 ligand (PD-L1) in tumor-infiltrating lymphocytes is associated with favorable spinal chordoma prognosis. *Am J Transl Res* (2016) 8(7):3274–87.

22. Sanchez K, Kim I, Chun B, Pucilowska J, Redmond W, Urba W, et al. Multiplex immunofluorescence to measure dynamic changes in tumor-infiltrating lymphocytes and PD-L1 in early-stage breast cancer. *Breast Cancer Res* (2021) 23(1):2. doi: 10.1186/s13058-020-01378-4

23. Berry S, Giraldo NA, Green BF, Cottrell TR, Stein JE, Engle EL, et al. Analysis of multispectral imaging with the AstroPath platform informs efficacy of PD-1 blockade. *Science* (2021) 372(6547):eaba2609. doi: 10.1126/science.aba2609

24. Uhlén M, Fagerberg L, Hallström BM, Lindskog C, Oksvold P, Mardinoglu A, et al. Proteomics. tissue-based map of the human proteome. *Science* (2015) 347(6220):1260419. doi: 10.1126/science.1260419

25. Sun S, Pan X, Zhao L, Zhou J, Wang H, Sun Y. The expression and relationship of CD68-Tumor-Associated macrophages and microvascular density with the prognosis of patients with laryngeal squamous cell carcinoma. *Clin Exp Otorhinolaryngol* (2016) 9(3):270–7. doi: 10.21053/ceo.2015.01305

26. Chistiakov DA, Killingsworth MC, Myasoedova VA, Orekhov AN, Bobryshev YV. CD68/macrosialin: not just a histochemical marker. *Lab Investig J Tech Methods Pathol* (2017) 97(1):4–13. doi: 10.1038/labinvest.2016.116

27. Tzankov A, Matter MS, Dirnhofer S. Refined prognostic role of CD68-positive tumor macrophages in the context of the cellular micromilieu of classical Hodgkin lymphoma. *Pathobiol J Immunopathol Mol Cell Biol* (2010) 77(6):301–8. doi: 10.1159/000321567

28. Sjödahl G, Lövgren K, Lauss M, Chebil G, Patschan O, Gudjonsson S, et al. Infiltration of $CD3^+$ and $CD68^+$ cells in bladder cancer is subtype specific and affects the outcome of patients with muscle-invasive tumors. *Urol Oncol* (2014) 32(6):791–7. doi: 10.1016/j.urolonc.2014.02.007

29. Coiffier B, Li W, Henitz ED, Karkera JD, Favis R, Gaffney D, et al. Prespecified candidate biomarkers identify follicular lymphoma patients who achieved longer progression-free survival with bortezomib-rituximab versus rituximab. *Clin Cancer Res Off J Am Assoc Cancer Res* (2013) 19(9):2551–61. doi: 10.1158/1078-0432.CCR-12-3069

30. Kong L-Q, Zhu X-D, Xu H-X, Zhang J-B, Lu L, Wang W-Q, et al. The clinical significance of the CD163+ and CD68+ macrophages in patients with hepatocellular carcinoma. *PloS One* (2013) 8(3):e59771. doi: 10.1371/journal.pone.0059771

31. Bronte V, Brandau S, Chen S-H, Colombo MP, Frey AB, Greten TF, et al. Recommendations for myeloid-derived suppressor cell nomenclature and characterization standards. *Nat Commun* (2016) 7:12150. doi: 10.1038/ncomms12150

32. Delaunay M, Guibert N, Lusque A, Farella M, Boubekeur N, Gouin S, et al. Baseline circulating myeloid-derived suppressor cells and response to PD-1 inhibitor in non-small cell lung cancer patients. *J Clin Oncol* (2018) 36(5_suppl):145–5. doi: 10.1200/JCO.2018.36.5_suppl.145

33. Sun L, Clavijo PE, Robbins Y, Patel P, Friedman J, Greene S, et al. Inhibiting myeloid-derived suppressor cell trafficking enhances T cell immunotherapy. *JCI Insight* (2019) 4(7):126853. doi: 10.1172/jci.insight.126853

34. Seiwert TY, Bao R, Tan Y-HC, Acharya R, Brisson RJ, Kochanny S, et al. Correlation of constitutive PD-1 resistance in HNC with GM-CSF expression and presence of myeloid derived suppressor cells (MDSCs). *J Clin Oncol* (2017) 35(15_suppl):6049–9. doi: 10.1200/JCO.2017.35.15_suppl.6049

35. Horiguchi H, Sano T, Qian ZR, Hirokawa M, Kagawa N, Yamaguchi T, et al. Expression of cell adhesion molecules in chordomas: an immunohistochemical study of 16 cases. *Acta Neuropathol (Berl)* (2004) 107(2):91–6. doi: 10.1007/s00401-003-0770-6

36. Chen M-L, Pittet MJ, Gorelik L, Flavell RA, Weissleder R, von Boehmer H, et al. Regulatory T cells suppress tumor-specific CD8 T cell cytotoxicity through TGF-beta signals in vivo. *Proc Natl Acad Sci U.S.A.* (2005) 102(2):419–24. doi: 10.1073/pnas.0408197102

37. Li C, Jiang P, Wei S, Xu X, Wang J. Regulatory T cells in tumor microenvironment: new mechanisms, potential therapeutic strategies and future prospects. *Mol Cancer* (2020) 19(1):116. doi: 10.1158/1557-3125.HIPPO19-B11

38. Yang Q, Guo N, Zhou Y, Chen J, Wei Q, Han M. The role of tumor-associated macrophages (TAMs) in tumor progression and relevant advance in targeted therapy. *Acta Pharm Sin B* (2020) 10(11):2156–70. doi: 10.1016/j.apsb.2020.04.004

39. Karpathiou G, Casteillo F, Giroult J-B, Forest F, Fournel P, Monaya A, et al. Prognostic impact of immune microenvironment in laryngeal and pharyngeal squamous cell carcinoma: Immune cell subtypes, immuno-suppressive pathways and clinicopathologic characteristics. *Oncotarget* (2016) 8(12):19310–22. doi: 10.18632/oncotarget.14242

40. Sugimura K, Miyata H, Tanaka K, Takahashi T, Kurokawa Y, Yamasaki M, et al. High infiltration of tumor-associated macrophages is associated with a poor response to chemotherapy and poor prognosis of patients undergoing neoadjuvant chemotherapy for esophageal cancer. *J Surg Oncol* (2015) 111(6):752–9. doi: 10.1002/jso.23881

41. Zhang Q, Liu L, Gong C, Shi H, Zeng Y, Wang X, et al. Prognostic significance of tumor-associated macrophages in solid tumor: a meta-analysis of the literature. *PLoS One* (2012) 7(12):e50946. doi: 10.1371/journal.pone.0050946

42. Karpathiou G, Giroult J-B, Forest F, Fournel P, Monaya A, et al. Clinical and histologic predictive factors of response to induction chemotherapy in head and neck squamous cell carcinoma. *Am J Clin Pathol* (2016) 146(5):546–53. doi: 10.1093/ajcp/aqw145

43. Xia C, Huang W, Chen Y-L, Fu H-B, Tang M, Zhang T-L, et al. Coexpression of HHLA2 and PD-L1 on tumor cells independently predicts the survival of spinal chordoma patients. *Front Immunol* (2021) 12:797407. doi: 10.3389/fimmu.2021.797407

44. Zou M-X, Pan Y, Huang W, Zhang T-L, Escobar D, Wang X-B, et al. A four-factor immune risk score signature predicts the clinical outcome of patients with spinal chordoma. *Clin Transl Med* (2020) 10(1):224–37. doi: 10.1002/ctm2.4

45. Zou M-X, Zheng B-W, Liu F-S, Wang X-B, Hu J-R, Huang W, et al. The relationship between tumor-stroma ratio, the immune microenvironment, and survival in patients with spinal chordoma. *Neurosurgery* (2019) 85(6):E1095–110. doi: 10.1093/neuros/nyz333

46. Gounder M, Zhu G, Roshal L, Lis E, Daigle SR, Blakemore SJ, et al. Immunologic correlates of the abscopal effect in a SMARCB1/INI1-negative poorly differentiated chordoma after EZH2 inhibition and radiotherapy. *Clin Cancer Res Off J Am Assoc Cancer Res* (2019) 25(7):2064–71. doi: 10.1158/1078-0432.CCR-18-3133

47. Zhou J, Sun J, Bai HX, Haung X, Zou Y, Tan X, et al. Prognostic factors in patients with spinal chordoma: An integrative analysis of 682 patients. *Neurosurgery* (2017) 81(5):812–23. doi: 10.1093/neuros/nyx081

frontiers | Frontiers in Oncology

TYPE Review
PUBLISHED 27 October 2022
DOI 10.3389/fonc.2022.1009193

OPEN ACCESS

EDITED BY
Jiwei Bai,
Beijing Tiantan Hospital, Capital Medical University, China

REVIEWED BY
Christopher Asquith,
University of Eastern Finland, Finland
Ming-Xiang Zou,
University of South China, China

*CORRESPONDENCE
Daniel M. Freed
dan@chordoma.org

SPECIALTY SECTION
This article was submitted to Neuro-Oncology and Neurosurgical Oncology, a section of the journal Frontiers in Oncology

RECEIVED 01 August 2022
ACCEPTED 11 October 2022
PUBLISHED 27 October 2022

CITATION
Freed DM, Sommer J and Punturi N (2022) Emerging target discovery and drug repurposing opportunities in chordoma.
Front. Oncol. 12:1009193.
doi: 10.3389/fonc.2022.1009193

Emerging target discovery and drug repurposing opportunities in chordoma

Daniel M. Freed*, Josh Sommer and Nindo Punturi

Chordoma Foundation, Durham, NC, United States

The development of effective and personalized treatment options for patients with rare cancers like chordoma is hampered by numerous challenges. Biomarker-guided repurposing of therapies approved in other indications remains the fastest path to redefining the treatment paradigm, but chordoma's low mutation burden limits the impact of genomics in target discovery and precision oncology efforts. As our knowledge of oncogenic mechanisms across various malignancies has matured, it's become increasingly clear that numerous properties of tumors transcend their genomes – leading to new and uncharted frontiers of therapeutic opportunity. In this review, we discuss how the implementation of cutting-edge tools and approaches is opening new windows into chordoma's vulnerabilities. We also note how a convergence of emerging observations in chordoma and other cancers is leading to the identification and evaluation of new therapeutic hypotheses for this rare cancer.

KEYWORDS

chordoma, rare cancer, drug repurposing, target discovery, multi-omics, functional genomics, synthetic lethality, precision oncology

Introduction

Chordoma is an ultra-rare bone cancer that arises in the skull base or spine of pediatrics and adults, and originates from vestigial remnants of the embryonic notochord. Normally a low-grade but locally invasive disease, current standard of care for chordoma involves maximum surgical resection and/or radiotherapy (1). Despite significant advances in surgical techniques and radiotherapy strategies, the majority of chordoma patients eventually develop recurrent and/or metastatic disease and ultimately require systemic therapy to control further progression (2). To date, no drugs are approved for the treatment of advanced chordoma and conventional chemotherapy is generally ineffective (1, 2), resulting in a poor prognosis in the advanced disease setting. Research efforts over the past two decades have focused intensively on evaluating drug

repurposing opportunities, primarily guided by detection of activated signaling pathways (3–5), focused drug screens (6–8), or anecdotal clinical responses to therapies (9, 10). These investigations inspired several Phase II clinical trials primarily involving multi-kinase inhibition with agents such as imatinib (11), sorafenib (12), lapatinib (13), or everolimus plus imatinib (14), for example, although modest efficacy and low objective response rates were observed in each study. In parallel, efforts to discover novel drug targets indicate that chordoma relies on the lineage-specific transcription factor brachyury (15–17), positioning it as arguably the most attractive – though, as of yet undruggable – target in chordoma.

Over the same time period, the continued growth of genome-guided precision oncology prompted an explosion of drug repurposing efforts for molecularly-defined tumor types – a trend that also extended into the realm of rare cancers. For example, following its approval in chronic myelogenous leukemia, imatinib was successfully repurposed for KIT-mutant gastrointestinal stromal tumors (18), and dabrafenib plus trametinib was repositioned for BRAF V600-mutated anaplastic thyroid cancer (19) after the approval of this combination in non-small cell lung cancer (NSCLC) and melanoma. These and other success stories motivated a series of genomic profiling efforts in chordoma (20–27), with the hope that lifting the veil on chordoma genomes might reveal actionable therapeutic opportunities. Instead, these studies revealed that, similar to most sarcomas and pediatric cancers (28–30), chordoma appears to be characterized by a low and infrequently-actionable mutation burden – with only ~14% of chordomas harboring genomic biomarkers predictive of response to FDA-approved or investigational therapies in other indications (Table 1) (31).

Although this observation limits the current impact of traditional genomic profiling on drug repurposing campaigns and precision oncology efforts in chordoma, it does not mean that chordoma is devoid of exploitable alterations *per se* (32). Indeed, genomic profiling studies have identified several potentially actionable alterations based on emerging science – many of which we discuss further below – and validating these therapeutic opportunities may increase the number of advanced-stage chordoma patients that can benefit from genomics-guided precision oncology. Moreover, systematic functional studies in other rare cancers argue that multiple therapeutically actionable vulnerabilities nonetheless exist in the context of a genomically "quiet" background (33–35). In this review, we provide a snapshot of the emerging drug repurposing landscape in chordoma, while highlighting state-of-the-art approaches that can open new windows into chordoma biology to extend our view beyond that provided by genomics. We also discuss opportunities to repurpose lessons learned in other cancers to catalyze the identification of novel therapeutic hypotheses in chordoma. The synthesis of this emerging knowledge may lead to the discovery of new targets and the development of personalized drug repurposing opportunities for chordoma.

Emerging genomics-guided drug repurposing opportunities in chordoma

Although ~95-97% of chordomas belong to a single histological subtype, multiple observations suggest that its biology and disease mechanisms are heterogeneous. For example, over half of patients experience disease recurrence following complete tumor resection (2), and exhibit vastly different responses to systemic therapies in the advanced disease setting (36). Additionally, many chordomas are defined by complex genomic rearrangements (20, 37) or recurrent copy number losses (38), whereas other tumors harbor no detectable alterations. This molecular heterogeneity is also reflected in recent chordoma tumor profiling studies, which have utilized next-generation sequencing to identify potentially actionable alterations in chordoma (Table 1) (20–23). These studies indicate that only ~14% of chordomas have biomarkers predictive of response to FDA-approved or investigational therapies in other indications. However, several opportunities for molecularly-guided drug repurposing are emerging based on recent scientific advances in chordoma and other cancers, and validation of these therapeutic hypotheses may increase the number of chordoma patients that can benefit from precision oncology (Figure 1A).

Growth factor signaling

In one large cohort (20), PI3K pathway alterations were observed in 16% of cases (n = 17/104), indicating an opportunity to explore repurposing of inhibitors targeting PI3K or its downstream effector mTOR. One of the most frequently altered genes in chordoma is PTEN (Figure 1A); the resulting potential dependence on PI3Kβ signaling (40) suggests an opportunity to evaluate PI3Kβ inhibitors in chordoma (41). Indeed, a recent preclinical study revealed significant tumor growth inhibition by the pan-PI3K inhibitor buparlisib (BKM120) in patient-derived xenograft models (42). Downstream of PI3K, clinical trials involving mTOR inhibitor combinations have demonstrated modest clinical benefit in chordoma patients, particularly in tumors with mTOR effector activation (14, 43). Intriguingly, chordoma sometimes occurs in patients with tuberous sclerosis complex (44–46), which is characterized by loss of the mTOR negative regulators TSC1/2, further hinting at a role for the PI3K/mTOR pathway in chordoma pathogenesis. Moreover, PI3K and mTOR are regulated by receptor tyrosine kinases (RTKs), of which several appear to be activated in most chordoma tumors (4). Several studies have analyzed the activation state or effects of targeting RTKs including MET (47, 48), IGF1R (49, 50), and the FGFR family (51), though PDGFRβ (5, 10) and EGFR (3, 52) have received the most attention, primarily owing to evidence of some clinical benefit from agents targeting these RTKs (9–11, 13). Since

TABLE 1 Chordoma mutations reported in genes of potential therapeutic significance.

Gene	Process	Type	Mutation	Reference
PIK3CA	Growth Factor Signaling	Single Nucleotide Variant	–	(21)
		Homozygous Deletion	NA	(21)
		Missense (n=2)	p.E545K	(20), (25)
		Missense	p.M1043I	(20)
		Missense	p.N345S	(25)
PTEN		Missense	p.N48S	(20)
		Frameshift Indel	p.P246fs*8	(25)
		Homozygous Deletion	NA	(25)
		Nonsense	p.R335*	(25)
		Frameshift Indel	–	(21)
		Frameshift Indel	–	(23)
		Missense	p.G251V	(22)
		Nonsense	p.R233*	(22)
PIK3R1		Frameshift Indel	p.M271fs*9	(20)
BRCA2	DNA Damage Repair	Missense	p.A75S	(20)
		Missense	p.R2842C	(25)
		Rearrangement	BRCA2-SPATA13	(25)
		Missense	p.E714A	(26)
		Nonsense	p.G715*	(26)
		Missense	p.I1173F	(26)
		Nonsense	p.C1200*	(26)
		Missense	p.E1593D	(26)
		Missense	p.K1690N	(26)
		Missense	p.E2301G	(26)
		Missense	p.T2337I	(26)
		Missense	p.S2522F	(26)
		Missense	p.N2706S	(26)
		Missense	p.R2784W	(26)
CHEK2		Frameshift Indel	p.T367fs*15	(25)
ATM		Missense	–	(23)
PALB2		Missense	p.S133T	(26)
		Missense (n=2)	p.Q348K	(26)
		Missense	p.S543A	(26)
		Missense	p.V919I	(26)
		Missense	p.I1035V	(26)
		Missense	p.S1165L	(26)
SMARCB1	Chromatin Remodeling	Missense	p.E95K	(24)
		Nonsense	p.E360*	(22)
PBRM1		Single Nucleotide Variant	–	(21)
		Structural Variant (n=5)	–	(21)
		Indel (n=4)	–	(21)
		Missense	p.I555K	(20)
		Frameshift Indel	p.F1007fs*6	(20)
		Nonsense	p.R889*	(20)
		Frameshift Indel	p.F120fs*54	(25)
		Frameshift Indel	p.S383fs*1	(25)
		Homozygous Deletion	NA	(25)
		Frameshift Indel	–	(23)

(Continued)

TABLE 1 Continued

Gene	Process	Type	Mutation	Reference
		Missense	–	(23)
		Nonsense	–	(23)
		Frameshift Indel	–	(23)
		Missense	p.S1315F	(24)
		Nonsense	p.E924*	(22)
ARID1A		Frameshift Indel	p.D641Vfs*8	(20)
		Indel	p.A345_A349del	(25)
		Missense	–	(23)
		Frameshift Indel	–	(23)
		Nonsense	–	(23)
		Nonsense	p.S320*	(22)
ARID1B		Missense	–	(23)
		Missense	p.V602A	(24)
		Indel	p.315_315del	(24)
ARID2		Single Nucleotide Variant	–	(21)
		Homozygous Deletion	NA	(25)
SETD2		Single Nucleotide Variant (n=2)	–	(21)
		Structural Variant	–	(21)
		Frameshift Indel	p.S2253fs*56	(20)
		Frameshift Indel	p.T2338fs*31	(25)
		Missense	–	(23)
		Indel	p.2517_2519del	(24)
		Frameshift Indel	p.P2381fs*	(24)

Mutations denoted with a "-" signify that the mutation type was reported in the associated study without a specific protein alteration call. In such cases, sometimes multiple mutations of the same type were reported, which is signified in parentheses. For alterations classified as single nucleotide or structural variants, no further detail regarding the specific nature of these alterations was provided in the associated study. Alterations colored in red text are existing standard care or investigational biomarkers predictive of response to an FDA-approved or investigational drug in another indication (OncoKB Therapeutic Level 3B; AMP/ASCO/CAP Level C Evidence), and those in blue text may be predictive of response to a drug as supported by compelling biological evidence (OncoKB Therapeutic Level 4; AMP/ASCO/CAP Level D Evidence). The alterations colored red and blue make up 14% of all tumors sequenced across each published profiling study.

RTK mutations are not frequently seen in chordoma, these receptors are presumably activated through alternative mechanisms such as aberrant growth factor production, which may be directly regulated by brachyury (53). The frequent activation of RTKs observed in chordoma may be related to the role of the notochord in regulating embryonic tissue patterning; in this context RTKs are thought to dictate proliferation and differentiation through the interpretation of morphogen gradients (54, 55). Inhibitors of wild-type EGFR, such as afatinib and cetuximab, have reproducibly shown promising activity against chordoma cell lines (3, 6, 7) and xenograft models (39, 47), which has motivated two Phase II clinical trials (NCT03083678 and NCT05041127). Since these strategies rely on inhibition of wild-type EGFR, it remains to be seen whether skin and gastrointestinal toxicities will limit their efficacy in the clinic (56).

Growth factor signaling drives cell proliferation by upregulation of cyclin D, CDK4/6 activation, and progression through the G1/S cell cycle checkpoint. RTK activation along with frequent loss of the cell cycle tumor suppressor CDKN2A in chordomas (24, 38, 57, 58) has motivated preclinical repurposing studies with CDK4/6 inhibitors (39, 59, 60) and a Phase II trial involving palbociclib in CDKN2A-null chordoma patients (NCT03110744). It remains unclear, however, whether CDKN2A loss is a faithful predictor of sensitivity to CDK4/6 inhibition (61, 62) – possibly because, in addition to $p16^{INK4A}$, CDKN2A encodes $p14^{ARF}$, whose loss results in CDK2 deregulation and compensatory G1/S cell cycle progression. Nevertheless, tumors with co-deletion of the CDKN2A-proximal MTAP gene may present an opportunity for combinations involving CDK4/6 inhibitors and antagonists of the PRMT5 axis (63–65). Notably, CDK4/6 inhibition has been reported to potentiate T cell immunity in several contexts (66, 67), and we discuss opportunities for evaluating CDK4/6 inhibitor combinations in this context further below.

DNA damage repair

Genomic profiling studies have also revealed potential synthetic lethality strategies in chordoma. Several deleterious alterations have been reported in genes involved in DNA damage repair and response, including BRCA2, CHEK2, PALB2 and ATM (20, 23,

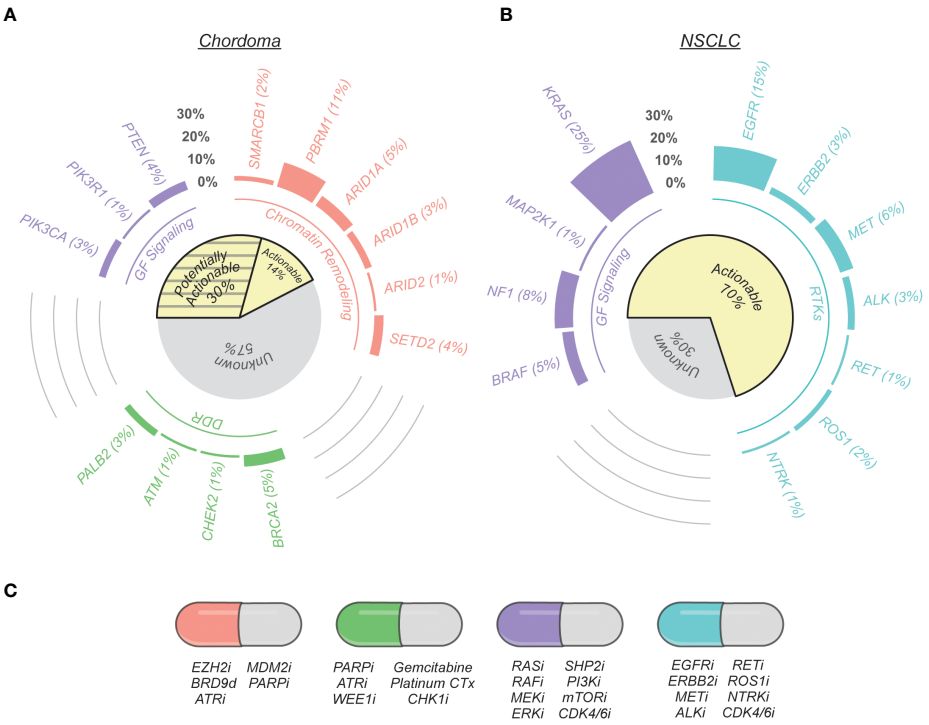

FIGURE 1
Therapeutically relevant genomic alterations found in chordoma and non-small cell lung cancer (NSCLC). **(A)** Nonsynonymous mutation call data from chordoma tumors were compiled from seven published genomic profiling studies (20–26). Genes are grouped by their protein functionality (chromatin remodeling, DNA damage repair (DDR), growth factor (GF) signaling, and receptor tyrosine kinases (RTKs)) and were selected by on their association with potential therapeutic opportunities based on current scientific literature, as reviewed here. The cohort of tumors analyzed for potentially targetable alterations varied on a per gene basis to account for variation between sequencing techniques and data presentation across studies: SMARCB1 (n = 2 altered/123 total), PBRM1 (22/203), ARID1A (6/123), ARID1B (3/104), ARID2 (2/203), SETD2 (8/203), PTEN (8/179), PIK3CA (6/203), PIK3R1 (1/123), BRCA2 (12/260), CHEK2 (1/123), ATM (1/123), PALB2 (7/260). The subset of actionable gene alterations are existing standard care or investigational biomarkers predictive of response to an FDA-approved or investigational drug in another indication (OncoKB Therapeutic Level 3B; AMP/ASCO/CAP Level C Evidence) or are predictive of response to a drug as supported by compelling biological evidence (OncoKB Therapeutic Level 4; AMP/ASCO/CAP Level D Evidence). Potentially actionable alterations are variants of currently-unknown significance (31). **(B)** Actionable gene alterations in metastatic NSCLC (39). **(C)** Examples of potential therapeutic opportunities indicated by specific gene alterations. The letter "i" signifies an inhibitor, whereas "d" denotes a degrader.

25, 26). In one recent study, a novel defective homologous recombination signature was identified in advanced chordomas that appears to impart a "BRCAness" phenotype and sensitivity to PARP inhibition (22). This strategy is being explored further in a Phase 2 clinical trial combining olaparib plus trabectedin for solid tumors with this defective homologous recombination signature (NCT03127215). Future studies aimed at examining the potential link between DNA damage repair defects and complex genomic rearrangements in chordoma may provide further mechanistic insight into this therapeutic opportunity.

Chromatin remodeling

Other studies have identified alterations in chromatin remodeling genes such as SETD2 and SWI/SNF complex members SMARCB1, ARID1A, and PBRM1 (20, 21, 24). Notably, biallelic loss of SMARCB1 defines an aggressive, poorly differentiated histopathological subtype of chordoma (<5% of cases) that most commonly afflicts the pediatric patient population (68, 69). Based on the apparent EZH2 dependence bestowed by SWI/SNF alterations (70, 71), a Phase II study is underway to explore repurposing of tazemetostat for SMARCB1-null chordoma (NCT02601950). The presence of SWI/SNF alterations also suggests opportunities for therapeutically exploiting aberrant SWI/SNF function, for example through resulting synthetic lethality with BRD9 antagonists (72–74), inhibitors of DNA repair (75–77), or p53 activation (78). Implementation of functional genomics screens may lead to the discovery of additional chordoma-specific synthetic lethal strategies in this context, which we discuss in more detail below.

An interesting connection appears to exist between SWI/SNF, the Hippo pathway, and brachyury, chordoma's main

Achilles' heel (79). Hippo transcriptional effectors YAP and TEAD are critical for notochord differentiation during embryonic development (80). Indeed, a YAP/TEAD motif is one of the top brachyury binding sites in chordoma cells (81), and reports have linked brachyury-mediated YAP upregulation to stemness and growth (82) – suggesting convergence between the Hippo and brachyury signaling networks. Intriguingly, SWI/SNF appears to sequester YAP, preventing its association with TEAD and thus antagonizing oncogenic Hippo transcriptional outputs (83). A key role of loss-of-function SWI/SNF alterations in chordoma may therefore be de-sequestration of YAP, which, when augmented by brachyury-mediated upregulation of YAP synthesis and stability, drives Hippo pathway flux to an oncogenic level. These observations suggest opportunities for evaluating an emerging class of TEAD palmitoylation inhibitors (84–86) in chordoma.

Moving beyond genomics to identify new therapeutic strategies

Creating a multidimensional map of chordoma cell circuitry

Although genomic profiling studies have informed our understanding of chordoma biology and expanded the list of potentially actionable therapeutic targets, chordoma nevertheless remains largely devoid of the recurring, actionable genomic alterations that define other solid tumors. For example, therapeutic biomarkers guide care for over two-thirds of metastatic NSCLC patients, with response rates to targeted therapies often approaching 70-80%, while chordoma profiling studies indicate ~14% of cases have potentially actionable genomic alterations (Figure 1). As highlighted in the previous section, our developing understanding of cancer biology suggests up to an additional ~30% of chordomas might have actionable genomic alterations; nevertheless, a majority of advanced-stage patients lack clear or effective treatment options.

This creates a need to open new windows into chordoma biology that extend our view beyond the "single oncogenic driver" perspective of cancer's dependencies. To this end, studies across several cancers have revealed new categories of therapeutic targets, called "non-oncogene dependencies", that mediate epigenetic changes, dysregulated signal transduction, metabolic rewiring, immune evasion, and other hallmarks of cancer (32). Multiple efforts are underway to analyze and integrate data layers derived from different aspects of cell biology, with a view to providing a more detailed molecular-resolution view of chordoma pathogenesis. For example, a recent investigation of methylation signatures in circulating tumor DNA revealed the existence of two distinct epigenetic subtypes in chordoma with prognostic relevance (87). A gene-set enrichment analysis pointed to dysregulated signaling pathways operating within each subtype, uncovering potential therapeutic opportunities that prompt further evaluation in functional studies. The exploration of additional data layers may further elucidate chordoma's molecular subtypes, including their association with specific therapeutic vulnerabilities, risk of recurrence, and other features of the disease. Such multi-omics studies may also lead to the identification of tumor-specific or lineage-restricted cell surface proteins that can serve as targets for antibody-drug conjugates, bispecific antibodies, chimeric antigen receptor T cells, or other surface antigen-targeted modalities.

Tumor-host interactions in the tumor microenvironment

In addition to tumor cell intrinsic targets, therapeutic opportunities may exist within the tumor microenvironment, where crosstalk with various immune and stromal cell subsets can profoundly influence chordoma progression and therapy response (88, 89). Studies of the chordoma immune microenvironment to date have focused on the PD-1 axis (90, 91), as well as other potentially important immune checkpoints such as B7-H3 and HHLA2 (92, 93). A recent single-cell transcriptomic analysis of six chordoma tumors identified putative immunosuppressive contributions from regulatory T cells, tumor-associated macrophages, and TGFβ signaling (94). Notably, TGFβ pathway genes are upregulated by brachyury (81). These results point to a repurposing opportunity for antagonists of TGFβ signaling in combination with immune checkpoint blockade (95, 96). Interestingly, a chordoma patient treated with a bifunctional fusion protein targeting TGFβ and PD-L1 experienced late-onset tumor shrinkage in a Phase 1 trial (97). The set of factors that govern antitumor immunity is complex, and more comprehensive phenotyping of the chordoma immune microenvironment – through single-cell sequencing, digital spatial profiling, multispectral immunofluorescence and other approaches – will be important for creating an atlas of the various lineage states in chordoma and revealing therapeutically-reversible defects in the cancer-immunity cycle (98).

Tumor-host interactions at the physiological level

Other important tumor cell extrinsic features extend beyond the microenvironment, highlighting the need to study chordoma biology at various resolutions – including contributions from host physiology. For example, germline genetics are now understood to play a role in cancer predisposition (99) and tumor immunity (100). Additionally, the gut microbiome impacts immunotherapy efficacy in several solid tumor types

(101–103), and recent data indicate that certain dietary habits can modulate the composition of the gut microbiome and influence immunotherapy response (104). Though it remains unclear how these factors contribute to the biology or treatment response of chordoma tumors, some studies are beginning to explore these questions. For example, MD Anderson's Patient Mosaic initiative aims to collect genetic, immune, and microbiome profiles from thousands of cancer patients to inform treatment strategies. Biospecimens collected from chordoma patients enrolled on the cetuximab Phase II study at MD Anderson will be included in the Patient Mosaic protocol, shedding light on how host (and other tumor extrinsic) factors shape chordoma tumor biology.

Recent advances in the establishment and availability of chordoma models

The functional validation of new therapeutic targets and strategies resulting from multi-omics studies requires appropriate patient-derived samples and preclinical models. To this end, a variety of chordoma models have been developed by several groups (105, 106). In addition, the Chordoma Foundation has built a tumor biobank of over 500 biospecimens and a model repository currently consisting of 26 cell lines, 12 patient-derived xenograft (PDX) models, and a PBMC-humanized mouse model (www.chordoma.org/research). The majority of these models have been characterized by whole-exome and whole-transcriptome sequencing and will undergo additional multi-omics characterization in the future, with a view to facilitating hypothesis testing through the establishment of models representing the full diversity of chordoma. Moreover, these models are available to the research community, as are in-kind drug testing services offered through the Chordoma Foundation's Drug Screening Program. As emerging drug repurposing concepts are evaluated in the Drug Screening Program, resulting data are publicly shared, whenever possible (107), to provide justification for further evaluation of the most promising therapeutic opportunities.

Unbiased functional assays for target discovery and personalized medicine

Patient-derived models for target discovery and precision oncology

In translational cancer research, PDX models have been the gold standard for preclinical drug testing because they accurately recapitulate features of the patient's tumor (108, 109); this has motivated the development of over two dozen chordoma PDXs by the Chordoma Foundation and others (47, 105) that represent the anatomical, age, histopathological, and known molecular diversity of chordoma. More recently, patient-derived organoids (PDOs) have generated significant interest as functional models because they provide faithful representations of patient tumors, while improving on initiation time, cost, and efficiency scales compared to PDXs (110). This technology is now being actively explored in chordoma; one recent proof-of-concept study reportedly developed chordoma PDOs from five different patients and screened them against various drugs to nominate personalized repurposing opportunities (111). In other cancer types, PDOs accurately mimic patient drug response (112–114) and have been utilized for personalized therapy (115, 116). The slow growth rate of chordoma tumors provides a large window of opportunity to develop protocols for establishing, validating, screening chordoma PDOs from high-risk or relapsing patients to enable identification of effective drug repurposing opportunities within the timeframe required to make treatment decisions.

Implementing systematic functional screens to develop new therapeutic hypotheses

Patient avatars like PDXs, PDOs and cell lines also serve as key platforms for target discovery because they allow functional studies capable of revealing or validating non-oncogene dependencies in chordoma. Genome-scale loss-of-function screens in various cancer cell lines have enabled the creation of "dependency maps" (33, 117), and this cutting-edge approach has recently been applied to chordoma to identify selective genetic dependencies (79). Perhaps unsurprisingly, *T* (or *TBXT*), the gene encoding brachyury, appears to be the most selectively essential gene in chordoma. Since brachyury (like most transcription factors) is a challenging drug target, the authors performed a drug repurposing screen and found that inhibitors of CDK9 or CDK7/12/13 (118) downregulate *TBXT* transcription and suppress chordoma cell proliferation. These results have motivated further *in vivo* testing of transcriptional CDK inhibitors, including KB-0742 (119), in the Chordoma Foundation's Drug Screening Program (120).

Ongoing systematic screening of genetic and chemical vulnerabilities in chordoma is facilitating the development of new therapeutic hypotheses. For example, CDK6 – but not CDK4 – appears to be a genetic essentiality in some chordoma cell lines (79). Outside of their common cell-cycle target RB1, CDK6 possesses a much broader substrate repertoire than does CDK4 (121) – suggesting that one or more non-RB1 targets may be mechanistically linked to chordoma's CDK6 dependence. One interesting possibility relates to the observation that chordoma cells are sensitive to the lipid hydroperoxidase

inhibitor RSL3 (79), which is known to promote ferroptotic cell death via antagonism of GPX4. CDK6 can upregulate glutathione and NADPH via phosphorylation of two glycolytic enzymes (122); depletion of these antioxidants can prime cells for ferroptosis (123). CDK6 may therefore be crucial for maintaining redox homeostasis in chordoma to safeguard against ferroptosis, providing rationale for evaluation of CDK4/6 inhibitors in combination with ferroptosis inducers.

Chordoma's apparent CDK6 dependence and potential ferroptosis susceptibility raises intriguing and unexpected parallels with clear-cell carcinomas (124, 125). Histologically, clear-cell renal cell carcinoma (ccRCC) is almost indistinguishable from chordoma, owing to morphological similarities between ccRCC's characteristic lipid droplets and the physaliferous cells that define conventional chordoma (126). Notably, ferroptosis susceptibility in clear-cell carcinomas has been linked to HIF-1/2α-dependent accumulation of polyunsaturated lipids within the intracellular droplets that give rise to the clear-cell morphology (124). Both brachyury and mTOR are known to upregulate HIF-1α (81, 127–129), suggesting a possible connection between dysregulated hypoxia signaling, physaliferous morphology, and establishment of a ferroptosis-susceptible state in chordoma (Figure 2A). Although the precise composition of physaliferous vacuoles remains unclear (130–132), chordoma and ccRCC share additional similarities, including resistance to chemotherapy and modest mutational burdens enriched in chromatin modifier and PI3K/mTOR pathway alterations (133). Collectively, these observations suggest these cancers of different tissue origins share a similar cellular context, and potentially associated therapeutic vulnerabilities – providing opportunities for repurposing lessons learned from a well-studied and common cancer.

Functional screens to identify synthetic lethalities

Another key implementation of systematic functional screens involves the discovery of synthetic lethal and combination therapy strategies. Loss-of-function screens in large cell line panels have led to identification of new synthetic lethal interactions (117, 134, 135), including PRMT5 dependence in cells with MTAP loss (63, 64). As noted above, the CDKN2A/MTAP locus is frequently deleted in chordoma (20, 21), suggesting an opportunity for repurposing PRMT5 or MAT2A inhibitors (136, 137). Exploiting such synthetic lethalities not only provides an avenue for targeting tumor suppressor loss in cancer, but is a particularly important approach to explore in genomically quiet malignancies. In addition to potential vulnerabilities created by loss of MTAP, SWI/SNF, or homologous recombination repair (as noted above), an intriguing candidate for synthetic lethality screening is LYST – a lysosomal trafficking protein of unknown function that's lost in 10% of chordomas (20). Functional genomics screens in chordoma cell lines with LYST loss may reveal targetable vulnerabilities created by this unique alteration.

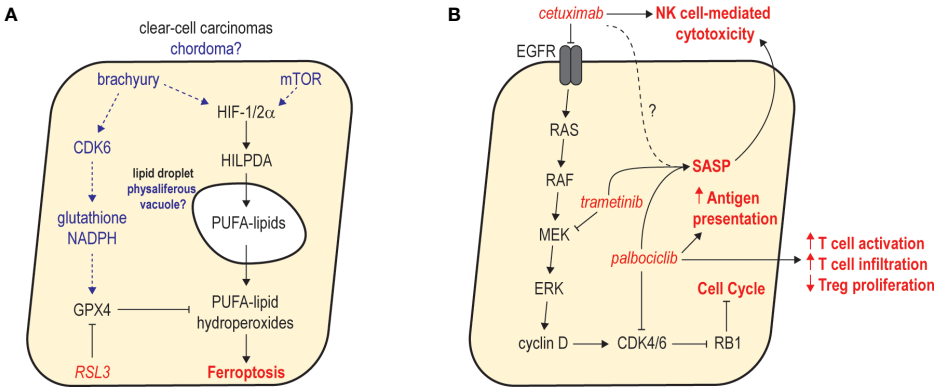

FIGURE 2
Examples of emerging therapeutic hypotheses in chordoma. **(A)** Potential mechanisms of ferroptosis susceptibility in chordoma and parallels with clear-cell carcinomas. In clear-cell carcinomas, dysregulated HIF-1/2α functions through HILPDA to promote deposition of polyunsaturated fatty acid (PUFA) lipids in intracellular lipid droplets. GPX4 activity counteracts PUFA-lipid oxidation and protects cells from ferroptosis. In chordoma, brachyury and mTOR activity may upregulate HIF-1/2α, resulting in deposition of PUFA lipids in physaliferous vacuoles. CDK6 activity may be critical for antioxidant production to protect chordoma cells against ferroptosis. **(B)** Combined inhibition of MAPK signaling and CDK4/6 activity promotes robust cell cycle arrest and antitumor immunity. Studies in other cancers revealed that combined inhibition of MEK and CDK4/6 with trametinib and palbociclib leads to sustained proliferative arrest and a senescence-associated secretory phenotype (SASP) that promotes NK and T cell immunity. As single agents, cetuximab and palbociclib reportedly augment NK and T cell immunity, respectively. Thus, combining cetuximab with palbociclib may synergistically inhibit tumor growth while stimulating a SASP that augments the activation of NK and T cell-based immunity promoted by each agent.

The next frontiers

Combination therapy strategies

Preclinical and clinical research has yet to identify a therapy capable of producing frequent responses in chordoma (36), motivating the development of combination strategies aimed at increasing the magnitude and duration of therapeutic benefit. One approach with this goal in mind involves performing unbiased anchor screens, in which genome-wide CRISPR screening is utilized to identify genes whose loss sensitizes cells to a given targeted therapy 'anchor' (136). Such genes – if druggable – may serve as attractive targets for combination therapy regimens. A similar approach can also be employed to identify candidate resistance mechanisms – that is, genes whose loss (or gain) reduce sensitivity to the anchor drug.

As one of the most well-validated therapeutic targets in chordoma, inhibitors of wild-type EGFR are arguably the best 'anchors' to initially explore in unbiased screens or rational combination studies. Indeed, combination therapy investigations with afatinib (47) or cetuximab (138) have yielded encouraging results. One interesting hypothesis involves combining cetuximab with a CDK4/6 inhibitor (Figure 2B). Since CDK4/6-mediated G1/S cell cycle progression is highly dependent on RTK/MAPK signaling, concomitant antagonism of EGFR-mediated cyclin D upregulation and CDK4/6 kinase activity may cause a more complete cell cycle arrest. This effect has been observed in lung (139) and pancreatic cancers (140), where combined MEK and CDK4/6 inhibition induced a profound G1/S arrest, resulting in a senescence-associated secretory phenotype (SASP) that promoted increased NK cell-mediated cytotoxicity and infiltration of CD8+ T cells, respectively. Importantly, as an IgG1 antibody, cetuximab monotherapy appears to promote antibody-dependent NK cell-mediated cytotoxicity in several cancers including chordoma (141). A cetuximab/CDK4/6 inhibitor combination may therefore act synergistically to halt the growth of chordoma tumor cells and provoke a strong NK- and T-cell based antitumor response. As a result, further exploration of this concept may be warranted, particularly once the single-agent activity of cetuximab (NCT05041127) and palbociclib (NCT03110744) in chordoma is benchmarked in the clinic. Notably, similar combination immunotherapy approaches aiming to enhance NK cell-mediated killing have recently been described in chordoma (138), and these strategies were reported to selectively target the reservoir of cancer stem-like cells that promote recurrence and therapy resistance.

Immunotherapy strategies

Achieving deep and durable responses in chordoma will likely require identification of therapeutic concepts capable of invigorating antitumor immunity. Despite a low tumor mutational burden, a significant proportion of chordomas appear to be characterized by complex genomic rearrangements (20, 37), which may lead to high neoantigen expression. In addition to the examples noted above, documented patient responses to vaccines (142) and PD-1 inhibitors (143–146) provide important proof-of-concept for the use of immunotherapies in chordoma, and prompt evaluation of different immune checkpoints and combinations thereof. For example, strong scientific rationale exists for co-blockade of the PD-1 and TIGIT checkpoints in cancer (147), and a new clinical study enrolling chordoma patients is testing this concept with atezolizumab plus tiragolumab (NCT05286801). Another promising approach involves the cell-surface protein CD24, which is frequently expressed in chordomas and – along with brachyury and low molecular weight cytokeratins – has been used as a diagnostic marker for chordoma in some cases (148). Intriguingly, tumor-derived CD24 was recently identified as a key anti-phagocytic "don't eat me" signal in other solid tumors (149), making it a promising immunotherapeutic target and prompting evaluation of CD24 blockade in chordoma. The evaluation of immunotherapy combinations in chordoma, such as PD-1 antagonism plus inhibition of TIGIT or TGFβ signaling as noted above, may reinvigorate the tumor-immunity cycle at multiple points. Multi-omics studies of chordoma may be valuable in guiding these efforts and revealing key molecular details governing the chordoma immune microenvironment.

New drug discovery driving repurposing in reverse

Tumorigenesis appears to require three main ingredients: an oncogenic signaling input, deregulation of the signal through tumor suppressor loss (150, 151), and a permissive transcriptional environment for interpretation of oncogenic signaling (152, 153). Lineage-specific transcription factors – such as brachyury in chordoma – are essential for creating a permissive environment (79), and thus represent attractive drug targets. While oncogenic signaling and tumor suppressor loss can be targeted by kinase inhibitors and synthetic lethal strategies, respectively, transcription factors like brachyury are inherently challenging drug targets (Figure 3A). However, advances in drug discovery and the development of new targeted protein degradation technologies, such as proteolysis targeting chimeras (PROTACs) and molecular glues, provide opportunities to redefine this paradigm (154). To this end, numerous projects have recently been launched to develop novel compounds that bind brachyury with high affinity, which can either serve as functional inhibitors, molecular glues, or warheads for PROTACS. Notably, an open-source project through the Structural Genomics Consortium is

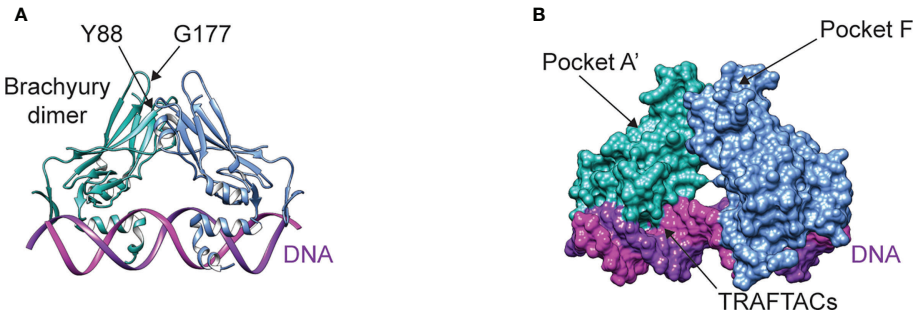

FIGURE 3
(A) Structure of the brachyury dimer bound to DNA (PDB ID 6F58). The alpha carbons of residues Y88 and G177 are separated by a distance of ~9 Å **(B)** Brachyury rendered in surface representation, showing the two main pockets being targeted by open-source drug discovery efforts and the DNA binding interface targeted by TRAFTACs.

focusing on the development of high-quality probes that bind pockets identified in brachyury crystal structures (Figure 3B) to induce industry investment in further brachyury drug discovery.

The development of functional inhibitors is a challenging endeavor, given that brachyury lacks the deep binding pockets commonly associated with enzymatic activity. Yet, transcription factors like brachyury are often involved in multiprotein complexes, pointing to the development of compounds that modulate protein-protein interactions as an attractive strategy. For example, brachyury associates with the histone acetyltransferase p300 using an interface involving amino acid residue Y88 (Figure 3A) (155). The proximity of Y88 to residue G177 (Figure 3A) is interesting, as a G177D germline variant is strongly associated with chordoma (15). Because residue G177 is on a flexible, solvent-exposed loop, the G177D mutation is unlikely to affect brachyury structure – however this substitution may stabilize intermolecular contacts with p300 or other binding partners, thus modulating brachyury function. Indeed, the interaction between brachyury and p300 appears to regulate histone 3 lysine 27 acetylation (155) – a modification associated with active enhancers. Since association of brachyury with super-enhancers appears to be crucial to its role in chordoma (79, 81), designing compounds that can block or allosterically modulate this protein-protein interaction – for example, by targeting pocket A' or F (Figure 3B) – may represent an attractive therapeutic strategy. Another novel approach to functionally modulating brachyury involves the development of Transcription Factor Targeting Chimeras (TRAFTACs) (156). In contrast to PROTACs, TRAFTACs utilize a transcription factor-specific DNA sequence to achieve target specificity, which is linked to an E3 ligase-recruiting moiety that directs brachyury to the proteasome for degradation.

Although new drug discovery in an ultra-rare indication presents numerous challenges, the concept of "reverse" drug repurposing – that is, repurposing drugs initially developed in a rare cancer to more common indications – represents a promising path. Further highlighting the intriguing parallels between chordoma and kidney cancer, brachyury expression is associated with poor survival in ccRCC and papillary RCC (Figure 4) (133, 157). Interestingly, expression of CDK6 – an apparent dependency in both chordoma and ccRCC (125), as noted above – appears to be regulated by brachyury (79). Numerous additional studies indicate brachyury is associated with poor prognosis and implicated in driving recurrence, metastasis, and/or resistance to standard of care therapy in several more common cancers including breast (158–161), lung (162–166), and colon (167). Thus, chordoma represents a "pure" and target-rich setting for the initial development of brachyury antagonists, which can then be expanded into larger indications where brachyury plays a role in disease progression.

Perspective

Even when macroscopic complete resection is achieved using cutting-edge surgical approaches, the majority of chordoma patients experience disease recurrence and are unlikely to be cured (1, 2). At some point, local therapies such as surgery and/or radiation are no longer safe or feasible, and treatment options become limited due to a lack of effective systemic therapies. This has motivated intensive research to identify effective therapeutic strategies in chordoma, but drug repurposing efforts have been hampered by chordoma's resistance to conventional chemotherapy and a paucity of actionable genomic alterations.

In this review, we highlight several therapeutic hypotheses inspired by developing knowledge of chordoma biology and its parallels with other cancer types. In particular, we focus on emerging therapeutic opportunities based on emerging knowledge linking drug sensitivity to specific biomarkers. Nevertheless, through the lens of genomic sequencing, most chordomas still lack actionable alterations – underscoring the need to implement more sophisticated multi-omics approaches.

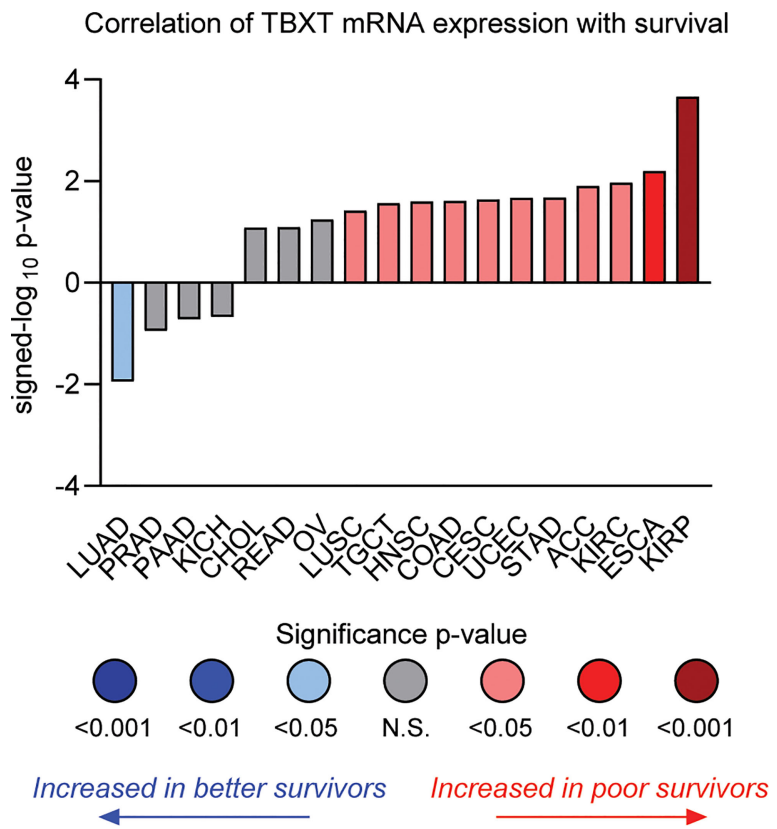

FIGURE 4
Correlation of *TBXT* (brachyury) mRNA expression with overall survival by tumor type in TCGA datasets. The individual values are sign-corrected $\log_{10}$ p-values of correlation. Negative signed-$\log_{10}$ p-values (y-axis) indicate that high *TBXT* expression is associated with better survival, whereas positive values indicate high *TBXT* expression predicts poor survival. Cancer types are listed by their respective TCGA study abbreviations (e.g., KIRP, kidney renal papillary cell carcinoma; ESCA, esophageal carcinoma; KIRC, kidney renal clear-cell carcinoma; LUAD, lung adenocarcinoma). The results shown in this figure are in whole or part based upon data generated through the Lumin Bioinformatics Software of Champions Oncology, Inc.

Indeed, genomics is only one piece of the puzzle; tumor growth is controlled by multiple integrated systems, with each contributing uniquely to chordoma's biology. Therapeutic opportunities exist within each of these systems, and efforts focused on elucidating and integrating them will provide a fuller view of chordoma's biology. A key goal of multi-omics profiling efforts will be the identification of molecular subtypes, stratified by risk and therapeutic vulnerabilities, as has been demonstrated in other cancers (168–170).

In parallel, unbiased functional assays, utilizing genome-wide CRISPR or high-throughput drug screening, may reveal non-oncogene dependencies or combination therapy strategies that would otherwise be difficult to detect through multi-omics profiling approaches. The identification of additive or synergistic therapeutic combinations is of particular interest, given the low historical response rates in chordoma (36). In addition to guiding target discovery campaigns, functional assays can provide personalized medicine opportunities. For example, if multi-omics studies identify patients at high risk for recurrence, the ability to establish and profile drug sensitivity of PDXs or PDOs at time of initial surgery may allow nomination of potential therapeutic options upon disease recurrence, as successfully demonstrated recently in breast cancer (116). Due to the intrinsically slow growth of chordoma tumors, such an approach could also be considered at the time of recurrence.

Finally, we highlight how technological advances are opening the door to targeting the transcription factor brachyury, the main Achilles heel of chordoma. The identification of binding pockets on brachyury can serve as target sites for PROTAC warheads or molecular glues, but they may also be functionally important. One such potential site is pocket A' or F (Figure 3B), near the putative p300 interface and residue G177, which is the site of a germline variant strongly associated with chordoma development. If efforts to target brachyury are ultimately successful, these drugs can be repurposed for more common cancers in circumstances where brachyury drives resistance to standard of care therapy.

Author contributions

All authors listed have made a substantial, direct, and intellectual contribution to the work and approved it for publication.

Funding

This work was funded by the generous donors to Chordoma Foundation.

Acknowledgments

We acknowledge and thank our patient community for giving us constant motivation to help identify and develop better treatments for chordoma. We are also grateful for our generous donors who provide the necessary funding – and to our colleagues at Chordoma Foundation and the research community for their efforts – to work towards this goal. Finally, we thank Champions Oncology for their assistance with figure generation.

Conflict of interest

The authors declare that the research was conducted in the absence of any commercial or financial relationships that could be construed as a potential conflict of interest.

Publisher's note

All claims expressed in this article are solely those of the authors and do not necessarily represent those of their affiliated organizations, or those of the publisher, the editors and the reviewers. Any product that may be evaluated in this article, or claim that may be made by its manufacturer, is not guaranteed or endorsed by the publisher.

References

1. Stacchiotti S, Sommer JG. Chordoma Global Consensus. Building a global consensus approach to chordoma: A position paper from the medical and patient community. *Lancet Oncol* (2015) 16(2):e71–83. doi: 10.1016/S1470-2045(14)71190-8

2. Stacchiotti S, Gronchi A, Fossati P, Akiyama T, Alapetite C, Baumann M, et al. Best practices for the management of local-regional recurrent chordoma: A position paper by the chordoma global consensus group. *Ann Oncol* (2017) 28 (6):1230–42. doi: 10.1093/annonc/mdx054

3. Shalaby A, Presneau N, Ye H, Halai D, Berisha F, Idowu B, et al. The role of epidermal growth factor receptor in chordoma pathogenesis: A potential therapeutic target. *J Pathol* (2011) 223(3):336–46. doi: 10.1002/path.2818

4. Tamborini E, Virdis E, Negri T, Orsenigo M, Brich S, Conca E, et al. Analysis of receptor tyrosine kinases (RTKs) and downstream pathways in chordomas. *Neuro Oncol* (2010) 12(8):776–89. doi: 10.1093/neuonc/noq003

5. Tamborini E, Miselli F, Negri T, Lagonigro MS, Staurengo S, Dagrada GP, et al. Molecular and biochemical analyses of platelet-derived growth factor receptor (PDGFR) b, PDGFRA, and KIT receptors in chordomas. *Clin Cancer Res* (2006) 12 (23):6920–8. doi: 10.1158/1078-0432.CCR-06-1584

6. Scheipl S, Barnard M, Cottone L, Jorgensen M, Drewry DH, Zuercher WJ, et al. EGFR inhibitors identified as a potential treatment for chordoma in a focused compound screen. *J Pathol* (2016) 239(3):320–34. doi: 10.1002/path.4729

7. Magnaghi P, Salom B, Cozzi L, Amboldi N, Ballinari D, Tamborini E, et al. Afatinib is a new therapeutic approach in chordoma with a unique ability to target EGFR and brachyury. *Mol Cancer Ther* (2018) 17(3):603–13. doi: 10.1158/1535-7163.MCT-17-0324

8. Cottone L, Cribbs AP, Khandelwal G, Wells G, Ligammari L, Philpott M, et al. Inhibition of histone H3K27 demethylases inactivates brachyury (TBXT) and promotes chordoma cell death. *Cancer Res* (2020) 80(20):4540–51. doi: 10.1158/0008-5472.CAN-20-1387

9. Hof H, Welzel T, Debus J. Effectiveness of cetuximab/gefitinib in the therapy of a sacral chordoma. *Onkologie* (2006) 29(12):572–4. doi: 10.1159/000096283

10. Casali PG, Messina A, Stacchiotti S, Tamborini E, Crippa F, Gronchi A, et al. Imatinib mesylate in chordoma. *Cancer* (2004) 101(9):2086–97. doi: 10.1002/cncr.20618

11. Stacchiotti S, Longhi A, Ferraresi V, Grignani G, Comandone A, Stupp R, et al. Phase II study of imatinib in advanced chordoma. *J Clin Oncol* (2012) 30 (9):914–20. doi: 10.1200/JCO.2011.35.3656

12. Bompas E, Le Cesne A, Tresch-Bruneel E, Lebellec L, Laurence V, Collard O, et al. Sorafenib in patients with locally advanced and metastatic chordomas: A phase II trial of the French sarcoma group (GSF/GETO). *Ann Oncol* (2015) 26(10):2168–73. doi: 10.1093/annonc/mdv300

13. Stacchiotti S, Tamborini E, Lo Vullo S, Bozzi F, Messina A, Morosi C, et al. Phase II study on lapatinib in advanced EGFR-positive chordoma. *Ann Oncol* (2013) 24(7):1931–6. doi: 10.1093/annonc/mdt117

14. Stacchiotti S, Morosi C, Lo Vullo S, Casale A, Palassini E, Frezza AM, et al. Imatinib and everolimus in patients with progressing advanced chordoma: A phase 2 clinical study. *Cancer* (2018) 124(20):4056–63. doi: 10.1002/cncr.31685

15. Pillay N, Plagnol V, Tarpey PS, Lobo SB, Presneau N, Szuhai K, et al. A common single-nucleotide variant in T is strongly associated with chordoma. *Nat Genet* (2012) 44(11):1185–7. doi: 10.1038/ng.2419

16. Presneau N, Shalaby A, Ye H, Pillay N, Halai D, Idowu B, et al. Role of the transcription factor T (brachyury) in the pathogenesis of sporadic chordoma: A genetic and functional-based study. *J Pathol* (2011) 223(3):327–35. doi: 10.1002/path.2816

17. Vujovic S, Henderson S, Presneau N, Odell E, Jacques TS, Tirabosco R, et al. Brachyury, a crucial regulator of notochordal development, is a novel biomarker for chordomas. *J Pathol* (2006) 209(2):157–65. doi: 10.1002/path.1969

18. Demetri GD, von Mehren M, Blanke CD, Van den Abbeele AD, Eisenberg B, Roberts PJ, et al. Efficacy and safety of imatinib mesylate in advanced gastrointestinal stromal tumors. *N Engl J Med* (2002) 347(7):472–80. doi: 10.1056/NEJMoa020461

19. Subbiah V, Kreitman RJ, Wainberg ZA, Cho JY, Schellens JHM, Soria JC, et al. Dabrafenib and trametinib treatment in patients with locally advanced or metastatic BRAF V600-mutant anaplastic thyroid cancer. *J Clin Oncol* (2018) 36 (1):7–13. doi: 10.1200/JCO.2017.73.6785

20. Tarpey PS, Behjati S, Young MD, Martincorena I, Alexandrov LB, Farndon SJ, et al. The driver landscape of sporadic chordoma. *Nat Commun* (2017) 8(1):890. doi: 10.1038/s41467-017-01026-0

21. Bai J, Shi J, Li C, Wang S, Zhang T, Hua X, et al. Whole genome sequencing of skull-base chordoma reveals genomic alterations associated with recurrence and chordoma-specific survival. *Nat Commun* (2021) 12(1):757. doi: 10.1038/s41467-021-21026-5

22. Groschel S, Hubschmann D, Raimondi F, Horak P, Warsow G, Frohlich M, et al. Defective homologous recombination DNA repair as therapeutic target in advanced chordoma. *Nat Commun* (2019) 10(1):1635. doi: 10.1038/s41467-019-09633-9

23. Mattox AK, Yang B, Douville C, Lo SF, Sciubba D, Wolinsky JP, et al. The mutational landscape of spinal chordomas and their sensitive detection using circulating tumor DNA. *Neurooncol Adv* (2021) 3(1):vdaa173. doi: 10.1093/noajnl/vdaa173

24. Wang L, Zehir A, Nafa K, Zhou N, Berger MF, Casanova J, et al. Genomic aberrations frequently alter chromatin regulatory genes in chordoma. *Genes Chromosomes Cancer* (2016) 55(7):591–600. doi: 10.1002/gcc.22362

25. Gounder MM, Agaram NP, Trabucco SE, Robinson V, Ferraro RA, Millis SZ, et al. Clinical genomic profiling in the management of patients with soft tissue and bone sarcoma. *Nat Commun* (2022) 13(1):3406. doi: 10.1038/s41467-022-30496-0

26. Xia B, Biswas K, Foo TK, Torres T, Riedel-Topper M, Southon E, et al. Rare germline variants in PALB2 and BRCA2 in familial and sporadic chordoma. *Hum Mutat* (2022) 43(10):1396–407. doi: 10.1002/humu.24427

27. Liang WS, Dardis C, Helland A, Sekar S, Adkins J, Cuyugan L, et al. Identification of therapeutic targets in chordoma through comprehensive genomic and transcriptomic analyses. *Cold Spring Harb Mol Case Stud* (2018) 4(6):a003418 . doi: 10.1101/mcs.a003418

28. Ma X, Liu Y, Liu Y, Alexandrov LB, Edmonson MN, Gawad C, et al. Pan-cancer genome and transcriptome analyses of 1,699 paediatric leukaemias and solid tumours. *Nature* (2018) 555(7696):371–6. doi: 10.1038/nature25795

29. Grobner SN, Worst BC, Weischenfeldt J, Buchhalter I, Kleinheinz K, Rudneva VA, et al. The landscape of genomic alterations across childhood cancers. *Nature* (2018) 555(7696):321–7. doi: 10.1038/nature25480

30. Cancer Genome Atlas Research Network. Electronic address and N. Cancer Genome Atlas Research. Comprehensive and integrated genomic characterization of adult soft tissue sarcomas. *Cell* (2017) 171(4):950–965 e28. doi: 10.1016/j.cell.2017.10.014

31. Chakravarty D, Gao J, Phillips S, Kundra R, Zhang H, Wang J, et al. OncoKB: A precision oncology knowledge base. *JCO Precis Oncol* (2017) PO.17.00011. doi: 10.1200/PO.17.00011

32. Hahn WC, Bader JS, Braun TP, Califano A, Clemons PA, Druker BJ, et al. An expanded universe of cancer targets. *Cell* (2021) 184(5):1142–55. doi: 10.1016/j.cell.2021.02.020

33. Dharia NV, Kugener G, Guenther LM, Malone CF, Durbin AD, Hong AL, et al. A first-generation pediatric cancer dependency map. *Nat Genet* (2021) 53 (4):529–38. doi: 10.1038/s41588-021-00819-w

34. Hong AL, Tseng YY, Cowley GS, Jonas O, Cheah JH, Kynnap BD, et al. Integrated genetic and pharmacologic interrogation of rare cancers. *Nat Commun* (2016) 7:11987. doi: 10.1038/ncomms11987

35. Oberlick EM, Rees MG, Seashore-Ludlow B, Vazquez F, Nelson GM, Dharia NV, et al. Small-molecule and CRISPR screening converge to reveal receptor tyrosine kinase dependencies in pediatric rhabdoid tumors. *Cell Rep* (2019) 28 (9):2331–2344 e8. doi: 10.1016/j.celrep.2019.07.021

36. Wedekind MF, Widemann BC, Cote G. Chordoma: Current status, problems, and future directions. *Curr Probl Cancer* (2021) 45(4):100771. doi: 10.1016/j.currproblcancer.2021.100771

37. Stephens PJ, Greenman CD, Fu B, Yang F, Bignell GR, Mudie LJ, et al. Massive genomic rearrangement acquired in a single catastrophic event during cancer development. *Cell* (2011) 144(1):27–40. doi: 10.1016/j.cell.2010.11.055

38. Le LP, Nielsen GP, Rosenberg AE, Thomas D, Batten JM, Deshpande V, et al. Recurrent chromosomal copy number alterations in sporadic chordomas. *PloS One* (2011) 6(5):e18846. doi: 10.1371/journal.pone.0018846

39. Blakely CM, Watkins TBK, Wu W, Gini B, Chabon JJ, McCoach CE, et al. Evolution and clinical impact of co-occurring genetic alterations in advanced-stage EGFR-mutant lung cancers. *Nat Genet* (2017) 49(12):1693–704. doi: 10.1038/ng.3990

40. Jia S, Liu Z, Zhang S, Liu P, Zhang L, Lee SH, et al. Essential roles of PI(3)K-p110beta in cell growth, metabolism and tumorigenesis. *Nature* (2008) 454 (7205):776–9. doi: 10.1038/nature07091

41. Mateo J, Ganji G, Lemech C, Burris HA, Han SW, Swales K, et al. A first-Time-in-Human study of GSK2636771, a phosphoinositide 3 kinase beta-selective inhibitor, in patients with advanced solid tumors. *Clin Cancer Res* (2017) 23 (19):5981–92. doi: 10.1158/1078-0432.CCR-17-0725

42. Michmerhuizen NL, Owen JH, Heft Neal ME, Mann JE, Leonard E, Wang J, et al. Rationale for the advancement of PI3K pathway inhibitors for personalized chordoma therapy. *J Neurooncol* (2020) 147(1):25–35. doi: 10.1007/s11060-020-03418-7

43. Stacchiotti S, Marrari A, Tamborini E, Palassini E, Virdis E, Messina A, et al. Response to imatinib plus sirolimus in advanced chordoma. *Ann Oncol* (2009) 20 (11):1886–94. doi: 10.1093/annonc/mdp210

44. Borgel J, Olschewski H, Reuter T, Miterski B, Epplen JT. Does the tuberous sclerosis complex include clivus chordoma? a case report. *Eur J Pediatr* (2001) 160 (2):138. doi: 10.1007/s004310000645

45. Lee-Jones L, Aligianis I, Davies PA, Puga A, Farndon PA, Stemmer-Rachamimov A, et al. Sacrococcygeal chordomas in patients with tuberous sclerosis complex show somatic loss of TSC1 or TSC2. *Genes Chromosomes Cancer* (2004) 41(1):80–5. doi: 10.1002/gcc.20052

46. McMaster ML, Goldstein AM, Parry DM. Clinical features distinguish childhood chordoma associated with tuberous sclerosis complex (TSC) from chordoma in the general paediatric population. *J Med Genet* (2011) 48(7):444–9. doi: 10.1136/jmg.2010.085092

47. Zhao T, Siu IM, Williamson T, Zhang H, Ji C, Burger PC, et al. AZD8055 enhances *in vivo* efficacy of afatinib in chordomas. *J Pathol* (2021) 255(1):72–83. doi: 10.1002/path.5739

48. Scheipl S, Barnard M, Lohberger B, Zettl R, Brcic I, Liegl-Atzwanger B, et al. Drug combination screening as a translational approach toward an improved drug therapy for chordoma. *Cell Oncol (Dordr)* (2021) 44(6):1231–42. doi: 10.1007/s13402-021-00632-x

49. Sommer J, Itani DM, Homlar KC, Keedy VL, Halpern JL, Holt GE, et al. Methylthioadenosine phosphorylase and activated insulin-like growth factor-1 receptor/insulin receptor: potential therapeutic targets in chordoma. *J Pathol* (2010) 220(5):608–17. doi: 10.1002/path.2679

50. Aleksic T, Browning L, Woodward M, Phillips R, Page S, Henderson S, et al. Durable response of spinal chordoma to combined inhibition of IGF-1R and EGFR. *Front Oncol* (2016) 6:98. doi: 10.3389/fonc.2016.00098

51. Hu Y, Mintz A, Shah SR, Quinones-Hinojosa A, Hsu W. The FGFR/MEK/ERK/brachyury pathway is critical for chordoma cell growth and survival. *Carcinogenesis* (2014) 35(7):1491–9. doi: 10.1093/carcin/bgu014

52. Dewaele B, Maggiani F, Floris G, Ampe M, Vanspauwen V, Wozniak A, et al. Frequent activation of EGFR in advanced chordomas. *Clin Sarcoma Res* (2011) 1(1):4. doi: 10.1186/2045-3329-1-4

53. Nelson AC, Pillay N, Henderson S, Presneau N, Tirabosco R, Halai D, et al. An integrated functional genomics approach identifies the regulatory network directed by brachyury (T) in chordoma. *J Pathol* (2012) 228(3):274–85. doi: 10.1002/path.4082

54. Shilo BZ. Regulating the dynamics of EGF receptor signaling in space and time. *Development* (2005) 132(18):4017–27. doi: 10.1242/dev.02006

55. Darras S, Nishida H. The BMP signaling pathway is required together with the FGF pathway for notochord induction in the ascidian embryo. *Development* (2001) 128(14):2629–38. doi: 10.1242/dev.128.14.2629

56. Politi K, Ayeni D, Lynch T. The next wave of EGFR tyrosine kinase inhibitors enter the clinic. *Cancer Cell* (2015) 27(6):751–3. doi: 10.1016/j.ccell.2015.05.012

57. Choy E, MacConaill LE, Cote GM, Le LP, Shen JK, Nielsen GP, et al. Genotyping cancer-associated genes in chordoma identifies mutations in oncogenes and areas of chromosomal loss involving CDKN2A, PTEN, and SMARCB1. *PloS One* (2014) 9(7):e101283. doi: 10.1371/journal.pone.0101283

58. Cottone L, Eden N, Usher I, Lombard P, Ye H, Ligammari L, et al. Frequent alterations in p16/CDKN2A identified by immunohistochemistry and FISH in chordoma. *J Pathol Clin Res* (2020) 6(2):113–23. doi: 10.1002/cjp2.156

59. Anderson E, Havener TM, Zorn KM, Foil DH, Lane TR, Capuzzi SJ, et al. Synergistic drug combinations and machine learning for drug repurposing in chordoma. *Sci Rep* (2020) 10(1):12982. doi: 10.1038/s41598-020-70026-w

60. von Witzleben A, Goerttler LT, Marienfeld R, Barth H, Lechel A, Mellert K, et al. Preclinical characterization of novel chordoma cell systems and their targeting by pharmocological inhibitors of the CDK4/6 cell-cycle pathway. *Cancer Res* (2015) 75(18):3823–31. doi: 10.1158/0008-5472.CAN-14-3270

61. Gong X, Litchfield LM, Webster Y, Chio LC, Wong SS, Stewart TR, et al. Genomic aberrations that activate d-type cyclins are associated with enhanced sensitivity to the CDK4 and CDK6 inhibitor abemaciclib. *Cancer Cell* (2017) 32 (6):761–776 e6. doi: 10.1016/j.ccell.2017.11.006

62. Finn RS, Crown JP, Lang I, Boer K, Bondarenko IM, Kulyk SO, et al. The cyclin-dependent kinase 4/6 inhibitor palbociclib in combination with letrozole versus letrozole alone as first-line treatment of oestrogen receptor-positive, HER2-negative, advanced breast cancer (PALOMA-1/TRIO-18): a randomised phase 2 study. *Lancet Oncol* (2015) 16(1):25–35. doi: 10.1016/S1470-2045(14)71159-3

63. Kryukov GV, Wilson FH, Ruth JR, Paulk J, Tsherniak A, Marlow SE, et al. MTAP deletion confers enhanced dependency on the PRMT5 arginine methyltransferase in cancer cells. *Science* (2016) 351(6278):1214–8. doi: 10.1126/science.aad5214

64. Mavrakis KJ, McDonald ER3rd, Schlabach MR, Billy E, Hoffman GR, deWeck A, et al. Sellers: Disordered methionine metabolism in MTAP/CDKN2A-deleted cancers leads to dependence on PRMT5. *Science* (2016) 351 (6278):1208–13. doi: 10.1126/science.aad5944

65. Aggarwal P, Vaites LP, Kim JK, Mellert H, Gurung B, Nakagawa H, et al. Nuclear cyclin D1/CDK4 kinase regulates CUL4 expression and triggers neoplastic growth *via* activation of the PRMT5 methyltransferase. *Cancer Cell* (2010) 18 (4):329–40. doi: 10.1016/j.ccr.2010.08.012

66. Goel S, DeCristo MJ, Watt AC, BrinJones H, Sceneay J, Li BB, et al. CDK4/6 inhibition triggers anti-tumour immunity. *Nature* (2017) 548(7668):471–5. doi: 10.1038/nature23465

67. Deng J, Wang ES, Jenkins RW, Li S, Dries R, Yates K, et al. CDK4/6 inhibition augments antitumor immunity by enhancing T-cell activation. *Cancer Discovery* (2018) 8(2):216–33. doi: 10.1158/2159-8290.CD-17-0915

68. Hasselblatt M, Thomas C, Hovestadt V, Schrimpf D, Johann P, Bens S, et al. Poorly differentiated chordoma with SMARCB1/INI1 loss: a distinct molecular entity with dismal prognosis. *Acta Neuropathol* (2016) 132(1):149–51. doi: 10.1007/s00401-016-1574-9

69. Shih AR, Cote GM, Chebib I, Choy E, DeLaney T, Deshpande V, et al. Clinicopathologic characteristics of poorly differentiated chordoma. *Mod Pathol* (2018) 31(8):1237–45. doi: 10.1038/s41379-018-0002-1

70. Kim KH, Kim W, Howard TP, Vazquez F, Tsherniak A, Wu JN, et al. SWI/SNF-mutant cancers depend on catalytic and non-catalytic activity of EZH2. *Nat Med* (2015) 21(12):1491–6. doi: 10.1038/nm.3968

71. Wilson BG, Wang X, Shen X, McKenna ES, Lemieux ME, Cho YJ, et al. Epigenetic antagonism between polycomb and SWI/SNF complexes during oncogenic transformation. *Cancer Cell* (2010) 18(4):316–28. doi: 10.1016/j.ccr.2010.09.006

72. Michel BC, D'Avino AR, Cassel SH, Mashtalir N, McKenzie ZM, McBride MJ, et al. A non-canonical SWI/SNF complex is a synthetic lethal target in cancers driven by BAF complex perturbation. *Nat Cell Biol* (2018) 20(12):1410–20. doi: 10.1038/s41556-018-0221-1

73. Wang X, Wang S, Troisi EC, Howard TP, Haswell JR, Wolf BK, et al. BRD9 defines a SWI/SNF sub-complex and constitutes a specific vulnerability in malignant rhabdoid tumors. *Nat Commun* (2019) 10(1):1881. doi: 10.1038/s41467-019-09891-7

74. Brien GL, Remillard D, Shi J, Hemming ML, Chabon J, Wynne K, et al. Targeted degradation of BRD9 reverses oncogenic gene expression in synovial sarcoma. *Elife* (2018) 7:e41305. doi: 10.7554/eLife.41305

75. Chabanon RM, Morel D, Eychenne T, Colmet-Daage L, Bajrami I, Dorvault N, et al. PBRM1 deficiency confers synthetic lethality to DNA repair inhibitors in cancer. *Cancer Res* (2021) 81(11):2888–902. doi: 10.1158/0008-5472.CAN-21-0628

76. Jones SE, Fleuren EDG, Frankum J, Konde A, Williamson CT, Krastev DB, et al. ATR is a therapeutic target in synovial sarcoma. *Cancer Res* (2017) 77 (24):7014–26. doi: 10.1158/0008-5472.CAN-17-2056

77. Williamson CT, Miller R, Pemberton HN, Jones SE, Campbell J, Konde A, et al. ATR inhibitors as a synthetic lethal therapy for tumours deficient in ARID1A. *Nat Commun* (2016) 7:13837. doi: 10.1038/ncomms13837

78. Howard TP, Arnoff TE, Song MR, Giacomelli AO, Wang X, Hong AL, et al. MDM2 and MDM4 are therapeutic vulnerabilities in malignant rhabdoid tumors. *Cancer Res* (2019) 79(9):2404–14. doi: 10.1158/0008-5472.CAN-18-3066

79. Sharifnia T, Wawer MJ, Chen T, Huang QY, Weir BA, Sizemore A, et al. Small-molecule targeting of brachyury transcription factor addiction in chordoma. *Nat Med* (2019) 25(2):292–300. doi: 10.1038/s41591-018-0312-3

80. Sawada A, Kiyonari H, Ukita K, Nishioka N, Imuta Y, Sasaki H. Redundant roles of Tead1 and Tead2 in notochord development and the regulation of cell proliferation and survival. *Mol Cell Biol* (2008) 28(10):3177–89. doi: 10.1128/MCB.01759-07

81. Sheppard HE, Dall'Agnese A, Park WD, Shamim MH, Dubrulle J, Johnson HL, et al. Targeted brachyury degradation disrupts a highly specific autoregulatory program controlling chordoma cell identity. *Cell Rep Med* (2021) 2(1):100188. doi: 10.1016/j.xcrm.2020.100188

82. Shah SR, David JM, Tippens ND, Mohyeldin A, Martinez-Gutierrez JC, Ganaha S, et al. Brachyury-YAP regulatory axis drives stemness and growth in cancer. *Cell Rep* (2017) 21(2):495–507. doi: 10.1016/j.celrep.2017.09.057

83. Chang L, Azzolin L, Di Biagio D, Zanconato F, Battilana G, Lucon Xiccato R, et al. The SWI/SNF complex is a mechanoregulated inhibitor of YAP and TAZ. *Nature* (2018) 563(7730):265–9. doi: 10.1038/s41586-018-0658-1

84. Noland CL, Gierke S, Schnier PD, Murray J, Sandoval WN, Sagolla M, et al. Palmitoylation of TEAD transcription factors is required for their stability and function in hippo pathway signaling. *Structure* (2016) 24(1):179–86. doi: 10.1016/j.str.2015.11.005

85. Holden JK, Crawford JJ, Noland CL, Schmidt S, Zbieg JR, Lacap JA, et al. Small molecule dysregulation of TEAD lipidation induces a dominant-negative inhibition of hippo pathway signaling. *Cell Rep* (2020) 31(12):107809. doi: 10.1016/j.celrep.2020.107809

86. Tang TT, Konradi AW, Feng Y, Peng X, Ma M, Li J, et al. Small molecule inhibitors of TEAD auto-palmitoylation selectively inhibit proliferation and tumor growth of NF2-deficient mesothelioma. *Mol Cancer Ther* (2021) 20(6):986–98. doi: 10.1158/1535-7163.MCT-20-0717

87. Zuccato JA, Patil V, Mansouri S, Liu JC, Nassiri F, Mamatjan Y, et al. DNA Methylation-based prognostic subtypes of chordoma tumors in tissue and plasma. *Neuro Oncol* (2022) 24(3):442–54. doi: 10.1093/neuonc/noab235

88. Zou MX, Lv GH, Wang XB, Huang W, Li J, Jiang Y, et al. Clinical impact of the immune microenvironment in spinal chordoma: Immunoscore as an independent favorable prognostic factor. *Neurosurgery* (2019) 84(6):E318–33. doi: 10.1093/neuros/nyy274

89. Zou MX, Zheng BW, Liu FS, Wang XB, Hu JR, Huang W, et al. The relationship between tumor-stroma ratio, the immune microenvironment, and survival in patients with spinal chordoma. *Neurosurgery* (2019) 85(6):E1095–110. doi: 10.1093/neuros/nyz333

90. Feng Y, Shen J, Gao Y, Liao Y, Cote G, Choy E, et al. Expression of programmed cell death ligand 1 (PD-L1) and prevalence of tumor-infiltrating lymphocytes (TILs) in chordoma. *Oncotarget* (2015) 6(13):11139–49. doi: 10.18632/oncotarget.3576

91. Mathios D, Ruzevick J, Jackson CM, Xu H, Shah SR, Taube JM, et al. PD-1, PD-L1, PD-L2 expression in the chordoma microenvironment. *J Neurooncol* (2015) 121(2):251–9. doi: 10.1007/s11060-014-1637-5

92. Xia C, Huang W, Chen YL, Fu HB, Tang M, Zhang TL, et al. Coexpression of HHLA2 and PD-L1 on tumor cells independently predicts the survival of spinal chordoma patients. *Front Immunol* (2021) 12:797407. doi: 10.3389/fimmu.2021.797407

93. Long C, Li G, Zhang C, Jiang T, Li Y, Duan X, et al. B7-H3 as a target for CAR-T cell therapy in skull base chordoma. *Front Oncol* (2021) 11:659662. doi: 10.3389/fonc.2021.659662

94. Duan W, Zhang B, Li X, Chen W, Jia S, Xin Z, et al. Single-cell transcriptome profiling reveals intra-tumoral heterogeneity in human chordomas. *Cancer Immunol Immunother* (2022) 71(9):2185–95. doi: 10.1007/s00262-022-03152-1

95. Mariathasan S, Turley SJ, Nickles D, Castiglioni A, Yuen K, Wang Y, et al. Powles: TGFbeta attenuates tumour response to PD-L1 blockade by contributing to exclusion of T cells. *Nature* (2018) 554(7693):544–8. doi: 10.1038/nature25501

96. Tauriello DVF, Palomo-Ponce S, Stork D, Berenguer-Llergo A, Badia-Ramentol J, Iglesias M, et al. TGFbeta drives immune evasion in genetically reconstituted colon cancer metastasis. *Nature* (2018) 554(7693):538–43. doi: 10.1038/nature25492

97. Strauss J, Heery CR, Schlom J, Madan RA, Cao L, Kang Z, et al. Phase I trial of M7824 (MSB0011359C), a bifunctional fusion protein targeting PD-L1 and TGFbeta, in advanced solid tumors. *Clin Cancer Res* (2018) 24(6):1287–95. doi: 10.1158/1078-0432.CCR-17-2653

98. Chen DS, Mellman I. Oncology meets immunology: the cancer-immunity cycle. *Immunity* (2013) 39(1):1–10. doi: 10.1016/j.immuni.2013.07.012

99. Huang KL, Mashl RJ, Wu Y, Ritter DI, Wang J, Oh C, et al. Pathogenic germline variants in 10,389 adult cancers. *Cell* (2018) 173(2):355–370 e14. doi: 10.1016/j.cell.2018.03.039

100. Sayaman RW, Saad M, Thorsson V, Hu D, Hendrickx W, Roelands J, et al. Germline genetic contribution to the immune landscape of cancer. *Immunity* (2021) 54(2):367–386 e8. doi: 10.1016/j.immuni.2021.01.011

101. Matson V, Fessler J, Bao R, Chongsuwat T, Zha Y, Alegre ML, et al. The commensal microbiome is associated with anti-PD-1 efficacy in metastatic melanoma patients. *Science* (2018) 359(6371):104–8. doi: 10.1126/science.aao3290

102. Gopalakrishnan V, Spencer CN, Nezi L, Reuben A, Andrews MC, Karpinets TV, et al. Gut microbiome modulates response to anti-PD-1 immunotherapy in melanoma patients. *Science* (2018) 359(6371):97–103. doi: 10.1126/science.aan4236

103. Routy B, Le Chatelier E, Derosa L, Duong CPM, Alou MT, Daillere R, et al. Gut microbiome influences efficacy of PD-1-based immunotherapy against epithelial tumors. *Science* (2018) 359(6371):91–7. doi: 10.1126/science.aan3706

104. Spencer CN, McQuade JL, Gopalakrishnan V, McCulloch JA, Vetizou M, Cogdill AP, et al. Dietary fiber and probiotics influence the gut microbiome and melanoma immunotherapy response. *Science* (2021) 374(6575):1632–40. doi: 10.1126/science.aaz7015

105. Passeri T, Dahmani A, Masliah-Planchon J, Naguez A, Michou M, El Botty R, et al. Dramatic *In vivo* efficacy of the EZH2-inhibitor tazemetostat in PBRM1-mutated human chordoma xenograft. *Cancers (Basel)* (2022) 14(6):1486. doi: 10.3390/cancers14061486

106. Walker RL, Hornicek FJ, Duan Z. Advances in the development of chordoma models for drug discovery and precision medicine. *Biochim Biophys Acta Rev Cancer* (2022), 1877(6):188812. doi: 10.1016/j.bbcan.2022.188812

107. Chordoma Foundation*Chordoma foundation in vivo drug screening program data*. figshare. Available at: https://figshare.com/projects/Chordoma_Foundation_In_Vivo_Drug_Screening_Program/25948.

108. Woo XY, Giordano J, Srivastava A, Zhao ZM, Lloyd MW, de Bruijn R, et al. Eur: Conservation of copy number profiles during engraftment and passaging of patient-derived cancer xenografts. *Nat Genet* (2021) 53(1):86–99. doi: 10.1038/s41588-020-00750-6

109. Gao H, Korn JM, Ferretti S, Monahan JE, Wang Y, Singh M, et al. High-throughput screening using patient-derived tumor xenografts to predict clinical trial drug response. *Nat Med* (2015) 21(11):1318–25. doi: 10.1038/nm.3954

110. Drost J, Clevers H. Organoids in cancer research. *Nat Rev Cancer* (2018) 18 (7):407–18. doi: 10.1038/s41568-018-0007-6

111. Al Shihabi A, Davarifar A, Nguyen HTL, Tavanaie N, Nelson SD, Yanagawa J, et al. Personalized chordoma organoids for drug discovery studies. *Sci Adv* (2022) 8(7):eabl3674. doi: 10.1126/sciadv.abl3674

112. Vlachogiannis G, Hedayat S, Vatsiou A, Jamin Y, Fernandez-Mateos J, Khan K, et al. Patient-derived organoids model treatment response of metastatic gastrointestinal cancers. *Science* (2018) 359(6378):920–6. doi: 10.1126/science.aao2774

113. Tiriac H, Belleau P, Engle DD, Plenker D, Deschenes A, Somerville TDD, et al. Organoid profiling identifies common responders to chemotherapy in pancreatic cancer. *Cancer Discovery* (2018) 8(9):1112–29. doi: 10.1158/2159-8290.CD-18-0349

114. Ooft SN, Weeber F, Dijkstra KK, McLean CM, Kaing S, van Werkhoven E, et al. Patient-derived organoids can predict response to chemotherapy in metastatic colorectal cancer patients. *Sci Transl Med* (2019) 11(513):eaay2574. doi: 10.1126/scitranslmed.aay2574

115. Pauli C, Hopkins BD, Prandi D, Shaw R, Fedrizzi T, Sboner A, et al. Personalized *In vitro* and *In vivo* cancer models to guide precision medicine. *Cancer Discovery* (2017) 7(5):462–77. doi: 10.1158/2159-8290.CD-16-1154

116. Guillen KP, Fujita M, Butterfield AJ, Scherer SD, Bailey MH, Chu Z, et al. A human breast cancer-derived xenograft and organoid platform for drug discovery and precision oncology. *Nat Cancer* (2022) 3(2):232–50. doi: 10.1038/s43018-022-00337-6

117. Tsherniak A, Vazquez F, Montgomery PG, Weir BA, Kryukov G, Cowley GS, et al. Defining a cancer dependency map. *Cell* (2017) 170(3):564–576 e16. doi: 10.1016/j.cell.2017.06.010

118. Vervoort SJ, Devlin JR, Kwiatkowski N, Teng M, Gray NS, Johnstone RW. Targeting transcription cycles in cancer. *Nat Rev Cancer* (2022) 22(1):5–24. doi: 10.1038/s41568-021-00411-8

119. Richters A, Doyle SK, Freeman DB, Lee C, Leifer BS, Jagannathan S, et al. Modulating androgen receptor-driven transcription in prostate cancer with selective CDK9 inhibitors. *Cell Chem Biol* (2021) 28(2):134–147 e14. doi: 10.1016/j.chembiol.2020.10.001

120. Day MAS, Hood T, Obholzer N, Pandey A, Lin CY, Kumar P, et al. CDK9 inhibition *via* KB-0742 is a potential strategy to treat transcriptionally addicted cancers. *Cancer Res* (2022) 82(12_Supplement):2564. doi: 10.1158/1538-7445.AM2022-2564

121. Anders L, Ke N, Hydbring P, Choi YJ, Widlund HR, Chick JM, et al. A systematic screen for CDK4/6 substrates links FOXM1 phosphorylation to senescence suppression in cancer cells. *Cancer Cell* (2011) 20(5):620–34. doi: 10.1016/j.ccr.2011.10.001

122. Wang H, Nicolay BN, Chick JM, Gao X, Geng Y, Ren H, et al. The metabolic function of cyclin D3-CDK6 kinase in cancer cell survival. *Nature* (2017) 546(7658):426–30. doi: 10.1038/nature22797

123. Stockwell BR, Friedmann Angeli JP, Bayir H, Bush AI, Conrad M, Dixon SJ, et al. Ferroptosis: A regulated cell death nexus linking metabolism, redox biology, and disease. *Cell* (2017) 171(2):273–85. doi: 10.1016/j.cell.2017.09.021

124. Zou Y, Palte MJ, Deik AA, Li H, Eaton JK, Wang W, et al. A GPX4-dependent cancer cell state underlies the clear-cell morphology and confers sensitivity to ferroptosis. *Nat Commun* (2019) 10(1):1617. doi: 10.1038/s41467-019-09277-9

125. Nicholson HE, Tariq Z, Housden BE, Jennings RB, Stransky LA, Perrimon N, et al. HIF-independent synthetic lethality between CDK4/6 inhibition and VHL loss across species. *Sci Signal* (2019) 12(601):eaay0482. doi: 10.1126/scisignal.aay0482

126. Coffin CM, Swanson PE, Wick MR, Dehner LP. An immunohistochemical comparison of chordoma with renal cell carcinoma, colorectal adenocarcinoma, and myxopapillary ependymoma: a potential diagnostic dilemma in the diminutive biopsy. *Mod Pathol* (1993) 6(5):531–8.

127. Duvel K, Yecies JL, Menon S, Raman P, Lipovsky AI, Souza AL, et al. Activation of a metabolic gene regulatory network downstream of mTOR complex 1. *Mol Cell* (2010) 39(2):171–83. doi: 10.1016/j.molcel.2010.06.022

128. Dodd KM, Yang J, Shen MH, Sampson JR, Tee AR. mTORC1 drives HIF-1alpha and VEGF-a signalling *via* multiple mechanisms involving 4E-BP1, S6K1 and STAT3. *Oncogene* (2015) 34(17):2239–50. doi: 10.1038/onc.2014.164

129. Li X, Ji Z, Ma Y, Qiu X, Fan Q, Ma B. Expression of hypoxia-inducible factor-1alpha, vascular endothelial growth factor and matrix metalloproteinase-2 in sacral chordomas. *Oncol Lett* (2012) 3(6):1268–74. doi: 10.3892/ol.2012.645

130. Lam R. The nature of cytoplasmic vacuoles in chordoma cells. a correlative enzyme and electron microscopic histochemical study. *Pathol Res Pract* (1990) 186 (5):642–50. doi: 10.1016/S0344-0338(11)80228-1

131. Pandiar D, Thammaiah S. Physaliphorous cells. *J Oral Maxillofac Pathol* (2018) 22(3):296–7. doi: 10.4103/jomfp.JOMFP_265_18

132. Ellis K, Bagwell J, Bagnat M. Notochord vacuoles are lysosome-related organelles that function in axis and spine morphogenesis. *J Cell Biol* (2013) 200 (5):667–79. doi: 10.1083/jcb.201212095

133. N. Cancer Genome Atlas Research. Comprehensive molecular characterization of clear cell renal cell carcinoma. *Nature* (2013) 499(7456):43–9. doi: 10.1038/nature12222

134. McDonald ER3rd, de Weck A, Schlabach MR, Billy E, Mavrakis KJ, Hoffman GR, et al. Sellers: Project DRIVE: A compendium of cancer dependencies and synthetic lethal relationships uncovered by Large-scale, deep RNAi screening. *Cell* (2017) 170(3):577–592 e10. doi: 10.1016/j.cell.2017.07.005

135. Behan FM, Iorio F, Picco G, Goncalves E, Beaver CM, Migliardi G, et al. Prioritization of cancer therapeutic targets using CRISPR-Cas9 screens. *Nature* (2019) 568(7753):511–6. doi: 10.1038/s41586-019-1103-9

136. Huang A, Garraway LA, Ashworth A, Weber B. Synthetic lethality as an engine for cancer drug target discovery. *Nat Rev Drug Discovery* (2020) 19(1):23–38. doi: 10.1038/s41573-019-0046-z

137. Kalev P, Hyer ML, Gross S, Konteatis Z, Chen CC, Fletcher M, et al. MAT2A inhibition blocks the growth of MTAP-deleted cancer cells by reducing PRMT5-dependent mRNA splicing and inducing DNA damage. *Cancer Cell* (2021) 39(2):209–224 e11. doi: 10.1016/j.ccell.2020.12.010

138. Hoke ATK, Padget MR, Fabian KP, Nandal A, Gallia GL, Bilusic M, et al. Combinatorial natural killer cell-based immunotherapy approaches selectively target chordoma cancer stem cells. *Cancer Res Commun* (2021) 1(3):127–39. doi: 10.1158/2767-9764.crc-21-0020

139. Ruscetti M, Leibold J, Bott MJ, Fennell M, Kulick A, Salgado NR, et al. NK cell-mediated cytotoxicity contributes to tumor control by a cytostatic drug combination. *Science* (2018) 362(6421):1416–22. doi: 10.1126/science.aas9090

140. Ruscetti M, t. Morris JP, Mezzadra R, Russell J, Leibold J, Romesser PB, et al. Senescence-induced vascular remodeling creates therapeutic vulnerabilities in pancreas cancer. *Cell* (2020) 181(2):424–441 e21. doi: 10.1016/j.cell.2020.03.008

141. Fujii R, Schlom J, Hodge JW. A potential therapy for chordoma *via* antibody-dependent cell-mediated cytotoxicity employing NK or high-affinity NK cells in combination with cetuximab. *J Neurosurg* (2018) 128(5):1419–27. doi: 10.3171/2017.1.JNS162610

142. DeMaria PJ, Lee-Wisdom K, Donahue RN, Madan RA, Karzai F, Schwab A, et al. Phase 1 open-label trial of intravenous administration of MVA-BN-brachyury-TRICOM vaccine in patients with advanced cancer. *J Immunother Cancer* (2021) 9(9):e003238. doi: 10.1136/jitc-2021-003238

143. Migliorini D, Mach N, Aguiar D, Vernet R, Landis BN, Becker M, et al. First report of clinical responses to immunotherapy in 3 relapsing cases of chordoma after failure of standard therapies. *Oncoimmunology* (2017) 6(8): e1338235. doi: 10.1080/2162402X.2017.1338235

144. Williamson LM, Rive CM, Di Francesco D, Titmuss E, Chun HE, Brown SD, et al. Clinical response to nivolumab in an INI1-deficient pediatric chordoma correlates with immunogenic recognition of brachyury. *NPJ Precis Oncol* (2021) 5 (1):103. doi: 10.1038/s41698-021-00238-4

145. Wu X, Lin X, Chen Y, Kong W, Xu J, Yu Z. Response of metastatic chordoma to the immune checkpoint inhibitor pembrolizumab: A case report. *Front Oncol* (2020) 10:565945. doi: 10.3389/fonc.2020.565945

146. Blay JY, Penel N, Ray-Coquard IL, Cousin S, Bertucci F, Bompas E, et al. High clinical activity of pembrolizumab in chordoma, alveolar soft part sarcoma (ASPS) and other rare sarcoma histotypes: The French AcSe pembrolizumab study from unicancer. *J Clin Oncol* (2021) 39(no. 15_suppl):11520–0. doi: 10.1200/JCO.2021.39.15_suppl.11520

147. Banta KL, Xu X, Chitre AS, Au-Yeung A, Takahashi C, O'Gorman WE, et al. Mechanistic convergence of the TIGIT and PD-1 inhibitory pathways necessitates co-blockade to optimize anti-tumor CD8(+) T cell responses. *Immunity* (2022) 55(3):512–526 e9. doi: 10.1016/j.immuni.2022.02.005

148. Fujita N, Miyamoto T, Imai J, Hosogane N, Suzuki T, Yagi M, et al. CD24 is expressed specifically in the nucleus pulposus of intervertebral discs. *Biochem Biophys Res Commun* (2005) 338(4):1890–6. doi: 10.1016/j.bbrc.2005.10.166

149. Barkal AA, Brewer RE, Markovic M, Kowarsky M, Barkal SA, Zaro BW, et al. CD24 signalling through macrophage siglec-10 is a target for cancer immunotherapy. *Nature* (2019) 572(7769):392–6. doi: 10.1038/s41586-019-1456-0

150. Serrano M, Lin AW, McCurrach ME, Beach D, Lowe SW. Oncogenic ras provokes premature cell senescence associated with accumulation of p53 and p16INK4a. *Cell* (1997) 88(5):593–602. doi: 10.1016/s0092-8674(00)81902-9

151. Michaloglou C, Vredeveld LC, Soengas MS, Denoyelle C, Kuilman T, van der Horst CM, et al. BRAFE600-associated senescence-like cell cycle arrest of human naevi. *Nature* (2005) 436(7051):720–4. doi: 10.1038/nature03890

152. Baggiolini A, Callahan SJ, Montal E, Weiss JM, Trieu T, Tagore MM, et al. Developmental chromatin programs determine oncogenic competence in melanoma. *Science* (2021) 373(6559):eabc1048. doi: 10.1126/science.abc1048

153. Patel SA, Hirosue S, Rodrigues P, Vojtasova E, Richardson EK, Ge J, et al. The renal lineage factor PAX8 controls oncogenic signalling in kidney cancer. *Nature* (2022) 606(7916):999–1006. doi: 10.1038/s41586-022-04809-8

154. Dale B, Cheng M, Park KS, Kaniskan HU, Xiong Y, Jin J. Advancing targeted protein degradation for cancer therapy. *Nat Rev Cancer* (2021) 21 (10):638–54. doi: 10.1038/s41568-021-00365-x

155. Beisaw A, Tsaytler P, Koch F, Schmitz SU, Melissari MT, Senft AD, et al. BRACHYURY directs histone acetylation to target loci during mesoderm development. *EMBO Rep* (2018) 19(1):118–34. doi: 10.15252/embr.201744201

156. Samarasinghe KTG, Jaime-Figueroa S, Burgess M, Nalawansha DA, Dai K, Hu Z, et al. Targeted degradation of transcription factors by TRAFTACs: TRAnscription factor TArgeting chimeras. *Cell Chem Biol* (2021) 28(5):648–661 e5. doi: 10.1016/j.chembiol.2021.03.011

157. N. Cancer Genome Atlas Research, Linehan WM, Spellman PT, Ricketts CJ, Creighton CJ, Fei SS, et al. Comprehensive molecular characterization of papillary renal-cell carcinoma. *N Engl J Med* (2016) 374(2):135–45. doi: 10.1056/NEJMoa1505917

158. Palena C, Roselli M, Litzinger MT, Ferroni P, Costarelli L, Spila A, et al. Overexpression of the EMT driver brachyury in breast carcinomas: association with poor prognosis. *J Natl Cancer Inst* (2014) 106(5):dju054. doi: 10.1093/jnci/dju054

159. Hamilton DH, Roselli M, Ferroni P, Costarelli L, Cavaliere F, Taffuri M, et al. Brachyury, a vaccine target, is overexpressed in triple-negative breast cancer. *Endocr Relat Cancer* (2016) 23(10):783–96. doi: 10.1530/ERC-16-0037

160. Li K, Ying M, Feng D, Du J, Chen S, Dan B, et al. Brachyury promotes tamoxifen resistance in breast cancer by targeting SIRT1. *BioMed Pharmacother* (2016) 84:28–33. doi: 10.1016/j.biopha.2016.09.011

161. Lee KH, Kim EY, Yun JS, Park YL, Do SI, Chae SW, et al. Prognostic significance of expression of epithelial-mesenchymal transition driver brachyury in breast cancer and its association with subtype and characteristics. *Oncol Lett* (2018) 15(1):1037–45. doi: 10.3892/ol.2017.7402

162. Miettinen M, Wang Z, Lasota J, Heery C, Schlom J, Palena C. Nuclear brachyury expression is consistent in chordoma, common in germ cell tumors and small cell carcinomas, and rare in other carcinomas and sarcomas: An immunohistochemical study of 5229 cases. *Am J Surg Pathol* (2015) 39 (10):1305–12. doi: 10.1097/PAS.0000000000000462

163. Roselli M, Fernando RI, Guadagni F, Spila A, Alessandroni J, Palmirotta R, et al. Brachyury, a driver of the epithelial-mesenchymal transition, is overexpressed in human lung tumors: an opportunity for novel interventions against lung cancer. *Clin Cancer Res* (2012) 18(14):3868–79. doi: 10.1158/1078-0432.CCR-11-3211

164. Huang B, Cohen JR, Fernando RI, Hamilton DH, Litzinger MT, Hodge JW, et al. The embryonic transcription factor brachyury blocks cell cycle progression and mediates tumor resistance to conventional antitumor therapies. *Cell Death Dis* (2013) 4:e682. doi: 10.1038/cddis.2013.208

165. Xu K, Liu B, Liu Y. Impact of brachyury on epithelial-mesenchymal transitions and chemosensitivity in non-small cell lung cancer. *Mol Med Rep* (2015) 12(1):995–1001. doi: 10.3892/mmr.2015.3348

166. Shimamatsu S, Okamoto T, Haro A, Kitahara H, Kohno M, Morodomi Y, et al. Prognostic significance of expression of the epithelial-mesenchymal transition-related factor brachyury in intrathoracic lymphatic spread of non-small cell lung cancer. *Ann Surg Oncol* (2016) 23(Suppl 5):1012–20. doi: 10.1245/s10434-016-5530-7

167. Kilic N, Feldhaus S, Kilic E, Tennstedt P, Wicklein D, Wasielewski R, et al. Brachyury expression predicts poor prognosis at early stages of colorectal cancer. *Eur J Cancer* (2011) 47(7):1080–5. doi: 10.1016/j.ejca.2010.11.015

168. Guinney J, Dienstmann R, Wang X, de Reynies A, Schlicker A, Soneson C, et al. The consensus molecular subtypes of colorectal cancer. *Nat Med* (2015) 21 (11):1350–6. doi: 10.1038/nm.3967

169. Parker JS, Mullins M, Cheang MC, Leung S, Voduc D, Vickery T, et al. Supervised risk predictor of breast cancer based on intrinsic subtypes. *J Clin Oncol* (2009) 27(8):1160–7. doi: 10.1200/JCO.2008.18.1370

170. Chapuy B, Stewart C, Dunford AJ, Kim J, Kamburov A, Redd RA, et al. Molecular subtypes of diffuse large b cell lymphoma are associated with distinct pathogenic mechanisms and outcomes. *Nat Med* (2018) 24(5):679–90. doi: 10.1038/s41591-018-0016-8

frontiers | Frontiers in Oncology

TYPE Review
PUBLISHED 16 November 2022
DOI 10.3389/fonc.2022.1029670

OPEN ACCESS

EDITED BY
Haotian Zhao,
New York Institute of Technology,
United States

REVIEWED BY
Jinpeng Zhou,
Fourth Military Medical
University, China
Mingxuan Li,
Beijing Neurosurgical Institute, China
Zhenlin Wang,
Xuanwu Hospital, Capital Medical
University, China

*CORRESPONDENCE
Cheng Yang
ddyc2001@163.com
Jianru Xiao
cz_xiaojianru@163.com

†These authors have contributed
equally to this work and share
first authorship

SPECIALTY SECTION
This article was submitted to
Neuro-Oncology and
Neurosurgical Oncology,
a section of the journal
Frontiers in Oncology

RECEIVED 27 August 2022
ACCEPTED 19 October 2022
PUBLISHED 16 November 2022

CITATION
Zhao C, Tan T, Zhang E, Wang T,
Gong H, Jia Q, Liu T, Yang X, Zhao J,
Wu Z, Wei H, Xiao J and Yang C (2022)
A chronicle review of new techniques
that facilitate the understanding and
development of optimal individualized
therapeutic strategies for chordoma.
Front. Oncol. 12:1029670.
doi: 10.3389/fonc.2022.1029670

A chronicle review of new techniques that facilitate the understanding and development of optimal individualized therapeutic strategies for chordoma

Chenglong Zhao[1†], Tao Tan[2†], E. Zhang[1†], Ting Wang[1], Haiyi Gong[1], Qi Jia[1], Tielong Liu[1], Xinghai Yang[1], Jian Zhao[1], Zhipeng Wu[1], Haifeng Wei[1], Jianru Xiao[1*] and Cheng Yang[1*]

[1]Spinal Tumor Center, Department of Orthopedic Oncology, Changzheng Hospital, Shanghai, China, [2]Department of Orthopedics, 905 Hospital of People's Liberation Army Navy, Shanghai, China

Chordoma is a rare malignant bone tumor that mainly occurs in the sacrum and the clivus/skull base. Surgical resection is the treatment of choice for chordoma, but the local recurrence rate is high with unsatisfactory prognosis. Compared with other common tumors, there is not much research and individualized treatment for chordoma, partly due to the rarity of the disease and the lack of appropriate disease models, which delay the discovery of therapeutic strategies. Recent advances in modern techniques have enabled gaining a better understanding of a number of rare diseases, including chordoma. Since the beginning of the 21st century, various chordoma cell lines and animal models have been reported, which have partially revealed the intrinsic mechanisms of tumor initiation and progression with the use of next-generation sequencing (NGS) techniques. In this study, we performed a systematic overview of the chordoma models and related sequencing studies in a chronological manner, from the first patient-derived chordoma cell line (U-CH1) to diverse preclinical models such as the patient-derived organoid-based xenograft (PDX) and patient-derived organoid (PDO) models. The use of modern sequencing techniques has discovered mutations and expression signatures that are considered potential treatment targets, such as the expression of Brachyury and overactivated receptor tyrosine kinases (RTKs). Moreover, computational and bioinformatics techniques have made drug repositioning/repurposing and individualized high-throughput drug screening available. These advantages facilitate the research and development of comprehensive and personalized treatment strategies for indicated patients and will dramatically improve their prognoses in the near feature.

KEYWORDS

chordoblast, organoid, NGS—next-generation sequencing, precision treatment, drug discovery

Introduction

Chordomas are extremely rare malignant bone tumors originating from the remnant notochord (1, 2). The estimated annual incidence is approximately 0.8–1 out of 1,000,000, with male dominance (3, 4). Almost all primary tumors accumulate in the axial skeleton, with a predilection of the sacrum and the clivus/skull base. According to the WHO classification (5th edition), chordomas are pathologically classified into three subtypes: conventional (including the chondroid), poorly differentiated, and dedifferentiated (5). The conventional subtype is the most common, accounting for more than 95% of all cases (6).

Chordomas are considered as low- to intermediate-grade malignancies with a moderate growth rate, but with locally aggressive features. The ideal treatment is en bloc resection of the primary tumor without metastasis (7, 8). However, most patients with chordoma lack the typical clinical symptoms in the early stage due to the indolent characteristic of this tumor. Most chordoma tumors are large at the first diagnosis, with a pseudo-capsule that is vulnerably violated intraoperatively. On the other hand, as most chordoma tumors originate from the cranio-caudal ends of axial skeletons, vital structures such as the pituitary, spinal cord or cervical/sacral nerve roots, vertebral/iliac arteries, rectum, and the sigmoid colon are often involved or even enrolled by the tumor mass, which constitutes a great challenge in the surgical intervention of this malignancy. Subtotal resection with adjuvant radiotherapy is considered as an alternative treatment, but insufficient resection of the tumor often leads to a high risk of subsequent local recurrence or even metastasis (9).

The 5-year recurrence-free survival (RFS) of chordoma is over 50% for patients with adequate resection margins, but the rate may drop dramatically to less than 20% in the presence of contamination (7, 9, 10). Few advanced cases can be cured radically by surgery, and systemic treatment is required, but the effect is limited (6, 8, 9). Conventional chordomas are considered as indolent to cytotoxic chemotherapy, while the poorly differentiated and dedifferentiated subtypes are considered as sensitive to chemotherapy. Systemic treatment is considered as upfront management for chordoma by most researchers and clinicians, but more evidence-based verification is required (11–14).

To some extent, the current clinical dilemma is attributed to the lack of basic research on chordoma compared with other tumors. Given the low occurrence rate and the indolent biological feature of chordoma, it is usually difficult to develop stable cell lines and suitable xenograft animal models, which hinders gaining a deeper understanding of the intrinsic mechanism of the biological processes of chordoma. It was not until 2001 that the first chordoma cell line was established and well characterized (15). With the joint efforts of clinicians, biologists, pharmacologists, and numerous other multidisciplinary teams, chordoma research has made great progress in the new century. New treatment strategies, including tumor vaccines, targeted therapies, and immunotherapies, have been developed and have shown promising prospects. In the current review, we focus on the progress in the basic research of chordoma in recent years and its far-reaching impact on clinical practices. In addition, we provide an overview of modern individualized drug screening systems for chordoma.

The research tools: Chordoma cell lines and animal models

The importance of cell lines and animal models for disease research cannot be doubted. However, since the identification of the first case in 2000, chordoma research has mainly focused on the clinical symptoms, radiological expressions, and pathological manifestations. Compared with other types of malignant tumors, the lack of understanding of the pathogenesis of chordoma and effective medical therapies is the partial reason for the delayed establishment of model systems. There is limited basic research in identifying karyotype abnormalities and characteristic molecules from clinical samples. It was not until 2001 that the first human chordoma cell line, U-CH1, was established (15), and about 10 years later, the first xenograft model was reported (16). Today, over 20 chordoma cell lines and several different types of animal models have been established, which substantially expands our understanding of the pathogenesis of chordoma.

Cell lines

The U-CH1 cell line was developed from a sacrum tumor of a 46-year-old male patient who received radiotherapy for local recurrence of the tumor 4 years after the primary resection. Further characterization proved typical physaliphorous morphological features and stable expression of several markers, including Brachyury, vimentin, and cytokeratin (15). Since its establishment, the U-CH1 cell line has become one of the most widely used chordoma cell lines worldwide. Several interesting intrapersonal models of cell line families with unique characteristics have been established. The U-CH11 and U-CH11R cell lines were established from the primary and the recurrent sacral chordoma (recurred 4 years after primary resection) of the same patient, respectively (17). The primary tumor tissue, the U-CH11 cell line, and the corresponding recurrent cell lines were compared using RNA sequencing (RNA-seq). The results demonstrated that transcriptomic reprogramming occurred during chordoma recurrence, which did not derive from genomic events. Similar conclusions were

also drawn from another series of cell lines originating from the same patient. U-CH17P, U-CH17M, and U-CH17S were established from the primary site, lung metastasis, and skin metastasis, respectively (18). Although there was some loss of genetic variations compared with the parental chordoma tissues, such cell line model systems are meaningful for the investigation and understanding of the intrinsic mechanisms underlying the process of tumor progression.

Compared with cell lines established from sacrococcygeal tumors, clivus-originated chordoma cell lines are even more difficult to breed. Lucia et al. reported a technical note on establishing three clival chordoma cell lines from patients, but the cells were not permanent (19): the cells underwent crisis with continued passaging for about 40 generations. Owen et al. established the first permanent human clival chordoma cell line, UM-Chor1, and successfully transduced it with a luciferase lentiviral vector (20). A para-sacral xenograft model in non-obese diabetic/severe combined immunodeficiency (NOD/SCID) mice was also built, which showed slow growth *via* bioluminescence. The lack of clival chordoma cell lines could possibly be explained by the role of aggressive telomerase in chordoma and the destruction or damage of tumor cells intraoperatively (19). Gellner et al. thoroughly analyzed such suspects and successfully bred the clival cell line MUG-CC1 using a full endoscopic technique under suitable culture conditions (21). Since non-tumorigenic notochordal cell lines are unlikely to be available in near future, their team also creatively presented a non-tumorigenic, spontaneously established lymphoblastoid cell line originating from the same chordoma patient (termed as MUG-CC1-LCL) for comparative analysis. Recently, Kino et al. have established a novel skull base chordoma cell line, TSK-CHO1 (22), which has been proven to be neoplastic and which exhibited pleomorphic features. It was also revealed that the TSK-CHO1 cell line secretes Brachyury and SOX9 into conditioned medium (CM), which can further induce human dental pulp stem cell differentiation and promote the production of hyaluronic acid and type II collagen. This new cell line is expected to be used for elucidating the pathogenesis of skull base chordoma and investigating the mechanism underlying the production of fibrocartilage.

Most currently available cell lines have been derived from conventional chordomas, but the origin of the other subtypes is unknown. Kim et al. successfully established a chordoma cell line from a patient with recurrent dedifferentiated chordoma and named it DTC (23). Compared with U-CH1 cells, DTC cells showed a unique polygonal morphology and higher clonogenic activity. Compared with conventional chordomas, a distinct expression spectrum was also identified, with a high expression of platelet-derived growth factor receptor-β (PDGFR-β) and stemness- and epithelial-to-mesenchymal transition (EMT)-related proteins, but low levels of Brachyury and cytokeratins. DTC cells were also demonstrated to have a high surface expression of CXCR4 and the capacity to form xenograft subcutaneous tumors in nude mice.

3D cultures of chordoma cell lines

It is well documented that chordoma cells are embedded in a massive extracellular myxoid matrix *in vivo*. The extracellular components not only function as a passive scaffold within the tumor architecture but also play a more active role, thus facilitating the communication between cells and participating in the regulation of cellular proliferation, differentiation, and motility. Therefore, 3D cultures are considered to have obvious superiority over traditional 2D cultures (24, 25). Cao et al. reported their experience using 3D cultures of chordoma cell lines (26). They cultured three cell lines (U-CH1, CH8, and GB60) the growth factor-reduced Matrigel by using an assay medium with the addition of extra growth factor 12 (DMEM/F12) containing 2% horse serum, 0.5 g/ml hydrocortisone, 100 ng/ml cholera toxin, 10 g/ml insulin, 100 U/ml penicillin G, and 100 mg/ml streptomycin after the tumor was seeded on the reconstituted basement membrane. The clusters and acini-like spheroids formed by the cells partially restored the *in vivo* morphology. Locquet et al. prepared 3D cellular models using cell lines representative of three different stages of the disease: U-CH12 for primary, U-CH1 for relapsed, and CH22 for metastatic tumor (27). Their tumor spheroids recapitulated the main histological and morphological features, as well as the radioresistant environment of chordoma.

The 3D cultures of the patient-derived primary tumor cells were named as organoids (patient-derived organoids, PDOs). More advantages of organoids over conventional 2D patient-derived cell cultures (PDCs) have been recognized and documented (28–30). However, similar obstacles, such as indolent tumor growth and difficulty in stable passage, need to be overcome by establishing chordoma organoid models in tumor cell lines. Scognamiglio et al. reported their experience in predicting the response of patients to the checkpoint inhibitors (ICIs) programmed cell death 1/programmed death ligand 1 (PD-1/PD-L1) (31). In their brief communication, they reported the first evidence of using chordoma PDOs to examine individual responses to treatment. In a recent report, Shihabi et al. have documented their experience in establishing the PDO model with a 100% success rate, stating that the model mimicked the immunohistopathological characteristics of the parental tumor (32). Furthermore, they built an effective and timely high-throughput drug screening platform with their PDO model. Additionally, the PDO model was obviously more cost-effective than the patient-derived xenograft (PDX) model. Details are presented in the subsequent section.

Collectively, the 3D culture and PDO models can serve as important supplements to traditional *in vitro* and *in vivo* animal models, which can greatly accelerate the study of such a rare disease and help in the discovery of potential therapeutic drugs. Details are presented in subsequent discussions.

Animal models

Two types of animal models have been established: the xenograft tumor model and the zebrafish tumor model. The former was derived based on chordoma cell lines or patient-derived tumors, while the latter is mostly a spontaneous animal model used to facilitate the understanding of the mechanisms of tumor initiation and progression.

Wesley et al. injected JHC7 cells into immunodeficient mice subcutaneously and successfully constructed the first cell line-derived (CLD) chordoma xenograft animal model (16). Further experiments demonstrated that the injected tumor vividly resembled the parental tumor phenotype. Siu et al. established the first serial transplantable PDX model (33). Compared with the CLD model, the PDX model more closely mimicked the original tumor and was more valuable for effective therapeutics (34). Using this model, Siu et al. (35) further evaluated the efficacy of the epidermal growth factor receptor (EGFR) inhibitor erlotinib *in vivo*. Subsequently, several PDX models reflecting different tumor characteristics were established, including primary or recurrent tumors involving the cervical spine or sacrum (36–38). However, all these tumors were subcutaneously injected; *in situ* transplanted models continue to be pursued.

Diaz et al. (34) established a clival chordoma xenograft to mimic *in situ* tumor characteristics (34). The tumors were harvested intraoperatively, digested, resuspended, and mixed with Matrigel. NOD/SCID gamma (NSG) mice were prepared by scraping the outer cortex of the parietal bone with a scalpel. The obtained tumor cells were implanted into the subcutaneous epicranial space above the posterior parietal bone and the sub-occipital musculature thereafter. Although not on each PDX model, bony invasion was observed in each generation, which partially restored the clinical features of patients compared with the primary tumor. Salle et al. (39) developed an orthotopic primary PDX model with tumors implanted in the lumbosacral area. Compared with the clivus, the lumbosacral area was preferred in order to allow tumor growth and avoid animal suffering and mortality related to the growth of the tumor. The success rate of tumor engraftment was significantly increased using this orthotopic technique, from about 30%–40% to 60%–80%.

Compared with the xenograft model, the tumorigenic model was more suitable for the investigation and understanding of tumor development and progression. In the new century, zebrafish has emerged as a powerful genetic model of human cancer with the advantages of high genetic conservation, operable genetic manipulations, and feasibility for observation (40). Burger et al. reported the first zebrafish model for chordoma research (41). They built a notochord-specific expression of HRASV12 in the Gal4/upstream activating sequence (UAS) system, which was one of the first inducible transgenic methods providing a unique opportunity to induce oncogene expression in a tissue-specific manner in zebrafish. Although no evidence of *HRAS* mutations has been reported in human chordomas, their model firstly observed a chordoma-like tissue malformation of the notochord with positive expressions of Brachyury and cytokeratin. A primary distinction observed between the examined zebrafish notochord tumors and the human chordoma is the rapid phenotype onset in the fish model compared with the slow growth of human cancer. These features facilitated an application in high-throughput drug screening. With this *in vivo* platform, the authors further investigated other potential drivers of chordoma initiation (42). Notably, their data imply that Brachyury per se might be insufficient to initiate chordoma and that the active receptor tyrosine kinase may potently induce a chordoma phenotype.

Several other genes were examined for their ability to induce tumor initiation in zebrafish models. The upregulation of the metastasis-associated gene *PRL-3* and the downregulation of the transforming growth factor-β family member *TGFB3* have been proven to be correlated with chordoma formation (43). Although there was no direct evidence of the contribution of *FAS*/*FASL* dysregulation to chordoma formation, the knockdown of this pair of genes in zebrafish strikingly impaired notochord formation in the zebrafish model, suggesting their possible involvement in chordoma occurrence (44). In addition to these genetic manipulated models, an interesting finding should be noted. Cooper et al. (45) reported a series of 24 cases of spontaneous primary intestinal chordomas in zebrafish and nine cases of spontaneous vertebral chordoma. The former represents a novel tumor type that had not been previously described in any species.

At present, most chordoma cell lines and several serial passable PDX models are well documented by the Chordoma Foundation (https://www.chordomafoundation.org/research/disease-models/) and are available to researchers. With the help of these valuable research models, chordoma research has made great strides and accelerated the development of comprehensive therapeutic drug discovery.

Leap to the next generation: Advances in genetic research

The identification of driver mutations and downstream regulatory abnormalities in malignancies is beneficial to revealing the intrinsic mechanisms of tumor initiation, progression, and recurrence and has dramatically changed the treatment landscape for many tumors. Multiple techniques for genetic analysis have been applied to karyotype analysis, comparative genetic hybridization (CGH), high-throughput microarray, and the NGS of chordoma. Some recent studies

have applied modern sequencing techniques to chordoma investigation, including single-cell RNA sequencing (scRNA-seq), whole-genome bisulfite sequencing (WGBS), transposable accessible chromatin by high-throughput sequencing (ATAC-seq), and Hi-C.

Early exploration of cytogenetic changes in chordoma

Due to restrictions in the investigation techniques, only limited studies with 18 chordoma cases focusing on cytogenetic changes were reported before 2000 (46). Few specific or characteristic chromosomal anomalies have been determined, except in one study by Butler et al., which reported the results of cytogenetic analysis of five chordomas (46). Only random abnormalities in one tumor cell out of 100 cells from Patient No. 5 were identified. However, their study identified elongation, but not reduction as in other tumors, of telomere length and an increase of telomerase activity. In the new century, several studies have demonstrated loss of heterozygosity for different loci in chordoma. In Klingler's cohort of 12 patients with chordoma, microsatellite instability (MIN) was demonstrated in six patients and loss of heterozygosity (LOH) for at least one locus in two patients (47). Several other LOH and comparative genomic hybridization (CGH) studies demonstrated more chromosome abnormalities that showed a feature of more loss than gain, including loss of 1p36, 7q33, and 9p21 as an important mechanism for tumor development (48–50). Furthermore, candidate genes mainly located in the locus of interest were mapped and identified using PCR, gene chips, and immunohistochemistry (IHC). At the same time, researchers firstly attempted to use imatinib mesylate, a selective tyrosine kinase inhibitor (TKI) of *c-KIT* and platelet-derived growth factor receptors, for patients with chordoma as it was shown to be highly effective in gastrointestinal stromal tumors (GIST) (51). Although some benefits in tumor control have been demonstrated in clinical practice, most of the samples were negative with activating mutations but overexpression of the receptor tyrosine kinase (RTK) genes, which can be identified with RT-PCR or IHC (52–54). Since then, many studies concerning the expression and functional analyses of RTK and other candidate genes have been performed with tissue microarray, with the results indicating a promising pattern for corresponding inhibitors in the treatment of chordoma (55–59).

High-throughput microarray has further promoted our understanding of such a rare tumor. The first array-based study characterizing DNA copy number changes in chordoma identified copy number alterations in all samples (50). Deletions were more common than gains, and no high-level amplification was found. Henderson et al. firstly drew a molecular map of mesenchymal tumors and identified a gene expression signature of chordoma through gene expression microarray (GEM) in a machine learning model (60). Among which, the T-box transcription factor (*TBXT*) Brachyury was first identified, which was mainly expressed in the developing notochord and strongly linked the embryonic structure with chordoma. Pillay et al. identified *TBXT* amplification in both familial and sporadic chordomas, finding that it was the rs2305089 polymorphism that altered the binding ability of *TBXT*, which is known to be closely correlated with tumor initiation in individuals of European ancestry (61). Further mutation studies also identified other common variants of *TBXT* with risk of chordomas, such as rs3816300 in sporadic chordomas and rs1056048 in familial cases (62). Since then, large numbers of studies have verified the important roles of Brachyury in the initiation, progression, and prognosis of chordoma. As the results have been well collective and compared in several other reviews (63–65), we will not discuss them herein. However, a recent randomized, double-blind, placebo-controlled phase II trial failed to observe advantages of the yeast–Brachyury vaccine combined with standard-of-care radiotherapy in locally advanced unresectable chordoma (66). Although the results of the yeast–Brachyury vaccine are not consistent, the idea of targeting Brachyury with other immune or targeted methods for chordoma therapy is still worth further exploration.

Since only a few driver mutations but dramatic functional gene expression signatures were identified in chordomas, exploration of the epigenetic changes was conducted (67, 68). Rinner et al. (69) reviewed 10 chordoma samples and found that the PI3K pathway played a potential important role in the development of chordoma. They first provided evidence of the DNA methylation of tumor suppressor genes in chordoma, suggesting that they could serve as markers for its early detection. Another study (70) identified a subset of probes that were differentially methylated between recurrent and non-recurrent chordomas. Identification of the DNA methylation features of chordoma has provided a wealth of information in establishing useful biomarkers for diagnosis, prognosis prediction, and disease monitoring, and these biomarkers could also be potential therapeutic targets for this rare tumor.

NGS techniques provide a deeper understanding of chordoma

Due to the urgent need to gain more thorough insights into the molecular biology and genetics of chordoma, ultra-deep NGS analysis was performed (as listed in Table 1). Fischer et al. (71) performed the first panel-based NGS study in nine patients with chordoma for the mutations of 48 cancer genes, but failed to identify somatic mutations in "hotspots" of genes known to be involved in cancer development; very low mutation rates of *KDR*, *KIT*, and *TP53* were determined. Another panel-based study of 341 key cancer-associated genes was performed in 23

chordoma samples (72). The results revealed non-random copy number losses across the genome and a very low mutation rate, with an average of 0.5 mutation per sample. However, about 40% of the mutation events were grouped as chromatin regulatory genes, including *SETD2*, *PBRM1*, *ARID1B*, and *SMARCB1*, and the co-occurrence of alterations in *CDKN2A*/*CDKN2B* was fairly common. These findings hinted that chordoma might belong to the C class tumors in terms of copy number changes whose oncogenic signature was a non-random multiple copy number loss across the genome, and these genomic aberrations frequently alter chromatin regulatory genes.

Restricted by the limited number of genes investigated in panel-based studies, a number of studies used whole-exome and whole-genome sequencing (WES and WGS, respectively), as these techniques can shed further light into the pathogenesis of and potential treatment options for chordoma. Jason et al. (74) combined WES and whole-transcriptome sequencing on 10 clivus chordomas and identified a novel gene fusion of *SMAD5–SASH1* for the first time in the skull base, which can be employed as a therapeutic and prognostic marker (74). Tarpey et al. (76) constructed a driver landscape of 104 cases of sporadic chordoma with 11 WGS, 26 WES, and 67 panel-based sequencing. WGS/WES studies were used as the discovery cohort and the remaining studies used as the validation cohort. This study identified somatic duplications of *TBXT*, recurrent mutations of *PI3K* signaling genes, and driver events in chromatin modeling genes, consistent with the results of the aforementioned studies. In addition, they also identified non-random enrichment of truncating mutations in the lysosomal trafficking regulator (LYST) protein for the first time and found that the expression of LYST was correlated with the function of lysosomes, a histological hallmark of physaliphorous vacuole-packed cells that characterize chordoma. *LYST* may work as a cancer gene in chordoma and prove to be an adjunct diagnostic marker.

The genomic features differed between ethnicities, tumor locations, and pathological subtypes. As aforementioned, the rs2305089 polymorphism in *TBXT* was associated with a sixfold increase in the risk of developing chordoma in a European population, but it was not found to be correlated with an increased risk in East Asians (81). On the other hand, somatic duplications of *TBXT* and mutations in *PI3K* signaling genes are rare in skull base chordomas, which was different from that observed in sacral chordoma. In a Chinese patient-based study of sacral chordomas, Xu et al. (79) identified a new *CLDN9* T120A substitution as a potential oncogene in indicated populations, which had not been previously reported. Previous analyses have identified pathological changes in chordomas (12). Compared with benign notochordal cell tumors, the conventional and dedifferentiated chordoma subtypes showed an increased genomic instability (78). In dedifferentiated chordomas, Brachyury was expressed in the conventional/chondroid components, but was completely lost in the dedifferentiated component. Poorly differentiated chordomas are characterized by the loss of *INI1*/*SMARCB1* and may also represent a discrete entity with a more aggressive phenotype, which is more similar to rhabdoid tumors. However, driver gene alterations are critical in tumor initiation and progression, but may not be involved in tumor dedifferentiation and high-grade transformation (82).

WES/WGS in chordoma tissues demonstrate a low-frequency mutation rate compared with that in other cancer tissues. Apart from genetic alterations, epigenetic regulators and chromatin spatial organization are also crucial for gene regulation by regulating the accessibility of DNA to sequence-specific binding proteins and bringing distant promoters, enhancers, and other *cis*-regulatory regions together (85, 86). Meng et al. (87) performed a multi-omics analysis with RNA-seq, ATAC-seq, and Hi-C and found that the bone microenvironment played an important role in chordoma tumorigenesis. In addition, they identified carbonic anhydrase II (*CA2*) as a novel therapeutic target in chordoma. ScRNA-seq could elucidate the mechanisms underlying carcinogenesis and the molecular features of cancers. Duan et al. (84) first delineated the transcriptomic landscape of chordoma using scRNA-seq. Their results identified six subclusters of chordoma cells, which exhibited properties of an epithelial-like extracellular matrix, and stem cells with immunosuppression. They also identified a strong immunosuppressive effect exerted by regulatory T cells (Tregs) and M2 macrophages and an enhanced TGF-β signaling pathway in tumor progression. Immune therapy is considered as a promising strategy for tumor control, and several clinical cases have been reported to respond to immune ICIs. The study of Duan et al. partially explained the rationale for immune therapy in patients with chordoma, although in-depth research is still required.

With the development of NGS techniques, the design of individualized therapy using comprehensive genomic analysis has been attempted and clinically practiced. Screening for hotspot mutations in cancer-associated genes prior to a personalized treatment approach in patients with limited therapeutic options can provide a rationale for genomics-guided therapy. Liang et al. (88) reported their experience on the combined use of WES and RNA-seq in four patients with chordoma and found that the incorporation of different sequencing techniques could help further clarify which DNA alterations are expressed or could be used as therapeutic targets. Another more detailed analysis of WES/WGS-guided therapy was reported by Stefan et al. (77). The authors observed that advanced chordomas were characterized with frequently impaired DNA repair *via* homologous recombination (HR) and with mutations of HR-related genes, including *BRCA2*, *NBN*, and *CHEK2*. Treatment with the poly(ADP-ribose) polymerase (PARP) inhibitor showed promising clinical prospects for such patients. However, one case gained olaparib resistance after a 10-month treatment, when tumor reprogression occurred due to a second mutation of the p.T910A allele and restored the activity of PARP. Gene expression-based estimates of immune cell abundance have the potential to identify patients that may respond to ICI treatment (89–91). Growing evidence has also shown responses to ICIs in

TABLE 1 Next-generation sequencing (NGS) studies on chordoma.

Reference	No. of patients	Sequencing technique	Tumor sites	Primary/ recurrent	Subtypes
Pillary et al. (59)	20 (European ancestry)	WES	NA	NA	NA
Fischer et al. (71)	9 (Caucasians)	NGS (the TruSeq Amplicon Cancer Panel)	3 skull base, 4 spine, and 2 sacrum/coccyx	Primary	Conventional (7 classic and 2 chondroid)
Wang et al. (72)	24	NGS (MSK-IMPACT)	3 spine, 18 sacrum, and 3 pelvic	21 primary and 3 recurrent	Conventional
Bell et al. (73)	14	RNA-seq analysis	Skull base	NA	13 conventional (including 3 chondroid) and 1 dedifferentiated
Sa et al. (74)	10	WES in 8 patients and RNA-seq analysis in 5 patients	Skull base	6 primary and 4 recurrent	Conventional (5 classic and 5 chondroid)
Bell et al. (75)	12	RNA-seq analysis in 12 patients	Spine	Primary	Conventional
Tarpey et al. (76)	104	WGS in 11 patients, WES in 26 patients, and NGS (targeted sequencing) in 67 patients	19 skull base, 25 spine, 50 sacrum/ coccyx, 3 extra axial, and 7 unknown	NA	89 conventional, 5 dedifferentiated, 4 poorly differentiated, and 6 unknowns
Gröschel et al. (77)	11	WES in 9 patients and WGS in 2 patients	3 skull base, 5 spine, and 3 sacurm	NA	NA
Hung et al. (12)	4	WES in 4 patients	NA	4 primary and 1 Paired metastatic	Dedifferentiated
Zhu et al. (78)	11	NGS (MSK-IMPACT)	NA	NA	NA
Bai et al. (79)	80 (Chinese patients)	WGS	Skull base	80 primary and 11 paired recurrences	78 conventional (including 14 chondroid) and 2 dedifferentiated
Mattox et al. (80)	32	WES	14 spine, 15 sacrum, 2 pelvic, and 1 chest	31 primary and 1 metastatic	NA
Yepes et al. (81)	138 (European ancestry)	WES	55.7% skull base, 23% spinal, and 20.3% sacral	NA	NA
Wen et al. (82)	3	NGS (MSK-IMPACT)	Extra-axial	Primary	1 conventional and 2 poorly differentiated
Xu et al. (83)	8 (Chinese patients)	WES	Sacrum	4 primary and 4 recurrent	NA
Duan et al. (84)	6 (Chinese patients)	scRNA-seq	3 spine, 1 sacrum, and 2 skull base	NA	NA

WES, whole-exome sequencing; NGS, next-generation sequencing; RNA-seq, RNA sequencing; WGS, whole-genome sequencing; scRNA-seq, single-cell RNA sequencing; NA, not available.

tumors deficient in SWI/SNF chromatin remodeling genes (92, 93). Therefore, poorly differentiated chordoma with a characteristic *SMARCB1* deficit is a potential candidate for ICI treatment. Williamson et al. (94) performed multi-omics sequencing including WGS, RNA-seq, and WGBS and successfully identified a recurrent pediatric poorly differentiated chordoma with features of single copy losses affecting *SMARCB1*, hypomethylation of the *TBXT* promoter, overexpression of the Brachyury tumor antigen and *CD274* (PD-L1), and $CD8^+$ T-cell, $CD79a^+$ B-cell, and plasma cell infiltration. All these features hinted of a potential effect of ICIs, which have been used in clinical practice and with proven satisfactory outcomes.

Collectively, genetic research on chordoma using multiple techniques revealed a relatively quiet cancer genome driven by a limited repertoire of cancer genes, and epigenetic regulations may play an important role in tumor initiation and progression. The combination of multi-omics analyses helps in the comprehensive understanding of the tumor landscape and facilitates the design of individualized treatment strategies.

New era: Modern personalized precision drug treatment

At present, surgery remains the mainstay of treatment for chordoma. However, complete tumor resection is not always available; therefore, there is an urgent need to develop new therapeutic options for this tumor (1, 8, 9). Conventionally, chordoma is considered resistant to chemotherapy, and only anecdotal cases have provided limited evidence for the clinical

employment of cytotoxic agents (6, 95). Recent studies have reported responses to agents such as anthracyclines, alkylating agents, cisplatin, and etoposide in the ultra-rare subtype of dedifferentiated chordoma (96–98). The combined use of cytotoxic drugs as sensitizers for radiotherapy or targeted therapy has also garnered attention (99, 100). Through sequencing efforts in chordoma, targeted therapies have shown promising prospects in tumor management. Nevertheless, unclear indications for individualized application of the limited available drugs have hindered comprehensive treatment of patients with chordoma. Drug discovery for this rare tumor has attracted significant interest from investigators with approaches such as drug repositioning, computational-assisted high-throughput drug screening, and PDO-based drug screening.

Multidimensional drug discovery strategies for chordoma

Chordoma is a type of tumor with a low-frequency mutation rate, and the number of suitable medications identified by sequencing is limited. Preclinical studies have identified several targeted medications for the systemic management of chordoma, and indicated clinical trials have provided the efficacy and safety data (101). However, no medications have been approved so far as first-line treatments for chordoma. The main obstacles for the identification of novel therapeutic avenues include the extremely low incidence of morbidity and the lack of appropriate models for preclinical research. Conventional drug discovery pipeline is long-lasting and is not cost-effective for rare diseases such as chordoma, for which new strategies are required (102).

Given the fact that chordoma has not been sufficiently covered by target-based approaches and that it is difficult for single-agent therapies to provide lasting effects, the combined use of phenotypic screening drugs may help in the development of novel therapeutic strategies. Anderson et al. examined the combination of synergistic drugs in chordoma with a machine learning method and demonstrated a synergistic effect of palbociclib and AZD2014 with afatinib for chordoma cells *in vitro* (103). Scheipl et al. (104) performed drug screening of 133 clinically approved anticancer drugs as single agents and in combination with EGFR inhibitors (EGFRis; e.g., afatinib and erlotinib) (100) and demonstrated that the combination of crizotinib, panobinostat, and doxorubicin with EGFRis showed a promising prospect of application. The histone deacetylase (HDAC) inhibitor panobinostat exerted a moderate synergistic effect when used in combination with afatinib. Although the study has not shown groundbreaking success of these treatments as monotherapeutics in solid tumors, including chordoma (104), there appears to be a role for this class in combination therapy and multi-target inhibition (104, 105).

The combined administration of different drugs has shown advantages of prolonged efficacy, avoidance or delayed occurrence of drug resistance, and synergistic effects with increased clinical outcomes. Combination screening as a translational approach will pave the way for improved personalized drug therapies for orphan diseases like chordoma.

Drug repositioning/repurposing has become an important approach to identifying new uses for already-approved regimens beyond original indications (106, 107). Previously, drug repositioning/repurposing has often been initiated by serendipitous observation of unexpected effects (108, 109). Now, however, it has gradually shifted to a rational, computer-assisted method. Computational techniques have facilitated the drug repositioning process, which is considered time-saving and cost-effective. It offers an opportunity for secondary analysis of vetted therapies with optimized pharmacokinetics and acceptable toxicity profiles for candidates with rare diseases in clinical trials (110). A deep learning strategy featured with combination and comprehensive analyses of gene expression features, signaling pathways, clinical prognoses, and pharmacochemical characteristics has promoted the implementation of precision medicine and our understanding and management of rare diseases including chordoma (102). Integrative mining approaches include ksRepo processing, Swanson's ABC approach, Chemotext, and ROBOKOP (Reasoning Over Biomedical Objects linked Knowledge-Oriented Pathways) (111–114). Traylor et al. (115) compared the differentially expressed genes (DEGs) of chordoma tissue samples with pharmacogenomic interactions in the Comparative Toxicogenomics Database using a drug repositioning platform named ksRepo. Alves et al. (102) reported a case of knowledge-based approach for drug repurposing with chordoma by building a connection between metformin and chordoma using the ROBOKOP platform. Their results suggested a potential treatment value by targeting osteoblast differentiation.

Personalized drug therapies for chordoma

As a typically fatal and extremely rare disease with complex molecular mechanisms, chordoma is suitable for personalized drug therapies. Individualized identification and testing of suitable agents can provide optimal application in indicated patients. Sequencing-based computational-assisted identification of molecular targeted therapies are generally accepted by patients and clinicians (8). Medications such as TKIs, CDK4/6 inhibitors, PARP inhibitors, and EZH2 inhibitors have been widely used for patients with corresponding molecular characteristics (116). However, the response of patients to medications as identified by sequencing may not be as expected, and considering the adverse effects of medications, personalized *in vivo* or *in vitro* screening of the indicated drugs with PDC, PDX, or PDO models is considered extremely valuable.

There are several obstacles that may hinder the process of personalized drug screening with PDC and PDX models. Firstly, the establishment and the passages of PDC or PDX models are time-consuming and have low success rates. Patients need to wait for about 1–3 months after subjecting the tumor tissue to drug screening, during which the disease may have already progressed (32, 36). Secondly, PDC models are highly dependent on sampling and often fail to recapitulate the heterogeneity of the tumor microstructures and microenvironments, resulting in changes to the drug response (117). The PDX model could provide more simultaneous features as parental tumors, but is more expensive and is not suitable for high-throughput screening (37, 39).

As aforementioned, Shihabi et al. (32) reported their experience in a proof-of-concept study of personalized drug discovery with PDO models. They successfully established a high-throughput drug screening platform of personalized organoids with the following advantages compared with the previous platforms: the PDOs could be established from biopsies or tumor resections and restored most features of primary tumors, which is superior to PDCs and similar to PDXs, but is more cost-effective; moreover, it is more time-saving, as the results can be available within a week from surgery (118, 119). Based on such a high-throughput platform, the authors also established a comprehensive analysis algorithm. A dot map was then generated and subjected to clinical consideration based on the combination analysis of BioAssay from the PubChem database and the WikiPathways database.

Shihabi's research is a typical example that illustrates the considerable value of new techniques in facilitating our understanding and management of chordoma. Successful establishment of such a screening platform profited from the advantages of the models, sequences, and bioinformatics analysis techniques, finally promoting personalized precision clinical management. Research tools and modern NGS techniques served as the two "wheels" of the "chordoma motorbike." Comprehensive use of these two "wheels" will strikingly accelerate our understanding and management of chordoma. Efforts are still needed in the future to benefit chordoma patients by building more precise disease models, determining the intrinsic mechanisms in tumor initiation and progression, and developing optimal cutting-edge technologies for clinical application.

Author contributions

CZ, JX, and CY conceived the study. CZ, TT, TW and XY reviewed the cell line and animal model part. CZ, EZ, HG, TL and JZ reviewed the sequencing study part. CZ, ZW, QJ and HW reviewed the personalized treatment part. CZ, TT, and EZ drafted the manuscript. JX and CY reviewed and modified the Manuscript. All authors contributed to the article and approved the submitted version.

Funding

National Natural Science Foundation of China (Award number(s): 81902732) to CZ; Shanghai Municipal Health and Family Planning Commission (Award number(s): 201840209) and Beijing Xisike Clinical Oncology Research Foundation (Award number(s): Y-HR2020MS-0751) to CY.

Conflict of interest

The authors declare that the research was conducted in the absence of any commercial or financial relationships that could be construed as a potential conflict of interest.

Publisher's note

References

1. Strauss SJ, Frezza AM, Abecassis N, Bajpai J, Bauer S, Biagini R, et al. Bone sarcomas: ESMO-EURACAN-GENTURIS-ERN PaedCan clinical practice guideline for diagnosis, treatment and follow-up. *Ann Oncol* (2021) 32(12):1520–36. doi: 10.1016/j.annonc.2021.08.1995

2. McMaster ML, Goldstein AM, Bromley CM, Ishibe N, Parry DM. Chordoma: incidence and survival patterns in the united states, 1973-1995. *Cancer Causes Control* (2001) 12(1):1–11. doi: 10.1023/a:1008947301735

3. Chambers KJ, Lin DT, Meier J, Remenschneider A, Herr M, Gray ST. Incidence and survival patterns of cranial chordoma in the united states. *Laryngoscope* (2014) 124(5):1097–102. doi: 10.1002/lary.24420

4. Yu E, Koffer PP, DiPetrillo TA, Kinsella TJ. Incidence, treatment, and survival patterns for sacral chordoma in the united states, 1974-2011. *Front Oncol* (2016) 6:203. doi: 10.3389/fonc.2016.00203

5. Schaefer IM, Gronchi A. WHO pathology: Highlights of the 2020 sarcoma update. *Surg Oncol Clin N Am* (2022) 31(3):321–40. doi: 10.1016/j.soc.2022.03.001

6. Wedekind MF, Widemann BC, Cote G. Chordoma: Current status, problems, and future directions. *Curr Probl Cancer* (2021) 45(4):100771. doi: 10.1016/j.currproblcancer.2021.100771

7. Meng T, Yin H, Li B, Li Z, Xu W, Zhou W, et al. Clinical features and prognostic factors of patients with chordoma in the spine: A retrospective analysis

of 153 patients in a single center. *Neuro Oncol* (2015) 17(5):725–32. doi: 10.1093/neuonc/nou331

8. Stacchiotti S, Sommer J. Chordoma global consensus G: Building a global consensus approach to chordoma: a position paper from the medical and patient community. *Lancet Oncol* (2015) 16(2):e71–83. doi: 10.1016/S1470-2045(14)71190-8

9. Stacchiotti S, Gronchi A, Fossati P, Akiyama T, Alapetite C, Baumann M, et al. Best practices for the management of local-regional recurrent chordoma: a position paper by the chordoma global consensus group. *Ann Oncol* (2017) 28(6):1230–42. doi: 10.1093/annonc/mdx054

10. Passer JZ, Alvarez-Breckenridge C, Rhines L, DeMonte F, Tatsui C, Raza SM. Surgical management of skull base and spine chordomas. *Curr Treat Options Oncol* (2021) 22(5):40. doi: 10.1007/s11864-021-00838-z

11. Yeter HG, Kosemehmetoglu K, Soylemezoglu F. Poorly differentiated chordoma: review of 53 cases. *APMIS* (2019) 127(9):607–15. doi: 10.1111/apm.12978

12. Hung YP, Diaz-Perez JA, Cote GM, Wejde J, Schwab JH, Nardi V, et al. Dedifferentiated chordoma: Clinicopathologic and molecular characteristics with integrative analysis. *Am J Surg Pathol* (2020) 44(9):1213–23. doi: 10.1097/PAS.0000000000001501

13. Nachwalter RN, Rothrock RJ, Katsoulakis E, Gounder MM, Boland PJ, Bilsky MH, et al. Treatment of dedifferentiated chordoma: a retrospective study from a large volume cancer center. *J Neurooncol* (2019) 144(2):369–76. doi: 10.1007/s11060-019-03239-3

14. Rekhi B, Michal M, Ergen FB, Roy P, Puls F, Haugland HK, et al. Poorly differentiated chordoma showing loss of SMARCB1/INI1: Clinicopathological and radiological spectrum of nine cases, including uncommon features of a relatively under-recognized entity. *Ann Diagn Pathol* (2021) 55:151809. doi: 10.1016/j.anndiagpath.2021.151809

15. Scheil S, Bruderlein S, Liehr T, Starke H, Herms J, Schulte M, et al. Genome-wide analysis of sixteen chordomas by comparative genomic hybridization and cytogenetics of the first human chordoma cell line, U-CH1. *Genes Chromosomes Cancer* (2001) 32(3):203–11. doi: 10.1002/gcc.1184

16. Hsu W, Mohyeldin A, Shah SR, ap Rhys CM, Johnson LF, Sedora-Roman NI, et al. Generation of chordoma cell line JHC7 and the identification of brachyury as a novel molecular target. *J Neurosurg* (2011) 115(4):760–9. doi: 10.3171/2011.5.JNS11185

17. Seeling C, Lechel A, Svinarenko M, Moller P, Barth TFE, Mellert K. Molecular features and vulnerabilities of recurrent chordomas. *J Exp Clin Cancer Res* (2021) 40(1):244. doi: 10.1186/s13046-021-02037-y

18. Jager D, Lechel A, Tharehalli U, Seeling C, Moller P, Barth TFE, et al. U-CH17P, -m and -s, a new cell culture system for tumor diversity and progression in chordoma. *Int J Cancer* (2018) 142(7):1369–78. doi: 10.1002/ijc.31161

19. Ricci-Vitiani L, Pierconti F, Falchetti ML, Petrucci G, Maira G, De Maria R, et al. Establishing tumor cell lines from aggressive telomerase-positive chordomas of the skull base. *Tech note J Neurosurg* (2006) 105(3):482–4. doi: 10.3171/jns.2006.105.3.482

20. Owen JH, Komarck CM, Wang AC, Abuzeid WM, Keep RF, McKean EL, et al. UM-Chor1: Establishment and characterization of the first validated clival chordoma cell line. *J Neurosurg* (2018) 128(3):701–9. doi: 10.3171/2016.10.JNS16877

21. Gellner V, Tomazic PV, Lohberger B, Meditz K, Heitzer E, Mokry M, et al. Establishment of clival chordoma cell line MUG-CC1 and lymphoblastoid cells as a model for potential new treatment strategies. *Sci Rep* (2016) 6:24195. doi: 10.1038/srep24195

22. Kino H, Akutsu H, Ishikawa H, Takano S, Takaoka S, Toyomura J, et al. Inducing substances for chondrogenic differentiation of dental pulp stem cells in the conditioned medium of a novel chordoma cell line. *Hum Cell* (2022) 35(2):745–55. doi: 10.1007/s13577-021-00662-5

23. Kim JY, Lee J, Koh JS, Park MJ, Chang UK. Establishment and characterization of a chordoma cell line from the tissue of a patient with dedifferentiated-type chordoma. *J Neurosurg Spine* (2016) 25(5):626–35. doi: 10.3171/2016.3.SPINE151077

24. Anders M, Hansen R, Ding RX, Rauen KA, Bissell MJ, Korn WM. Disruption of 3D tissue integrity facilitates adenovirus infection by deregulating the coxsackievirus and adenovirus receptor. *Proc Natl Acad Sci U.S.A.* (2003) 100(4):1943–8. doi: 10.1073/pnas.0337599100

25. Lee GY, Kenny PA, Lee EH, Bissell MJ. Three-dimensional culture models of normal and malignant breast epithelial cells. *Nat Methods* (2007) 4(4):359–65. doi: 10.1038/nmeth1015

26. Yang C, Hornicek FJ, Wood KB, Schwab JH, Choy E, Iafrate J, et al. Characterization and analysis of human chordoma cell lines. *Spine (Phila Pa 1976)* (2010) 35(13):1257–64. doi: 10.1097/BRS.0b013e3181c2a8b0

27. Locquet MA, Dechaume AL, Berchard P, Abbes L, Pissaloux D, Tirode F, et al. Aldehyde dehydrogenase, a therapeutic target in chordoma: Analysis in 3D cellular models. *Cells* (2021) 10(2):399. doi: 10.3390/cells10020399

28. Barker HE, Scott CL. Preclinical rare cancer research to inform clinical trial design. *Nat Rev Cancer* (2019) 19(9):481–2. doi: 10.1038/s41568-019-0172-2

29. de Witte CJ, Espejo Valle-Inclan J, Hami N, Lohmussaar K, Kopper O, Vreuls CPH, et al. Patient-derived ovarian cancer organoids mimic clinical response and exhibit heterogeneous inter- and intrapatient drug responses. *Cell Rep* (2020) 31(11):107762. doi: 10.1016/j.celrep.2020.107762

30. Vlachogiannis G, Hedayat S, Vatsiou A, Jamin Y, Fernandez-Mateos J, Khan K, et al. Patient-derived organoids model treatment response of metastatic gastrointestinal cancers. *Science* (2018) 359(6378):920–6. doi: 10.1126/science.aao2774

31. Scognamiglio G, De Chiara A, Parafioriti A, Armiraglio E, Fazioli F, Gallo M, et al. Patient-derived organoids as a potential model to predict response to PD-1/PD-L1 checkpoint inhibitors. *Br J Cancer* (2019) 121(11):979–82. doi: 10.1038/s41416-019-0616-1

32. Al Shihabi A, Davarifar A, Nguyen HTL, Tavanaie N, Nelson SD, Yanagawa J, et al. Personalized chordoma organoids for drug discovery studies. *Sci Adv* (2022) 8(7):eabl3674. doi: 10.1126/sciadv.abl3674

33. Siu IM, Salmasi V, Orr BA, Zhao Q, Binder ZA, Tran C, et al. Establishment and characterization of a primary human chordoma xenograft model. *J Neurosurg* (2012) 116(4):801–9. doi: 10.3171/2011.12.JNS111123

34. Diaz RJ, Luck A, Bondoc A, Golbourn B, Picard D, Remke M, et al. Characterization of a clival chordoma xenograft model reveals tumor genomic instability. *Am J Pathol* (2018) 188(12):2902–11. doi: 10.1016/j.ajpath.2018.08.004

35. Siu IM, Ruzevick J, Zhao Q, Connis N, Jiao Y, Bettegowda C, et al. Erlotinib inhibits growth of a patient-derived chordoma xenograft. *PloS One* (2013) 8(11):e78895. doi: 10.1371/journal.pone.0078895

36. Trucco MM, Awad O, Wilky BA, Goldstein SD, Huang R, Walker RL, et al. A novel chordoma xenograft allows *in vivo* drug testing and reveals the importance of NF-kappaB signaling in chordoma biology. *PloS One* (2013) 8(11):e79950. doi: 10.1371/journal.pone.0079950

37. Bozzi F, Manenti G, Conca E, Stacchiotti S, Messina A, Dagrada G, et al. Development of transplantable human chordoma xenograft for preclinical assessment of novel therapeutic strategies. *Neuro Oncol* (2014) 16(1):72–80. doi: 10.1093/neuonc/not152

38. Davies JM, Robinson AE, Cowdrey C, Mummaneni PV, Ducker GS, Shokat KM, et al. Generation of a patient-derived chordoma xenograft and characterization of the phosphoproteome in a recurrent chordoma. *J Neurosurg* (2014) 120(2):331–6. doi: 10.3171/2013.10.JNS13598

39. Salle H, Pocard M, Lehmann-Che J, Bourthoumieu S, Labrousse F, Pimpie C, et al. Development of a novel orthotopic primary human chordoma xenograft model: A relevant support for future research on chordoma. *J Neuropathol Exp Neurol* (2020) 79(3):314–24. doi: 10.1093/jnen/nlz121

40. Hayes MN, Langenau DM. Discovering novel oncogenic pathways and new therapies using zebrafish models of sarcoma. *Methods Cell Biol* (2017) 138:525–61. doi: 10.1016/bs.mcb.2016.11.011

41. Burger A, Vasilyev A, Tomar R, Selig MK, Nielsen GP, Peterson RT, et al. A zebrafish model of chordoma initiated by notochord-driven expression of HRASV12. *Dis Model Mech* (2014) 7(7):907–13. doi: 10.1242/dmm.013128

42. D'Agati G, Cabello EM, Frontzek K, Rushing EJ, Klemm R, Robinson MD, et al. Active receptor tyrosine kinases, but not brachyury, are sufficient to trigger chordoma in zebrafish. *Dis Model Mech* (2019) 12(7):dmm.039545. doi: 10.1242/dmm.039545

43. Li L, Shi H, Zhang M, Guo X, Tong F, Zhang W, et al. Upregulation of metastasis-associated PRL-3 initiates chordoma in zebrafish. *Int J Oncol* (2016) 48(4):1541–52. doi: 10.3892/ijo.2016.3363

44. Ferrari L, Pistocchi A, Libera L, Boari N, Mortini P, Bellipanni G, et al. FAS/FASL are dysregulated in chordoma and their loss-of-function impairs zebrafish notochord formation. *Oncotarget* (2014) 5(14):5712–24. doi: 10.18632/oncotarget.2145

45. Cooper TK, Murray KN, Spagnoli S, Spitsbergen JM. Primary intestinal and vertebral chordomas in laboratory zebrafish (Danio rerio). *Vet Pathol* (2015) 52(2):388–92. doi: 10.1177/0300985814537531

46. Butler MG, Dahir GA, Hedges LK, Juliao SF, Sciadini MF, Schwartz HS. Cytogenetic, telomere, and telomerase studies in five surgically managed lumbosacral chordomas. *Cancer Genet Cytogenet* (1995) 85(1):51–7. doi: 10.1016/0165-4608(95)00127-1

47. Klingler L, Shooks J, Fiedler PN, Marney A, Butler MG, Schwartz HS. Microsatellite instability in sacral chordoma. *J Surg Oncol* (2000) 73(2):100–3. doi: 10.1002/(SICI)1096-9098(200002)73:2<100::AID-JSO8>3.0.CO;2-M

48. Miozzo M, Dalpra L, Riva P, Volonta M, Macciardi F, Pericotti S, et al. A tumor suppressor locus in familial and sporadic chordoma maps to 1p36. *Int J*

Cancer (2000) 87(1):68–72. doi: 10.1002/1097-0215(20000701)87:1<68::AID-IJC10>3.0.CO;2-V

49. Kelley MJ, Korczak JF, Sheridan E, Yang X, Goldstein AM, Parry DM. Familial chordoma, a tumor of notochordal remnants, is linked to chromosome 7q33. *Am J Hum Genet* (2001) 69(2):454–60. doi: 10.1086/321982

50. Hallor KH, Staaf J, Jonsson G, Heidenblad M, Vult von Steyern F, Bauer HC, et al. Frequent deletion of the CDKN2A locus in chordoma: analysis of chromosomal imbalances using array comparative genomic hybridisation. *Br J Cancer* (2008) 98(2):434–42. doi: 10.1038/sj.bjc.6604130

51. Casali PG, Messina A, Stacchiotti S, Tamborini E, Crippa F, Gronchi A, et al. Imatinib mesylate in chordoma. *Cancer* (2004) 101(9):2086–97. doi: 10.1002/cncr.20618

52. Weinberger PM, Yu Z, Kowalski D, Joe J, Manger P, Psyrri A, et al. Differential expression of epidermal growth factor receptor, c-met, and HER2/neu in chordoma compared with 17 other malignancies. *Arch Otolaryngol Head Neck Surg* (2005) 131(8):707–11. doi: 10.1001/archotol.131.8.707

53. Tamborini E, Miselli F, Negri T, Lagonigro MS, Staurengo S, Dagrada GP, et al. Molecular and biochemical analyses of platelet-derived growth factor receptor (PDGFR) b, PDGFRA, and KIT receptors in chordomas. *Clin Cancer Res* (2006) 12 (23):6920–8. doi: 10.1158/1078-0432.CCR-06-1584

54. Fasig JH, Dupont WD, LaFleur BJ, Olson SJ, Cates JM. Immunohistochemical analysis of receptor tyrosine kinase signal transduction activity in chordoma. *Neuropathol Appl Neurobiol* (2008) 34(1):95–104. doi: 10.1111/j.1365-2990.2007.00873.x

55. Presneau N, Shalaby A, Idowu B, Gikas P, Cannon SR, Gout I, et al. Potential therapeutic targets for chordoma: PI3K/AKT/TSC1/TSC2/mTOR pathway. *Br J Cancer* (2009) 100(9):1406–14. doi: 10.1038/sj.bjc.6605019

56. Shalaby AA, Presneau N, Idowu BD, Thompson L, Briggs TR, Tirabosco R, et al. Analysis of the fibroblastic growth factor receptor-RAS/RAF/MEK/ERK-ETS2/brachyury signalling pathway in chordomas. *Mod Pathol* (2009) 22(8):996–1005. doi: 10.1038/modpathol.2009.63

57. Sommer J, Itani DM, Homlar KC, Keedy VL, Halpern JL, Holt GE, et al. Methylthioadenosine phosphorylase and activated insulin-like growth factor-1 receptor/insulin receptor: potential therapeutic targets in chordoma. *J Pathol* (2010) 220(5):608–17. doi: 10.1002/path.2679

58. Shalaby A, Presneau N, Ye H, Halai D, Berisha F, Idowu B, et al. The role of epidermal growth factor receptor in chordoma pathogenesis: A potential therapeutic target. *J Pathol* (2011) 223(3):336–46. doi: 10.1002/path.2818

59. Akhavan-Sigari R, Gaab MR, Rohde V, Brandis A, Tezval H, Abili M, et al. Expression of vascular endothelial growth factor receptor 2 (VEGFR-2), inducible nitric oxide synthase (iNOS), and ki-M1P in skull base chordoma: a series of 145 tumors. *Neurosurg Rev* (2014) 37(1):79–88. doi: 10.1007/s10143-013-0495-5

60. Henderson SR, Guiliano D, Presneau N, McLean S, Frow R, Vujovic S, et al. A molecular map of mesenchymal tumors. *Genome Biol* (2005) 6(9):R76. doi: 10.1186/gb-2005-6-9-r76

61. Pillay N, Plagnol V, Tarpey PS, Lobo SB, Presneau N, Szuhai K, et al. A common single-nucleotide variant in T is strongly associated with chordoma. *Nat Genet* (2012) 44(11):1185–7. doi: 10.1038/ng.2419

62. Kelley MJ, Shi J, Ballew B, Hyland PL, Li WQ, Rotunno M, et al. Characterization of T gene sequence variants and germline duplications in familial and sporadic chordoma. *Hum Genet* (2014) 133(10):1289–97. doi: 10.1007/s00439-014-1463-z

63. Nibu Y, Jose-Edwards DS, Di Gregorio A. From notochord formation to hereditary chordoma: the many roles of brachyury. *BioMed Res Int* (2013) 2013:826435. doi: 10.1155/2013/826435

64. Gill CM, Fowkes M, Shrivastava RK. Emerging therapeutic targets in chordomas: A review of the literature in the genomic era. *Neurosurgery* (2020) 86(2):E118–23. doi: 10.1093/neuros/nyz342

65. Chen M, Wu Y, Zhang H, Li S, Zhou J, Shen J. The roles of embryonic transcription factor BRACHYURY in tumorigenesis and progression. *Front Oncol* (2020) 10:961. doi: 10.3389/fonc.2020.00961

66. DeMaria PJ, Bilusic M, Park DM, Heery CR, Donahue RN, Madan RA, et al. Randomized, double-blind, placebo-controlled phase II study of yeast-brachyury vaccine (GI-6301) in combination with standard-of-Care radiotherapy in locally advanced, unresectable chordoma. *Oncologist* (2021) 26(5):e847–58. doi: 10.1002/onco.13720

67. Yu X, Li Z. Epigenetic deregulations in chordoma. *Cell Prolif* (2015) 48 (5):497–502. doi: 10.1111/cpr.12204

68. Tu K, Lee S, Roy S, Sawant A, Shukla H. Dysregulated epigenetics of chordoma: Prognostic markers and therapeutic targets. *Curr Cancer Drug Targets* (2022) 22(8):678–90. doi: 10.2174/1568009622666220419122716

69. Rinner B, Weinhaeusel A, Lohberger B, Froehlich EV, Pulverer W, Fischer C, et al. Chordoma characterization of significant changes of the DNA methylation pattern. *PloS One* (2013) 8(3):e56609. doi: 10.1371/journal.pone.0056609

70. Alholle A, Brini AT, Bauer J, Gharanei S, Niada S, Slater A, et al. Genome-wide DNA methylation profiling of recurrent and non-recurrent chordomas. *Epigenetics* (2015) 10(3):213–20. doi: 10.1080/15592294.2015.1006497

71. Fischer C, Scheipl S, Zopf A, Niklas N, Deutsch A, Jorgensen M, et al. Mutation analysis of nine chordoma specimens by targeted next-generation cancer panel sequencing. *J Cancer* (2015) 6(10):984–9. doi: 10.7150/jca.11371

72. Wang L, Zehir A, Nafa K, Zhou N, Berger MF, Casanova J, et al. Genomic aberrations frequently alter chromatin regulatory genes in chordoma. *Genes Chromosomes Cancer* (2016) 55(7):591–600. doi: 10.1002/gcc.22362

73. Bell D, Raza SM, Bell AH, Fuller GN, DeMonte F. Whole-transcriptome analysis of chordoma of the skull base. *Virchows Arch* (2016) 469(4):439–49. doi: 10.1007/s00428-016-1985-y

74. Sa JK, Lee IH, Hong SD, Kong DS, Nam DH. Genomic and transcriptomic characterization of skull base chordoma. *Oncotarget* (2017) 8(1):1321–8. doi: 10.18632/oncotarget.13616

75. Bell AH, DeMonte F, Raza SM, Rhines LD, Tatsui CE, Prieto VG, et al. Transcriptome comparison identifies potential biomarkers of spine and skull base chordomas. *Virchows Arch* (2018) 472(3):489–97. doi: 10.1007/s00428-017-2224-x

76. Tarpey PS, Behjati S, Young MD, Martincorena I, Alexandrov LB, Farndon SJ, et al. The driver landscape of sporadic chordoma. *Nat Commun* (2017) 8(1):890. doi: 10.1038/s41467-017-01026-0

77. Groschel S, Hubschmann D, Raimondi F, Horak P, Warsow G, Frohlich M, et al. Defective homologous recombination DNA repair as therapeutic target in advanced chordoma. *Nat Commun* (2019) 10(1):1635. doi: 10.1038/s41467-019-09633-9

78. Zhu GG, Ramirez D, Chen W, Lu C, Wang L, Frosina D, et al. Chromosome 3p loss of heterozygosity and reduced expression of H3K36me3 correlate with longer relapse-free survival in sacral conventional chordoma. *Hum Pathol* (2020) 104:73–83. doi: 10.1016/j.humpath.2020.07.002

79. Bai J, Shi J, Li C, Wang S, Zhang T, Hua X, et al. Whole genome sequencing of skull-base chordoma reveals genomic alterations associated with recurrence and chordoma-specific survival. *Nat Commun* (2021) 12(1):757. doi: 10.1038/s41467-021-21026-5

80. Mattox AK, Yang B, Douville C, Lo SF, Sciubba D, Wolinsky JP, et al. The mutational landscape of spinal chordomas and their sensitive detection using circulating tumor DNA. *Neurooncol Adv* (2021) 3(1):vdaa173. doi: 10.1093/noajnl/vdaa173

81. Yepes S, Shah NN, Bai J, Koka H, Li C, Gui S, et al. Rare germline variants in chordoma-related genes and chordoma susceptibility. *Cancers (Basel)* (2021) 13 (11):2704. doi: 10.3390/cancers13112704

82. Wen X, Cimera R, Aryeequaye R, Abhinta M, Athanasian E, Healey J, et al. Recurrent loss of chromosome 22 and SMARCB1 deletion in extra-axial chordoma: A clinicopathological and molecular analysis. *Genes Chromosomes Cancer* (2021) 60(12):796–807. doi: 10.1002/gcc.22992

83. Xu Z, Zhang L, Wen L, Chao H, Wang Q, Sun M, et al. Clinical and molecular features of sacrum chordoma in Chinese patients. *Ann Transl Med* (2022) 10(2):61. doi: 10.21037/atm-21-6617

84. Duan W, Zhang B, Li X, Chen W, Jia S, Xin Z, et al. Single-cell transcriptome profiling reveals intra-tumoral heterogeneity in human chordomas. *Cancer Immunol Immunother* (2022) 71(9):2185–95. doi: 10.21203/rs.3.rs-167938/v1

85. Buenrostro JD, Giresi PG, Zaba LC, Chang HY, Greenleaf WJ. Transposition of native chromatin for fast and sensitive epigenomic profiling of open chromatin, DNA-binding proteins and nucleosome position. *Nat Methods* (2013) 10(12):1213–8. doi: 10.1038/nmeth.2688

86. Vian L, Pekowska A, Rao SSP, Kieffer-Kwon KR, Jung S, Baranello L, et al. The energetics and physiological impact of cohesin extrusion. *Cell* (2018) 173 (5):1165–1178.e1120. doi: 10.1016/j.cell.2018.03.072

87. Meng T, Huang R, Jin J, Gao J, Liu F, Wei Z, et al. A comparative integrated multi-omics analysis identifies CA2 as a novel target for chordoma. *Neuro Oncol* (2021) 23(10):1709–22. doi: 10.1093/neuonc/noab156

88. Liang WS, Dardis C, Helland A, Sekar S, Adkins J, Cuyugan L, et al. Identification of therapeutic targets in chordoma through comprehensive genomic and transcriptomic analyses. *Cold Spring Harb Mol Case Stud* (2018) 4(6):a003418. doi: 10.1101/mcs.a003418

89. Jelinic P, Ricca J, Van Oudenhove E, Olvera N, Merghoub T, Levine DA, et al. Immune-active microenvironment in small cell carcinoma of the ovary, hypercalcemic type: Rationale for immune checkpoint blockade. *J Natl Cancer Inst* (2018) 110(7):787–90. doi: 10.1093/jnci/djx277

90. Miao D, Margolis CA, Gao W, Voss MH, Li W, Martini DJ, et al. Genomic correlates of response to immune checkpoint therapies in clear cell renal cell carcinoma. *Science* (2018) 359(6377):801–6. doi: 10.1126/science.aan5951

91. Leruste A, Tosello J, Ramos RN, Tauziede-Espariat A, Brohard S, Han ZY, et al. Clonally expanded T cells reveal immunogenicity of rhabdoid tumors. *Cancer Cell* (2019) 36(6):597–612 e598. doi: 10.1016/j.ccell.2019.10.008

92. Forrest SJ, Al-Ibraheemi A, Doan D, Ward A, Clinton CM, Putra J, et al. Genomic and immunologic characterization of INI1-deficient pediatric cancers. *Clin Cancer Res* (2020) 26(12):2882–90. doi: 10.1158/1078-0432.CCR-19-3089

93. Pender A, Titmuss E, Pleasance ED, Fan KY, Pearson H, Brown SD, et al. Genome and transcriptome biomarkers of response to immune checkpoint inhibitors in advanced solid tumors. *Clin Cancer Res* (2021) 27(1):202–12. doi: 10.1158/1078-0432.CCR-20-1163

94. Williamson LM, Rive CM, Di Francesco D, Titmuss E, Chun HE, Brown SD, et al. Clinical response to nivolumab in an INI1-deficient pediatric chordoma correlates with immunogenic recognition of brachyury. *NPJ Precis Oncol* (2021) 5 (1):103. doi: 10.1038/s41698-021-00238-4

95. Chugh R, Dunn R, Zalupski MM, Biermann JS, Sondak VK, Mace JR, et al. Phase II study of 9-nitro-camptothecin in patients with advanced chordoma or soft tissue sarcoma. *J Clin Oncol* (2005) 23(15):3597–604. doi: 10.1200/JCO.2005.02.170

96. Al-Rahawan MM, Siebert JD, Mitchell CS, Smith SD. Durable complete response to chemotherapy in an infant with a clival chordoma. *Pediatr Blood Cancer* (2012) 59(2):323–5. doi: 10.1002/pbc.23297

97. Lee MH, Kim SR, Jeong JS, Lee EJ, Lee YC. Pulmonary metastatic chordoma improved by platinum-based chemotherapy. *Lung Cancer* (2012) 76(2):255–7. doi: 10.1016/j.lungcan.2012.02.007

98. Dhall G, Traverso M, Finlay JL, Shane L, Gonzalez-Gomez I, Jubran R. The role of chemotherapy in pediatric clival chordomas. *J Neurooncol* (2011) 103 (3):657–62. doi: 10.1007/s11060-010-0441-0

99. Cao X, Lu Y, Liu Y, Zhou Y, Song H, Zhang W, et al. Combination of PARP inhibitor and temozolomide to suppress chordoma progression. *J Mol Med (Berl)* (2019) 97(8):1183–93. doi: 10.1007/s00109-019-01802-z

100. Scheipl S, Barnard M, Lohberger B, Zettl R, Brcic I, Liegl-Atzwanger B, et al. Drug combination screening as a translational approach toward an improved drug therapy for chordoma. *Cell Oncol (Dordr)* (2021) 44(6):1231–42. doi: 10.1007/s13402-021-00632-x

101. Colia V, Stacchiotti S. Medical treatment of advanced chordomas. *Eur J Cancer* (2017) 83:220–8. doi: 10.1016/j.ejca.2017.06.038

102. Alves VM, Korn D, Pervitsky V, Thieme A, Capuzzi SJ, Baker N, et al. Knowledge-based approaches to drug discovery for rare diseases. *Drug Discovery Today* (2022) 27(2):490–502. doi: 10.1016/j.drudis.2021.10.014

103. Anderson E, Havener TM, Zorn KM, Foil DH, Lane TR, Capuzzi SJ, et al. Synergistic drug combinations and machine learning for drug repurposing in chordoma. *Sci Rep* (2020) 10(1):12982. doi: 10.1038/s41598-020-70026-w

104. Shah RR. Safety and tolerability of histone deacetylase (HDAC) inhibitors in oncology. *Drug Saf* (2019) 42(2):235–45. doi: 10.1007/s40264-018-0773-9

105. Rodrigues DA, Pinheiro PSM, Fraga CAM. Multitarget inhibition of histone deacetylase (HDAC) and phosphatidylinositol-3-kinase (PI3K): Current and future prospects. *ChemMedChem* (2021) 16(3):448–57. doi: 10.1002/cmdc.202000643

106. Ekins S, Williams AJ, Krasowski MD, Freundlich JS. In silico repositioning of approved drugs for rare and neglected diseases. *Drug Discovery Today* (2011) 16 (7-8):298–310. doi: 10.1016/j.drudis.2011.02.016

107. Ashburn TT, Thor KB. Drug repositioning: identifying and developing new uses for existing drugs. *Nat Rev Drug Discovery* (2004) 3(8):673–83. doi: 10.1038/nrd1468

108. Pushpakom S, Iorio F, Eyers PA, Escott KJ, Hopper S, Wells A, et al. Drug repurposing: Progress, challenges and recommendations. *Nat Rev Drug Discovery* (2019) 18(1):41–58. doi: 10.1038/nrd.2018.168

109. Franks ME, Macpherson GR, Figg WD. Thalidomide. *Lancet* (2004) 363 (9423):1802–11. doi: 10.1016/S0140-6736(04)16308-3

110. Govindaraj RG, Naderi M, Singha M, Lemoine J, Brylinski M. Large-Scale computational drug repositioning to find treatments for rare diseases. *NPJ Syst Biol Appl* (2018) 4:13. doi: 10.1038/s41540-018-0050-7

111. Brown AS, Kong SW, Kohane IS, Patel CJ. ksRepo: a generalized platform for computational drug repositioning. *BMC Bioinf* (2016) 17:78. doi: 10.1186/s12859-016-0931-y

112. Swanson DR. Medical literature as a potential source of new knowledge. *Bull Med Libr Assoc* (1990) 78(1):29–37.

113. Capuzzi SJ, Thornton TE, Liu K, Baker N, Lam WI, O'Banion CP, et al. Chemotext: A publicly available web server for mining drug-Target-Disease relationships in PubMed. *J Chem Inf Model* (2018) 58(2):212–8. doi: 10.1021/acs.jcim.7b00589

114. Bizon C, Cox S, Balhoff J, Kebede Y, Wang P, Morton K, et al. ROBOKOP KG and KGB: Integrated knowledge graphs from federated sources. *J Chem Inf Model* (2019) 59(12):4968–73. doi: 10.1021/acs.jcim.9b00683

115. Traylor JI, Sheppard HE, Ravikumar V, Breshears J, Raza SM, Lin CY, et al. Computational drug repositioning identifies potentially active therapies for chordoma. *Neurosurgery* (2021) 88(2):428–36. doi: 10.1093/neuros/nyaa398

116. Barber SM, Sadrameli SS, Lee JJ, Fridley JS, Teh BS, Oyelese AA, et al. Chordoma-current understanding and modern treatment paradigms. *J Clin Med* (2021) 10(5):1054. doi: 10.3390/jcm10051054

117. Honkala A, Malhotra SV, Kummar S, Junttila MR. Harnessing the predictive power of preclinical models for oncology drug development. *Nat Rev Drug Discovery* (2022) 21(2):99–114. doi: 10.1038/s41573-021-00301-6

118. Phan N, Hong JJ, Tofig B, Mapua M, Elashoff D, Moatamed NA, et al. A simple high-throughput approach identifies actionable drug sensitivities in patient-derived tumor organoids. *Commun Biol* (2019) 2:78. doi: 10.1038/s42003-019-0305-x

119. Nguyen HTL, Soragni A. Patient-derived tumor organoid rings for histologic characterization and high-throughput screening. *STAR Protoc* (2020) 1 (2):100056. doi: 10.1016/j.xpro.2020.100056

frontiers | Frontiers in Oncology

TYPE Systematic Review
PUBLISHED 25 November 2022
DOI 10.3389/fonc.2022.1016857

OPEN ACCESS

EDITED BY
Cheng Yang,
Shanghai Changzheng Hospital, China

REVIEWED BY
Francesco Doglietto,
Agostino Gemelli University Polyclinic (IRCCS), Italy
Qing Liu,
Xiangya Hospital, Central South University, China

*CORRESPONDENCE
Xiaoguang Qiu
qiuxiaoguang@bjtth.org

†These authors have contributed equally to this work and share first authorship

SPECIALTY SECTION
This article was submitted to Neuro-Oncology and Neurosurgical Oncology, a section of the journal Frontiers in Oncology

RECEIVED 11 August 2022
ACCEPTED 31 October 2022
PUBLISHED 25 November 2022

CITATION
Nie M, Chen L, Zhang J and Qiu X (2022) Pure proton therapy for skull base chordomas and chondrosarcomas: A systematic review of clinical experience. *Front. Oncol.* 12:1016857. doi: 10.3389/fonc.2022.1016857

Pure proton therapy for skull base chordomas and chondrosarcomas: A systematic review of clinical experience

Menglin Nie[1†], Liying Chen[2†], Jing Zhang[1] and Xiaoguang Qiu[1*]

[1]Department of Radiation Oncology, Beijing Tiantan Hospital, Capital Medical University, Beijing, China, [2]Laboratory of Pathology, Hebei Cancer Institute, The Fourth Hospital of Hebei Medical University, Shijiazhuang, Hebei, China

Background: Skull base chordoma and chondrosarcoma are exceptionally rare bone tumors with high propensity for local recurrence. Different postoperative radiation modalities are often used to improve the clinical efficacy. Proton therapy (PT) might be among the most promising ones because of the unique ballistic characteristics of high-energy particles. However, previous meta-analysis often included studies with combined radiation techniques. No systematic review to date has directly analyzed the survival and toxicity of pure PT for these two types of malignancies.

Methods: By following the PRISMA guidelines, a systematic search of three databases was conducted. Articles were screened and data were extracted according to a prespecified scheme. R 4.2.0 software was used to conduct the meta-analysis. Normal distribution test was used for the incidence rate of each subgroup.

Results: A total of seven studies involving 478 patients were included in this analysis. The quality of included articles ranged from moderate to high quality. All patients were histopathologically diagnosed with chordoma or chondrosarcoma, and the follow-up time of the cohort ranged from 21 to 61.7 months. For PT planning, the median target volume ranged from 15 cc to 40 cc, and the administered median dose varied from 63 to 78.4 Gy_{RBE} at 1.8–2.0 Gy_{RBE} per fraction. The 1-, 2-, 3-, 5-, and 7-year local control and overall survival rates were 100%, 93%, 87%, 78%, and 68%, and 100%, 99%, 89%, 85%, and 68%, respectively. The late grade 3 or higher toxicities were reported in only two involved articles.

Conclusions: Until now, medical centers worldwide have exerted PT to improve outcomes of skull base chordomas and chondrosarcomas. PT not combined with other radiation modalities showed favorable local control and survival with a low incidence of severe radiation-induced toxicities, which manifests promising clinical benefits. However, high-quality evidence is still limited, requiring future clinical trials and prospective studies in selected patients.

KEYWORDS

proton therapy, chordoma, chondrosarcoma, skull base, efficacy, toxicity

Introduction

Chordoma and chondrosarcoma are slowly progressive, locally aggressive bone tumors with extremely low incidence (1). The common locations often include the skull base, as well as the extracranial skeleton, mostly in the sacrococcygeal area and spine. Skull base chordomas mainly arise from remnants of the notochord in the clivus of sphenoid bone, usually presenting with typical symptoms, such as headache and diplopia (2). Chordoma is mainly divided into three common categories, namely, conventional, chondroid, and dedifferentiated histopathologic subtypes (3). Chondrosarcomas are rare malignant cartilaginous neoplasms comprising 6% of all skull base primary malignant bone tumors (4, 5). Both of these rare pathological tumors require maximal debulking resection so as to achieve optimal clinical outcomes, whereas a bloc clean surgical resection is difficult to achieve because of the complex anatomy of the skull base. In addition, due to the intrinsic aggressive pathological features, tumors tend to relapse and progress frequently even after achieving optimal surgical resection (1). As a result, postoperative adjuvant therapies are crucial to achieve favorable local control and long-term survival of these patients (6, 7).

To date, radiotherapies with different modalities and radioactive particles have been developed. Radiotherapy used curatively or postoperatively seems to be an effective measure to precisely eliminate the residual or subclinical lesions, reduce local recurrence, and improve prognosis (8–10).

Conventional photon radiotherapy (CRT) has been employed since the last century and is the most accessible radiation therapy modality. Despite the fact that CRT can deliver nearly 60–70 Gy to a highly conformed tumor target, dose escalation to greater than 70 Gy might be required for chordomas and chondrosarcomas to achieve better tumor control (11, 12). However, tumors located in the skull base represent a challenge for CRT because adjacent critical neurologic structures, such as optic pathways, brainstem, and cervical spinal cord, limit the prescription dose. Charged particles such as protons were then explored to improve the biological effect of radiotherapy, as well as to protect organs at risk and minimize both early and late radiation-related toxicities (13, 14). Compared to photon therapy, the ballistic characteristics of proton beams loaded with sharp kinetic energy allow more dose escalation to the precise target while limiting the exposure dose of adjacent critical structures (15, 16).

To date, medical centers worldwide have gathered more information about the effects of PT used as either radical or adjuvant therapy in skull base chordomas and chondrosarcomas (17–19). However, access to PT is still limited and much more costly compared with conventional photon therapy; thus, the included patients in some existing systematic reviews were not purely receiving PT. In this systematic review, we analyzed the clinical outcomes and potential toxicities of skull base chordomas and chondrosarcomas after PT-only plannings without combination of any other radiation modalities. A better insight into delivering proton beams alone in skull base chordomas and chondrosarcomas should be achieved, and the accuracy together with reliability of published research should be clarified.

Abbreviations: PT, proton therapy; GTR, gross total resection; STR, subtotal resection; LC, local control; OS, overall survival; NOS, Newcastle–Ottawa Scale; GRADE, Grading of Recommendations, Assessment, Development and Evaluations; CRT, conventional photon radiotherapy; SRS/SRT, stereotactic radiosurgery/stereotactic radiotherapy; CIRT, carbon ion radiotherapy

Methods

Search strategy

The systematic search was conducted on three electronic literature databases (1997–present), namely, PubMed, the Cochrane Library, and MEDLINE, to identify articles appropriate for this study. The Medical Subject Headings (MeSH) terms and keywords used for searching were as follows: ("chordoma" [MeSH Terms] OR "chordomas" [All Fields]) AND ("skull base neoplasms" [MeSH Terms] OR "skull base" [All Fields] OR "clivus" [All Fields] OR "cranial" [All Fields] OR "intracranial" [All Fields] OR "atlas" [All Fields]) AND ("proton therapy" [MeSH Terms] OR "proton therapies" [All Fields] OR "proton beam therapy" [All Fields] OR "proton beam radiation therapy" [All Fields]) AND ("radiotherapy" [MeSH Terms] OR "radiotherapies" [All Fields] OR "radiation therapy" [All Fields] OR "radiation therapies" [All Fields]) AND ("survival" [All Fields] OR "mortality" [All Fields] OR "prognosis" [All Fields] OR "prognostic factor" [All Fields] OR "recurrence" [All Fields]).

Selection criteria

The review was conducted in compliance with the Preferred Reporting Items for Systematic reviews and Meta-Analysis (PRISMA) guidelines and recommendations [1]. Only English-language articles were included. All retrieved articles were screened by two reviewers (MN and LC). The inclusion criteria were as follows (1): primary or recurrent chordoma or chondrosarcoma located in the skull base location, (2) managed by proton-only radiotherapy after surgical resection or biopsy, and (3) the observation indicator included either survival outcomes and/or toxicity incidence. Either local control (LC) or overall survival (OS) could be considered as survival outcomes. The exclusion criteria were the combined photon–proton radiotherapy and median follow-up of less than 1 year. Rare presentations or metastases due to clival chordoma should also be excluded.

Metadata extraction

The full text of all eligible articles should be available and then a data extraction form was made. All the observation indicators, including authors and year of study, study period, location of the study conducted, trial design, cohort size, median age and follow-up, pathological diagnosis, surgical resection, median target volume, proton radiotherapy regimen, survival outcomes, and toxicity, were extracted from each included article.

Statistical techniques

R 4.2.0 software (R-4.2.0, 64 bit, The Cochrane Collaboration, Oxford, UK) was used to make a single-arm meta-analysis. Normal distribution test was performed before further analysis. All the W-values were close to 1 and p-value > 0.05. The Cochran Q test and I^2 statistics were used to assess the heterogeneity. The forest plots were used to show the results of a single study and summary analysis. The funnel plots and Egger's linear regression test were conducted to analyze the bias assessment of all studies. Sensitivity analysis was also used to analyze the publication bias.

Certainty, quality, and bias assessments

To assess the quality of included articles, the Newcastle–Ottawa Scale (NOS) (20) was used. Items for assessment included representativeness of the exposed cohort, whether it was histopathologically confirmed, whether the follow-up was long enough for outcomes to occur, whether all important data were cited in the report, and whether the outcome was correctly ascertained. The Grading of Recommendations, Assessment, Development and Evaluations (GRADE) (21) criteria were used to assess the certainty of the results based on the information of the included studies. Publication bias was assessed using funnel plots and Egger's regression. Asymmetry in plots indicated publication bias (22), and Egger's regression test provided a statistical verification of funnel plot asymmetry.

Results

Search strategy

A total of 141 candidate articles were identified from systematic searches of the literature databases, and no additional studies were identified from other sources (Figure 1). After screening by title, 4 case reports and 19 reviews were excluded, and 36 studies were inconsistent with our research content. Furthermore, by reading the abstract, 57 articles were filtered. There were then 25 articles remaining for full-text analysis, of which 8 studies were excluded because the treatment methods were mixed with combined proton–photon therapy, 8 studies were excluded because the tumor location was not limited to the skull base, 1 article was excluded because the full text could not be found, and 1 article was excluded because it failed to show enough survival data records. Finally, only seven articles were included in this meta-analysis: one came from the Radiological Research Center of Russia (23), two studies originated from different institutes in Japan (24, 25), two studies were conducted by the Paul Scherrer Institute in Switzerland (26, 27), and two studies were finished by different cancer centers in the USA (28, 29). Of note, one study was specific to chordoma (25), and one study reported only survival outcomes (27).

Demographics

This study analyzed the clinical data of 478 patients from six centers around the world. Two of the studies did not list the proportions of chordoma and chondrosarcoma separately. In the remaining five studies, there were 211 patients with chordoma and 92 patients with chondrosarcoma. Overall, the median age and follow-up time of the cohort ranged from 38 to 52 years and 21 to 61.7 months, respectively. The proportion of male and female patients in this analysis was about 47% and 53%. The characteristics of the included cohort are summarized in Table 1.

Clinical features

All patients included in the analysis were histopathologically diagnosed with chordoma or chondrosarcoma by gross total resection (GTR) or subtotal resection (STR) or biopsy, among which the proportion of recurrent disease was 6.7% to 36.8%. One of the studies did not clearly report the extent of surgical resection for each patient (24), the proportions who underwent GTR and STR procedures in the remaining six studies were approximately 13% and 83.6%, respectively, and only about 3.4% of the patients received histological biopsies. The clinical features of all included studies are summarized in Table 2.

Proton radiotherapy

For PT, the median target volume ranges from 15 to 40 cc, and the median total dose for proton radiotherapy regimen varies from 63 to 78.4 Gy_{RBE}, most of which with a single fraction dose of 1.8–2.0 Gy_{RBE} (Table 2). For one of the studies conducted in Japan, Hayashi et al. (25) evaluated the hyperfractionated high-dose proton beam therapy for patients with clival chordomas; the prescribed dose for the first 9 consecutive patients was 77.44 Gy_{RBE} in 64 fractions, and the latter 10 patients were treated with 78.4 Gy_{RBE} in 56 fractions. The dose per fraction was set at 1.2 Gy_{RBE} and 1.4 Gy_{RBE},

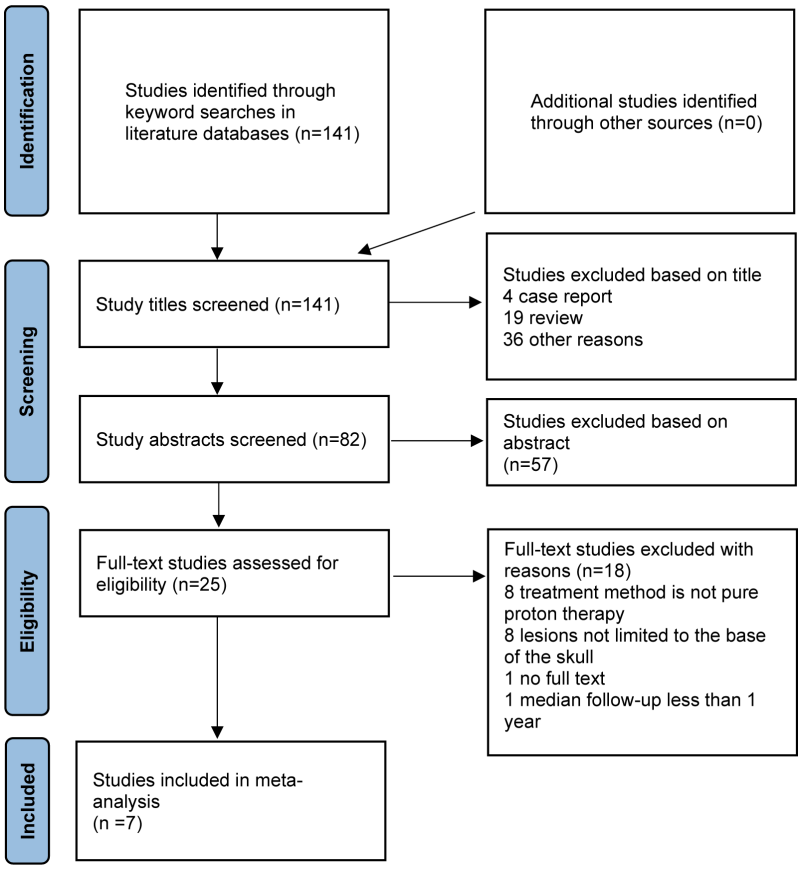

FIGURE 1
PRISMA flowchart of the literature screening process.

respectively. Survival analysis showed that the 5-year LC, cause-specific, and OS rates of the latter 10 cases were higher than all 19 cases, indicating that a hyperfractionated high-dose scheme after maximum surgical resection seems to be efficient for patients with clival chordomas. For another study conducted in Paul Scherrer Institute, Switzerland, Hottinger et al. (27) utilized a total dose of 72.6–80.0 Gy at 1.8–2.5 Gy per fraction.

Local control

Data were extracted from seven included studies for LC analysis (Figure 2 and Table 3). For the 1-year LC, six studies (23, 25–29) were analyzed, and the incidence was 100% (95% CI 98–100%, I^2 = 34%). Five studies (23–28) were included in the analysis of the 2-year and 3-year LC rates, with an incidence of 93% (95% CI 89%–97%, I^2 = 56%) and 87% (95% CI 84%–91%, I^2 = 0%), respectively. The incidence of 5-year LC was 78% (95% CI 72%–84%, I^2 = 24%), calculated from three articles (25–27). As to the 7-year LC rate, only two studies (25, 26) were analyzed, and the incidence was 68% (95% CI 43%–93%, I^2 = NA).

Overall survival

The outcomes of OS were calculated from a total of seven studies, including 1-, 2-, 3-, 5-, and 7-year incidence and 95% CI (Figure 3 and Table 3). The 1-year OS was 100% (95% CI 98%–100%, I^2 = 0%) calculated from five articles (23–25, 28, 29). For the 2-year OS, four studies were analyzed and the incidence was 99% (95% CI 94%–100%, I^2 = 64%). Analysis of 3- and 5-year OS included three studies (23–27), and the incidence was 89% (95% CI 70%–100%, I^2 = 83%) and 85% (95% CI 82%–89%, I^2 = 0%), respectively. As to the 7-year OS, only two studies (25, 26) were analyzed, and the incidence was 68% (95% CI 43%–93%, I^2 = NA).

Toxicity

For the seven studies included in the analysis, only one study did not report toxicity (27), and none of the remaining studies reported early grade 3 or higher toxicity. As to the late grade 3 or higher toxicity, two studies were involved. Weber et al. (26) showed that high-grade late toxicity was observed in 8.1% of the

10.3389/fonc.2022.1016857

TABLE 1 Study characteristics and cohort demographics of all included studies.

Study	Outcomes		Study period	Location	Design	Cohort			Median age (years)	Female (*n*)	Male (*n*)	Median follow-up (months)
	Survival	Toxicity				Size (*n*)	Chordoma (*n*)	Chondrosarcoma (*n*)				
Fuji, H. (2011)	Survival	Toxicity	June 2003–November 2008	Japan	ROCS	16	8	8	38 (9–78)	6	10	42 (9–80)
Deraniyagala, R.L. (2014)	Survival	Toxicity	2007–2011	USA	ROCS	33	NR	NR	NR	7	26	21 (3–58)
Grosshans, D.R. (2014)	Survival	Toxicity	June 2010–August 2011	USA	ROCS	15	10	5	43 (25–69)	10	5	27 (13–42)
Hayashi, Y. (2016)	Survival	Toxicity	February 2006–May 2013	Japan	ROCS	19	19	0	52 (13–76)	11	8	61.7 (31.5–115.4)
Weber, D.C. (2016)	Survival	Toxicity	1998–2012	Switzerland	ROCS	222	151	71	40.8	105	117	50 (4–176)
Hottinger, A.L. (2020)	Survival	NR	2004–2016	Switzerland	ROCS	142	NR	NR	42 (1–79)	66	76	52 (3–152)
Gordon, K. (2021)	Survival	Toxicity	2016–2020	Russia	ROCS	31	23	8	50 (27–71)	20	11	21 (4–52)

overall patients, which consisted of grade 3 unilateral optic neuropathy in 5 (25%) patients, grade 3 temporal lobe necrosis and grade 3 cerebellum brain parenchyma necrosis in 13 (56%) patients and 1 (8%) patient, respectively, grade 3 unilateral hearing loss in 3 (12%) patients, grade 4 bilateral optic neuropathy in 2 (8%) patients, and 1 (8%) patient with grade 4 spinal cord necrosis. Gordon et al. (23) reported two cases of ≥ grade 3 late toxicity, with one case of grade 3 myelitis (11 months after PT) and one case of grade 5 brainstem injury. According to the included studies, reported early or late toxicities of less than grade 3 included otitis media, temporal lobe necrosis, diplopia, unilateral hearing loss, fatigue, vomiting, headache, mild cognitive and memory impairment, keratitis, and laryngeal mucositis.

Quality assessment and publication bias

The quality of the included articles was assessed according to the NOS (Supplementary Table 1). All of the studies were considered moderate to high quality. GRADE assessment results showed that the certainty of the evidence was very low to moderate (Supplementary Table 2), mainly due to the high heterogeneity between studies and wide confidence intervals. For the data used for survival analysis, we firstly verified with several methods, including PRAW, PLN, PLOGIT, PAS, and PFT, to ensure that the data conformed to normal distribution. The funnel plots appeared symmetrical in comparison models except the 2- and 3-year OS (Supplementary Figure 1), mainly due to high heterogeneity. Sensitivity analysis was performed on the 2- and 3-year OS analysis, and the included articles were separately excluded for re-analysis. Results showed that when the article by Deraniyagala (2014) was excluded, the I^2 for the 2-year OS decreased to 0, and when the article of Gordon (2021) was excluded from the analysis, I^2 decreases to 0 for the 3-year OS.

Discussion

The main treatment of chordoma and chondrosarcoma is surgery, and the extent of surgical resection is often related to survival outcomes. However, GTR is hard to achieve. Thus, compared with surgery alone, residual tumors have been treated with adjuvant local radiation therapy. A retrospective review of 20 patients diagnosed with clival chordoma indicated that adjuvant RT after GTR may play a vital role in the elevated progression-free survival and OS (30). However, there remains heterogeneity in literature on the effects of different radiotherapy modalities adopted in skull base chordoma and chondrosarcoma. A meta-analysis indicated that adjuvant radiotherapy improved the survival of patients undergoing partial resection, and the 5-year OS of patients treated with surgery followed by adjuvant radiotherapy was 90% compared

TABLE 2 Clinical features of all included studies.

Study	Pathology	Surgical resection	Diagnostic resection (%)	Recurrent disease (%)	Median target volume (cc)	Proton radiotherapy regimen		
						Total dose (Gy_{RBE})	Fractions (*n*)	Dose/ fraction (Gy_{RBE})
Fuji, H. (2011)	Yes	NR	100%	NR	40 (7–546) (GTV)	63 (50–70)	NR	1.8
Deraniyagala, R.L. (2014)	Yes	GTR 27%; STR 67%; Biopsy only 6%	100%	9%	NR	74 (70–79)	NR	1.8–2.0
Grosshans, D.R. (2014)	Yes	GTR 20%; STR 80%	100%	6.70%	15–26.2	69.8 (68–70) chordoma; 68.4 (66–70) chondrosarcoma	NR	1.8–2.0
Hayashi, Y. (2016)	Yes	GTR 42.1%; STR 47.3%; Biopsy only 10.6%	100%	36.80%	NR	9 cases: 77.44; 10 cases: 78.4	77.44/64 bid; 78.4/56 bid	1.2–1.4
Weber, D.C. (2016)	Yes	GTR 3.2%; STR 96.8%	100%	23%	35.7 ± 29.1 (GTV)	72.5 ± 2.2	NR	1.8–2.0
Hottinger, A.L. (2020)	Yes	GTR 13%; STR 83%; Biopsy4%	100%	24%	26.3 (0.0–130.4) (GTV)	74.0 (72.6–80.0)	NR	1.8–2.5
Gordon, K. (2021)	Yes	GTR 32.2%; STR 48.4%	80.6%	12.90%	25.6 (4.2–115.6) (GTV)	70 (60–74)	NR	2

with 70% of those treated by surgery alone, but it failed to show significant statistical benefits in this subgroup (31).

To date, apart from conventional photon radiotherapy (CRT), various radiation techniques have been applied for chordoma and chondrosarcoma, such as stereotactic radiosurgery or hypofractionated stereotactic radiotherapy (SRS/SRT), proton therapy (PT), and other heavy charged particles like carbon ion radiotherapy (CIRT), aiming to improve clinical efficacy. However, a previous systematic review showed no difference in 5-year PFS and OS between the various particle types of radiotherapy (32). Thus, the role of radiation therapy for skull base chordomas should be well established.

SRS/SRT could be performed in skull base chordoma by delivering a relatively high and homogenous dose to target volume. An international multi-institutional study analyzed 93 patients who underwent single-session SRS for intracranial chordoma. The mean margin and maximum doses utilized were 17 Gy and 34.2 Gy, respectively. The 5- and 10-year OS rates could reach 83% and 70%, respectively (33). Other articles reported that a better LC can be reached by a higher prescription dose of at least more than 20 Gy (34). However, the adoption of SRS/SRT is usually limited by tumor volume, which made it more appropriate for a small tumor of less than 10 cc to remain after surgery to avoid severe toxicities.

Carbon ion radiotherapy (CIRT) is an emerging radiation modality used in skull base tumor. Lu et al. conducted a meta-analysis of nine studies including 632 patients with skull base chordoma or chondrosarcoma. This research showed favorable results concerning survival outcomes. For chordoma-only studies, the LC incidence at 1, 5, and 10 years was 99%, 80%, and 56%, respectively. As for the 1-, 5-, and 10-year OS probability, the estimated results were 100%, 94%, and 78%, respectively (35). The existing articles showed a low incidence of severe early and late toxicity (grade ≥ 3), ranging from 0 to 4%. However, this new treatment pattern can only be accessible at a limited number of centers around the world.

PT is increasingly becoming the preferred treatment modality because of its unique ballistic characteristics of high-energy particles that allow dose escalation to the tumor and delivery of substantially lower doses to critical structures compared to other radiation modalities (36). However, most systematic reviews on this respect usually included publications that incorporated patients receiving combined beam planning like proton–photon- based radiotherapy. Since the innate dose distribution characteristics were different between photons and protons, combined radiation mode may cause suboptimal dose sparing to the adjacent tissues, which would impair the intended biological effects of the dose-escalated tumor region (37, 38). At the same time, combined mode led to unfavorable protection of the organ at risk, consequently indicating that clinically relevant acute or late toxicities might increase (39). Hence, a systematic review focusing on PT not combined with other radiation modalities can represent one of just a few methods to evaluate the true clinical efficacy of PT on skull base chordoma and chondrosarcoma.

A total of seven retrospective observational cohort studies met the inclusion and exclusion criteria for this analysis and our outcomes were able to load unique metadata to indicate actual clinical efficacy of delivering PT. Herein, we present our results

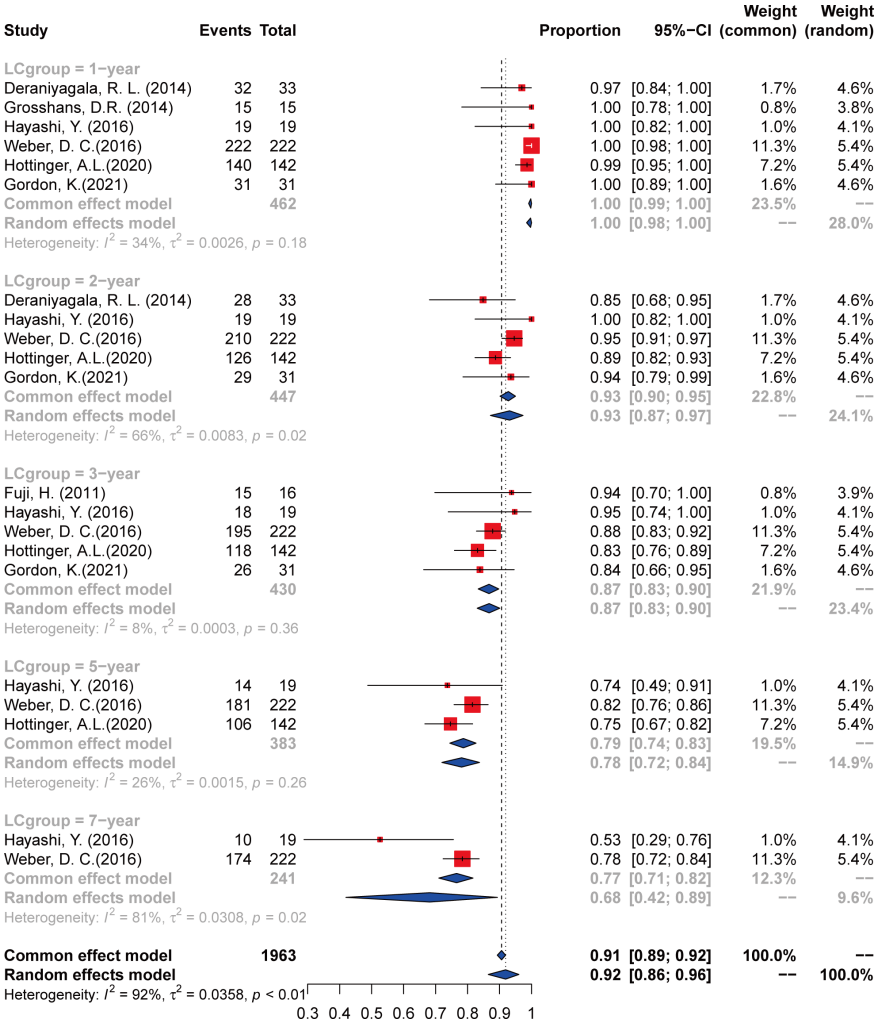

FIGURE 2
The local control of chordoma and chondrosarcoma treated with PT.

TABLE 3 Local control and overall survival incidence and error estimates as indicated by the contemporary literature, with certainty assessed for each outcome per the GRADE criteria.

All studies (n = 478 patients)	Local Control						Overall Survival					
	Number at risk (n)	Incidence (%)	95% CI	I^2 (%)	Studies (n)	Certainty	Number at risk (n)	Incidence (%)	95% CI	I^2 (%)	Studies (n)	Certainty
1 year	459	100	98–100	34	6	Moderate	114	100	98–100	0	5	Moderate
2 years	412	93	89–97	56	5	Moderate	96	99	94–100	64	4	Low
3 years	372	87	84–91	0	5	Moderate	55	89	70–100	83	3	Very low
5 years	301	78	72–84	24	3	Very low	326	85	82–89	0	3	Very low
7 years	184	68	43–93	NA	2	Very low	184	68	43–93	NA	2	Very low

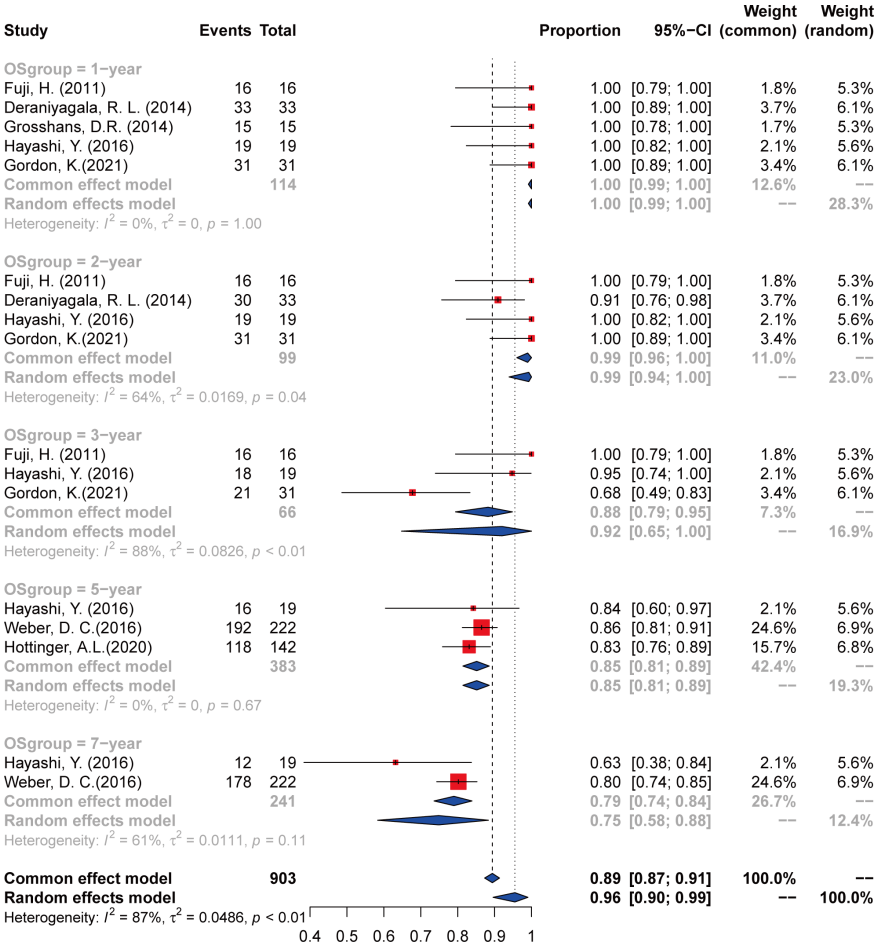

FIGURE 3
The overall survival of chordoma and chondrosarcoma treated with PT.

of a systematic review of seven articles concerning PT in a total of 478 patients. Through metadata extraction and analysis, we achieved 100% 1-year LC and OS. The 2- and 3-year LC was 93% and 87%, and 2- and 3-year OS was 99% and 89%, respectively. The symmetry of the funnel plots for 2- and 3-year OS was poor, and sensitivity analysis results indicated that the heterogeneity stemmed from the publications by Deraniyagala (2014) and Gordon et al. (2021). It was believed that the possible reasons were the small number of enrolled patients, and the relatively lower proportion of patients undergoing GTR surgery compared with other involved literatures. With respect to long-term clinical analysis, LC and OS over 5 years were the major concern. Three included articles reported 5-year LC and OS (25–27), and we determined the corresponding incidence to be 78% and 89%, respectively. Only two articles documented the 7-year OS rate (25, 26), and the calculated incidence was 68%. Because of the limited number of involved studies, further analysis between the two pathologic subgroups was not conducted. However, as a whole, our study was consistent with different institutional findings concerning PT, with 5-year OS rates ranging from 62% to 88% for chordoma and 91% to 100% for chondrosarcoma (28, 40–43). A recent meta-analysis revealed that PT was more effective following surgery for chordoma than CRT and confirmed the benefit of PT in chordoma, which showed an OS advantage for protons over conventional radiotherapy at 3 (89% *vs.* 70%), 5 (78% *vs.* 46%), and 10 years (60% *vs.* 21%) (44). A retrospective study of the NCDB also demonstrated improved 5-year OS to be associated with the PT for definitive radiotherapy (45). For long-term survival, typically after 5 years, PT seems to be more beneficial than other radiation management.

Though dose escalation for skull base chordoma and chondrosarcoma shows superiority in survival aspects, it may also be latently treacherous on some critical adjacent structures, specifically the anterior optic pathway. Visual toxicity is an irreversible severe late complication induced by a higher

maximum dose (Dmax), among which vision loss is the most detrimental outcome (46). Alexandra et al. (47) analyzed 148 patients and 283 individual eyes with functional vision at baseline receiving a minimum of 30 Gy_{RBE} to 0.1 cm^3 of the anterior optic pathway. The reported median time to vison loss was 15.2 months following high-dose proton-based radiotherapy. The 5-year incidence of functional blindness was 2.1%. It further demonstrated the acceptable long-term complication of vision loss with an incidence rate of 3.6% over 60 Gy_{RBE} and no blindness occurred under 60 Gy_{RBE}. As to our systematic review, Weber et al. (26) showed that high-grade late toxicity was observed in 8.1% of the overall patients, with grade 3 unilateral optic neuropathy occurring in 2.3% of the patients. No late grade 3 or higher toxicities were found in most of the other involved studies. Feuvret et al. (39) compared treatment planning between combined photon–proton planning and proton planning for skull base tumors, so as to assess the potential limitations of combined planning for these tumors. In this research, mean doses delivered to the GTVs and CTVs were not significantly different between the two groups. However, the dose inhomogeneity was drastically increased with the combined beam group. In the proton-only planning, it could significantly reduce the tumor dose inhomogeneity and the delivered sharp kinetic energy to adjacent normal tissues. This may give us a hint that proton-only modality is more suitable for children or patients with longer life expectations, which might achieve better protection against radiation-induced functional impairment and improve quality of life.

Our systematic review also has some limitations that need to be addressed in future studies. In the first place, since chordoma is a slowly progressive bone tumor with a relatively long natural history, the involved seven studies did not have follow-up statistics for more than 7 years, which prompted us to figure out the long-term oncologic outcomes such as recurrence pattern and radiation-induced secondary malignancies. Second, greater cohort studies or prospective studies were encouraged, which would provide us with a more reliable and comprehensive understanding of the management of PT. Last but not least, neurocognitive evaluation and other neuro-oncological relative outcomes, such as quality of life, should be included, since such information is critical to distinguish PT from other radiation modalities so that we could make the best individual recommendations to patients.

Conclusions

Our analyses have shown the satisfactory survival outcomes and acceptable toxicity of PT. PT might be a promising option to treat chordomas and chondrosarcomas especially for the skull base location. However, currently, a major concern in the use of PT is the limited literature, most of which are retrospective observational cohort studies. With this concern, multicenter randomized controlled studies and prospective clinical trials should be conducted in the future to truly validate the existing outcomes to date. Standardized procedures and observational endpoints of PT in the skull base chordomas and chondrosarcomas are encouraged so as to establish a clear guideline to select the optimal method that is most beneficial to patients.

Data availability statement

The original contributions presented in the study are included in the article/Supplementary Material. Further inquiries can be directed to the corresponding author.

Author contributions

Conception and design: XQ and MN. Search and collection of data: MN and LC. Data analysis and interpretation: MN and JZ. Manuscript writing: MN and LC. MN and LC contributed equally to this article. All authors contributed to the article and approved the submitted version.

Conflict of interest

The authors declare that the research was conducted in the absence of any commercial or financial relationships that could be construed as a potential conflict of interest.

Publisher's note

Supplementary material

The Supplementary Material for this article can be found online at: https://www.frontiersin.org/articles/10.3389/fonc.2022.1016857/full#supplementary-material

SUPPLEMENTARY FIGURE 1
The funnel plot of 2- and 3-year overall survival.

References

1. Walcott BP, Nahed BV, Mohyeldin A, Coumans JV, Kahle KT, Ferreira MJ. Chordoma: Current concepts, management, and future directions. *Lancet Oncol* (2012) 13(2):e69–76. doi: 10.1016/s1470-2045(11)70337-0

2. Aydin AL, Sasani M, Oktenoglu T, Solaroglu I, Ozer AF. A case of chordoma invading multiple neuroaxial bones: Report of ten years follow up. *Turk Neurosurg* (2013) 23(4):551–6. doi: 10.5137/1019-5149.JTN.5666-11.2

3. Choi JH, Ro JY. The 2020 who classification of tumors of bone: An updated review. *Adv anatomic Pathol* (2021) 28(3):119–38. doi: 10.1097/pap.0000000000000293

4. Sen CN, Sekhar LN, Schramm VL, Janecka IP. Chordoma and chondrosarcoma of the cranial base: An 8-year experience. *Neurosurgery* (1989) 25(6):931–40. doi: 10.1097/00006123-198912000-00013

5. Volpe NJ, Liebsch NJ, Munzenrider JE, Lessell S. Neuro-ophthalmologic findings in chordoma and chondrosarcoma of the skull base. *Am J Ophthalmol* (1993) 115(1):97–104. doi: 10.1016/s0002-9394(14)73531-7

6. Mendenhall WM, Mendenhall CM, Lewis SB, Villaret DB, Mendenhall NP. Skull base chordoma. *Head Neck* (2005) 27(2):159–65. doi: 10.1002/hed.20144

7. Yoneoka Y, Tsumanuma I, Fukuda M, Tamura T, Morii K, Tanaka R, et al. Cranial base chordoma–long term outcome and review of the literature. *Acta neurochir* (2008) 150(8):773–8; discussion 8. doi: 10.1007/s00701-008-1600-3

8. Konieczkowski DJ, DeLaney TF, Yamada YJ. Radiation strategies for spine chordoma: Proton beam, carbon ions, and stereotactic body radiation therapy. *Neurosurg Clinics North America* (2020) 31(2):263–88. doi: 10.1016/j.nec.2019.12.002

9. Hug EB, Slater JD. Proton radiation therapy for chordomas and chondrosarcomas of the skull base. *Neurosurg Clinics North America* (2000) 11 (4):627–38. doi: 10.1016/S1042-3680(18)30088-3

10. Pennicooke B, Laufer I, Sahgal A, Varga PP, Gokaslan ZL, Bilsky MH, et al. Safety and local control of radiation therapy for chordoma of the spine and sacrum: A systematic review. *Spine* (2016) 41 Suppl 20(Suppl 20):S186–s92. doi: 10.1097/brs.0000000000001831

11. Kim JW, Suh CO, Hong CK, Kim EH, Lee IJ, Cho J, et al. Maximum surgical resection and adjuvant intensity-modulated radiotherapy with simultaneous integrated boost for skull base chordoma. *Acta neurochir* (2017) 159(10):1825–34. doi: 10.1007/s00701-016-2909-y

12. Chen ATC, Hong CBC, Narazaki DK, Rubin V, Serante AR, Ribeiro Junior U, et al. High dose image-guided, intensity modulated radiation therapy (Ig-imrt) for chordomas of the sacrum, mobile spine and skull base: Preliminary outcomes. *J neuro-oncol* (2022) 158(1):23–31. doi: 10.1007/s11060-022-04003-w

13. Durante M, Loeffler JS. Charged particles in radiation oncology. *Nat Rev Clin Oncol* (2010) 7(1):37–43. doi: 10.1038/nrclinonc.2009.183

14. Loeffler JS, Durante M. Charged particle therapy–optimization, challenges and future directions. *Nat Rev Clin Oncol* (2013) 10(7):411–24. doi: 10.1038/nrclinonc.2013.79

15. Rotondo RL, Folkert W, Liebsch NJ, Chen YL, Pedlow FX, Schwab JH, et al. High-dose proton-based radiation therapy in the management of spine chordomas: Outcomes and clinicopathological prognostic factors. *J Neurosurg Spine* (2015) 23 (6):788–97. doi: 10.3171/2015.3.Spine14716

16. Aibe N, Demizu Y, Sulaiman NS, Matsuo Y, Mima M, Nagano F, et al. Outcomes of patients with primary sacral chordoma treated with definitive proton beam therapy. *Int J Radiat oncol biol Phys* (2018) 100(4):972–9. doi: 10.1016/j.ijrobp.2017.12.263

17. Parzen JS, Li X, Zheng W, Ding X, Kabolizadeh P. Proton therapy for skull-base chordomas and chondrosarcomas: Initial results from the Beaumont proton therapy center. *Cureus* (2021) 13(5):e15278. doi: 10.7759/cureus.15278

18. Indelicato DJ, Rotondo RL, Mailhot Vega RB, Holtzman AL, Looi WS, Morris CG, et al. Local control after proton therapy for pediatric chordoma. *Int J Radiat oncol biol Phys* (2021) 109(5):1406–13. doi: 10.1016/j.ijrobp.2020.11.051

19. Holtzman AL, Rotondo RL, Rutenberg MS, Indelicato DJ, De Leo A, Rao D, et al. Clinical outcomes following dose-escalated proton therapy for skull-base chordoma. *Int J particle Ther* (2021) 8(1):179–88. doi: 10.14338/ijpt-20-00066.1

20. Stang A. Critical evaluation of the Newcastle-Ottawa scale for the assessment of the quality of nonrandomized studies in meta-analyses. *Eur J Epidemiol* (2010) 25(9):603–5. doi: 10.1007/s10654-010-9491-z

21. Guyatt GH, Oxman AD, Schünemann HJ, Tugwell P, Knottnerus A. Grade guidelines: A new series of articles in the journal of clinical epidemiology. *J Clin Epidemiol* (2011) 64(4):380–2. doi: 10.1016/j.jclinepi.2010.09.011

22. Page MJ, Sterne JAC, Higgins JPT, Egger M. Investigating and dealing with publication bias and other reporting biases in meta-analyses of health research: A review. *Res synthesis Methods* (2021) 12(2):248–59. doi: 10.1002/jrsm.1468

23. Gordon K, Gulidov I, Koryakin S, Smyk D, Makeenkova T, Gogolin D, et al. Proton therapy with a fixed beamline for skull-base chordomas and chondrosarcomas: Outcomes and toxicity. *Radiat Oncol (London England)* (2021) 16(1):238. doi: 10.1186/s13014-021-01961-9

24. Fuji H, Nakasu Y, Ishida Y, Horiguchi S, Mitsuya K, Kashiwagi H, et al. Feasibility of proton beam therapy for chordoma and chondrosarcoma of the skull base. *Skull base* (2011) 21(3):201–6. doi: 10.1055/s-0031-1275636

25. Hayashi Y, Mizumoto M, Akutsu H, Takano S, Matsumura A, Okumura T, et al. Hyperfractionated high-dose proton beam radiotherapy for clival chordomas after surgical removal. *Br J Radiol* (2016) 89(1063):20151051. doi: 10.1259/bjr.20151051

26. Weber DC, Malyapa R, Albertini F, Bolsi A, Kliebsch U, Walser M, et al. Long term outcomes of patients with skull-base low-grade chondrosarcoma and chordoma patients treated with pencil beam scanning proton therapy. *Radiother Oncol* (2016) 120(1):169–74. doi: 10.1016/j.radonc.2016.05.011

27. Hottinger AL, Bojaxhiu B, Ahlhelm F, Walser M, Bachtiary B, Zepter S, et al. Prognostic impact of the "Sekhar grading system for cranial chordomas" in patients treated with pencil beam scanning proton therapy: An institutional analysis. *Radiat Oncol (London England)* (2020) 15(1):96. doi: 10.1186/s13014-020-01547-x

28. Deraniyagala RL, Yeung D, Mendenhall WM, Li Z, Morris CG, Mendenhall NP, et al. Proton therapy for skull base chordomas: An outcome study from the university of Florida proton therapy institute. *J neurol Surg Part B Skull base* (2014) 75(1):53–7. doi: 10.1055/s-0033-1354579

29. Grosshans DR, Zhu XR, Melancon A, Allen PK, Poenisch F, Palmer M, et al. Spot scanning proton therapy for malignancies of the base of skull: Treatment planning, acute toxicities, and preliminary clinical outcomes. *Int J Radiat oncol biol Phys* (2014) 90(3):540–6. doi: 10.1016/j.ijrobp.2014.07.005

30. Sanusi O, Arnaout O, Rahme RJ, Horbinski C, Chandler JP. Surgical resection and adjuvant radiation therapy in the treatment of skull base chordomas. *World Neurosurg* (2018) 115:e13–21. doi: 10.1016/j.wneu.2018.02.127

31. Amit M, Na'ara S, Binenbaum Y, Billan S, Sviri G, Cohen JT, et al. Treatment and outcome of patients with skull base chordoma: A meta-analysis. *J neurol Surg Part B Skull base* (2014) 75(6):383–90. doi: 10.1055/s-0034-1376197

32. Di Maio S, Temkin N, Ramanathan D, Sekhar LN. Current comprehensive management of cranial base chordomas: 10-year meta-analysis of observational studies. *J Neurosurg* (2011) 115(6):1094–105. doi: 10.3171/2011.7.Jns11355

33. Pikis S, Mantziaris G, Peker S, Samanci Y, Nabeel AM, Reda WA, et al. Stereotactic radiosurgery for intracranial chordomas: An international multiinstitutional study. *J Neurosurg* (2022), 1:1–8. doi: 10.3171/2021.12.JNS212416

34. Shinya Y, Hasegawa H, Shin M, Kawashima M, Koga T, Hanakita S, et al. High dose radiosurgery targeting the primary tumor sites contributes to survival in patients with skull base chordoma. *Int J Radiat oncol biol Phys* (2022) 113(3):582–7. doi: 10.1016/j.ijrobp.2022.02.024

35. Lu VM, O'Connor KP, Mahajan A, Carlson ML, Van Gompel JJ. Carbon ion radiotherapy for skull base chordomas and chondrosarcomas: A systematic review and meta-analysis of local control, survival, and toxicity outcomes. *J Neurooncol* (2020) 147(3):503–13. doi: 10.1007/s11060-020-03464-1

36. Brada M, Pijls-Johannesma M, De Ruysscher D. Current clinical evidence for proton therapy. *Cancer J (Sudbury Mass)* (2009) 15(4):319–24. doi: 10.1097/PPO.0b013e3181b6127c

37. Weber DC, Trofimov AV, Delaney TF, Bortfeld T. A treatment planning comparison of intensity modulated photon and proton therapy for paraspinal sarcomas. *Int J Radiat oncol biol Phys* (2004) 58(5):1596–606. doi: 10.1016/j.ijrobp.2003.11.028

38. Miralbell R, Lomax A, Bortfeld T, Rouzaud M, Carrie C. Potential role of proton therapy in the treatment of pediatric Medulloblastoma/Primitive neuroectodermal tumors: Reduction of the supratentorial target volume. *Int J Radiat oncol biol Phys* (1997) 38(3):477–84. doi: 10.1016/s0360-3016(97)00004-7

39. Feuvret L, Noel G, Weber DC, Pommier P, Ferrand R, De Marzi L, et al. A treatment planning comparison of combined photon-proton beams versus proton beams-only for the treatment of skull base tumors. *Int J Radiat oncol biol Phys* (2007) 69(3):944–54. doi: 10.1016/j.ijrobp.2007.07.2326

40. Fung V, Calugaru V, Bolle S, Mammar H, Alapetite C, Maingon P, et al. Proton beam therapy for skull base chordomas in 106 patients: A dose adaptive radiation protocol. *Radiother Oncol* (2018) 128(2):198–202. doi: 10.1016/j.radonc.2017.12.017

41. Hug EB, Loredo LN, Slater JD, DeVries A, Grove RI, Schaefer RA, et al. Proton radiation therapy for chordomas and chondrosarcomas of the skull base. *J Neurosurg* (1999) 91(3):432–9. doi: 10.3171/jns.1999.91.3.0432

42. Ares C, Hug EB, Lomax AJ, Bolsi A, Timmermann B, Rutz HP, et al. Effectiveness and safety of spot scanning proton radiation therapy for chordomas and chondrosarcomas of the skull base: First long-term report. *Int J Radiat oncol biol Phys* (2009) 75(4):1111–8. doi: 10.1016/j.ijrobp.2008.12.055

43. Feuvret L, Bracci S, Calugaru V, Bolle S, Mammar H, De Marzi L, et al. Efficacy and safety of adjuvant proton therapy combined with surgery for chondrosarcoma of the skull base: A retrospective, population-based study. *Int J Radiat oncol biol Phys* (2016) 95(1):312–21. doi: 10.1016/j.ijrobp.2015.12.016

44. Zhou J, Yang B, Wang X, Jing Z. Comparison of the effectiveness of radiotherapy with photons and particles for chordoma after surgery: A meta-analysis. *World Neurosurg* (2018) 117:46–53. doi: 10.1016/j.wneu.2018.05.209

45. Palm RF, Oliver DE, Yang GQ, Abuodeh Y, Naghavi AO, Johnstone PAS. The role of dose escalation and proton therapy in perioperative or definitive treatment of chondrosarcoma and chordoma: An analysis of the national cancer data base. *Cancer* (2019) 125(4):642–51. doi: 10.1002/cncr.31958

46. Mayo C, Martel MK, Marks LB, Flickinger J, Nam J, Kirkpatrick J. Radiation dose-volume effects of optic nerves and chiasm. *Int J Radiat oncol biol Phys* (2010) 76(3 Suppl):S28–35. doi: 10.1016/j.ijrobp.2009.07.1753

47. De Leo AN, Holtzman AL, Ho MW, Morris CG, Rutenberg MS, Rotondo RL, et al. Vision loss following high-dose proton-based radiotherapy for skull-base chordoma and chondrosarcoma. *Radiother Oncol* (2021) 158:125–30. doi: 10.1016/j.radonc.2021.02.012

frontiers | Frontiers in Oncology

TYPE Original Research
PUBLISHED 25 November 2022
DOI 10.3389/fonc.2022.960720

OPEN ACCESS

EDITED BY
Domenico Solari,
Federico II University Hospital, Italy

REVIEWED BY
Shaan M. Raza,
University of Texas MD Anderson Cancer Center, United States
Daniel Freed,
Chordoma Foundation, United States

*CORRESPONDENCE
Thibault Passeri
thibault.passeri@neurochirurgie.fr

SPECIALTY SECTION
This article was submitted to Neuro-Oncology and Neurosurgical Oncology, a section of the journal Frontiers in Oncology

RECEIVED 03 June 2022
ACCEPTED 18 October 2022
PUBLISHED 25 November 2022

CITATION
Passeri T, Dahmani A, Masliah-Planchon J, El Botty R, Courtois L, Vacher S, Marangoni E, Nemati F, Roman-Roman S, Adle-Biassette H, Mammar H, Froelich S, Bièche I and Decaudin D (2022) *In vivo* efficacy assessment of the CDK4/6 inhibitor palbociclib and the PLK1 inhibitor volasertib in human chordoma xenografts. *Front. Oncol.* 12:960720. doi: 10.3389/fonc.2022.960720

In vivo efficacy assessment of the CDK4/6 inhibitor palbociclib and the PLK1 inhibitor volasertib in human chordoma xenografts

Thibault Passeri[1,2,3]*, Ahmed Dahmani[1], Julien Masliah-Planchon[2], Rania El Botty[1], Laura Courtois[2], Sophie Vacher[2], Elisabetta Marangoni[1], Fariba Nemati[1], Sergio Roman-Roman[4], Homa Adle-Biassette[5], Hamid Mammar[6], Sébastien Froelich[3], Ivan Bièche[2] and Didier Decaudin[1,7]

[1]Laboratory of Preclinical Investigation, Translational Research Department, Institut Curie, University of Paris Saclay, Paris, France, [2]Department of Genetics, Institut Curie, University of Paris Saclay, Paris, France, [3]Department of Neurosurgery, Lariboisière Hospital, Assistance Publique des Hôpitaux de Paris, University of Paris, Paris, France, [4]Department of Translational Research, Institut Curie, University of Paris Saclay, Paris, France, [5]Department of Pathology, Lariboisière Hospital, Assistance Publique des Hôpitaux de Paris, University of Paris, Paris, France, [6]Department of Radiotherapy - Proton Therapy Center, Institut Curie, Paris-Saclay University, Orsay, France, [7]Department of Medical Oncology, Institut Curie, Paris, France

Background: Management of advanced chordomas remains delicate considering their insensitivity to chemotherapy. Homozygous deletion of the regulatory gene *CDKN2A* has been described as the most frequent genetic alteration in chordomas and may be considered as a potential theranostic marker. Here, we evaluated the tumor efficacy of the CDK4/6 inhibitor palbociclib, as well as the PLK1 inhibitor volasertib, in three chordoma patient-derived xenograft (PDX) models to validate and identify novel therapeutic approaches.

Methods: From our chordoma xenograft panel, we selected three models, two of them harboring a homozygous deletion of *CDKN2A/2B* genes, and the last one a *PBRM1* pathogenic variant (as control). For each model, we tested the palbociclib and volasertib drugs with pharmacodynamic studies together with RT-PCR and RNAseq analyses.

Results: For palbociclib, we observed a significant tumor response for one of two models harboring the deletion of *CDKN2A/2B* ($p = 0.02$), and no significant tumor response in the *PBRM1*-mutated PDX; for volasertib, we did not observe any response in the three tested models. RT-PCR and RNAseq analyses showed a correlation between cell cycle markers and responses to palbociclib; finally, RNAseq analyses showed a natural enrichment of the oxidative phosphorylation genes (OxPhos) in the palbociclib-resistant PDX ($p = 0.02$).

Conclusion: CDK4/6 inhibition appears as a promising strategy to manage advanced chordomas harboring a loss of *CDKN2A/2B*. However, further preclinical studies are strongly requested to confirm it and to understand acquired or *de novo* resistance to palbociclib, in the peculiar view of a targeting of the oxidative phosphorylation genes.

KEYWORDS

CDKN2A/2B deletion, chordoma patient's derived xenograft, CDK4/6 inhibitor, palbocicib, PLK1 inhibitor, volasertib

Introduction

Chordomas are rare bone tumors of the skull-base and spine which originate from remnants of the notochord, explaining their common location along the neuraxis. They are characterized by a locally invasive extension despite slow growth. Considering their chemoradioresistance, a radical resection associated with a high-dose radiation is the gold-standard therapeutic strategy (1). However, despite this aggressive treatment, the disease-free survival is generally short (2, 3) due to the fact that locoregional recurrence is a common event following the initial treatment (4). The management of these tumor relapses or progression after surgery and proton beam therapy is a clinical challenge, especially for patients with metastases and inoperable recurrence disease. Difficulties in managing advanced chordomas explain the poor long-term prognosis of this cancer with an overall survival evaluated at ~30% at 10 years (3). There is, therefore, an unmet need for systemic therapies, which are especially difficult to raise given the lack of data (5–15) concerning the tumor biology (genetic driver events), and that chordomas have a relatively low mutation burden with few therapeutically actionable alterations (5, 6). Over the years, a wider use of new targeted therapies, such as tyrosine kinase inhibitors (TKI), has been developed. Unfortunately, the proportion of objective responses to all these agents was very low in chordomas (16–24). The limited number of patients included in these studies, as well as the lack of follow-up, interfere with the preliminary proof of effectiveness of these drugs, that encourages the development of several pre-clinical models (25–34).

Recently, we established and well-characterized a large panel of 12 chordoma patient-derived xenografts (PDXs) (35), including all relevant clinical features, their immunohistochemical and genomic profiles, serving as a support for preclinical drug testing. In this way, the Next Sequencing Generation (NGS) genomic characterization of our models showed a preponderance (58%) of homozygous deletions of *CDKN2A/2B* and mutations affecting the mammalian SWItch/Sucrose Non-Fermentable (SWI/SNF) chromatin remodeling complexes (such as *PBRM1*, *SMARCB1*, *ARID1A* pathogenic mutations), as described in a majority of chordomas (5, 6, 14). Mutations in the SWI/SNF complexes were also mutually exclusive with homozygous deletions of *CDKN2A/2B* in our panel. Genes encoding subunits of SWI/SNF complexes are collectively altered in over 20% of human malignancies (36) and became an interesting target for new therapies as enhancer of zeste homolog 2 (EZH2) inhibitors (35, 37, 38).

Cyclin-dependent kinase (CDK) inhibitor 2A (*CDKN2A*) is a tumor suppressor gene encoding the $p16^{ink4a}$ protein which plays an important role in cell-cycle regulation through the inhibition of cyclin-dependent kinases (CDK) 4/6 that protects the p53 protein from degradation (39). *CDKN2A* loss or mutation is found in a wide range of malignancies and may lead to an increased CDK activity, bypassing a critical senescent signal (40). In chordomas, the regulatory gene *CDKN2A* is also frequently lost (5, 6), and thus, CDK4/6 may be in an over-activated state (41), although multiple upstream seem to be the input in the dysregulation of CDK4/6 activity (42). Palbociclib (PD 0332991), a selective inhibitor of CDK4/6, approved for the treatment of hormone-receptor positive breast cancer (43), has been recently tested in *in vitro* cell-line chordoma models harboring the loss of *CDKN2A* (41), suggesting a potential *in vivo* action of anti-CDK4/6 in chordomas harboring this genomic alteration.

The Polo-like kinase (PLK) family, particularly PLK1, has recently become an attractive oncogenic target considering its regular roles in the G2/M cell cycle checkpoint, *via* its effects on chromosome segregation, spindle assembly, and cytokinesis (44). Volasertib (BI 2536), a selective PLK1-inhibitor, showed a promising antitumor activity in other cancer preclinical models (45–47). Considering that several genomic analyses of chordoma samples reveal widespread cell cycle dysregulation (48), testing the inhibition of PLK1 in chordomas makes sense.

In this study, we therefore focused our pharmacological expertise on the CDK4/6 inhibitor palbociclib and the PLK1-inhibitor volasertib in two xenograft models harboring homozygous deletions of *CDKN2A/2B*, and in a third *PBRM1*-mutated model (control), in order to evaluate the *CDKN2A/2B* loss as a theranostic biomarker in chordomas.

Materials and methods

Chordoma patient-derived xenografts

Three previously established and characterized chordoma PDXs were used for *in vivo* experiments: cluster of differentiation (CD) 3, CD7, and CD39 (35). The main clinical, histological, and genomic features of our xenografts panel have been previously described (35). PDX models of chordomas were obtained by engrafting a primary tumor sample into *nude* mice (Charles River Laboratories). All *in vivo* experimental procedures, animal care, and housing were performed in accordance with the recommendations of the European Community (2010/63/UE) for the care and use of laboratory animals. Experimental procedures were specifically approved by the ethics committee of the Institut Curie CEEA-IC #118 (Authorization APAFiS# 25870-2020060410487032-v1 given by National Authority) in compliance with the international guidelines.

Next-generation sequencing

DNA was extracted from frozen tumor samples using a standard phenol/chloroform procedure. RNA was extracted from microdissected areas using the RNeasy Mini Kit (Qiagen, Valencia, CA, USA).

DNA from xenografts and a part of patients' tumors were then analyzed for gene mutations by targeted next-generation sequencing (NGS). The in-house NGS panel includes 571 genes of interest in oncology for diagnosis, prognosis, and theranostics including chordoma genes of interest such as *PIK3CA*, *PTEN*, *CDKN2A/2B*, *PBRM1*, *SETD2*, and *ARID1A*. The library preparation was performed using the Agilent Sureselect XT HS kit, and sequencing was completed on an Illumina NovaSeq 6000 sequencer. All variants, called using Varscan2 (v2.4.3-0), that passed the following thresholds were validated: allelic ratio above 5% and population frequency lower than 0.1% in 1000 g, ESP, or gnomAD. This large targeted NGS panel also allowed molecular analysis of tumors for CNV (copy number variation) status including *CDKN2A* homozygous deletion detection. In case of doubt concerning the originating link between the patient's tumors and PDXs, an identity monitoring was performed based on polymorphisms.

Antitumor efficacy of targeted therapy drugs

Considering the results of the molecular analysis of our chordoma xenograft panel, two drugs on three PDXs (CD3, CD7, and CD39) were considered in our pharmacological program, i.e. the CDK4/6 inhibitor palbociclib (Ibrance®, Pfizer) and the PLK1 inhibitor volasertib (Boehringer Ingelheim). This last targeted treatment was tested in the field of our huge expertise developed in various types of human cancers, such as non-small cell lung cancers (46) and breast cancers (47). Palbociclib was administered orally at a dose of 75 mg/kg/day (tween 80 0.5% + methylcellulose 0.5% + water 99%), once daily, 5 days per week; volasertib was administered orally at the dose of 10 mg/kg/day (methylcellulose 0.5% + tween 80 0.5% + DMSO 2% + water 97%), once daily, 4 days per week. The treatment was administered from day 1 to mouse sacrifice. Drugs were sourced from the oncological department of Institut Curie, Paris, France.

For *in vivo* therapeutic studies, a 15 mm^3 tumor fragment was grafted into 30 female immunodeficiency *nude* mice. Mice bearing growing tumors with a volume of 60–150 mm^3 were randomly assigned to control or treatment groups. Animals with tumor volumes outside this range were excluded. Mice were weighted and tumors were measured once a week. Considering the slow growth of these tumors, xenografted mice were sacrificed when tumor volume reached a mean volume of 500 mm^3.

Tumor volumes were calculated using two perpendicular diameters with calipers as follows: $V\ (volume) = (a \times b)^2/2$ where a and b are the largest and smallest perpendicular tumor diameters (in mm). Relative tumor volumes (RTV) were calculated from the following formula: $RTV = (V_x/V1)$, where V_x is the tumor volume on day x and V1 is the tumor volume at initiation of therapy (day 1). Antitumor activity was evaluated according to tumor growth inhibition (TGI), calculated according to the following formula: percent GI = 100 − (RTVt/RTVc ×100), where RTVt is the median RTV of treated mice and RTVc is the median RTV of controls, both at a given time point when the antitumor effect was optimal. A meaningful biological effect was defined as a TGI of at least 50% (49). The statistical significance of differences observed between the individual RTVs corresponding to the treated mice and control groups was calculated using the two-tailed Mann–Whitney U test.

Moreover, to evaluate the response to treatments observed in the three models according to individual mouse variability, we decided to consider each mouse as one tumor-bearing entity. Hence, in all *in vivo* experiments, a relative tumor variation (RTVV)) was calculated for each treated mouse as follows: [(RTVt/mRTVc)], where RTVt is the relative tumor volume of the treated mouse and mRTVc is the median relative tumor volume of the corresponding control group at the end of treatment. We then calculated an overall response rate (ORR) for each treated mouse as follows: ORR = [(RTVV) - 1]. A tumor was considered to be responding to treatment, if the ORR was below -0.5. The statistical significance of the ORR between tested treatments was determined using Fisher's Exact test. Finally, we evaluated the impact of treatments on tumor progression, by evaluating all progression-free survival probabilities taking

tumor doubling time (RTV × 2) and time for RTV × 4 into account. A log-rank (Mantel–Cox) test was used to perform treatment comparisons.

Pharmacodynamics study by RT-PCR analysis and RNAseq after *in vivo* pharmacological experiments

A RT-PCR study was performed after the administration of palbociclib and volasertib drugs on the two models CD3 and CD7. The RT-PCR technique has been previously described by our group (50). Results, expressed as N-fold differences in target gene expressions relative to the murine and human *TBP* genes (both the murine and the human TBP transcripts), and termed N_{target}, were determined as $N_{target} = 2^{\Delta Ctsample}$, where the ΔCt value of the sample was determined by subtracting the Ct value of the specific target gene from the Ct value of the TBP. The N_{target} values of the samples were subsequently normalized so that the value for "basal mRNA level" (smallest amount of quantifiable target gene mRNA, Ct = 35) was 1 for selected genes. The expression of the following cancer genes potentially implied in palbociclib resistance (51, 52) was studied: *CCNE1*, *CDK4*, *PTEN*, *RB1*, and *E2F1*. The *PLK1* gene was also studied, as the target of PLK1 inhibitors. Finally, we studied some genes implied in the proliferation, or overexpressed in chordomas: MKI67, *MYC*, *TBXT* and *EGFR (*53). The nucleotide sequences of the gene primers used are available on request.

For RNAseq analyses, RNA was extracted from microdissected areas using the RNeasy Mini Kit (Qiagen, Valencia, CA, USA). Library preparation was performed using the QuantSeq 3′ mRNA-Seq reverse (REV) Library Prep Kit (Lexogen, Vienna, Austria) using 150 ng of total RNA, and according to the manufacturer's instruction. The pool was sequenced on a NovaSeq 6000 SP 2x75bp flow cell (Illumina Inc., San Diego, CA, USA). RNA sequencing data were analyzed using the BlueBee Genomics Platform (Lexogen, Vienna, Austria). Gene Ontology Enrichment Analysis was performed using the ShinyGO (http://bioinformatics.sdstate.edu/go/) and gProfiler (https://biit.cs.ut.ee/gprofiler/gost) Web sites.

Statistical analyses

Statistical analyses were performed using the Prism v9.0 software (GraphPad Software, Inc., La Jolla, CA, USA). Statistical characteristics were used to describe all variables. Numerical variables were expressed as the median or mean and standard deviation, as appropriate. Categorical variables were expressed as the count and percentage. Variables were tested by the Mann-Whitney *U* test, Fisher's Exact test, or chi-squared test, as appropriate. Survival distributions were determined using the Kaplan–Meier method and the log-rank (Mantel–Cox) test was used to compare groups. Every statistical test used in this manuscript was two-tailed, and p-values less than 0.05 were considered as significant.

Results

Patient-derived xenograft selection

The histological and genomic features of the three PDXs are described in Table 1. CD3 was obtained from a patient's sacral primary tumor previously operated on and displaying a homozygous deletion of *CDKN2A/2B;* CD7 was obtained from a skull base primary tumor previously operated on and irradiated and displaying a homozygous deletion of *CDKN2A/2B;* CD39 was obtained from a skull base primary tumor previously operated on and presenting a pathogenic *PBRM1* variant (c.599C>G), without *CDKN2A/2B* deletion (Figure 1). The CD39 model which does not harbor any loss-of-function genomic alteration of *CDKN2A* or *CDKN2B* but a *PBRM1*-variant was chosen as a negative control in order to reinforce the fact that *CDKN2A/2B* might be a biomarker of response to palbociclib. None of these models harbored another CNV or pathogenic variant of theranostic interest.

In vivo antitumor efficacy of targeted therapies

In vivo therapeutic experiments with palbociclib and volasertib were done on these three xenografts. For each model, PDX tumor-bearing mice were randomized into treatment and control groups (n = 4–7 mice per group). For the palbociclib drug, TGI was calculated at 80, 49, and 85 days, for CD3, CD7, and CD39, respectively. For the volasertib drug, TGI was calculated at 77, 28, and 51 days, for CD3, CD7, and CD39, respectively.

In vivo responses to palbociclib and volasertib are shown in the Figure 2. For the CD3 xenograft, palbociclib induced a significant TGI (p = 0.02) with an optimal TGI of 60%, whereas

TABLE 1 Histopathological and molecular features of the three selected PDX models.

Models	Histology type*	Molecular alteration	Targeted-therapy
CD3	Conventional	*CDKN2A/2B* loss	Palbociclib Volasertib
CD7	Conventional	*CDKN2A/2B* loss	Palbociclib Volasertib
CD39	Conventional	*PBRM1* variant (c.599C>G; p.(Ser200Ter))	Palbociclib Volasertib

*According to the WHO (World Health Organization) 2020.
CD, cluster of differentiation.

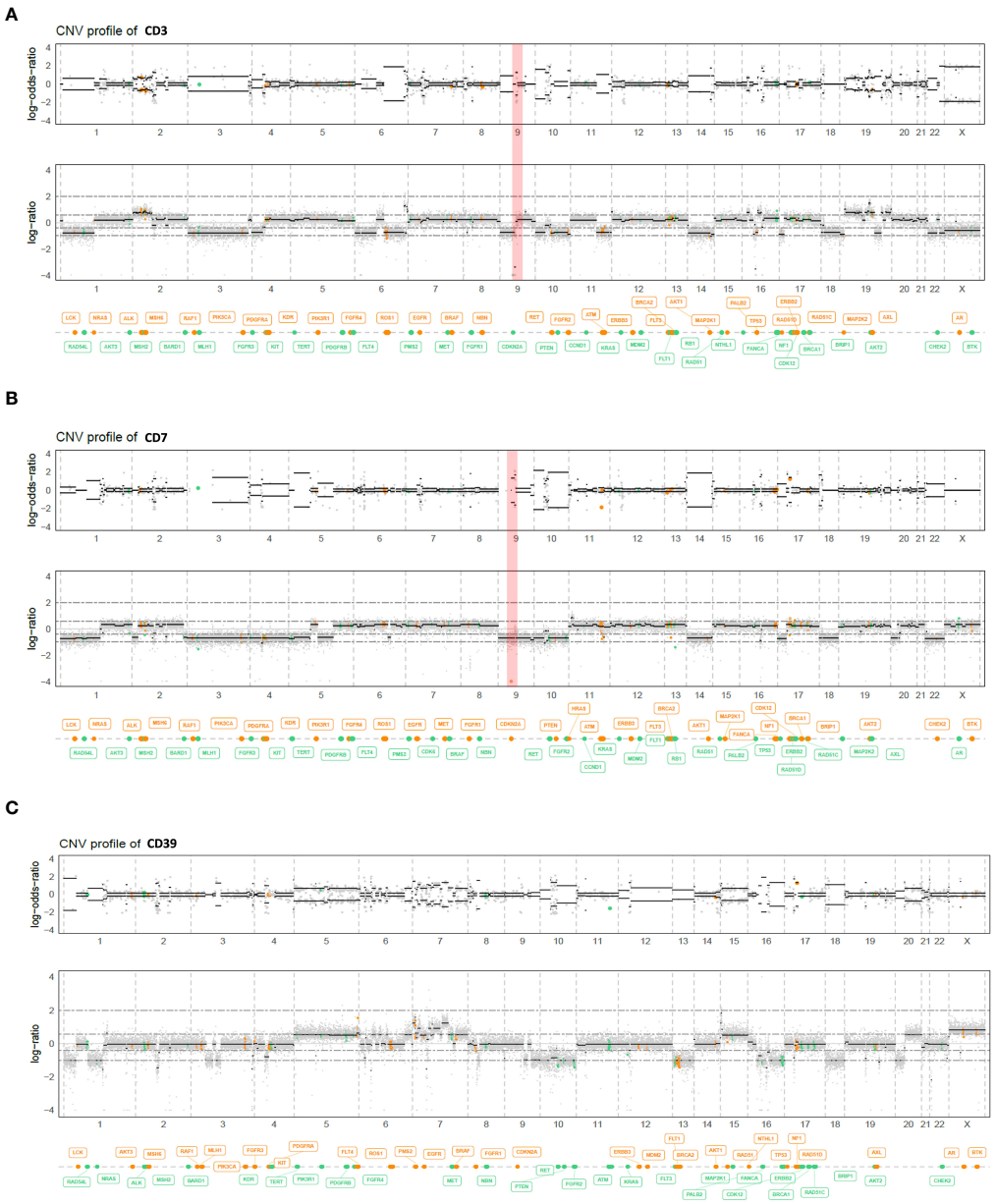

FIGURE 1
Genome view profiles of the allele-specific copy number of the CD3 **(A)**, CD7 **(B)**, and CD39 **(C)** chordoma PDX models. The top graph log-odds-ratio represents the B-Allele Frequency (BAF), and the bottom graph the log depth ratio between tumor and a healthy witness. Both CD3 and CD7 chordoma PDX models harbored a homozygous deletion of *CDKN2A/2B* (red bar), whereas CD39 did not.

volasertib showed a slight tumor growth response close to statistical significance (p = 0.065) (Figure 2A). The probability of progression-free survival at RTV × 4 was significantly longer in the palbociclib and volasertib treatments groups than in the control (p = 0.03 and p = 0.02, respectively), but not at RTV× 2 (p = 0.09 and p = 0.052, respectively) (Figure 2B).

For the CD7 xenograft, we did not observe any tumor growth response to both palbociclib and volasertib (p = 0.85 and p > 0.99, respectively), as well as for the CD39 xenograft without *CDKN2A/2B* deletion (p = 0.40 and 0.058, respectively).

Hence, when we looked at the individual tumor responses in the three treated models (Figure 3A), the ORRs lower than -0.5 were 33.3% and 18.8% after palbociclib and volasertib, respectively (p = 0.25). Finally, the study of the progression-free survival across the three PDX models at RTV × 2 and RTV × 4 did not show any significant effect for palbociclib (p = 0.39 and

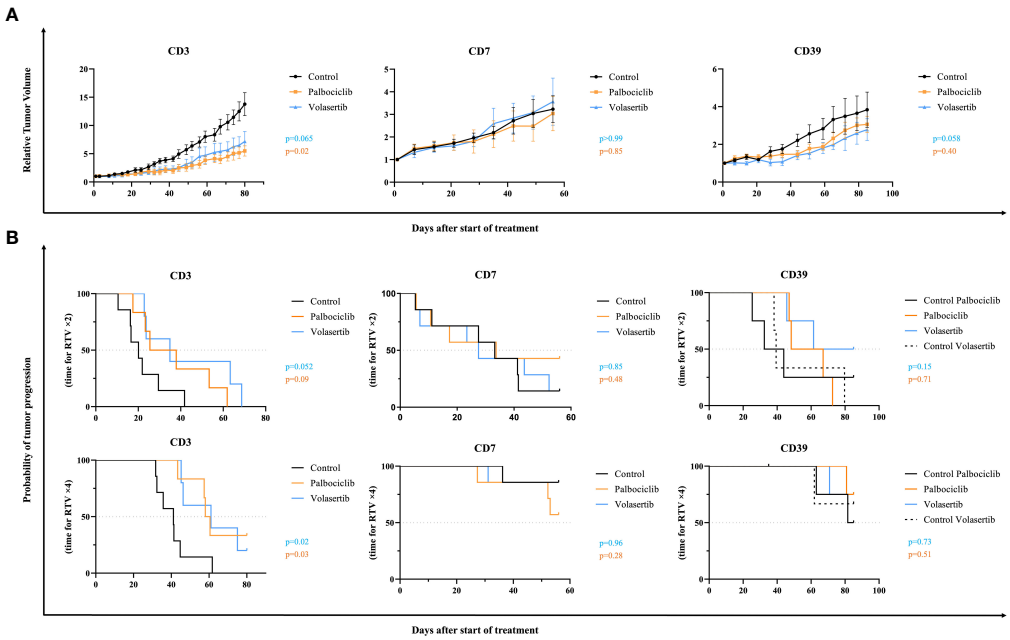

FIGURE 2
In vivo efficacy of palbociclib and volasertib, in the CD3, CD7, and CD39 chordoma PDXs. PDX tumor-bearing mice were randomized into each treatment group (n = 4–7 mice per group), and treated with palbociclib 75 mg/kg, 5 days per week (orange), or volasertib 10 mg/kg, 4 days per week (blue). Untreated control is shown in black. **(A)** Relative tumor volumes. Tumor growth was evaluated by plotting the mean of the relative tumor volume ± SD per group. **(B)** Probability of tumor progression. The time to reach RTV × 2 and RTV × 4 for each treated mouse has been calculated using Kaplan Meier curves and log-rank test.

p = 0.39 for RTV × 2 and RTV × 4, respectively) nor with volasertib (p=0.13 and p=0.27 for RTV x 2 and RTV x 4 respectively) (Figures 3B, C).

Pharmacodynamics study

Using RT-PCR analyses, we first looked at modifications of candidate gene expression occurring after palbociclib and volasertib *in vivo* therapies in CD3 and CD7 models compared to the control groups (Figure 4). For that, we applied RT-qPCR on the genes of interest (described in the materials and methods section) on 28 samples assigned to the control or treatment group. After palbociclib treatment, we observed a significant decrease in human *MKI67* (p = 0.008), *E2F1* (p = 0.016), and *PLK1* (p = 0.016) gene expression in the *in vivo* responding CD3 xenograft; in contrast, we only observed decreased gene expression in *E2F1* (p = 0.029) in the non-responding model CD7. No significant modification of gene expression was noted for *CDK4* (palbociclib target), *MYC*, *TBXT*, *EGFR*, *CCNE1*, and *RB1* in both studied models. After volasertib administration, we observed a significant gene expression modification of *RB1* (p = 0.03) in the CD3 model. No significant modification of gene expression was noted for the other genes, including *PLK1* (volasertib target).

To better understand the opposite efficacy of palbociclib in the two *CDKN2A/2B* deleted CD3 and CD7 PDXs, we then performed RNAseq analyses in both control and treated groups (three tumors per group). In a differential supervised analysis, comparing control tumors and tumors treated with palbociclib in both PDX models, we observed a more important modification of gene expression in the responding CD3 PDX model (n = 318 genes, Supplementary Table S1) compared to the non-responding CD7 PDX model (n = 12 genes; Supplementary Table S2), which correlated with *in vivo* observations. Next, we tested the enrichment of the set of genes resulting from the KEGG database. As expected, we found a significant decrease in the enrichment of cell cycle genes in the responding CD3 tumors (p = 0.04), such as *TOP2A* (p = 2.2 e^{-26}), *MKI67* (p = 4.3 e^{-20}), and *AURKB* (2.5 e^{-8}). Moreover, we compared in a supervised analysis the gene expression of control untreated CD3 PDX tumors and control untreated CD7 PDX tumors in order to find predictive biomarkers of intrinsic palbociclib resistance (Supplementary Table S3). We observed an upregulation of genes implied in hypoxia such as *S100A4* (p = 6.5 e^{-79}) and *CA3* (p = 3.8 e^{-56}) in the resistant CD7 PDX model (Figure 5A). Among the top 1000 genes in which we observed a significant gene expression variation in both the models (adjusted p-value), we noted an enrichment of the oxidative phosphorylation genes in the resistant CD7 PDX model (p = 0.02) using the KEGG data

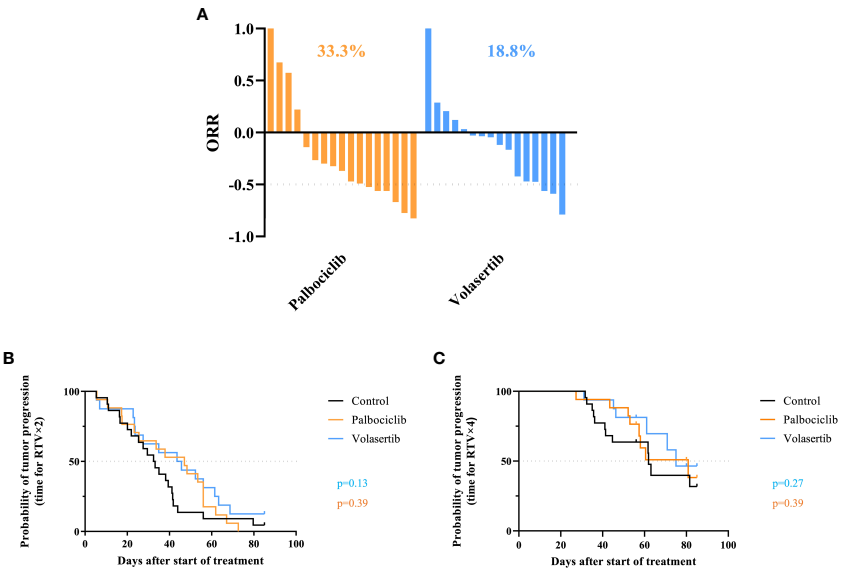

FIGURE 3
Individual tumor responses in the three treated models. **(A)** Overall response rate (ORR) in all treated chordoma PDXs after palbociclib (n = 17) and volasertib (n = 16). A tumor was considered to be responding to treatment if ORR was below -0.5. **(B, C)** Probability of progression (RTV × 2 and RTV × 4) in all treated chordoma PDXs after palbociclib and volasertib treatments.

base, such as *NDUFA1* ($p = 6.5\ e^{-14}$), *NDUFB2* ($p = 1.2\ e^{-07}$), *COX6C* ($p = 4.4\ e^{-07}$), *COX7A2* ($p = 1.9\ e^{-05}$), *COX7C* ($p = 3.2\ e^{-7}$), and *COX17* ($p = 4.2\ e^{-10}$) (Figure 5B). To resume the pharmacodynamic study, we observed a decrease in the expression of genes implied in the cell cycle in the responding CD3 compared to the CD7 PDX model treated by palbociclib. Moreover, we noted a significant enrichment of the expression of genes implied in oxidative phosphorylation (OxPhos) into the non-responding control CD7 PDX model in comparison with the responding control CD3 PDX model.

Discussion

In this current study, we explored the antitumor effect of the targeted therapy palbociclib in three PDX chordoma models in order to consider the homozygous deletion of *CDKN2A/2B* as a theranostic biomarker of response to palbociclib, as suggested in other cancer types (43, 54, 55). We observed various responses to palbociclib concerning both models (CD3, CD7) harboring a loss of *CDKN2A/2B*, and no tumor efficacy in the non-*CDKN2A/2B*-deleted *PBRM1*-mutated PDX (CD39). We also tested the PLK1 inhibitor volasertib in these three PDXs and did not observe any significant anti-tumor response.

Chordoma tumors are known to overexpress multiple kinases (56) (included PDGFR-α, PDGFR-β, c-Kit, c-Met, pAKT, mTOR, HER2, VEGFR, and EGFR) which are involved in a multitude of cellular functions relevant to cancer pathogenesis. These kinases are well-studied in the field of oncology, and several FDA-approved drugs on the market targeting each kinase can be used as repurposing candidates for advanced chordomas. The first pre- and clinical results of some FDA-approved drugs targeting EGFR, PDGFR-α, PDGFR-β, and c-Kit, have shown partial objective response and clinical benefit in chordomas (57). The lack of data concerning the biology of chordomas (genetic driver events) and theranostic markers hampers the selection of molecularly guided therapies and may explain these sparse results. As kinases, CDK4 and CDK6 play a crucial role in the G1-S phase transition, which is an important restriction point in the normal cell cycle, often reduced in cancer, leading to uncontrolled cell proliferation (Figure 6). Importantly, in chordomas, as well as in our PDX chordoma panel (35), the CDK4/6 regulatory gene *CDKN2A* (also known as p16) is frequently lost (5, 6), leading to the fact that CDK4/6 may be found in an over-activated state (41). However, it should be noted that other signaling pathways, in addition to *CDKN2A* loss, are inputted in cyclin D overexpression and promote CDK4/6 activity, leading to uncontrolled cell proliferation (42). Palbociclib, a specific inhibitor of CDK4/6, has recently been tested in *in vitro* cell line chordoma models harboring the loss of *CDKN2A* and showed an efficient inhibition of the tumor cell growth (41). Finally, the efficacy of palbociclib has been tested in numerous clinical trials for cancers, and is also currently being tested in a phase II trial, in patients with locally advanced/metastatic chordomas (NCT03110744).

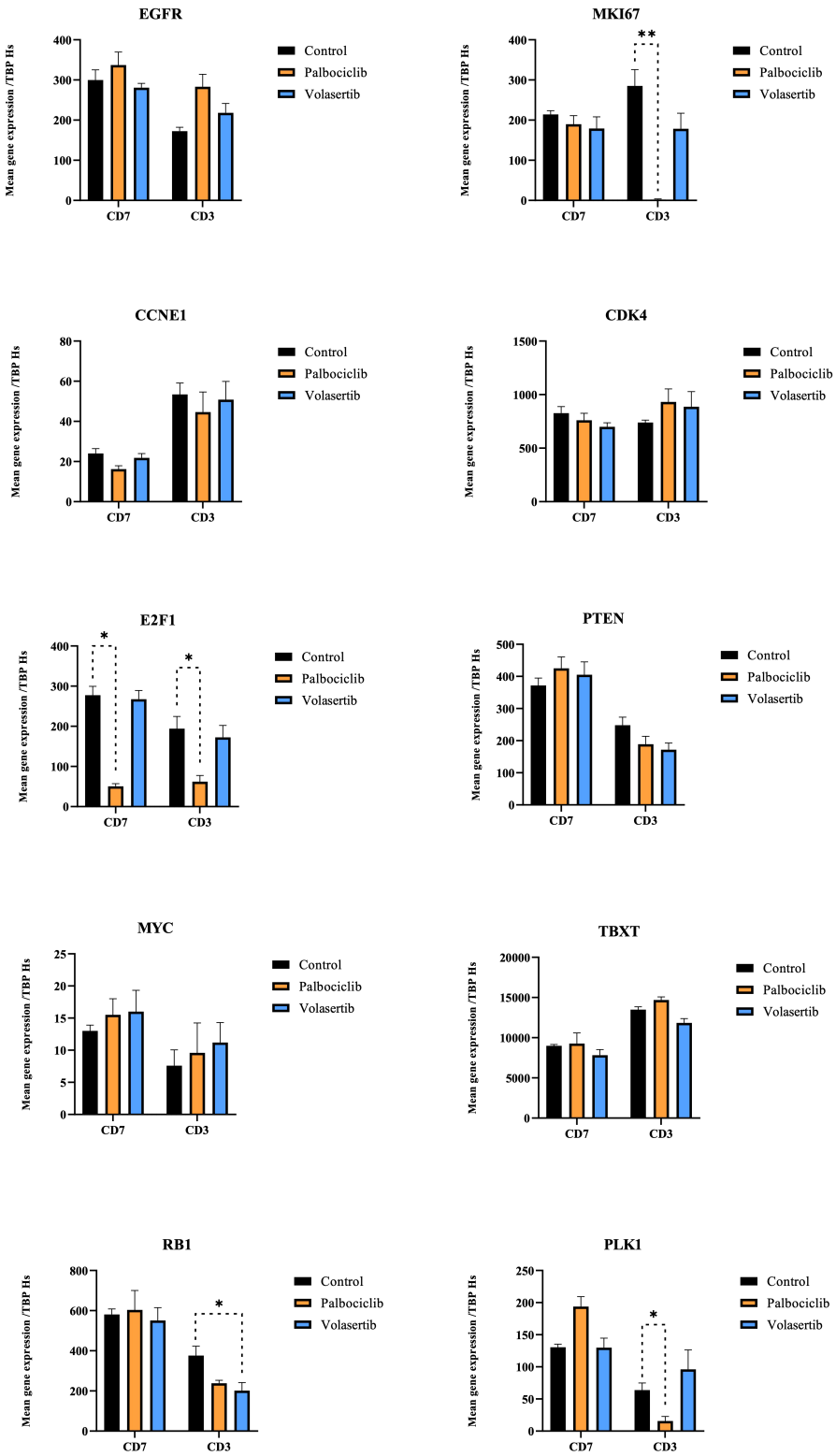

FIGURE 4
Gene expression modifications after treatments with palbociclib and volasertib (CD3 and CD7 models). Quantitative RT-PCR was performed to measure the expression of the target genes. Data are presented as level of gene expression compared to the standard level of *Homo sapien* (Hs) TBP. Genes expressions were compared between mice treated with the indicated agent and the control group. Error bars show the standard error of the mean. * and ** achieve statistical significance compared to control ($p < 0.05$ and $p < 0.01$, respectively) by Mann–Whitney *U* test.

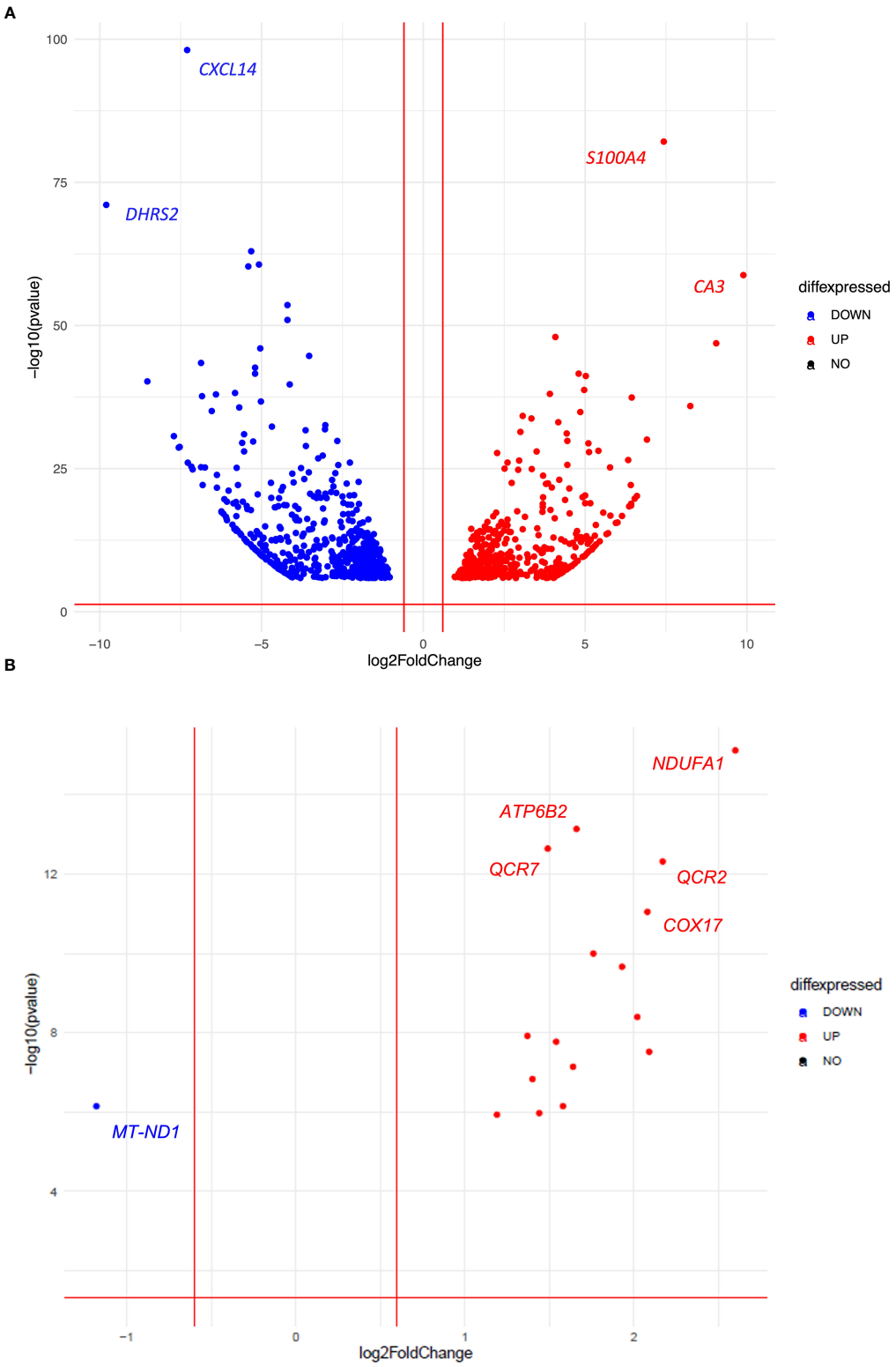

FIGURE 5
Volcanoplots illustrating the top 1000 genes **(A)** and all genes related to the oxidative phosphorylation (OxPhos) pathway **(B)**, in which we observed a significant gene expression variation in both untreated CD3 and CD7 PDX models (adjusted p-value).

In our *in vivo* pharmacological program, the CD3 model harboring *CDKN2A/2B* showed a significant tumor growth inhibition (p = 0.02), while the CD7 model showed no tumor response (p = 0.85). Pharmacodynamic study (RT PCR and RNAseq) confirmed the difference between both PDX models harboring both the loss of *CDKN2/2B*. Indeed, in the responding CD3 PDX model, we observed a decrease in the expression of genes implied in the cell cycle, such as *MKI67* (p = 0.008), *E2F1* (p = 0.016), *PLK1* (p = 0.016), *TOP2A* (p = 2.2 e^{-26}), and *AURKB* (p = 2.5 e^{-8}), compared to the non-responding model (CD7). We did not observe tumor response to palbociclib with the xenograft CD39 (p = 0.40) (which did not harbor a loss of *CDKN2A/2B)*; such an observation raises the possibility to consider *CDKN2A/2B* loss as a theranostic marker of palbociclib antitumor efficacy in chordomas. Considering the various sensitivities to palbociclib, we can formulate the hypothesis on which tumor heterogeneity and preexistence of a resistant clonal subtype to palbociclib in the CD7 PDX model might be present. Indeed, chordoma is known as a heterogeneous tumor (58) with various cell phenotypes. Genetic heterogeneity contributes to selecting a clonal cell population during tumor development and progression, and is well-known as a prominent contributor to therapeutic failure (59). This hypothesis is reinforced by genetic analyses performed on the CD7 chordoma PDX model, which confirmed the loss of *CDKN2A/2B* in treated and control mice, but not in the primary patient's tumor (35), suggesting a spatial tumor heterogeneity in which some cells harbor the homozygous deletion of *CDKN2A*, and others do not. Moreover, as observed

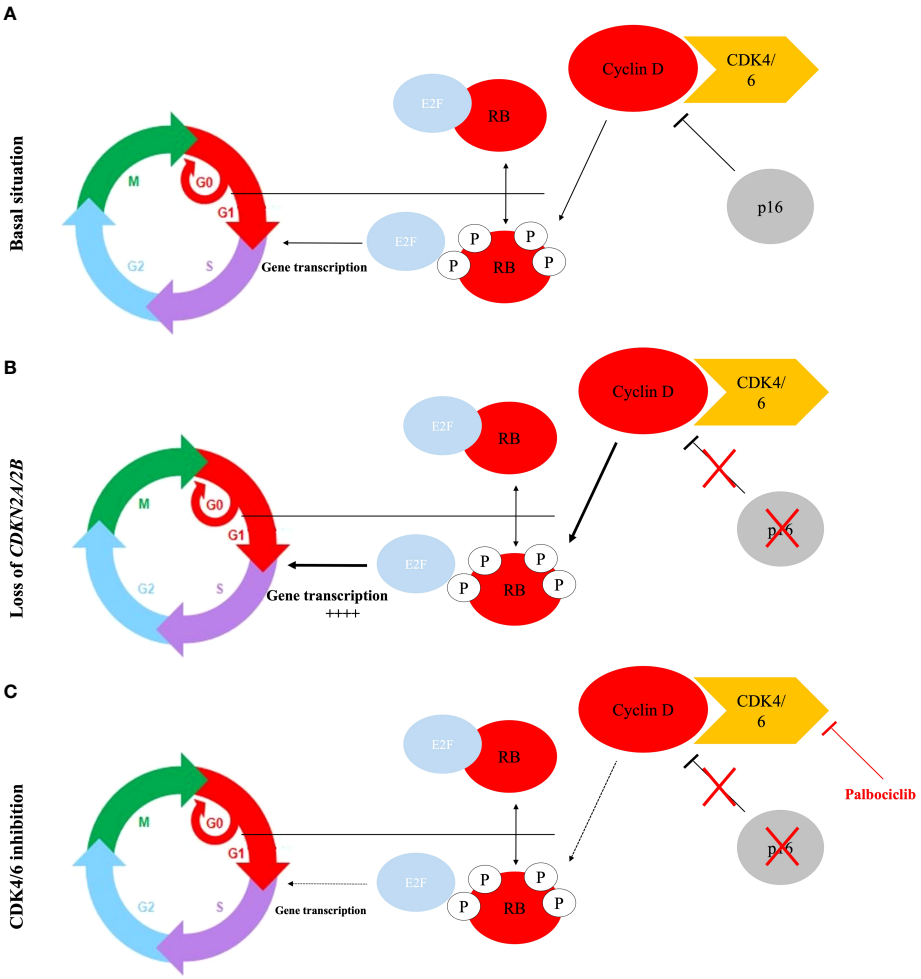

FIGURE 6
The classic model for the regulation of the G1/S transition by cyclins and CDK. **(A)** In basal situation, RB protein phosphorylation performed by cyclin D-CDK4/6 kinase induces E2F releasing and facilitates the expression of E2F target genes, which are critical for initiation of DNA synthesis and entry into S-phase. CDK4/6 activity is repressed by the p16 protein. **(B)** Loss of p16/CDKN2A/2B activity leads to an overactivation of the CDK4/6 activity and therefore an uncontrolled cell proliferation. **(C)** The CDK4/6 inhibitor re-establishes the activity of the RB protein activity as an inhibitor of cell division.

in hormone receptor-positive breast cancers, many tumors demonstrate *de novo* (or intrinsic) resistance to palbociclib, implying genomic alterations (60). When we compared the gene expression in the RNAseq-supervised analysis in non-treated CD3 and CD7 PDX tumors, we observed a significant enrichment of the expression of genes implied in oxidative phosphorylation (OxPhos) into the non-responding CD7 PDX model, as compared to the responding CD3 PDX model. Metabolism reprogramming is well known as a hallmark of cancer (61). While normal cells commonly use mitochondrial oxidative metabolism for energy generation, tumor cells often switch to aerobic glycolysis, described as the Warburg effect (62). Classically, glycolytic metabolism is involved in the induction of acquired drug resistance, such as in estrogen-receptor breast cancer treated with palbociclib (63). However, some authors also suggested that drug resistance could be associated with an upregulation of the oxidative phosphorylation (OxPhos) pathway, which may be explained by the "reverse Warburg effect" (64, 65). Evans et al. (66) recently showed an OxPhos dependence in chemotherapy-resistant triple-negative breast cancer. Moreover, radiation therapy seems to increase *in vitro* and *in vivo* OxPhos activity (67). Thus, we can suppose a selection of clonal subtypes to palbociclib in the CD7 PDX model, increased by the history of radiation, leading to a higher OxPhos activity in this model. Interestingly, drug resistance can be reversed by blocking OxPhos (68). In several cancers, new OxPhos inhibitors have already been identified, and are under preclinical and/or clinical evaluation (66, 69). Moreover, favorable results about the synergistic antitumoral effect of the combination of OxPhos inhibitors and palbociclib in a triple-negative breast cancer cell line (66), encourage testing the use of this drug combination or OxPhos inhibitors alone in palbociclib-resistant PDX chordoma models harboring the *CDKN2A/2B* loss. However, some authors revealed an upregulation of oxidative metabolism (OxPhos) in CDK4/6 inhibitor-tolerant uveal melanomas (70), suggesting further experimental research to conclude a causal association in the Oxphos dependency of palbociclib-resistant chordomas. Although being not fully understood, several other resistance mechanisms of CD4/6 inhibitors exist, as mechanisms bypassing the CDK4/6 inhibition *via* activating CDK2 signaling, which is another way that phosphorylates RB (52).

The PLK1 inhibitor showed a slight antitumor efficacy without significant activity ($p = 0.065$) in one model (CD3). These results could be explained by the absence of concomitant amplification or copy number gains of *CCND1* and *CCNE2* in our chordoma PDXs models (35), both of which are involved in RB inactivation driving tumor cells through the S phase (47). PLK1 inhibition seems to be more promising in a combination of treatments than in monotherapy (46, 71), therefore suggesting the importance of future preclinical trials in order to assess the combination of PLK1 inhibitors with other targeted drugs such as palbociclib. Indeed, PLK1 inhibition results in a G2-M arrest (72). Consequently, the combination of drugs resulting in a dual G1 (palbociclib) and G2-M arrest (volasertib) might therefore be addressed in chordomas.

Study limitations

Considering our disparate results and the low number of tested models ($n = 3$), there is a lack of support evidence to consider *CDKN2A/2B* loss as a potential biomarker for CDK4/6 inhibitor sensitivity, suggesting the importance of further studies on more preclinical models. Secondly, we did not perform drug combinations, especially with volasertib and palbociclib, considering the slow-growth of the tumor in PDX models (35). Moreover, we also hypothesized that the enrichment of the expression of genes implied in oxidative phosphorylation (OxPhos) could lead to primary resistance in chordoma. However, our results are insufficient to definitely conclude a causal association considering the few tested models and the absence of additional pharmacogenomic experiments.

Conclusion

Considering the frequency of genomic alterations affecting the *CDKN2A/2B* gene in chordomas, targeting this biomarker was fundamental. The present study described for the first time the *in vivo* activity of a CDK4/6 inhibitor and a PLK1 inhibitor in two human chordoma xenografts harboring homozygous deletions of *CDKN2A/2B*. We also hypothesized that OxPhos activity could lead to as a resistance mechanism to CDK4/6 inhibitors in chordomas. CDK4/6 inhibition may be effective, but further studies in several PDX models are strongly necessary to confirm such an observation, and to identify predictive markers of response or resistance to palbociclib in chordomas and reverse primary or secondary resistances. Investigating volasertib in combination with palbociclib could also provide a novel therapeutic strategy.

Data availability statement

The data presented in the study are deposited in the GEO repository, accession number GSE216419 (https://www.ncbi.nlm.nih.gov/geo/query/acc.cgi?acc=GSE216418).

Ethics statement

The animal study was reviewed and approved by Ethics committee of the Institut Curie CEEA-IC #118 (Authorization APAFiS# 25870-2020060410487032-v1 given by National Authority).

Author contributions

Conceptualization, TP, JM-P, HM, SF, IB and DD. Data curation, TP. Formal analysis, TP. Investigation, TP. Methodology, TP and DD. Project administration, DD. Resources, TP, AD, LC, RB, FN, SV, HA-B. Software, TP. Supervision, JMP, HAB, HM, SF, IB and DD. Validation, SR-R, EM, HM, SF, JM-P and IB. Visualization, TP. Writing – original draft, TP and DD. Writing – review and editing, JM-P and IB. All authors contributed to the article and approved the submitted version.

Acknowledgments

We wish to thank the Animal Platform of the Institut Curie and Raphaëlle Galy for English language editing.

Conflict of interest

The authors declare that the research was conducted in the absence of any commercial or financial relationships that could be construed as a potential conflict of interest.

Publisher's note

Supplementary material

The Supplementary Material for this article can be found online at: https://www.frontiersin.org/articles/10.3389/fonc.2022.960720/full#supplementary-material

SUPPLEMENTARY TABLE 1
Differential supervised analysis of the gene expression, comparing control tumors and tumors treated with palbociclib for the responding CD3 PDX model.

SUPPLEMENTARY TABLE 2
Differential supervised analysis of the gene expression, comparing control tumors and tumors treated with palbociclib for the non-responding CD7 PDX model.

SUPPLEMENTARY TABLE 3
Differential supervised analysis of the gene expression of control CD3 PDX tumors and control CD7 PDX tumors control PDX tumors.

References

1. Stacchiotti S, Sommer J. Chordoma global consensus group. building a global consensus approach to chordoma: A position paper from the medical and patient community. *Lancet Oncol* (2015) 16:e71–83. doi: 10.1016/S1470-2045(14)71190-8

2. Zou M-X, Lv G-H, Zhang Q-S, Wang S-F, Li J, Wang X-B. Prognostic factors in skull base chordoma: A systematic literature review and meta-analysis. *World Neurosurg* (2018) 109:307–27. doi: 10.1016/j.wneu.2017.10.010

3. Bohman L-E, Koch M, Bailey RL, Alonso-Basanta M, Lee JYK. Skull base chordoma and chondrosarcoma: Influence of clinical and demographic factors on prognosis: a SEER analysis. *World Neurosurg* (2014) 82:806–14. doi: 10.1016/j.wneu.2014.07.005

4. Stacchiotti S, Gronchi A, Fossati P, Akiyama T, Alapetite C, Baumann M, et al. Best practices for the management of local-regional recurrent chordoma: A position paper by the chordoma global consensus group. *Ann Oncol* (2017) 28:1230–42. doi: 10.1093/annonc/mdx054

5. Tarpey PS, Behjati S, Young MD, Martincorena I, Alexandrov LB, Farndon SJ, et al. The driver landscape of sporadic chordoma. *Nat Commun* (2017) 8. doi: 10.1038/s41467-017-01026-0

6. Bai J, Shi J, Li C, Wang S, Zhang T, Hua X, et al. Whole genome sequencing of skull-base chordoma reveals genomic alterations associated with recurrence and chordoma-specific survival. *Nat Commun* (2021) 12:757. doi: 10.1038/s41467-021-21026-5

7. Le LP, Nielsen GP, Rosenberg AE, Thomas D, Batten JM, Deshpande V, et al. Recurrent chromosomal copy number alterations in sporadic chordomas. *PloS One* (2011) 6:e18846. doi: 10.1371/journal.pone.0018846

8. Duan Z, Feng Y, Shen J, Hornicek F. Genomic and epigenetic instability in chordoma: Current insights. *AGG* (2014) 67. doi: 10.2147/AGG.S50523

9. Wang L, Zehir A, Nafa K, Zhou N, Berger MF, Casanova J, et al. Genomic aberrations frequently alter chromatin regulatory genes in chordoma. *Genes Chromosomes Cancer* (2016) 55:591–600. doi: 10.1002/gcc.22362

10. Diaz RJ, Guduk M, Romagnuolo R, Smith CA, Northcott P, Shih D, et al. High-resolution whole-genome analysis of skull base chordomas implicates FHIT loss in chordoma pathogenesis. *Neoplasia* (2012) 14:788–98. doi: 10.1593/neo.12526

11. Mattox AK, Yang B, Douville C, Lo S-F, Sciubba D, Wolinsky JP, et al. The mutational landscape of spinal chordomas and their sensitive detection using circulating tumor DNA. *Neurooncol Adv* (2021) 3:vdaa173. doi: 10.1093/noajnl/vdaa173

12. Cottone L, Eden N, Usher I, Lombard P, Ye H, Ligammari L, et al. Frequent alterations in p16/CDKN2A identified by immunohistochemistry and FISH in chordoma. *J Pathol Clin Res* (2020) 6:113–23. doi: 10.1002/cjp2.156

13. Zuccato JA, Patil V, Mansouri S, Liu JC, Nassiri F, Mamatjan Y, et al. DNA Methylation-based prognostic subtypes of chordoma tumors in tissue and plasma. *Neuro-Oncology* (2022) 24:442–54. doi: 10.1093/neuonc/noab235

14. Yang C, Sun J, Yong L, Liang C, Liu T, Xu Y, et al. Deficiency of PTEN and CDKN2A tumor-suppressor genes in conventional and chondroid chordomas: Molecular characteristics and clinical relevance. *Onco Targets Ther* (2020) 13:4649–63. doi: 10.2147/OTT.S252990

15. Choy E, MacConaill LE, Cote GM, Le LP, Shen JK, Nielsen GP, et al. Genotyping cancer-associated genes in chordoma identifies mutations in oncogenes and areas of chromosomal loss involving CDKN2A, PTEN, and SMARCB1. *PloS One* (2014) 9:e101283. doi: 10.1371/journal.pone.0101283

16. Singhal N, Kotasek D, Parnis FX. Response to erlotinib in a patient with treatment refractory chordoma. *Anticancer Drugs* (2009) 20:953–5. doi: 10.1097/CAD.0b013e328330c7f0

17. Stacchiotti S, Marrari A, Tamborini E, Palassini E, Virdis E, Messina A, et al. Response to imatinib plus sirolimus in advanced chordoma. *Ann Oncol* (2009) 20:1886–94. doi: 10.1093/annonc/mdp210

18. Lindèn O, Stenberg L, Kjellén E. Regression of cervical spinal cord compression in a patient with chordoma following treatment with cetuximab and gefitinib. *Acta Oncol* (2009) 48:158–9. doi: 10.1080/02841860802266672

19. Lebellec L, Chauffert B, Blay J-Y, Le Cesne A, Chevreau C, Bompas E, et al. Advanced chordoma treated by first-line molecular targeted therapies: Outcomes

and prognostic factors. a retrospective study of the French sarcoma group (GSF/GETO) and the association des neuro-oncologues d'Expression française (ANOCEF). *Eur J Cancer* (2017) 79:119–28. doi: 10.1016/j.ejca.2017.03.037

20. Stacchiotti S, Morosi C, Lo Vullo S, Casale A, Palassini E, Frezza AM, et al. Imatinib and everolimus in patients with progressing advanced chordoma: A phase 2 clinical study. *Cancer* (2018) 124:4056–63. doi: 10.1002/cncr.31685

21. Hindi N, Casali PG, Morosi C, Messina A, Palassini E, Pilotti S, et al. Imatinib in advanced chordoma: A retrospective case series analysis. *Eur J Cancer* (2015) 51:2609–14. doi: 10.1016/j.ejca.2015.07.038

22. George S, Merriam P, Maki RG, Van den Abbeele AD, Yap JT, Akhurst T, et al. Multicenter phase II trial of sunitinib in the treatment of nongastrointestinal stromal tumor sarcomas. *J Clin Oncol* (2009) 27:3154–60. doi: 10.1200/JCO.2008.20.9890

23. Stacchiotti S, Longhi A, Ferraresi V, Grignani G, Comandone A, Stupp R, et al. Phase II study of imatinib in advanced chordoma. *J Clin Oncol* (2012) 30:914–20. doi: 10.1200/JCO.2011.35.3656

24. Stacchiotti S, Tamborini E, Lo Vullo S, Bozzi F, Messina A, Morosi C, et al. Phase II study on lapatinib in advanced EGFR-positive chordoma. *Ann Oncol* (2013) 24:1931–6. doi: 10.1093/annonc/mdt117

25. Brüderlein S, Sommer JB, Meltzer PS, Li S, Osada T, Ng D, et al. Molecular characterization of putative chordoma cell lines. *Sarcoma* (2010) 2010:630129. doi: 10.1155/2010/630129

26. Liu X, Nielsen GP, Rosenberg AE, Waterman PR, Yang W, Choy E, et al. Establishment and characterization of a novel chordoma cell line: CH22. *J Orthop Res* (2012) 30:1666–73. doi: 10.1002/jor.22113

27. Scheil S, Brüderlein S, Liehr T, Starke H, Herms J, Schulte M, et al. Genome-wide analysis of sixteen chordomas by comparative genomic hybridization and cytogenetics of the first human chordoma cell line, U-CH1. *Genes Chromosomes Cancer* (2001) 32:203–11. doi: 10.1002/gcc.1184

28. Bosotti R, Magnaghi P, Di Bella S, Cozzi L, Cusi C, Bozzi F, et al. Establishment and genomic characterization of the new chordoma cell line chor-IN-1. *Sci Rep* (2017) 7:9226. doi: 10.1038/s41598-017-10044-3

29. Rinner B, Froehlich EV, Buerger K, Knausz H, Lohberger B, Scheipl S, et al. Establishment and detailed functional and molecular genetic characterisation of a novel sacral chordoma cell line, MUG-Chor1. *Int J Oncol* (2012) 40:443–51. doi: 10.3892/ijo.2011.1235

30. Hsu W, Mohyeldin A, Shah SR, a, Rhys CM, Johnson LF, Sedora-Roman NI, et al. Generation of chordoma cell line JHC7 and the identification of brachyury as a novel molecular target. *J Neurosurg* (2011) 115:760–9. doi: 10.3171/2011.5.JNS11185

31. Salle H, Pocard M, Lehmann-Che J, Bourthoumieu S, Labrousse F, Pimpie C, et al. Development of a novel orthotopic primary human chordoma xenograft model: A relevant support for future research on chordoma. *J Neuropathol Exp Neurol* (2020) 79:314–24. doi: 10.1093/jnen/nlz121

32. Dobrolecki LE, Airhart SD, Alferez DG, Aparicio S, Behbod F, Bentires-Alj M, et al. Patient-derived xenograft (PDX) models in basic and translational breast cancer research. *Cancer Metastasis Rev* (2016) 35:547–73. doi: 10.1007/s10555-016-9653-x

33. Diaz RJ, Luck A, Bondoc A, Golbourn B, Picard D, Remke M, et al. Characterization of a clival chordoma xenograft model reveals tumor genomic instability. *Am J Pathol* (2018) 188:2902–11. doi: 10.1016/j.ajpath.2018.08.004

34. Zhao T, Siu I-M, Williamson T, Zhang H, Ji C, Burger PC, et al. AZD8055 enhances *in vivo* efficacy of afatinib in chordomas. *J Pathol* (2021). doi: 10.1002/path.5739

35. Passeri T, Dahmani A, Masliah-Planchon J, Naguez A, Michou M, El Botty R, et al. Dramatic *In vivo* efficacy of the EZH2-inhibitor tazemetostat in PBRM1-mutated human chordoma xenograft. *Cancers* (2022) 14:1486. doi: 10.3390/cancers14061486

36. Masliah-Planchon J, Bièche I, Guinebretière J-M, Bourdeaut F, Delattre O. SWI/SNF chromatin remodeling and human malignancies. *Annu Rev Pathol Mech Dis* (2015) 10:145–71. doi: 10.1146/annurev-pathol-012414-040445

37. Duan R, Du W, Guo W. EZH2: A novel target for cancer treatment. *J Hematol Oncol* (2020) 13:104. doi: 10.1186/s13045-020-00937-8

38. Gounder MM, Zhu G, Roshal L, Lis E, Daigle SR, Blakemore SJ, et al. Immunologic correlates of the abscopal effect in a SMARCB1/INI1-negative poorly differentiated chordoma after EZH2 inhibition and radiotherapy. *Clin Cancer Res* (2019) 25:2064–71. doi: 10.1158/1078-0432.CCR-18-3133

39. Witkiewicz AK, Knudsen KE, Dicker AP, Knudsen ES. The meaning of p16 ^{ink4a} expression in tumors: Functional significance, clinical associations and future developments. *Cell Cycle* (2011) 10:2497–503. doi: 10.4161/cc.10.15.16776

40. Nobori T, Miura K, Wu DJ, Lois A, Takabayashi K, Carson DA. Deletions of the cyclin-dependent kinase-4 inhibitor gene in multiple human cancers. *Nature* (1994) 368:753–6. doi: 10.1038/368753a0

41. von Witzleben A, Goerttler LT, Marienfeld R, Barth H, Lechel A, Mellert K, et al. Preclinical characterization of novel chordoma cell systems and their targeting by pharmocological inhibitors of the CDK4/6 cell-cycle pathway. *Cancer Res* (2015) 75:3823–31. doi: 10.1158/0008-5472.CAN-14-3270

42. Yuan K, Wang X, Dong H, Min W, Hao H, Yang P. Selective inhibition of CDK4/6: A safe and effective strategy for developing anticancer drugs. *Acta Pharm Sin B* (2021) 11:30–54. doi: 10.1016/j.apsb.2020.05.001

43. Mayer EL, Dueck AC, Martin M, Rubovszky G, Burstein HJ, Bellet-Ezquerra M, et al. Palbociclib with adjuvant endocrine therapy in early breast cancer (PALLAS): Interim analysis of a multicentre, open-label, randomised, phase 3 study. *Lancet Oncol* (2021) 22:212–22. doi: 10.1016/S1470-2045(20)30642-2

44. Gjertsen BT, Schöffski P. Discovery and development of the polo-like kinase inhibitor volasertib in cancer therapy. *Leukemia* (2015) 29:11–9. doi: 10.1038/leu.2014.222

45. Steegmaier M, Hoffmann M, Baum A, Lénárt P, Petronczki M, Krssák M, et al. BI 2536, a potent and selective inhibitor of polo-like kinase 1, inhibits tumor growth. *vivo. Curr Biol* (2007) 17:316–22. doi: 10.1016/j.cub.2006.12.037

46. Montaudon E, El Botty R, Vacher S, Déas O, Naguez A, Chateau-Joubert S, et al. High *in vitro* and *in vivo* synergistic activity between mTORC1 and PLK1 inhibition in adenocarcinoma NSCLC. *Oncotarget* (2021) 12:859–72. doi: 10.18632/oncotarget.27930

47. Montaudon E, Nikitorowicz-Buniak J, Sourd L, Morisset L, El Botty R, Huguet L, et al. PLK1 inhibition exhibits strong anti-tumoral activity in CCND1 -driven breast cancer metastases with acquired palbociclib resistance. *Nat Commun* (2020) 11:4053. doi: 10.1038/s41467-020-17697-1

48. Barber SM, Sadrameli SS, Lee JJ, Fridley JS, Teh BS, Oyelese AA, et al. Chordoma–current understanding and modern treatment paradigms. *JCM* (2021) 10:1054. doi: 10.3390/jcm10051054

49. Johnson JI, Decker S, Zaharevitz D, Rubinstein LV, Venditti JM, Schepartz S, et al. Relationships between drug activity in NCI preclinical *in vitro* and *in vivo* models and early clinical trials. *Br J Cancer* (2001) 84:1424–31. doi: 10.1054/bjoc.2001.1796

50. Bièche I, Parfait B, Tozlu S, Lidereau R, Vidaud M. Quantitation of androgen receptor gene expression in sporadic breast tumors by real-time RT-PCR: evidence that MYC is an AR-regulated gene. *Carcinogenesis* (2001) 22:1521–6. doi: 10.1093/carcin/22.9.1521

51. Pandey K, An H, Kim SK, Lee SA, Kim S, Lim SM, et al. Molecular mechanisms of resistance to CDK4/6 inhibitors in breast cancer: A review. *Int J Cancer* (2019) 145:1179–88. doi: 10.1002/ijc.32020

52. Li Z, Zou W, Zhang J, Zhang Y, Xu Q, Li S, et al. Mechanisms of CDK4/6 inhibitor resistance in luminal breast cancer. *Front Pharmacol* (2020) 11:580251. doi: 10.3389/fphar.2020.580251

53. Rubino F, Alvarez-Breckenridge C, Akdemir K, Conley AP, Bishop AJ, Wang W-L, et al. Prognostic molecular biomarkers in chordomas: A systematic review and identification of clinically usable biomarker panels. *Front Oncol* (2022) 12:997506. doi: 10.3389/fonc.2022.997506

54. Al Baghdadi T, Halabi S, Garrett-Mayer E, Mangat PK, Ahn ER, Sahai V, et al. Palbociclib in patients with pancreatic and biliary cancer with CDKN2A alterations: Results from the targeted agent and profiling utilization registry study. *JCO Precis Oncol* (2019), 1–8. doi: 10.1200/PO.19.00124

55. Xue Z, Lui VWY, Li Y, Jia L, You C, Li X, et al. Therapeutic evaluation of palbociclib and its compatibility with other chemotherapies for primary and recurrent nasopharyngeal carcinoma. *J Exp Clin Cancer Res* (2020) 39:262. doi: 10.1186/s13046-020-01763-z

56. Anderson E, Havener TM, Zorn KM, Foil DH, Lane TR, Capuzzi SJ, et al. Synergistic drug combinations and machine learning for drug repurposing in chordoma. *Sci Rep* (2020) 10:12982. doi: 10.1038/s41598-020-70026-w

57. Gill CM, Fowkes M, Shrivastava RK. Emerging therapeutic targets in chordomas: A review of the literature in the genomic era. *Neurosurgery* (2019). doi: 10.1093/neuros/nyz342

58. El-Heliebi A, Kroneis T, Wagner K, Meditz K, Kolb D, Feichtinger J, et al. Resolving tumor heterogeneity: Genes involved in chordoma cell development identified by low-template analysis of morphologically distinct cells. *PloS One* (2014) 9:e87663. doi: 10.1371/journal.pone.0087663

59. Zhang J, Späth SS, Marjani SL, Zhang W, Pan X. Characterization of cancer genomic heterogeneity by next-generation sequencing advances precision medicine in cancer treatment. *Precis Clin Med* (2018) 1:29–48. doi: 10.1093/pcmedi/pby007

60. Wander SA, Cohen O, Gong X, Johnson GN, Buendia-Buendia JE, Lloyd MR, et al. The genomic landscape of intrinsic and acquired resistance to cyclin-dependent kinase 4/6 inhibitors in patients with hormone receptor–positive metastatic breast cancer. *Cancer Discovery* (2020) 10:1174–93. doi: 10.1158/2159-8290.CD-19-1390

61. Hanahan D, Weinberg RA. Hallmarks of cancer: The next generation. *Cell* (2011) 144:646–74. doi: 10.1016/j.cell.2011.02.013

62. Warburg O. On respiratory impairment in cancer cells. *Science* (1956) 124:269–70. doi: 10.1126/science.124.3215.269

63. Lorito N, Bacci M, Smiriglia A, Mannelli M, Parri M, Comito G, et al. Glucose metabolic reprogramming of ER breast cancer in acquired resistance to the CDK4/6 inhibitor palbociclib+. *Cells* (2020) 9:668. doi: 10.3390/cells9030668

64. Zaal EA, Berkers CR. The influence of metabolism on drug response in cancer. *Front Oncol* (2018) 8:500. doi: 10.3389/fonc.2018.00500

65. Pavlides S, Whitaker-Menezes D, Castello-Cros R, Flomenberg N, Witkiewicz AK, Frank PG, et al. The reverse warburg effect: Aerobic glycolysis in cancer associated fibroblasts and the tumor stroma. *Cell Cycle* (2009) 8:3984–4001. doi: 10.4161/cc.8.23.10238

66. Evans KW, Yuca E, Scott SS, Zhao M, Paez Arango N, Cruz Pico CX, et al. Oxidative phosphorylation is a metabolic vulnerability in chemotherapy-resistant triple negative breast cancer. *Cancer Res* (2021). doi: 10.1158/0008-5472.CAN-20-3242

67. Chen D, Barsoumian HB, Fischer G, Yang L, Verma V, Younes AI, et al. Combination treatment with radiotherapy and a novel oxidative phosphorylation inhibitor overcomes PD-1 resistance and enhances antitumor immunity. *J Immunother Cancer* (2020) 8:e000289. doi: 10.1136/jitc-2019-000289

68. Lee J-S, Lee H, Jang H, Woo SM, Park JB, Lee S-H, et al. Targeting oxidative phosphorylation reverses drug resistance in cancer cells by blocking autophagy recycling. *Cells* (2020) 9:2013. doi: 10.3390/cells9092013

69. Sica V, Bravo-San Pedro JM, Stoll G, Kroemer G. Oxidative phosphorylation as a potential therapeutic target for cancer therapy. *Int J Cancer* (2020) 146:10–7. doi: 10.1002/ijc.32616

70. Teh JLF, Purwin TJ, Han A, Chua V, Patel P, Baqai U, et al. Metabolic adaptations to MEK and CDK4/6 cotargeting in uveal melanoma. *Mol Cancer Ther* (2020) 19:1719–26. doi: 10.1158/1535-7163.MCT-19-1016

71. Posch C, Cholewa BD, Vujic I, Sanlorenzo M, Ma J, Kim ST, et al. Combined inhibition of MEK and Plk1 has synergistic antitumor activity in NRAS mutant melanoma. *J Invest Dermatol* (2015) 135:2475–83. doi: 10.1038/jid.2015.198

72. Gutteridge REA, Ndiaye MA, Liu X, Ahmad N. Plk1 inhibitors in cancer therapy: From laboratory to clinics. *Mol Cancer Ther* (2016) 15:1427–35. doi: 10.1158/1535-7163.MCT-15-0897

frontiers | Frontiers in Oncology

TYPE Original Research
PUBLISHED 16 December 2022
DOI 10.3389/fonc.2022.996262

OPEN ACCESS

EDITED BY
Hailiang Tang,
Fudan University, China

REVIEWED BY
Li Cai,
CHI St Vincent, United States
Sheng Han,
The First Affiliated Hospital of China Medical University, China
Emma D'Ippolito,
University of Campania Luigi Vanvitelli, Italy

*CORRESPONDENCE
Yazhuo Zhang
zyz2004520@yeah.net

†PRESENT ADDRESS
Yixuan Zhai,
Department of Neurosurgery,
The First Affiliated Hospital of Zhengzhou University, Zhengzhou, China

‡These authors have contributed equally to this work

SPECIALTY SECTION
This article was submitted to Neuro-Oncology and Neurosurgical Oncology, a section of the journal Frontiers in Oncology

RECEIVED 17 July 2022
ACCEPTED 01 December 2022
PUBLISHED 16 December 2022

CITATION
Zhai Y, Bai J, Xue Y, Li M, Mao W, Zhang X and Zhang Y (2022) Development and validation of a preoperative MRI-based radiomics nomogram to predict progression-free survival in patients with clival chordomas. *Front. Oncol.* 12:996262. doi: 10.3389/fonc.2022.996262

Development and validation of a preoperative MRI-based radiomics nomogram to predict progression-free survival in patients with clival chordomas

Yixuan Zhai[1†‡], Jiwei Bai[1‡], Yake Xue[2], Mingxuan Li[1], Wenbin Mao[2], Xuezhi Zhang[2] and Yazhuo Zhang[1,3,4,5*]

[1]Beijing Neurosurgical Institute, Capital Medical University, Beijing, China, [2]Department of Neurosurgery, The First Affiliated Hospital of Zhengzhou University, Zhengzhou, China, [3]Department of Neurosurgery, Beijing Tiantan Hospital, Capital Medical University, Beijing, China, [4]Center of Brain Tumor, Beijing Institute for Brain Disorders, Capital Medical University, Beijing, China, [5]China National Clinical Research Center for Neurological Diseases, Beijing, China

Objectives: The aim of this study was to establish and validate a MRI-based radiomics nomogram to predict progression-free survival (PFS) of clival chordoma.

Methods: A total of 174 patients were enrolled in the study (train cohort: 121 cases, test cohort: 53 cases). Radiomic features were extracted from multiparametric MRIs. Intraclass correlation coefficient analysis and a Lasso and Elastic-Net regularized generalized linear model were used for feature selection. Then, a nomogram was established *via* univariate and multivariate Cox regression analysis in the train cohort. The performance of this nomogram was assessed by area under curve (AUC) and calibration curve.

Results: A total of 3318 radiomic features were extracted from each patient, of which 2563 radiomic features were stable features. After feature selection, seven radiomic features were selected. Cox regression analysis revealed that 2 clinical factors (degree of resection, and presence or absence of primary chordoma) and 4 radiomic features were independent prognostic factors. The AUC of the established nomogram was 0.747, 0.807, and 0.904 for PFS prediction at 1, 3, and 5 years in the train cohort, respectively, compared with 0.582, 0.852, and 0.914 in the test cohort. Calibration and risk score stratified survival curves were satisfactory in the train and test cohort.

Conclusions: The presented nomogram demonstrated a favorable predictive accuracy of PFS, which provided a novel tool to predict prognosis and risk stratification. Our results suggest that radiomic analysis can effectively help neurosurgeons perform individualized evaluations of patients with clival chordomas.

KEYWORDS

radiomics, nomogram, chordoma, prognosis, prediction

Introduction

Chordoma is a rare malignant neoplasm that arises from the remnants of the primitive notochord (1). The annual incidence is lower than one case per million people (2). Chordoma mainly involves the axial skeleton, and about 25% of chordoma originates from the skull base (3). Skull base chordoma has the tendency to invade surrounding structures which makes it difficult to achieve gross-total resection (GTR) in the operation (4). Furthermore, chordoma isn't sensitive to chemotherapy and radiotherapy, resulting in extensive recurrences. The local recurrence rate is as high as 50% in four years after surgery. Until now, there is no effective method for predicting recurrence (5).

Radiomics generally refers to the extraction and analysis of large amounts of advanced quantitative imaging features with high throughput from medical images obtained using CT, MRI or PET. The researchers are able to develop models that may potentially improve diagnostic, prognostic, and predictive accuracy. Radiomics has been widely used in prediction of tumor consistency, prognosis, and blood supply in many tumors such as pituitary adenomas (6), gliomas (7), meningiomas (8) et al. It enables doctors to deliver more personalized treatment with regard to tumor detection, prediction of tumor subtypes, and prognosis. However, few studies have focused on radiomics application in chordoma. Therefore, in this study, we aimed to establish a radiomics nomogram to predict progression-free survival (PFS) in patients with clival chordomas.

Methods

Patients

Our study retrospectively analyzed skull base chordoma patients who received operations at Beijing Tiantan Hospital from September 2003 to September 2014. The inclusion criteria were as follows: 1) chordoma diagnosis was confirmed by the pathological report, 2) medical records were complete, and 3) lesions were located in the clival region. Exclusion criteria were as follows: 1) incomplete medical records, 2) poor quality imaging, and 3) lack of patient follow-up. Accordingly, 174 skull base chordoma patients were included in the study.

The patients were divided randomly into train cohort (n=121) and test cohort (n=53). Patients' data was collected, including gender, age, course of disease, chief complaint, KPS score, degree of resection, postoperative treatment, and complications. The gross total resection (GTR) was defined as no residual tumor in the post-operative image. Non-gross total resection (NGTR) was defined as residual tumor detected in the post-operative image.

MRI acquisition

All patients underwent MR imaging scan before operation. Three clinical scanners (Siemens Healthcare, Toshiba Medical Systems, and GE Medical Systems) were used in the study. The MR imaging protocol included T1-weighted contrast-enhanced imaging with fluid-attenuated inversion-recovery sequence (T1C), T1-weighted imaging with fluid-attenuated inversion-recovery sequence (T1WI), and T2-weighted imaging sequence (T2WI). The T1C sequence was acquired with the following parameters: Repetition time (TR):2031.01-2803.86ms, Echo time (TE): 10.35-19.76ms, Flip angle: 90°, and Slice thickness: 4-6.5mm. The T1WI sequence was acquired with the following parameters: TR: 2031.01-2458.22ms, TE:9.50-19.76ms, Flip angle: 90°, and Slice thickness: 5-6.5mm. The T2WI sequence was acquired with the following parameters: TR:2680-6000ms, TE:102.17-123.62ms, Flip angle: 90°, and Slice thickness: 5-6.5mm.

Tumor segmentation, preprocessing, and feature extraction

The tumors were manually drawn on T1C imaging by two neuroradiologists independently, using a free 3D-Slicer software (v4.9.0).

Preprocessing was performed by SimpleITK package (v1.2.4). First, image registration was performed to register T1, and T2 sequence images to the T1C sequence images. Next, N4 bias field correction was applied to each sequence images to correct non-uniformities in intensity. The feature extraction was performed using PyRadiomics package (v3.0). The detail parameter settings are provided in the Supplementary document. For each imaging sequence, a total of 1106 radiomics features were calculated. For each patient, a total of three imaging sequences were calculated, which generated 3318 radiomic features.

Radiomic feature selection

To avoid overfitting, feature selection was performed before model training. Features were selected by two steps. First, the ROIs drawn by the two neuroradiologists were compared, and intraclass correlation coefficients (ICCs) were calculated. If the ICCs > 0.7, the radiomic features were defined as stable features. Then, the stable features were analyzed by a Lasso and Elastic-Net regularized generalized linear model (glmnet). Five-fold cross-validation with minimizing deviance was performed to find the optimal λ. With the optimal λ, the coefficient of each feature was calculated, then features with non-zero coefficients were selected. This step was repeated 1000 times. The features

that appeared more than 150 times were selected as the prognostic radiomic features.

Survival model training and nomogram establishment

Cox regression analysis was used to identify the prognostic factors. First, prognostic radiomics features and all the clinical variables were analyzed by univariate Cox regression. Then, all the variables with p value < 0.1 were further analyzed by multivariate Cox regression with the backward model (9). After that, all the significant variables were identified as the independent prognostic variables.

The Rad-score for each patient was calculated using the sum of the values of selected radiomic features weighted by the corresponding mean non-zero coefficients (see Supplementary document). The nomogram was established with the Rad-score and the independent prognostic clinical variables.

Predictive performance of nomogram

To evaluate the nomogram performance, the area under curve (AUC) of receiver operating characteristic (ROC) was performed in the train and test cohorts. A value of AUC > 0.7 indicates a good discrimination. Then, to compare the consistency between the predicted value and actual value, a calibration curve was drawn (10). Lastly, we calculated the risk score for each patient according to the nomogram. Using the risk score, patients were divided into two groups (low-risk and high-risk). If the risk score was lower than the mean score of the train cohort, the patient was placed in the low-risk group, otherwise they were placed in the high-risk group. The PFS was compared between the low-risk and high-risk group using the Kaplan-Meier method. And Rad-scores were also compared between the two groups. The flowchart of this study is shown in Figure 1.

Statistical analysis

Statistical analysis was conducted in Python (v3.7.6) with the packages ("os", "pandas", "SimpleITK", "pyradiomics") and R software (v4.0.0) with the packages ("survival", "rms", "plyr", "glmnet", "timeROC", "survminer").

Results

Patient clinical characteristics

A total of 174 patients (97 male and 77 female) were included in the study. There are 140 primary chordomas and 34 recurrent chordomas. The mean age was 40.51 years old (range: 8-78 years old), the mean course of disease was 21.77 months (range: 1-360 months). The KPS score ranged from 50 to 90 (mean: 80). GTR was achieved in 48 patients, and NGTR was achieved in 126 patients. There were 65 patients (37.4%) receiving post-operative radiotherapy. The total radiotherapy dose was between 50 Gy and 64 Gy (mean: 54.1 Gy). The mean

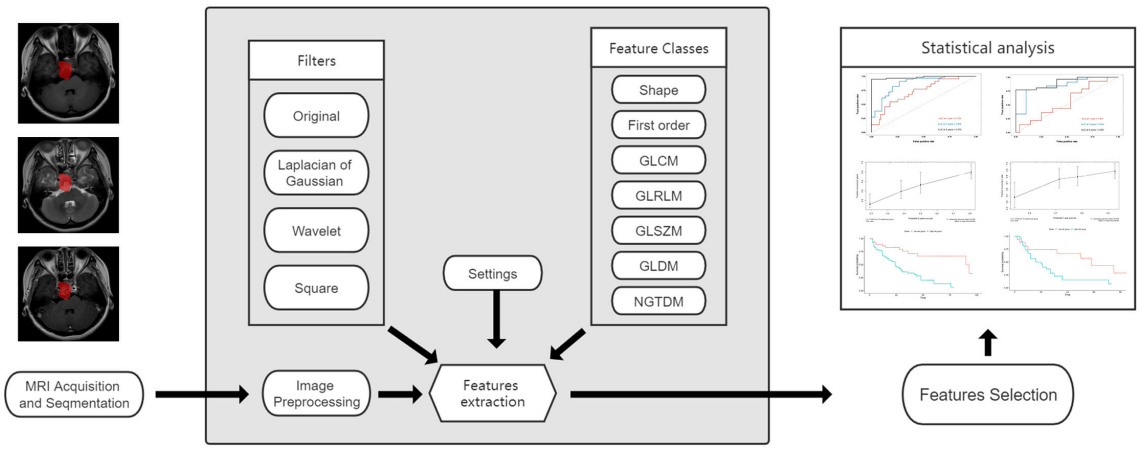

FIGURE 1
The flow chart of the study.

follow-up interval was 86 months (range: 52-185 months). Patient characteristics are shown in Table 1, which were similar overall between the train and test cohorts.

Radiomic feature selection

In total, 3318 radiomic features were extracted, and 2563 radiomic features were selected as stable features by ICCs (see Supplementary Table 1). Through Lasso and Elastic-Net regularized generalized linear model selection, seven radiomic features were selected.

Survival model training and nomogram establishment

Univariate Cox regression analysis was performed to detect the relationship between PFS and each of the seven radiomic features and clinical factors. Among the 7 radiomic features, 4 features were favorable prognostic features. Among the 10 clinical factors, 2 factors (GTR and primary chordoma) were favorable clinical factors. Multivariate Cox regression analysis was further performed. We found that 2 clinical factors and 4 radiomic features were significant prognostic factors (see Table 2).

The Rad-score for each patient was calculated in train and test cohorts. The formula of Rad-score is presented in the Supplementary Document. Based on the clinical factors and Rad-scores, we established a nomogram for easier clinical use (Figure 2).

For each patient, prognostic points were calculated by the following equation: Total points = 41.67 × (Rad-score + 1.8) + 1.39 × (primary chordoma or not) + 24.51 × (degree of resection). Higher total points indicated worse prognosis. The established 1-, 3-, and 5-year PFS rates were obtained according to the total points.

In the train cohort, the AUCs of the model were 0.747, 0.807 and 0.904 for PFS prediction at 1, 3 and 5 years, respectively (see Figure 3). This showed that the model had a satisfactory predictive ability. The calibration curves were drawn to test the model consistency which showed the nomogram had a satisfactory calibration curve (see Figure 4).

Model validation and comparison

The AUCs of the model in the test cohort were 0.582, 0.852, and 0.914 for PFS prediction at 1, 3 and 5 years, respectively.

TABLE 1 Patient characteristics.

Characteristics	Train cohort	Test cohort	*P* value
No. of patients	121	53	
Gender, n			
Male	72	25	0.18
Female	49	28	
Mean age (range), yrs	40.72 (11-78)	40.04 (8- 63)	0.77
Mean course of disease (range), mos	17.62 (1-240)	31.20 (1-360)	0.15
Primary chordoma, n	98	42	0.95
Recurrent chordoma, n	23	11	
Degree of resection, n			
GTR	34	14	0.96
NGTR	87	39	
Post-operative radiotherapy, n			
Yes	40	25	0.11
No	81	28	
Complications, n			
Yes	29	16	0.5
No	92	37	

GTR, gross total resection; NGTR, non-gross total resection.

10.3389/fonc.2022.996262

TABLE 2 Univariate and multivariate Cox regression analysis.

Variables	Univariate analysis			Multivariate analysis		
	HR	95%CI	*P value*	HR	95%CI	*P value*
Clinical factors						
Age	1.01	0.99-1.02	0.3653			
Gender (female vs male)	1.14	0.74-1.76	0.5617			
Course of disease	1	0.99-1	0.2571			
KPS score	0.99	0.96-1.02	0.4817			
Pituitary gland involved	1.04	0.67-1.6	0.8626			
Brainstem involved	1.14	0.71-1.85	0.5908			
Degree of resection (NGTR vs GTR)	5.05	2.71-9.43	<0.001	4.69	2.50-8.83	<0.001
Recurrent vs primary chordoma	2.35	1.41-3.92	0.001	1.77	1.06-2.96	0.03
With vs without post-operative radiotherapy	1.48	0.96-2.29	0.0757			
With vs without complication	1.04	0.64-1.72	0.8638			
Radiomics features						
T1_square_glrlm_ShortRunEmphasis	1.79	1.38-2.31	<0.001			
T1_wavelet.HLL_firstorder_Range	1.65	1.32-2.07	<0.001			
T1_wavelet.HLL_ngtdm_Complexity	1.66	1.33-2.08	<0.001	1.32	1.03-1.69	0.03
T1c_square_gldm_LowGrayLevelEmphasis	0.5	0.38-0.67	<0.001	0.57	0.41-0.78	<0.001
T1c_wavelet.HHH_firstorder_Range	1.47	1.18-1.82	<0.001	1.14	1.10-1.79	0.006
T2_wavelet.HLL_firstorder_Mean	1.89	1.44-2.48	<0.001	1.44	1.06-1.97	0.02
T2_square_firstorder_Median	0.55	0.42-0.71	<0.001			

CI, confidence interval; GTR, gross total resection; NGTR, non-gross total resection; HR, hazard ratio.

This demonstrated a satisfactory prediction performance (see Figure 3). The calibration curves of the test cohort also showed a satisfactory calibration (see Figure 4).

According to the established nomogram, the risk score of each patient was calculated. The mean risk score of the train cohort was 91.98 (range: 29.82-122.44). The mean risk score of the test cohort was 95.40 (range: 23.17-125.45). Patients were divided into two groups by the mean risk score of the train cohort. If the risk score was lower than the mean score of train cohort, the patient was placed in the low-risk group, otherwise

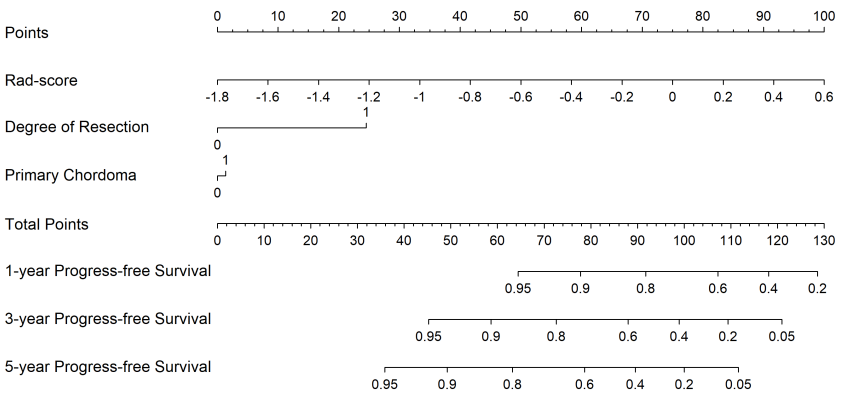

FIGURE 2
Radiomics nomogram for PFS prediction.

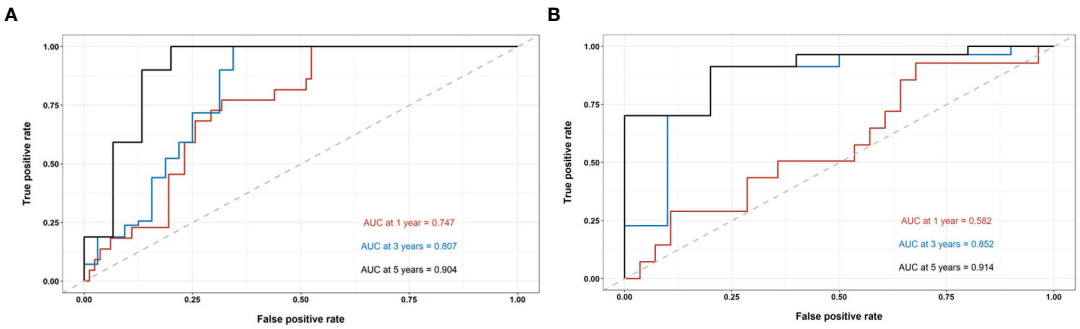

FIGURE 3
The performance evaluation of the radiomics nomogram. **(A)** The ROC curve in the train cohort; **(B)** The ROC curve in the test cohort.

they were placed in the high-risk group. In the train cohort, the median PFS of the low-risk group was 110 months, and the median PFS of the high-risk group was 16 months ($p<0.0001$). In the test cohort, the median PFS of the low-risk group was 60 months, and the median PFS of the high-risk group was 24 months ($p=0.0046$) (see Figure 5).

Discussion

The chordoma has the tendency of recurrence which results in poor prognosis. It has been reported that the 5-year PFS rate is as low as 59% (11). It has been reported that many factors are related to prognosis, such as total resection (12), post-operative radiotherapy (13), PBRM1 (14), PARP1, PDGFR-β (15), etc. A few prediction models were established using these prognostic factors. However, the performance of these models was not satisfactory. Therefore, we established a more efficient prediction model in this study.

Many studies have reported clinical factors that could predict patient PFS, but no consensus has been reached. In our study, we found that degree of resection was the independent prognostic factor. Radical resection can significantly prolong patient PFS. Sekhar et al (16) retrospectively studied 42 patients

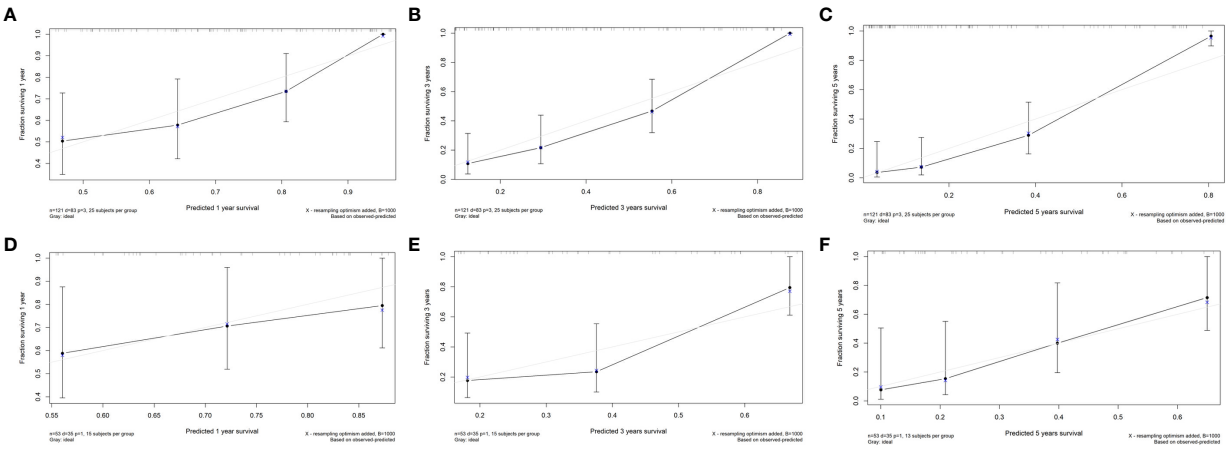

FIGURE 4
The calibration curves of the radiomics nomogram. **(A)** Calibration curve for prediction 1-year PFS in the train cohort; **(B)** Calibration curve for prediction 3-year PFS in the train cohort; **(C)** Calibration curve for prediction of 5-year PFS in the train cohort; **(D)** Calibration curve for prediction of 1-year PFS in the test cohort; **(E)** Calibration curve for prediction of 3-year PFS in the test cohort; **(F)** Calibration curve for prediction of 5-year PFS in the test cohort.

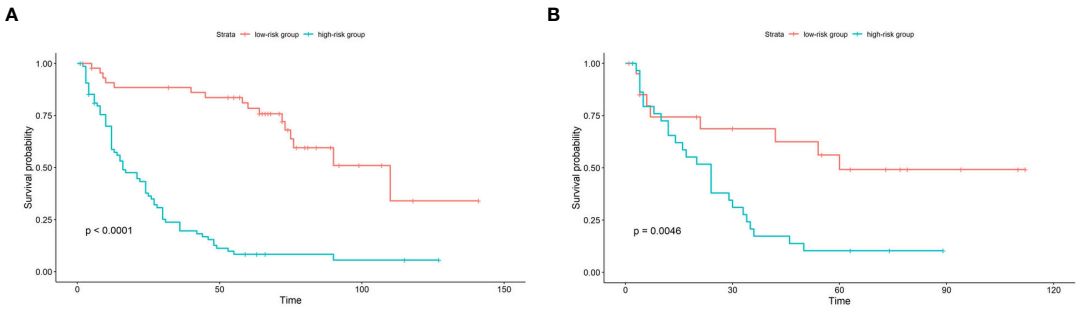

FIGURE 5
Kaplan-Meier survival curve of patients in the train cohort **(A)** and test cohort **(B)** stratified by nomogram predicted score. In the low-risk group, the score is lower than the mean score of the group; in the high-risk group, the score is higher than the mean score of the group.

and built a Chordoma Grading System. In these patients, complete resection rate was 36%, and subtotal resection rate was 64%. After Cox proportional hazards model analysis, they found that complete resection rate was significantly associated with PFS. Carl H Snyderman et al (17) present their endoscopic endonasal experience in the treatment of 60 patients with cranial base chordomas. The overall rate of GTR was as high as 66.7%. The mean PFS was 14.4 months. The recurrence rate of patients who underwent GTR was 20%, which was significantly lower than that of patients who underwent NGTR (60%). The high GTR rate can be attributed to the extensive experience of the surgeons. In most published studies, the GTR rate was about 30% to 50%. Thus, improvement of operative technique was the key to improve GTR rate. In this study, we also found that the PFS of primary chordoma was significantly longer than that of recurrent chordoma, which emphasized the importance of the first operation. If GTR is achieved in the primary chordoma, the prognosis will be significantly improved. Recently, some molecular features have been reported to be important prognostic factors in clival chordomas. Georgios A Zenonos et al (18) prospectively evaluated the 1p36 and 9p21 state, Ki-67 expression level in 105 clival chordomas samples, and found that homozygous 1p36 deletions and 9p21 deletions were independent prognostic factors.

Radiomics is a new area of study, which has been widely used in the differential diagnosis and prognosis prediction of many tumors (19–21). Nan Hong et al (22) developed a clinical-radiomics nomogram to differentiate sacral chordoma and sacral giant cell tumor before operation, which yielded an AUC of 0.948. Jie Tian et al (23) established a radiomic signature with multiparametric MRI for differentiating skull base chordoma and chondrosarcoma, which yielded an AUC of 0.975 and 0.872 in the train and test cohorts, respectively.

Only two articles that used radiomic features to predict prognosis of patients with clival chordoma have been published. Jie Tian et al (24) enrolled 80 patients with skull base chordomas, and selected 5 features from MR images to build a radiomics signature, which was used to train a logistic regression model. The model achieved an AUC=0.8600 in the train cohort and AUC=0.8568 in the test cohort. One year later, the author (25) developed a clinical-radiomic model to predict PFS of chordoma. They enrolled 148 patients, including 64 with disease progression. The Harrell's concordance index of their model was only 0.745 for the test cohort. In our study, we enrolled more patients with clival chordoma and extended follow-up time. Thus, our model achieved higher AUC and accuracy. The AUCs of our model were as high as 0.904 and 0.914 for PFS prediction at 5 years in the train and test cohorts, respectively. In addition, our model displayed a good calibration and discrimination ability. With the help of a nomogram, a neurosurgeon can stratify their patients. If the patient is classified in the high-risk group, the surgeon could shorten the follow-up interval and use more therapeutic measures. Thus, it is possible to develop an individualized treatment plan.

Our study has several limitations. First, all the patients were enrolled over the course of several years from one center, which may lead to patient selection bias. A multicenter study is needed for further analysis. Second, patient imaging was acquired by different scanners, which may increase the data heterogeneity bias. To avoid this, all imaging was subjected to imaging normalization before feature extraction.

Conclusion

In our study, we developed and validated a nomogram based on the multiparametric MRI radiomics signatures and clinical factors. The nomogram demonstrated a favorable predictive accuracy of PFS which provided a novel tool to predict prognosis and risk stratification. Our results suggest that radiomics analysis can effectively help neurosurgeons perform individualized evaluations of patients with clival chordomas.

Data availability statement

The raw data supporting the conclusions of this article will be made available by the authors, without undue reservation.

Author contributions

YXZ and YZZ designed the study. JB and ML collected clinical and MRI data. YX, WM, and XZ pre-processed patients MR imaging and drew the ROI. YXZ and JB analyzed the data and developed prediction model. YXZ wrote the manuscript. All authors contributed to the article and approved the submitted version.

Funding

This study was supported by the National Natural Science Foundation of China (82071559).

Conflict of interest

The authors declare that the research was conducted in the absence of any commercial or financial relationships that could be construed as a potential conflict of interest.

Publisher's note

Supplementary material

The Supplementary Material for this article can be found online at: https://www.frontiersin.org/articles/10.3389/fonc.2022.996262/full#supplementary-material

References

1. Walcott BP, Nahed BV, Mohyeldin A, Coumans JV, Kahle KT, Ferreira MJ. Chordoma: current concepts, management, and future directions. *Lancet Oncol* (2012) 13(2):e69–76. doi: 10.1016/S1470-2045(11)70337-0

2. McMaster ML, Goldstein AM, Bromley CM, Ishibe N, Parry DM. Chordoma: incidence and survival patterns in the united states, 1973-1995. *Cancer Causes Control.* (2001) 12(1):1–11. doi: 10.1023/a:1008947301735

3. Zhou J, Sun J, Bai HX, Huang X, Zou Y, Tan X, et al. Prognostic factors in patients with spinal chordoma: An integrative analysis of 682 patients. *Neurosurgery.* (2017) 81(5):812–23. doi: 10.1093/neuros/nyx081

4. Zhai Y, Bai J, Li M, Wang S, Li C, Wei X, et al. A nomogram to predict the progression-free survival of clival chordoma. *J Neurosurg* (2019) 134(1):144–52. doi: 10.3171/2019.10.JNS192414

5. Wang L, Wu Z, Tian K, Wang K, Li D, Ma J, et al. Clinical features and surgical outcomes of patients with skull base chordoma: a retrospective analysis of 238 patients. *J Neurosurg* (2017) 127(6):1257–67. doi: 10.3171/2016.9.JNS16559

6. Zhang Y, Shang L, Chen C, Ma X, Ou X, Wang J, et al. Machine-learning classifiers in discrimination of lesions located in the anterior skull base. *Front Oncol* (2020) 10:752. doi: 10.3389/fonc.2020.00752

7. Wang J, Zheng X, Zhang J, Xue H, Wang L, Jing R, et al. An MRI-based radiomics signature as a pretreatment noninvasive predictor of overall survival and chemotherapeutic benefits in lower-grade gliomas. *Eur Radiol* (2021) 31(4):1785–94. doi: 10.1007/s00330-020-07581-3

8. Park YW, Oh J, You SC, Han K, Ahn SS, Choi YS, et al. Radiomics and machine learning may accurately predict the grade and histological subtype in meningiomas using conventional and diffusion tensor imaging. *Eur Radiol* (2019) 29(8):4068–76. doi: 10.1007/s00330-018-5830-3

9. Montero PH, Yu C, Palmer FL, Patel PD, Ganly I, Shah JP, et al. Nomograms for preoperative prediction of prognosis in patients with oral cavity squamous cell carcinoma. *Cancer.* (2014) 120(2):214–21. doi: 10.1002/cncr.28407

10. Harrell FEJr., Lee KL, Mark DB. Multivariable prognostic models: issues in developing models, evaluating assumptions and adequacy, and measuring and reducing errors. *Stat Med* (1996) 15(4):361–87. doi: 10.1002/(SICI)1097-0258(19960229)15:4<361::AID-SIM168>3.0.CO;2-4

11. Zou Y, Neale N, Sun J, Yang M, Bai HX, Tang L, et al. Prognostic factors in clival chordomas: An integrated analysis of 347 patients. *World Neurosurg* (2018) 118:e375–e87. doi: 10.1016/j.wneu.2018.06.194

12. Li M, Bai J, Wang S, Zhai Y, Zhang S, Li C, et al. Mean platelet volume and platelet distribution width serve as prognostic biomarkers in skull base chordoma: a retrospective study. *BMC Cancer.* (2020) 20(1):988. doi: 10.1186/s12885-020-07497-7

13. Zhou Y, Hu B, Wu Z, Cheng H, Dai M, Zhang B. The clinical outcomes for chordomas in the cranial base and spine: A single center experience. *Med (Baltimore).* (2019) 98(23):e15980. doi: 10.1097/MD.0000000000015980

14. Bai J, Shi J, Li C, Wang S, Zhang T, Hua X, et al. Whole genome sequencing of skull-base chordoma reveals genomic alterations associated with recurrence and chordoma-specific survival. *Nat Commun* (2021) 12(1):757. doi: 10.1038/s41467-021-21026-5

15. Zhai Y, Bai J, Wang S, Gao H, Li M, Li C, et al. Analysis of clinical factors and PDGFR-beta in predicting prognosis of patients with clival chordoma. *J Neurosurg* (2018) 129(6):1429–37. doi: 10.3171/2017.6.JNS17562

16. Brito da Silva H, Straus D, Barber JK, Rostomily RC, Ferreira MJr., Sekhar LN. Cranial chordoma: A new preoperative grading system. *Neurosurgery.* (2018) 83(3):403–15. doi: 10.1093/neuros/nyx423

17. Koutourousiou M, Gardner PA, Tormenti MJ, Henry SL, Stefko ST, Kassam AB, et al. Endoscopic endonasal approach for resection of cranial base chordomas: outcomes and learning curve. *Neurosurgery.* (2012) 71(3):614–24. doi: 10.1227/NEU.0b013e31825ea3e0

18. Zenonos GA, Fernandez-Miranda JC, Mukherjee D, Chang YF, Panayidou K, Snyderman CH, et al. Prospective validation of a molecular prognostication panel for clival chordoma. *J Neurosurg* (2018) 130(5):1528–37. doi: 10.3171/2018.3.JNS172321

19. Lao J, Chen Y, Li ZC, Li Q, Zhang J, Liu J, et al. A deep learning-based radiomics model for prediction of survival in glioblastoma multiforme. *Sci Rep* (2017) 7(1):10353. doi: 10.1038/s41598-017-10649-8

20. Han W, Qin L, Bay C, Chen X, Yu KH, Miskin N, et al. Deep transfer learning and radiomics feature prediction of survival of patients with high-grade gliomas. *AJNR Am J Neuroradiol* (2020) 41(1):40–8. doi: 10.3174/ajnr.A6365

21. Fan Y, Hua M, Mou A, Wu M, Liu X, Bao X, et al. Preoperative noninvasive radiomics approach predicts tumor consistency in patients with acromegaly: Development and multicenter prospective validation. *Front Endocrinol (Lausanne).* (2019) 10:403. doi: 10.3389/fendo.2019.00403

22. Yin P, Mao N, Wang S, Sun C, Hong N. Clinical-radiomics nomograms for pre-operative differentiation of sacral chordoma and sacral giant cell tumor based

on 3D computed tomography and multiparametric magnetic resonance imaging. *Br J Radiol* (2019) 92(1101):20190155. doi: 10.1259/bjr.20190155

23. Li L, Wang K, Ma X, Liu Z, Wang S, Du J, et al. Radiomic analysis of multiparametric magnetic resonance imaging for differentiating skull base chordoma and chondrosarcoma. *Eur J Radiol* (2019) 118:81–7. doi: 10.1016/j.ejrad.2019.07.006

24. Wei W, Wang K, Tian K, Liu Z, Wang L, Zhang J, et al. A novel MRI-based radiomics model for predicting recurrence in chordoma. *Annu Int Conf IEEE Eng Med Biol Soc* (2018) 2018:139–42. doi: 10.1109/EMBC.2018.8512207

25. Wei W, Wang K, Liu Z, Tian K, Wang L, Du J, et al. Radiomic signature: A novel magnetic resonance imaging-based prognostic biomarker in patients with skull base chordoma. *Radiother Oncol* (2019) 141:239–46. doi: 10.1016/j.radonc.2019.10.002

frontiers | Frontiers in Oncology

TYPE Original Research
PUBLISHED 09 February 2023
DOI 10.3389/fonc.2022.1046238

OPEN ACCESS

EDITED BY
Cheng Yang,
Shanghai Changzheng Hospital, China

REVIEWED BY
Fang Fang,
Sichuan University, China
Zhiyuan Xu,
University of Virginia, United States

*CORRESPONDENCE
Shibin Sun
sunshibin711@163.com

SPECIALTY SECTION
This article was submitted to Neuro-Oncology and Neurosurgical Oncology, a section of the journal Frontiers in Oncology

RECEIVED 16 September 2022
ACCEPTED 26 October 2022
PUBLISHED 09 February 2023

CITATION
Wang K, Gao D, Pan J, Bao E and Sun S (2023) The role of Gamma Knife radiosurgery in the management of skull base chordoma.
Front. Oncol. 12:1046238.
doi: 10.3389/fonc.2022.1046238

The role of Gamma Knife radiosurgery in the management of skull base chordoma

Kuanyu Wang[1,2], Dezhi Gao[1,2], Jian Pan[1,2], Enmeng Bao[1,2] and Shibin Sun[1,2]*

[1]Gamma Knife Center, Beijing Tiantan Hospital, Capital Medical University, Beijing, China, [2]Gamma Knife Center, Beijing Neurosurgical Institute, Capital Medical University, Beijing, China

Objective: Chordoma is a slow-growing and locally aggressive cancer, which arises from the remnants of the primitive notochord. The first line treatment for the skull base chordoma is neurosurgery. Gamma Knife radiosurgery (GKS) is often be chosen especially in the setting of residual or recurrent chordomas. The purpose of this study is to evaluate the prognosis of patients with skull base chordoma who underwent GKS.

Methods: The present study was a retrospective analysis of 53 patients with skull base chordomas who underwent GKS. Univariate Cox and Kaplan-Meier survival analysis were performed to analyze the relationship between the tumor control time and the clinical characteristics.

Results: The 1-, 2-, 3-, and 5-year progression free survival (PFS) rates were 87, 71, 51, and 18%, respectively. After performing the univariate analysis, the clinical characteristics were not found to be significantly associated with the time of PFS; however, surgical history, peripheral dose, and tumor volume did have tendencies to predict the prognosis.

Conclusion: GKS provided a safe and relatively effective treatment for residual or recurrent chordomas after surgical resection. A higher tumor control rate depends on two approaches, an appropriate dose of radiation for the tumor and the accurate identification of the tumor margins.

KEYWORDS

Gamma Knife radiosurgery (GKS), chordoma, MDT, multi-procedure radiosurgery, multi-modality imaging

Introduction

Ribbert first described the term chordoma in 1894, as having a rare incidence rate of about 0.1 per 100,000 individuals (1). Chordoma, which arises from the remnants of the primitive notochord, is characteristically slow-growing and locally aggressive (2), and occurs more frequently in adults than children, with most diagnoses occurring between 40 to 60 years of age (3). Chordomas often occur in the skull base region (35%), the sacrococcygeal region (50%), and the vertebrae region (15%) (3, 4).

According to the World Health Organization (WHO) classification system, chordoma is divided into 3 distinct types: conventional chordoma (chondroid chordoma), dedifferentiated chordoma, and poorly differentiated chordoma (5). Patients with untreated chordomas have poor prognoses, with a mean survival < 1 year (6).

Although there is no doubt that neurosurgical therapy is the first line treatment option for the skull base chordoma, a total resection is often difficult to obtain, due to the invasion of the tumor into skull base and its location being adjacent to numerous important structures, along with a high tumor recurrence rate (7). The chemotherapy and traditional low-dose radiotherapy is not sensitive to this tumor (8). It is difficult to perform a repeat neurosurgical resection, necessitating the utilization of various radiotherapy approaches, including Gamma Knife radiosurgery (GKS), in an effort to control the tumor recurrence (9). GKS has been used for residual or recurrent chordoma as an effective treatment. In this study, we performed a large single-institution retrospective review of the prognosis for the skull base chordoma patients who underwent GKS. The purpose of this study is to define the role of GKS in the treatment of the chordoma patients.

Materials and methods

Patient demographics

We identified a total of 53 consecutive patients with chordomas who underwent GKS in Tiantan Hospital Gamma Knife Center between January 2006 and December 2019. The initial treatment for 52 of the patients was microsurgical resection, and the diagnosis of chordoma was confirmed by histopathology prior to the patients undergoing GKS, except for the 53rd patient, who underwent a remedial surgical resection post-GKS. Of the 53 patients, 34 (64%) were male and 19 (36%) were female. The mean age was 45 years (range, 16–71 years). Of the 53 patients, 8 had previously undergone radiotherapy – 5 underwent external beam radiotherapy and 3 underwent stereotactic radiosurgery (2 with GKS and 1 with cyber knife). Adjuvant GKS for the treatment of residual or recurrent chordomas occurred at an average of 11.9 months (range, 1–60 months) after the initial surgical resection. Of the 52 patients who were treated with salvage GKS, 1 patient underwent 8 surgical resections prior to GKS, 12 underwent 2 surgical resections, and 39 underwent 1 surgical resection (Table 1). Written informed consent was obtained from all patients involved in the present study.

Radiosurgical parameters

In all 53 cases, a Leksell stereotactic frame was fixed to the patient's skull under local anesthesia. High-resolution contrast-enhanced magnetic resonance imaging (MRI) was performed, utilizing a slice thickness of 2 mm for treatment planning. Radiosurgery was performed using the Leksell Gamma Knife model B (Elekta AB) before 2007, the Leksell Gamma Knife model C (Elekta AB) between January 2007 and October 2011, and the Leksell Gamma Knife Perfexion (Elekta AB) thereafter. Multiple dose planning sessions were carried out using the GammaPlan system (Elekta Instruments).

In the cohort evaluated in the present study, the mean prescribed radiation dose was 13.5 Gy (range, 10–16 Gy), for which the equivalent dose in 2-Gy fractions (EQD2; calculated assuming an $\alpha/\beta = 3$ for chordomas) ranged from 26 to 60.8 Gy (mean, 44.8 Gy). The mean isodose line was 45.8% (range, 40–50%); the mean maximum dose was 29.4 Gy (range 22–33.3 Gy); and the mean tumor volume was 17.1 cm^3 (range, 1.1–62.2 cm^3). Some patients had complicated radiotherapy histories, so the

TABLE 1 The basic information.

	Mean	Range
Gender	Male, 34	
	Female, 19	
Age	45	16–71
Surgery History	None, 1	
	Yes, 53	
Prior Radiotherapy	None, 45	
	Yes, 8	
Postoperative Interval (months)	12	1–60
Tumor Volume (cm^3)	17.1	1.08–62.6
Peripheral Dose (Gy)	13.5	10.0–16.0
Central Dose (Gy)	29.4	22.0–33.3
Follow-up (months)	53	8–168
EQD2 (Gy)	44.8	26–60.8

average total EQD2 for these patients was 60.3 Gy (range, 26–200 Gy) (Table 1).

Follow-up and statistical analysis

All patients were recommended to undergo MRI and clinical evaluations at 6-month intervals during the first year post-GKS, and every 6–12 months thereafter. Tumor recurrence was defined as an increase in the tumor size after GKS, or the development of a new tumor, as seen on follow-up MRI. Tumor recurrences were categorized as local (enlargement of the treated tumor), marginal (new tumor formation out of the prescribed line, but within the resection cavity), and distant (new tumor formation away from the resection cavity). In order to account for the variability between scanners and images, tumor shrinkage or growth was defined as a 25% decrease or increase in volume, respectively. Univariate Cox and Kaplan-Meier survival analysis were performed to analyze the relationship between the tumor control time and the clinical characteristics.

Results

For the present study, the mean duration of follow-up was 53 months (range 6–115 months). Of the 53 patients included in this study, follow-up MRI demonstrated that only 10 (19%) had good tumor control which remained stable, while 43 (81%) had varying degrees of tumor development, for an overall total tumor control rate of 19%. Of the 43 patients who experienced tumor development, 15 underwent repeat GKS, 1 underwent local radiotherapy, 12 underwent repeat surgical resection, 15 received only clinical observation or ceased follow-up, and 2 died from repeated tumor recurrence. The pattern of recurrence was as follows: local + marginal for 35 patients; distant for 3 patients; and local + marginal + distant for 5 patients. The 1-, 2-, 3-, and 5-year progression free survival (PFS) rates were 87, 71, 51% and 18%, respectively. Complex treatment strategies were adopted for most patients through their last follow-up, undergoing surgical resections as follows: 32 patients underwent a single surgical resection; 14 underwent 2 surgical resections; 5 underwent 3 surgical resections; 1 underwent 4 surgical resections; and 1 underwent 8 surgical resections. The patients underwent radiotherapy treatments as follows: 25 underwent a single radiotherapy treatment; 15 underwent 2 radiotherapy treatments; 7 underwent 3 radiotherapy treatments; 4 underwent 4 radiotherapy treatments; 1 underwent 5 radiotherapy treatments; and 1 underwent 6 radiotherapy treatments.

To evaluate the prognostic value of various factors in patients with chordomas who underwent GKS, the univariate Cox regression analysis was performed. The results of this analysis showed that several factors, including sex, age, surgical history, postoperative interval, number of shots, central dose, peripheral dose, and tumor volume, were not significantly associated with PFS ($P \geq 0.05$) (Table 2). Although there was no significant difference ($P < 0.05$) between these factors and PFS, the trend was existing, as the surgical history, peripheral dose, and tumor volume tended to predict the prognosis. Similar results were also obtained by Kaplan-Meier analysis (Figure 1), the results of which implied that PFS might be related to the surgical history, peripheral dose, and tumor volume in chordoma patients.

TABLE 2 Univariate analysis

	HR	95.0% CI	*P*-value
Sex	1.87	0.96–3.65	0.07
Age	1.00	0.98–1.03	0.77
Surgical History	1.17	0.94–1.45	0.15
Postoperative Interval	0.99	0.96–1.02	0.54
Central Dose	0.95	0.85–1.05	0.29
Peripheral Dose	0.86	0.69–1.06	0.16
Tumor Volume	1.01	0.99–1.03	0.19
EQD2	0.97	0.94–1.00	0.11

Discussion

Chordomas are often considered to be low-grade malignancies; however, the tumor cells frequently show locally aggressive growth, leading to a higher recurrence rate after the initial neurosurgical resection. The standard treatment for clival chordomas is complete or subtotal neurosurgical resection, while radiotherapy treatments are necessary for the residual or recurrent tumors after surgical management to improve local tumor control (10). The results of retrospective studies from multiple institutions have shown that GKS plays an important role in the treatment of residual or recurrent chordomas.

The first clinical report of GKS for chordoma was published in 1991 by Kondziolka from the University of Pittsburgh Medical Center, which revealed the confirmed efficacy of GKS with 20 Gy to the tumor margin for four patients. Subsequently Muthukumar et al. (11) also from the Pittsburgh group reported 9 patients with chordoma treated with GKS in 1998. A multicenter study investigated by Kano showed that the skull base chordomas patients who underwent GKS had a 5-year local control rate of 66% and a 5-year survival of 80%. The median marginal doses of 12.7–20 Gy were used in these studies of GKS for chordoma from Table 3. The clinical data from this table showed that the 5-year local control rate of chordoma after Gamma Knife treatment was 21.4%–76%, and the 5-year survival was 67-100 (1, 7, 11–20) (Table 3). The tumor control

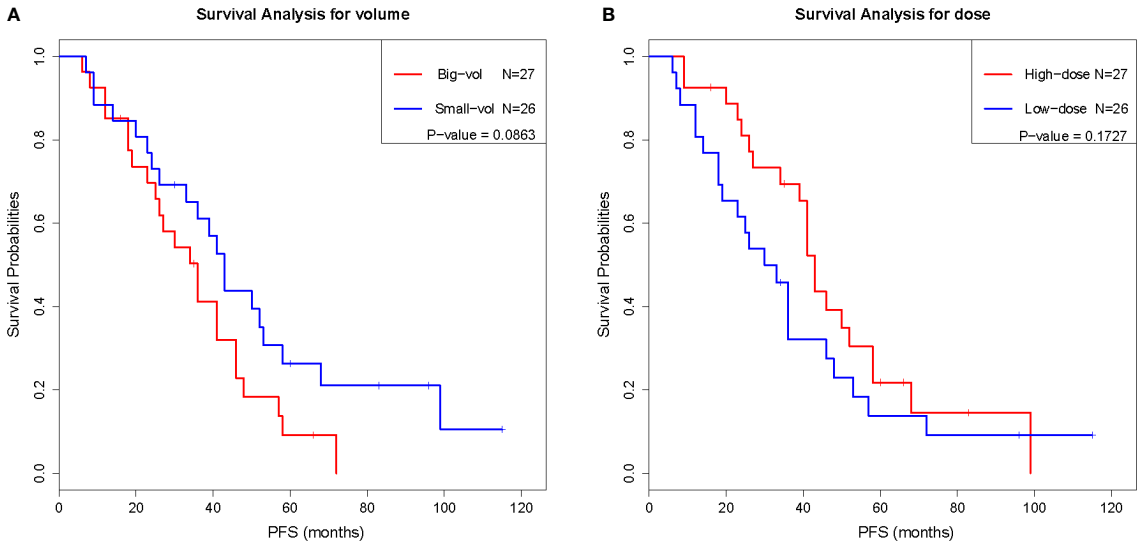

FIGURE 1
Kaplan-Meier analysis of tumor volume **(A)** and peripheral dose **(B)**.

rates from these clinical investigations varied widely, which demonstrated the radio-resistant characteristic of chordomas.

For the patients who underwent GKS at our center, the 3- and 5-year local control rates were 51 and 18%, respectively. As early as 2008, Liu et al. (21) had completed a retrospective study of 31 patients with skull base chordoma who underwent radiosurgery in our center. The results of that study showed that the 3- and 5-year local control rates were 64.2 and 21.4%, respectively. The mean follow-up time after the radiosurgery treatment was 30.2 months (range, 6–102 months) (21). In the present study, the mean follow-up was extended to 38.9 months (range, 6–115 months); however, there was no significant improvement in the tumor control rate between the two clinical investigations performed at our center. It is believed that the relatively low control effect may be related to the relatively large postoperative residual tumor volume, the

TABLE 3 Summary table of GKS studies for chordoma.

Author	Year	No.	Vol. (cm3)	Median Prescription Dose (Gy)	5-years Local Control (%)	5-years Survival (%)	Follow-Up (months)
Muthukumar et al.	1998	9	NA	18	66	NA	48
Krishnan et al.	2005	25	14.4	15	32	90	58
Hasegawa et al.	2007	27	19.7	14	76	80	59
Martin et al.	2007	18	9.8	16	63	63	NA
Liu et al.	2008	31	11.4	12.7	21.4	75.8	30.2
Dassoulas et al.	2009	15	5.8	15.3	50	NA	88
Ito et al.	2009	19	3.3	17.8	47.9	100	87
Koga et al.	2010	14	NA	15	43	NA	65
Kano et al.	2011	71	7.1	15	66	80.2	60
Mori et al.	2014	7	5.1	16.9	67	100	NA
Kim et al.	2014	5	10.7	20	35	73	53
Hafez et al.	2019	12	7	14.7	25	NA	45
Cahill et al.	2021	15	10	20	67	67	84

identification of the target area, and the relatively low peripheral radiation dose. From our experience, the ideal approach to improve tumor control of chordomas post-GKS depended on three aspects: how to appropriately increase the prescribed radiation dose for each tumor; how to strengthen the multi-disciplinary treatment (MDT) for each patient; and how to determine the real biological margins of each tumor.

Although the differences were not significant, the patient's surgical history, tumor volume, and peripheral dose had some correlation with the tumor control effect. Perfect total surgical resection and an appropriate increase in the peripheral radiation dose may improve the post-GSK tumor control in patients with chordoma. Several studies have reported that there was a correlation between the local control rate and the radiation dose, such as Koga et al. (18), who reported a significant difference between patients treated with GKS at different doses (18 vs. 12 Gy). The median marginal dose used in the study of Cahill et al. (1) was 20 Gy which is higher than many other studies, the tumor control rates at 5 and 10 years in the chordoma group were 67% and 49%, and the 5- and 10-year overall survival rates were 67% and 53% respectively. In the clinical practice, 20 Gy of prescription margin dose per fraction was difficult to be administered because of the adjacent critical structure. A prescription marginal dose of at least 16 Gy per fraction should be recommended to improve tumor control effect. Multi-procedure radiosurgery, including multi-stage radiosurgery and fractionated radiosurgery, could be performed to achieve the boost of irradiation dose.

To improve tumor control rates in patients with chordoma, it is necessary to introduce the concept of MDT to the diagnosis and treatment process. Neurosurgeons need to remove as much of the tumors as possible, on the premise of preserving nerve function and reducing the residual tumor volume. Radiologists and radiosurgeons should detect any residual tumor or tumor recurrence and perform a radiosurgical treatment as soon as possible. They also should pay attention to the location of the target area and appropriately increase the radiation dose, as necessary. We have recommended that the ideal window of opportunity for radiotherapy intervention when treating residual chordomas is approximately 3 months after the initial surgical resection.

The precise definition of the tumor target volume is crucial to the radiosurgery process, and for this it is necessary to determine which imaging techniques should be utilized for the identification of the real target area. The CT, MRI and PET characteristic features of chordomas have been revealed. CT displays osteolysis and a soft tissue component in almost all cases and frequently contain mineralized matrix or sequestered bone. The T1 sequence of MRI displays isointense signal with heterogeneous contrast enhancement. The T2 sequence displays a high signal intensity with heterogeneous hypointensity associated with mucous, hemorrhage, and calcification. Small foci of internal increased T1 and predominant T2 hyperintensity may also appear on MRIs of chordomas (22). PET generally displays heterogeneous ^{18}F-FDG activity with moderate but variable avidity. From our experience, the T2 sequence is of equal importance to the T1 contrast sequence in the MRI localization of the chordoma to outline the real tumor margin for GKS. Recent studies have demonstrated the uptake of multiple positron-emission tomography (PET) tracers in chordomas, which may have an important role in the diagnosis, follow-up, and personalized treatment of chordomas (23). We consider that multi-modality imaging localization fused with MRI, CT, and PET/MR or PET/CT will be utilized in the future for the identification of chordoma tumor margins to achieve higher local tumor control rate.

Additionally, the results of some recent studies have shown that certain adjuvant treatments also play an important role in improving disease control rates in patients with chordomas. A study published in 2021 by DeMaria et al. (2) showed that a novel yeast-brachyury vaccine could be used to treat patients with unresectable chordoma. The results, however, showed that this vaccine did not significantly improve the efficacy of radiotherapy in patients with chordoma (2). Another study, published in 2018 by Gregory et al. described the use of nilotinib, a kind of platelet-derived growth factor receptor (PDGFR) inhibitor, in addition to radiation in the treatment of high-risk chordomas. The results of their study showed that the median PFS was 58.15 months, with a 2-year overall survival rate was 95% (24). Studies such as these provide a research direction for the utilization of MDT in the treatment of chordomas.

This research was a retrospective study and the limitation of our study was that the number of cases was relatively small. The reason was related to the rare incidence of this disease. The univariate Cox analysis had no statistical significance might be related with the small sample size. In the future, we will further expand the sample size through multi-center cooperation.

Conclusions

GKS provides a safe and relatively effective management for residual or recurrent chordomas after the initial surgical resection. To achieve higher local tumor control of GKS for chordomas, three approaches can be recommended: Multi-procedure radiosurgery to increase the prescription margin dose, MDT management for the patients with chordomas, and Multi-modality imaging fusion to obtain the accurate identification of the tumor margins.

Data availability statement

The raw data supporting the conclusions of this article will be made available by the authors, without undue reservation.

Ethics statement

The study was reviewed and approved by the Ethics Review board of Beijing Tiantan Hospital and the written informed consent to participate in this study was obtained.

Author contributions

SS and KW designed the study, drafted the manuscript and revised the manuscript. DG, JP and EB contributed to the collection of the data. All authors read and approved the final manuscript.

Funding

The present study was funded by the National Natural Science Foundation of China (grant numbers 82003192) and the Cancer Precision Radiotherapy Spark Program of China International Medical Foundation (grant numbers 2019-N-11-37 and 2019-N-11-35).

Conflict of interest

The authors declare that the research was conducted in the absence of any commercial or financial relationships that could be construed as a potential conflict of interest.

Publisher's note

All claims expressed in this article are solely those of the authors and do not necessarily represent those of their affiliated organizations, or those of the publisher, the editors and the reviewers. Any product that may be evaluated in this article, or claim that may be made by its manufacturer, is not guaranteed or endorsed by the publisher.

Supplementary material

The Supplementary Material for this article can be found online at: https://www.frontiersin.org/articles/10.3389/fonc.2022.1046238/full#supplementary-material

References

1. Cahill J, Ibrahim R, Mezey G, Yianni J, Bhattacharyya D, Walton L, et al. Gamma knife stereotactic radiosurgery for the treatment of chordomas and chondrosarcomas. *Acta neurochirurgica* (2021) 163:1003–11. doi: 10.1007/s00701-021-04768-5

2. DeMaria PJ, Bilusic M, Park DM, Heery CR, Donahue RN, Madan RA, et al. Randomized, double-blind, placebo-controlled phase II study of yeast-brachyury vaccine (GI-6301) in combination with standard-of-Care radiotherapy in locally advanced, unresectable chordoma. *oncologist* (2021) 26:e847–58. doi: 10.1002/onco.13720

3. Wedekind MF, Widemann BC, Cote G. Chordoma: Current status, problems, and future directions. *Curr Problems Cancer* (2021) 45:100771. doi: 10.1016/j.currproblcancer.2021.100771

4. Krishnamurthy A. Mandibular metastasis as a presenting feature of a clival chordoma. *J Cancer Res Ther* (2020) 16:668–71. doi: 10.4103/jcrt.JCRT_613_18

5. Arvind V, Nevzati E, Ghaly M, Nasim M, Farshad M, Guggenberger R, et al. Primary extradural tumors of the spinal column: A comprehensive treatment guide for the spine surgeon based on the 5(th) edition of the world health organization bone and soft-tissue tumor classification. *J Craniovertebral Junction Spine* (2021) 12:336–60. doi: 10.4103/jcvjs.jcvjs_115_21

6. Eriksson B, Gunterberg B, Kindblom LG. Chordoma. A clinicopathologic and prognostic study of a Swedish national series. *Acta orthopaedica Scandinavica* (1981) 52:49–58. doi: 10.3109/17453678108991758

7. Mori Y, Kida Y, Matsushita Y, Mizumatsu S, Hatano M. Stereotactic radiosurgery and stereotactic radiotherapy for malignant skull base tumors. *Cureus* (2020) 12:e8401. doi: 10.7759/cureus.8401

8. Bai J, Li M, Xiong Y, Shen Y, Liu C , Zhao P, et al. Endoscopic endonasal surgical strategy for skull base chordomas based on tumor growth directions: Surgical outcomes of 167 patients during 3 years. *Front Oncol* (2021) 11:724972. doi: 10.3389/fonc.2021.724972

9. Kocher M, Voges J, Staar S, Treuer H, Sturm V, Mueller RP. Linear accelerator radiosurgery for recurrent malignant tumors of the skull base. *Am J Clin Oncol* (1998) 21:18–22. doi: 10.1097/00000421-199802000-00004

10. Forander P, Bartek JJr., Fagerlund M, Benmaklouf H, Dodoo E, Shamikh A, et al. Multidisciplinary management of clival chordomas; long-term clinical outcome in a single-institution consecutive series. *Acta neurochirurgica* (2017) 159:1857–68. doi: 10.1007/s00701-017-3266-1

11. Muthukumar N, Kondziolka D, Lunsford LD, Flickinger JC. Stereotactic radiosurgery for chordoma and chondrosarcoma: further experiences. *Int J Radiat oncology biology Phys* (1998) 41:387–92. doi: 10.1016/S0360-3016(98)00051-0

12. Kano H, Iqbal FO, Sheehan J, Mathieu D, Seymour ZA, Niranjan A, et al. Stereotactic radiosurgery for chordoma: A report from the north American gamma knife consortium. *Neurosurgery* (2011) 68:379–89. doi: 10.1227/NEU.0b013e3181ffa12c

13. Hafez RFA, Fahmy OM, Hassan HT. Gamma knife surgery efficacy in controlling postoperative residual clival chordoma growth. *Clin Neurol Neurosurg* (2019) 178:51–5. doi: 10.1016/j.clineuro.2019.01.017

14. Krishnan S, Foote RL, Brown PD, Pollock BE, Link MJ, Garces YI. Radiosurgery for cranial base chordomas and chondrosarcomas. *Neurosurgery* (2005) 56:777–84. doi: 10.1227/01.NEU.0000156789.10394.F5

15. Hasegawa T, Ishii D, Kida Y, Yoshimoto M, Koike J, Iizuka H. Gamma knife surgery for skull base chordomas and chondrosarcomas. *J Neurosurg* (2007) 107:752–7. doi: 10.3171/JNS-07/10/0752

16. Dassoulas K, Schlesinger D, Yen CP, Sheehan J. The role of gamma knife surgery in the treatment of skull base chordomas. *J neuro-oncology* (2009) 94:243–8. doi: 10.1007/s11060-009-9846-z

17. Ito E, Saito K, Okada T, Nagatani T, Nagasaka T. Long-term control of clival chordoma with initial aggressive surgical resection and gamma knife radiosurgery for recurrence. *Acta neurochirurgica* (2010) 152:57–67. doi: 10.1007/s00701-009-0535-7

18. Koga T, Shin M, Saito N. Treatment with high marginal dose is mandatory to achieve long-term control of skull base chordomas and chondrosarcomas by means of stereotactic radiosurgery. *J neuro-oncology* (2010) 98:233–8. doi: 10.1007/s11060-010-0184-y

19. Kim JH, Jung HH, Chang JH, Chang JW, Park YG, Chang WS. Gamma knife surgery for intracranial chordoma and chondrosarcoma: Radiosurgical perspectives and treatment outcomes. *J Neurosurg* (2014) 121 Suppl:188–97. doi: 10.3171/2014.7.GKS141213

20. Martin JJ, Niranjan A, Kondziolka D, Flickinger JC, Lozanne KA, Lunsford LD. Radiosurgery for chordomas and chondrosarcomas of the skull base. *J Neurosurg* (2007) 107:758–64. doi: 10.3171/JNS-07/10/0758

21. Liu AL, Wang ZC, Sun SB, Wang MH, Luo B, Liu P. Gamma knife radiosurgery for residual skull base chordomas. *Neurological Res* (2008) 30:557–61. doi: 10.1179/174313208X297878

22. Olson JT, Wenger DE, Rose PS, Petersen IA, Broski SM. Chordoma: (18)F-FDG PET/CT and MRI imaging features. *Skeletal Radiol* (2021) 50:1657–66. doi: 10.1007/s00256-021-03723-w

23. Santegoeds RGC, Temel Y, Beckervordersandforth JC, Overbeeke JJV, Hoeberigs CM. State-of-the-Art imaging in human chordoma of the skull base. *Curr Radiol Rep* (2018) 6:16. doi: 10.1007/s40134-018-0275-7

24. Cote GM, Barysauskas CM, DeLaney TF, Schwab J, Raskin K, Lozano-Calderon S, et al. A phase 1 study of nilotinib plus radiation in high-risk chordoma. *Int J Radiat Oncol Biol Phys* (2018) 102:1496–504. doi: 10.1016/j.ijrobp.2018.07.2013

Frontiers in Oncology

Advances knowledge of carcinogenesis and tumor progression for better treatment and management

The third most-cited oncology journal, which highlights research in carcinogenesis and tumor progression, bridging the gap between basic research and applications to imrpove diagnosis, therapeutics and management strategies.

Discover the latest Research Topics

See more →

Frontiers

Avenue du Tribunal-Fédéral 34
1005 Lausanne, Switzerland
frontiersin.org

Contact us

+41 (0)21 510 17 00
frontiersin.org/about/contact